

TABLE OF CONTENTS

Page	
INTRODUCTION	1
CHAPTER 1 LITERATURE REVIEW	5
1.1 Introduction.....	5
1.2 Turning.....	5
1.3 Machining lubrication modes	6
1.3.1 Wet.....	7
1.3.2 Dry	8
1.3.3 Semi-Dry.....	8
1.3.4 Properties of lubricant.....	9
1.4 Atomization.....	10
1.4.1 Definition	10
1.4.2 Mechanism of atomization.....	11
1.4.3 Theoretical and experimental studies (Theories).....	12
1.4.4 Atomization Summary	14
1.5 Atomizers and pulverization	14
1.5.1 Introduction.....	14
1.5.2 Different lubrication systems.....	15
1.5.3 Nozzle performance properties	20
1.5.4 Different types of atomizers.....	21
1.5.5 Common features of different twin-fluid atomizers	34
1.6 Prediction of mean drop size and drop size distribution.....	34
1.6.1 Introduction.....	34
1.6.2 Definition	35
1.6.3 The empirical correlations related on the mean drop diameter.....	37
1.6.4 The effects of variables on mean drop size.....	45
1.7 Cutting parameter effects on machining quality characteristics	48
1.7.1 Cutting parameter effects on Surface Roughness	48
1.7.2 Cutting parameter effects on cutting tool temperature	49
1.7.3 Cutting parameter effects on aerosol emission	51
1.8 Conclusion of literature review and refining of problematic.....	58
CHAPTER 2 INSTRUMENTS AND EXPERIMENTAL PROCEDURES	61
2.1 Introduction.....	61
2.2 Instruments.....	61
2.2.1 Injectors.....	61
2.2.2 Laser diffraction system.....	64
2.2.3 Pumps (GLS, SLS1.2-2 and DDA pumps) and flow sensor.....	65
2.2.4 TSI 8532 DustTrak – II aerosol monitor.....	71
2.2.5 Profilometer	72
2.3 Installation and experimental procedures	73

2.3.1	Particle sizing and injection angle measurement	73
2.3.2	Machining quality characteristics measurements	75
2.4	Conclusion	78

CHAPTER 3 EFFECTS OF ATOMIZER GEOMETRIES ON PARTICLE SIZING AND INJECTION ANGLE

3.1	Introduction.....	79
3.2	Effects of liquid orifice diameter	80
3.2.1	Sauter mean diameter (SMD)	80
3.2.2	Injection angle.....	84
3.3	Effects of atomizer length.....	89
3.3.1	Sauter mean diameter (SMD)	89
3.3.2	Injection angle.....	91
3.4	Effects of liquid orifice shape	93
3.4.1	Sauter mean diameter (SMD)	94
3.4.2	Injection angle.....	96
3.5	Atomizer geometry effects on SMD and injection angles when using continuous pump and high liquid flow rates	100
3.5.1	Liquid orifice diameter effects.....	100
3.5.2	Atomizer length effects.....	102
3.5.3	Liquid orifice shape effects.....	104
3.6	Validation of the Sauter mean diameter (SMD) experimental results	107
3.7	Conclusion	110

CHAPTER 4 MACHINING PERFORMANCE WHEN TURNING AA6061-T6 WITH PULSED AND CONTINUOUS COOLING/LUBRICATION

4.1	Introduction.....	111
4.2	Surface roughness investigation using the pulsed and continuous pumps when turning aluminum alloy 6061-T6.....	111
4.2.1	Introduction.....	111
4.2.2	Effect of cutting parameters on surface roughness when using pulsed pump	112
4.2.3	Effect of cutting parameters on surface roughness when using continuous pump	115
4.3	Cutting tool temperature and dust concentration investigation using the continuous pumps when turning of aa6061-t6	122
4.3.1	Introduction.....	122
4.3.2	Effect of cutting parameters on tool temperature	123
4.3.3	Effect of cutting parameters on dust concentration (Dc)	131
4.4	Multiple response optimization of machining	139
4.4.1	Introduction.....	139
4.4.2	Desirability Function	139

CONCLUSION	145
------------------	-----

RECOMMENDATIONS	149
-----------------------	-----

APPENDIX 1	151
APPENDIX 2	157
BIBLIOGRAPHY	163

LIST OF TABLES

	Page
Table 1.1	Applications of MQL & dry machining (DGUV, 2010)9
Table 1.2	The comparison between metering pump and pressure tank (Unfallversicherung, 2010)19
Table 1.3	Definitions and descriptions of mean particle diameter (Lee Black, McQuay and Bonin, 1996)36
Table 1.4	The parameters used in Kim and Marshall drop size measurements (Lefebvre, 1980)40
Table 1.5	The parameters used in Weiss and Worsham drop size measurements (Lefebvre, 1980)43
Table 1.6	The effects of the different variables on mean drop size (Lefebvre, 1980)46
Table 1.7	Dust generation when using different cutting conditions and chip morphologies (Khettabi, Songmene and Masounave, 2010)55
Table 2.1	Dimensions of atomizers.....63
Table 2.2	EMULTEC VG specifications64
Table 2.3	Mecagreen-550 specifications (CONDAT Lubrifiants)64
Table 2.4	Adjustment of Microlubrication systems67
Table 2.5	DDA reference specifications (GRUNDFOS, November 2010)69
Table 2.6	Flow sensor reference specifications (Manual, Aug 2012)70
Table 2.7	Gas and Liquid flow rates74
Table 2.8	Cutting parameters (Experiments using DDA pump).....76
Table 2.9	Cutting parameters (Experiments using SLS1.2-2 pump)77
Table 3.1	Dimensions of the atomizers.....79
Table 3.2	Gas and liquid flow rates80

Table 3.3	The ANOVA table of SMD when using nozzles with different diameters and GLS pump	81
Table 3.4	The ANOVA table of SMD when using nozzles with different diameters and DDA pump	81
Table 3.5	The ANOVA table of injection angle when using nozzles with different diameters and GLS pump	84
Table 3.6	The ANOVA table of injection angle when using nozzles with different diameters and DDA pump	85
Table 3.7	Percentage contribution of parameters affecting injection angle	85
Table 3.8	Examples of the measured injection angle	88
Table 3.9	The ANOVA table of SMD when using nozzles with different lengths and GLS pump	89
Table 3.10	The ANOVA table of SMD when using nozzles with different lengths and DDA pump	90
Table 3.11	The ANOVA table of injection angle when using nozzles with different lengths and GLS pump	91
Table 3.12	The ANOVA table of injection angle when using nozzles with different lengths and DDA pump	92
Table 3.13	Liquid orifice shapes	94
Table 3.14	The ANOVA table of SMD when using nozzles with different orifice shapes and GLS pump	95
Table 3.15	The ANOVA table of SMD when using nozzles with different orifice shapes and DDA pump	95
Table 3.16	The ANOVA table of injection angle when using nozzles with different orifice shapes and GLS pump	97
Table 3.17	The ANOVA table of injection angle when using nozzles with different orifice shapes and DDA pump	98
Table 3.18	Gas and liquid flow rates	100
Table 3.19	The ANOVA table of SMD when using nozzles with different liquid orifice diameter and DDA pump	101

Table 3.20	The ANOVA table of injection angle when using nozzles with different liquid orifice diameter and DDA pump	101
Table 3.21	The ANOVA table of SMD when using nozzles with different lengths and DDA pump	103
Table 3.22	The ANOVA table of injection angle when using nozzles with different lengths and DDA pump	103
Table 3.23	The ANOVA table of SMD when using nozzles with different liquid orifice shapes and DDA	105
Table 3.24	The ANOVA table of injection angle when using nozzles with different liquid orifice shapes and DDA	105
Table 3.25	Initial conditions of the experimental and theoretical studies	109
Table 3.26	Experimental air/liquid mass ratio	110
Table 4.1	The ANOVA table of surface roughness when using pulsed pump	114
Table 4.2	The ANOVA table of surface roughness when using Lg20.0dl0.25	119
Table 4.3	The ANOVA table of surface roughness when using Lg33.5dl1.00	120
Table 4.4	The ANOVA table of cutting tool temperature when using Lg20.0dl0.25	127
Table 4.5	The ANOVA table of cutting tool temperature when using Lg33.5dl1.00	128
Table 4.6	Quality responses statistical results	141
Table 4.7	Optimum setting level when using Lg20.0dl0.25 nozzle	142
Table 4.8	Optimum setting level when using Lg33.5dl1.00 nozzle	143
Table 4.9	Optimum response values for two different nozzles.....	144
Table 4.10	The ANOVA table of desirability function when using Lg33.5dl1.00 nozzle.....	144

LIST OF FIGURES

	Page
Figure 1.1	Important cutting parameters (Kalpakjian, 2008).....6
Figure 1.2	Atomization mechanism (Hede, Bach and Jensen, 2008).....11
Figure 1.3	Rayleigh Atomization Mechanism (Lightfoot, 2007).....13
Figure 1.4	One-channel and Two-channel systems (Unfallversicherung, 2010)16
Figure 1.5	One-channel system for internal feed (Unfallversicherung, 2010).....17
Figure 1.6	Two-channel system (Unfallversicherung, 2010).....17
Figure 1.7	Device with metering pump (Unfallversicherung, 2010)19
Figure 1.8	Device with pressure tank (Unfallversicherung, 2010)20
Figure 1.9	Plain orifice atomizer (Lefebvre, 1999).....22
Figure 1.10	Simplex atomizer1(Lefebvre, 1999)23
Figure 1.11	Dual orifice atomizer (Lefebvre, 1999)24
Figure 1.12	Spill return atomizers (Lefebvre, 1999).....25
Figure 1.13	Turbomeca slinger system (Lefebvre, 1999)26
Figure 1.14	Internal-mixing air assist atomizers (Lefebvre, 1999).....27
Figure 1.15	External-mixing air assist atomizers (Lefebvre, 1999).....27
Figure 1.16	Different types of the airblast atomizers (Lefebvre, 1999).....30
Figure 1.17	Plain-jet airblast atomizer (Lefebvre, 1999)31
Figure 1.18	Pre-filming airblast atomizer (Lefebvre, 1999)32
Figure 1.19	Prefilmer function in airblast atomizer (Batarseh, 2009).....33
Figure 1.20	Piloted airblast atomizer (Lefebvre, 1999)34

Figure 1.21	Nukiyama and Tanasawa plain-jet airblast atomizer (Lefebvre, 1980; Liu <i>et al.</i> , 2006).....	38
Figure 1.22	Kim & Marshall atomizer (Lefebvre, 1980)	40
Figure 1.23	Lorenzetto and Lefebvre atomizer (Lefebvre, 1980).....	41
Figure 1.24	Plain-jet atomizer used by Jasuja (Lefebvre, 1980).....	42
Figure 1.25	Rizkalla and Lefebvre atomizer (Lefebvre, 1980).....	44
Figure 1.26	Atomizing efficiency of the plain-jet and the prefilming atomizers (Lefebvre, 1980)	45
Figure 1.27	SMD variation related to liquid viscosity when using a plain-jet airblast atomizer (Lefebvre, 1980)	47
Figure 1.28	SMD variation related to surface tension when using for a plain-jet airblast atomizer (Lefebvre, 1980).....	47
Figure 1.29	SMD variation related to liquid density when using a plain-jet airblast atomizer (Lefebvre, 1980)	48
Figure 1.30	Heat generation zones (Sutter and Ranc, 2007).....	50
Figure 1.31	Average dust concentration when using A356 and AA6061 – T6 as a function of Workpiece Temperature (Balout, Songmene and Masounav, 2007)	52
Figure 1.32	Possible dust generation sources (micro level) (Balout, Songmene and Masounav, 2007).....	53
Figure 1.33	Dust emission varying on rake angle & cutting speed (dry machining of AA 6061-T6) (Khettabi <i>et al.</i> , 2010)	57
Figure 1.34	Dust emission varying on feed and cutting speed during (dry machining of AA6061) (Khettabi <i>et al.</i> , 2010).....	57
Figure 2.1	Coaxial plain-jet airblast atomizer (Steimes <i>et al.</i> , 2012).....	63
Figure 2.2	Helos-Vario/KR (www.sympatec.com), <i>consulted on 02/Sep/2012</i>	65
Figure 2.3	Microlubrication system (GLS pump) (Manual, Jan 2009).....	66
Figure 2.4	Microlubrication system (SLS1.2-2 pump) (Manual, 2009)	67
Figure 2.5	Digital Dosing Advanced Pump (DDA) (GRUNDFOS, November 2010)	68

Figure 2.6	Flow sensor (Manual, Aug 2012)	70
Figure 2.7	TSI 8532- DustTrak II aerosol monitor (Manual, Jan 2012)	71
Figure 2.8	Profilometer, Surtronic3+ (SalesBrochure) <i>consulted on 15/Aug./2012</i>	72
Figure 2.9	Profilometer, Mitutoyo	73
Figure 2.10	Injection angle experiment procedure.....	75
Figure 2.11	The position of injectors	76
Figure 2.12	The position of thermocouple	77
Figure 3.1	Pareto chart of SMD when using nozzles with different diameter and GLS pump.....	82
Figure 3.2	Pareto chart of SMD when using nozzles with different diameter and DDA pump.....	82
Figure 3.3	SMD related to gas flow rate for GLS and DDA pumps when using nozzles with different liquid orifice diameters	83
Figure 3.4	Pareto chart of injection angle when using nozzles with different diameters and GLS pump.....	86
Figure 3.5	Pareto chart of injection angle when using nozzles with different diameters and DDA pump	86
Figure 3.6	Injection angle related to gas flow rate for GLS pump when using nozzles with different liquid orifice diameters	87
Figure 3.7	Injection angle related to gas flow rate for DDA pump when using nozzles with different liquid orifice diameters	87
Figure 3.8	SMD related to gas flow rate when using nozzles with different lengths	90
Figure 3.9	Injection angle related to gas flow rate when using nozzles with different lengths and GLS pump.....	92
Figure 3.10	Injection angle related to gas flow rate when using nozzles with different lengths and DDA pump	93
Figure 3.11	SMD related to gas flow rate when using nozzles with different orifice shapes.....	96
Figure 3.12	Injection angle related to gas flow rate when using nozzles with different orifice shapes and GLS pump	98

Figure 3.13	Injection angle related to gas flow rate when using nozzles with different orifice shapes and DDA pump	99
Figure 3.14	Main effect plot of SMD when using nozzles with different liquid orifice diameters and DDA pump	102
Figure 3.15	Main effect plot of injection angle when using nozzles with different liquid orifice diameters and DDA pump.....	102
Figure 3.16	Main effect plot of SMD when using nozzles with different lengths and DDA pump	104
Figure 3.17	Main effect plot of injection angle when using nozzles with different lengths and DDA pump	104
Figure 3.18	Main effect plot of SMD when using nozzles with different liquid orifice shapes and DDA	106
Figure 3.19	Main effect plot of injection angle when using nozzles with different liquid orifice shapes and DDA.....	106
Figure 3.20	Particle sizing validation for the injector Lg20.0dl0.25	108
Figure 3.21	Particle sizing validation for the injector Lg33.5dl1.00	108
Figure 4.1	Surface roughness (μm) variations related to cutting speed (m/min) where feed rate = 0.10 mm/rev	112
Figure 4.2	Surface roughness (μm) variations related to cutting speed (m/min) where feed rate = 0.15 mm/rev	112
Figure 4.3	Surface roughness (μm) variations related to cutting speed (m/min) where feed rate = 0.20 mm/rev	113
Figure 4.4	Main effect plot of surface roughness analysis when using pulsed pump	114
Figure 4.5	Pareto chart of surface roughness analysis when using pulsed pump	115
Figure 4.6	Lg20.0dl0.25 – Surface roughness (μm) variations related to cutting speed (m/min)	116
Figure 4.7	Lg33.5dl1.00 - Surface roughness (μm) variations related to cutting speed (m/min)	118
Figure 4.8	Feed rate effects on surface roughness when using Lg20.0dl0.25	121

Figure 4.9	Feed rate effects on surface roughness when using Lg33.5dl1.00	121
Figure 4.10	Lg20.0dl0.25 – tool temperature (°C) variations related to cutting speed (m/min)	124
Figure 4.11	Lg20dl0.25 - tool temperature (°C) variations related to cutting speed (m/min)	126
Figure 4.12	Gas flow rate effects on tool temperature when using Lg20.0dl0.25	129
Figure 4.13	Liquid flow rate effects on tool temperature when using Lg20.0dl0.25	130
Figure 4.14	Gas flow rate effects on tool temperature when using Lg33.5dl1.0	130
Figure 4.15	Liquid flow rate effects on tool temperature when using Lg33.5dl1.0	131
Figure 4.16	Lg20.0dl0.25 – dust concentration (mg/m ³) variations related to cutting speed (m/min)	133
Figure 4.17	Lg33.5dl1.00 – dust concentration (mg/m ³) variations related to cutting speed (m/min)	134
Figure 4.18	Gas flow rate effects on dust concentration when using Lg20.0dl0.25	136
Figure 4.19	Gas flow rate effects on dust concentration when using Lg33.5dl1.00	136
Figure 4.20	Liquid flow rate effects on dust concentration when using Lg20.0dl0.25	137
Figure 4.21	Liquid flow rate effects on dust concentration when using Lg33.5dl1.00	137
Figure 4.22	Feed rate effects on dust concentration when using Lg20.0dl0.25	138
Figure 4.23	Feed rate effects on dust concentration when using Lg33.5dl1.00	138

LIST OF ABBREVIATIONS

SMD	sauter mean diameter
MMD	mass mean diameter
ML	minimum quantity lubrication
MQC	minimum quantity cooling
MQCL	minimum quantity cooling lubricant
ANOVA	analysis of variance
ALR	air/liquid mass ratio
Min	minimum value
Max	maximum value

LIST OF SYMBOLS

λ_{opt}	optimum wavelength
$f(\text{di})$	particle size distribution function
n_i	number of the droplets per unit volume
U	velocity (m/sec)
U_R	relative velocity of the gas to liquid (m/sec)
σ	surface tension (kg/sec ² , or N/m)
ρ	density (kg/m ³)
μ	dynamic viscosity (kg/msec, or Nsec/m ²)
Q	volumetric flow rate (l/sec)
D_p	prefilmer lip diameter (m)
β	flow localisation parameter defined by Xie et al.
D_u	dust unit (dimensionless)
E_A	energy activation
F_{sh}	shear force (N)
ϕ	shear angle (degree)
θ	tool rake angle (degree)
δ	material parameter
\dot{q}_g	gas flow rate (l/min)
\dot{q}_l	liquid flow rate (ml/min)
d_l	liquid orifice diameter (mm)
L	length of injector (mm)
R	liquid orifice shape (conical/straight)
d_{ge}	external gas orifice diameter (mm)
d_{gi}	internal gas orifice diameter (mm)
α	injection angle (degree)
\dot{m}	mass flow rate (kg/sec)
T_g	gas temperature (°K)
P_g	gas pressure (Pa)

XXVIII

Cs	cutting speed (m/min)
Fr	feed rate (mm/rev)
R _a	surface roughness (μm)
T	tool temperature (°C)
Dc	dust concentration (mg/m ³)
(d _i)	desirability of each response
D _i (x)	desirability function
w	weight value

INTRODUCTION

Manufacturing has been used for several thousand years by producing the stone, ceramic and metallic articles. From the first industrial revolution until now, there have been great improvements in manufacturing devices from traditional machines all the way to the online manufacturing machines in our days. This revolution allows customers to generate their own products using custom parts provided by online machine shops. Metal cutting is one of the best and useful methods of producing the final shape of parts.

Full understanding of the fundamentals of metal cutting mechanics and quantitative and qualitative analysis of the material removal mechanism are indispensable to achieve the optimum process performance.

The surface roughness, cutting temperature and aerosol emission are the important machining factors. Roughness of final product is considerable in many applications such as tires, floor surface and automobile brake linings. Because of the cutting temperature influence on cutting tool wear; its analysis is a crucial stage of machining studies. The cutting temperature produces the thermal damage and can impose the dimensional inaccuracies to the surfaces of machined workpiece. Nowadays, the manufacturers are interested in minimizing the environmental pollution to produce a cleaner workpiece as well as reducing the lubricant costs. Due to these reasons, dry and semi-dry machining are used frequently however dry machining produces the aerosols. The fine particles (less than $2.5\text{ }\mu\text{m}$) will go to deepest parts of the lung. The airborne particles introduce a health hazard because they remain suspended in the environment long enough to be inhaled by workers. Comparative study of the amounts of aerosol emission between dry and wet machining has shown that using cutting fluids can decrease the particle formation up to 40 – 50 % (Songmene, Balout and Masounave, 2008b).

The dominant factors on dust generation are tool geometry (rake angle and lead angle), cutting parameters (depth of cut, cutting speed and feed rate) and workpiece materials (Khettabi *et al.*, 2010).

Plastic deformation and friction are the other governing factors on particle emission. Therefore several studies are reported to investigate the friction and the quantity of particles generated. However these kinds of studies become difficult with micrometric or sub-micrometric particle sizes (Khettabi *et al.*, 2010). Considering the mentioned difficulties, this research study is performed based on MQC machining to find the cutting conditions which leads better machining part quality.

The main objectives of this research are summarized as follow:

1. Investigating governing factors on surface finish quality, heat generation in cutting tool and aerosol emission during turning of 6061-T6 aluminum alloy;
2. Comparing different lubrication mode such as dry, wet and MQC;
3. Presenting a strategy to find the optimum cutting conditions that leads to better machining performance.

Structure of thesis

The present work consists of 4 chapters which are organized as follow:

Chapter 1: Literature review

The first chapter presents a comprehensive literature review on various machining methods, atomization, different types of atomizers, laser based techniques for particle sizing, mean drop size prediction and drop size distribution. Furthermore factors governing machining quality index are also introduced, followed by a conclusion of the literature and refining the problematic.

Chapter 2: Instruments and Experimental procedures

This chapter describes the experimental apparatus and their installation methods.

Chapter 3: Effects of atomizer geometries on SMD and injection angles (Comparison between the pulsed and non-pulsed pumps)

This chapter consists of the investigation of the nozzle geometry effects on particle sizing and the injection angle which leads to choose the best nozzle geometry in order to use during the experimental study carried out in the following chapters. At the end of this chapter, the results of particle sizing obtained from the experiments performed by laser diffraction method are compared with the empirical equation to validate this experimental study.

Chapter 4: Machining performance when turning aa6061-t6 with pulsed and continuous cooling/lubrication

This chapter consists of three sections as follows:

- Study of the surface roughness using the pulsed and continuous pumps when turning 6061-T6 aluminum alloy.

In this chapter the effects of cutting parameters on surface roughness is studied using the pulsed and continuous pumps and two types of plain-jet airblast nozzles, which are geometrically different. The results discussion is performed to compare the different lubrication methods and to find the conditions which lead to the best surface quality. In this part of work, the effects of different pumps and nozzle geometries on surface roughness are investigated.

- Study of the cutting tool temperature and dust concentration using the continuous pumps when turning 6061-T6 aluminum alloy.

This section discusses about the cutting parameter effects on cutting tool temperature and dust concentration when using the different machining modes such as dry, wet and minimum quantity cooling. The main goal of this part is to find the conditions in which the minimum of heat generation occurred in cutting tool and the dust concentration reaches to its minimum value.

- Multiple response optimization of machining when using the minimum quantity cooling (MQC).

In industry and in different scientific researches, it is frequently happened that several dependent variables exist as response of an independent variable groupe as input data. In the present work, the different responses as machining quality indexes are investigated. Despite the existence of the conditions where each of these quality indicators can be in their optimum situation but these conditions are different from one to the other. In final section of this chapter of this research the multi response optimization is performed using the desirability function in order to find the optimum setting level of cutting parameters which determines the simultaneous minimization of all the responses.

CHAPTER 1

LITERATURE REVIEW

1.1 Introduction

The process of material removal from a workpiece to convert it into usable part is defined as machining. Metal cutting can be divided into two groups as follow:

- 1) Conventional machining process such as turning, drilling, grinding, milling, *etc.*;
- 2) Non – traditional manufacturing process such as e ultrasonic machining (USM), water jet and abrasive water jet machining (WJM & AWJM), electro discharge machining (EDM).

1.2 Turning

Turning is one of the conventional machining processes used for removing the metal from the outer diameter of a rotating cylindrical workpiece. This process is useful to shape the metal and generate a better surface finish. Turning is performed on a lathe machine in which the tool is stationary and the part is rotated. Using this machine, it is possible to perform four types of turning such as straight turning, taper turning, profiling or external grooving which can produce straight, conical, curved and grooved shaped parts.

In turning process, the most important factors which have to be adjusted before each process depends on material, cutting tool geometry, coating and cutting parameters (see Figure 1.1).

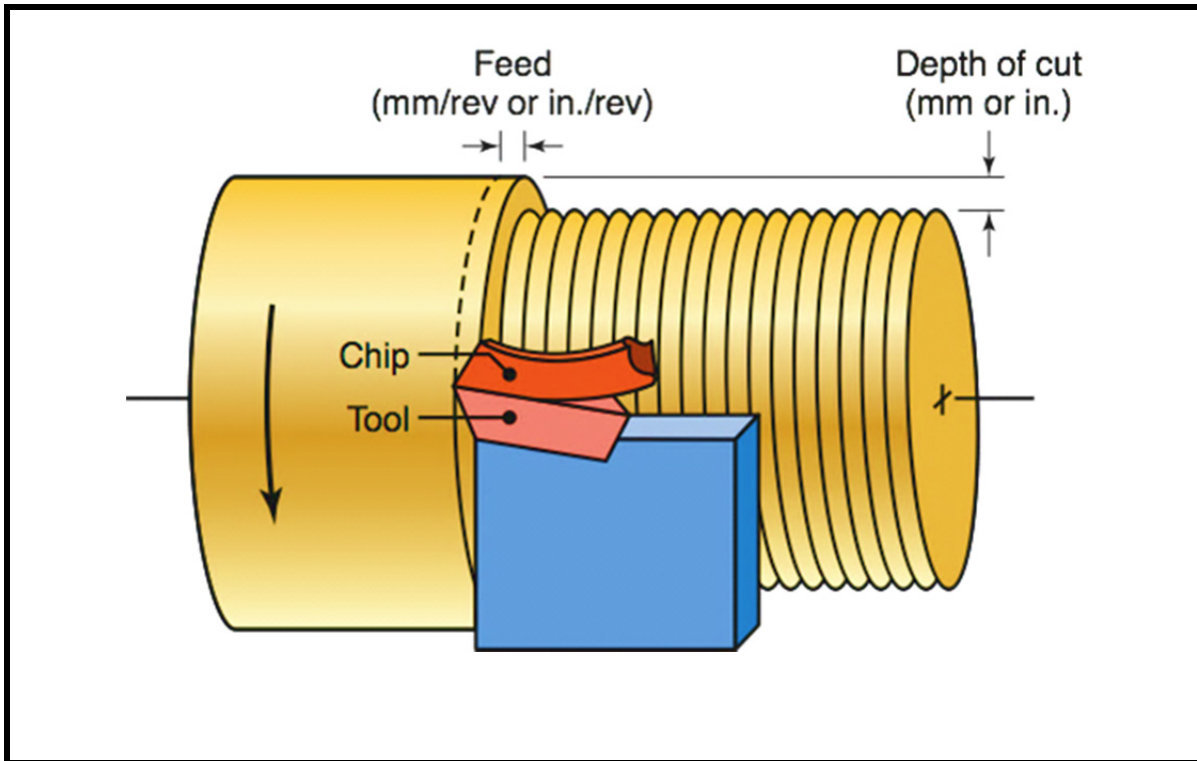


Figure 1.1 Important cutting parameters (Kalpakjian, 2008)

Revolution per minute as unit of cutting speed measurement shows the rotating speed and refers to the spindle and the workpiece. Feed rate is the rate at which the tool advances along its cutting path. The unit of feed rate is millimeter per revolution.

1.3 Machining lubrication modes

The important roles of cutting fluids during machining are decreasing the friction and the temperature by heat dissipation which increases tool life. However the use of cutting fluids is hazardous to operator health and the environment. Furthermore machining cost is anticipated when using cutting fluid.

To reduce the influence of cutting fluids on environment, the lubricants are improved by biodegradable fluids. However there is still bacterial contamination problem that is greatest problems encountered during lubricated machining. To eliminate all of these problems, other machining techniques such as dry and semi-dry machining or minimum quantity cooling lubricant (MQCL) are proposed. In cases with high heat generation, traditional oil can be

replaced with an emulsion which has a higher heat capacity due to its water content. The process in this case is referred to as minimum quantity cooling (MQC), making MQC distinct from MQL (minimum quantity lubrication). MQC is still largely unexplored, although it could provide a solution to processes with high heat generation (Diakodimitris, Hendrick and Iskandar)

These new methods help us to have clean machining and to increase and sometimes completely eliminate the serious problems associated with traditional machining. Most of these problems are caused by metallic particles and dust emissions generated during lubricated cutting.

1.3.1 Wet

Cutting fluids are used to lubricate the tool – chip and the tool – workpiece interface. These are useful for cooling the cutting zone in order to transfer heat. Lubrication is accomplished at low speeds by diffusion through the workpiece and by forming solid boundary layers from extreme pressure additives, but at high speeds, no lubrication is evident (Cassin and Boothroyd, 1965).

For the following three reasons, cutting fluids are not used during high speed machining (Shaw, Pigott and Richardson, 1951):

- 1) The chips carry the cutting fluid away from cutting zone;
- 2) The rate of reaction to the cutting fluid is too slow to be effective for high speed operations;
- 3) The rate of heat generation is greater for high speed operations than low speed operations.

Lower resulting values of friction, heat dissipation and better tool life time are the main advantages of wet machining. However the risk of operator health, environment hazard and machining cost increase are the most important disadvantages of wet machining.

1.3.2 Dry

Dry machining has been proposed in response to the environmental and health regulations and to reduce the machining costs. In high cutting speeds this type of machining leads to achieve the good surface finish. However the hard materials produce higher heat temperature to more than 1000 °C during higher speeds. (Charudatt).

1.3.3 Semi-Dry

In the metalworking industries, the health of operators and environmental pollution are affected by cutting fluids. In order to reduce these problems, the new method of machining, called Minimum Quantity Lubrication (MQL) is used. With respect to practical point of view, MQL cutting consumes an average of 50 ml of lubricant per processing hour. However, for certain operations (e.g. when using the workpiece with diameter of 40mm or larger), the lubrication consumption rate may exceed 150 ml/h (Unfallversicherung, 2010). Most important advantage of MQL system is that the lubricant supplies directly to the contact area. Due to this small droplet, the thermal shocking of the cutting tool is reduced, which increases the tool life and performance of its operation (Jun *et al.*, 2008). On the other hand, the MQL has also the disadvantages like the inability of complete heat transfer and moving out the chips from the cutting zone which is the cause of part corrosion. In this method, the nozzle must be located not more than 1 or 2 inches from the tool which enables the operator to precisely adjust the nozzle. The performance of MQL machining depends on many factors including lubricant; tools and suitable devices must be compatible. It is also very important that the conditions be properly inspected by the qualified machine operator. Dry machining and MQCL are possible for almost every cutting and non-cutting processes as well as turning, drilling, reaming, thread cutting, thread rolling, milling, hobbling, sawing and broaching (see Table 1.1).

Table 1.1 Applications of MQL & dry machining (DGUV, 2010)

Process	Material				
	Aluminum		Steel		Cast
	Cast alloy	Forged alloy	High-alloy Steels, rolling Bearing steel	Free-cutting Steel, quenched And tempered steel	GG20- GGG70
Drilling	MQCL	MQCL	MQCL	Dry	Dry
Reaming	MQCL	MQCL	MQCL	MQCL	MQCL
Thread cutting	MQCL	MQCL	MQCL	MQCL	MQCL
Thread rolling	MQCL	MQCL	MQCL	MQCL	MQCL
Deep drilling	MQCL	MQCL	-	MQCL	MQCL
Milling		MQCL	Dry	Dry	Dry
Turning	MQCL / Dry	MQCL / Dry	Dry	Dry	Dry
Hobbing	-	-	Dry	Dry	Dry
Sawing	MQCL	MQCL	MQCL	MQCL	MQCL
Broaching	-	-	MQCL	MQCL / Dry	MQCL / Dry

1.3.4 Properties of lubricant

Generally, there are several factors which are very important to choose a suitable lubricant. For example, the lubricant smell is substantial because spraying can increase the odor of lubricant. The lubricant must spray easily and also, the additives are very considerable because they should be adjusted to the processing requirements.

The lubricant must be easily removed from workpiece and machined parts and high flush point feature for them is very important because the flushing process should be done with the new lubricants. Viscosity range and corrosion protection are the other considerable characteristics to choose a lubricant. Khettabi *et al.* showed that the viscosity of 15 to 50 mm²/s is ideal to achieve the consistent results (Khettabi *et al.*, 2010).

MQCL machining improves the machinability and it increases the cutting performance more than dry and wet machining. Due to the injection of lubricant directly on the cutting zone, this type of machining reduces the cutting temperature which improves the chip-tool interaction. Also reducing the lubricant minimizes the amount of spray and mist which is better for operator health and environment. Finally using the minimum amount of cutting fluid in MQCL helps to reduce the machining cost.

1.4 Atomization

Nowadays, atomization of liquids is an important process in many industrial sectors such as pharmaceutical industries (spray-drying, tablet coating and spray congealing¹), automotive painting, combustion, gasification, agriculture and food processing of granular products, surface coating and *etc.* (Lefebvre, 1989; Liu *et al.*, 2006; Mandato *et al.*, 2012).

1.4.1 Definition

Liquid transformation into a large quantity of small drops is defined as atomization process (Lefebvre, 1980). The result of this phenomenon generates a high relative speed between the liquid and the surrounding gas. Atomization process provides a very high evaporation rates by increasing the surface to mass ratio in the liquid phase (Hede, Bach and Jensen, 2008). In this process, increase in relative speed decreases the frictional forces which generates droplets with smaller median diameters (Hede, Bach and Jensen, 2008).

Conversion of liquid into droplets depends on different parameters such as liquid physiochemical characteristics and nature of nozzle which has a large influence on spray quality (Mandato *et al.*, 2012). The physiochemical properties of liquid are influenced by the

¹ Congealing is the transition of a melt from a soft or fluid state to a rigid or solid state by cooling (http://www.niroinc.com/food_chemical/spray_cooling_congealing.asp) (consulted on 12/Aug/2012)

parameters such as surface tension, density and viscosity. For example, the increase in liquid density causes the increase in droplet size. Unfortunately, it is not a simple correlation between liquid characteristics and droplet size and this problem exists as a result of dependent variations of parameters such as viscosity and surface tension.

1.4.2 Mechanism of atomization

Despite of difficulties existence to understand and model the atomization process, the atomization occurs simply by creating a high relative velocity between the liquid and the surrounding gas. (Hede, Bach and Jensen, 2008; Lefebvre, 1980).

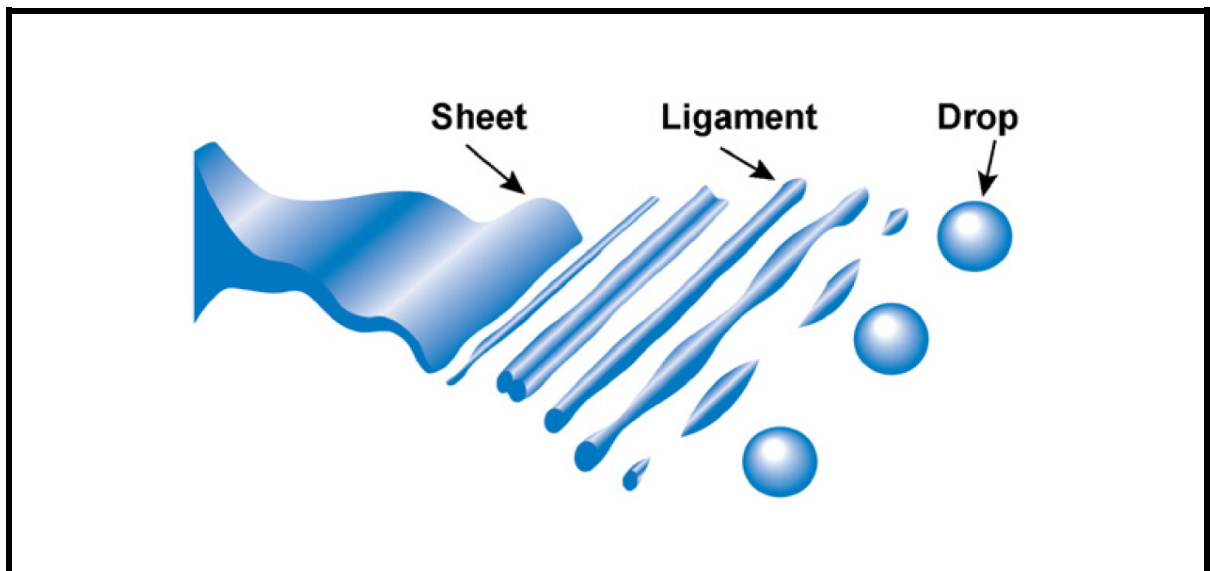


Figure 1.2 Atomization mechanism (Hede, Bach and Jensen, 2008)

Figure 1.2 shows the atomization mechanism. This process is performed during the following steps:

- 1) The increase in velocity of air or gas. This phase occurs before the contact between the gas and the unstable thin sheet of liquid which forms inside the nozzle. (Lefebvre, 1989).
- 2) The penetration of high speed gas into the low velocity liquid. This phase disintegrates the liquid into spray droplets due to creation of high frictional forces.



- 3) Providing the instability and the turbulence in fluid due to existence of disintegrated liquid accompanying the gas. In this phase, the atomization process is complete by breaking the liquid drops into tiny droplets (Hede, Bach and Jensen, 2008).

1.4.3 Theoretical and experimental studies (Theories)

Different theoretical and experimental studies carried out by Rayleigh (Strutt, 1879), Weber (Weber, 1931) and Castleman (Castleman, 1932) to understand the mechanism of atomization (Lefebvre, 1980). Rayleigh studied the atomization mechanism (see Figure 1.3) by preparing a laminar jet distribution through a circular orifice with initial jet diameter "d". He supposed that small instabilities which cause the breakup are increased when the perturbation increases rapidly at the wavelength equal to $4.51d$. After disintegration, the cylinder of length $4.51d$ becomes a spherical drop, as:

$$4.51d \times \left(\frac{\pi}{4}\right) d^2 = \left(\frac{\pi}{6}\right) D^3 \quad (1.1)$$

finally, the drop diameter, D , is:

$$D = 1.89d \quad (1.2)$$

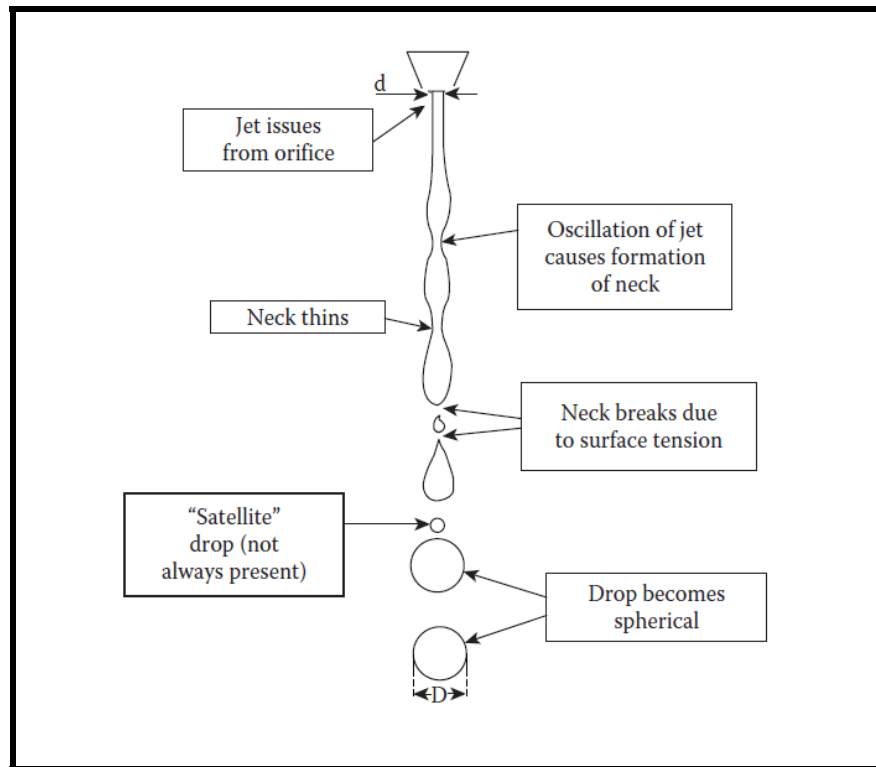


Figure 1.3 Rayleigh Atomization Mechanism (Lightfoot, 2007)

In the Rayleigh's analysis the viscosity and the influence of the surrounding air are not considered which is the inconvenience of his investigation (Lefebvre, 1989). Weber developed the Rayleigh's studies and in his analysis considered the effects of air resistance on drops which are being created during jet disintegration. In this case, he studied the influences of lower and higher relative velocities. He could show that in relatively low (zero) velocities, the wavelength has almost the same value which had been obtained by Rayleigh but the increase in relative velocity to 15 m/s reduced the λ_{opt} to $2.8d$ where the drop diameter became $1.6d$. This analysis showed that the optimum wavelength for jet breakup is influenced by relative velocity between the liquid jet and surrounding gas (Lefebvre, 1989). According to the Weber's studies, an increase in viscosity leads to an increase in the optimum wavelength of jet breakup. Castleman showed that in presence of air friction, the influence of relative movement between the air and the outer layer of spray is the most important factor for breaking the liquid surfaces and producing the unstable ligaments (Lefebvre, 1980).

1.4.4 Atomization Summary

Based on given explanations and depends on the relative velocity between liquid and surrounding air or gas, different modes of atomization are divided into four categories (Lefebvre, 1989):

1. At lower velocities, the spray is disintegrated into droplets with uniform sizes due to the increase in axisymmetric vibrations and the spray surface. This mechanism is explained by Rayleigh theory. Due to this theory the outlet drop diameter is approximately two times greater than initial spray diameter. According to Rayleigh's investigations, the increase in liquid viscosity and spray velocity, increases and decreases drop size respectively;
2. At higher velocities, the disintegration is due to the entire spray vibration with respect to the spray axis. This mode occurs on a relatively narrow range of speeds;
3. The interaction between liquid and high velocity surrounding air increases the instability of small waves on the spray surface which disintegrates the ligaments into drops with smaller diameters;
4. Atomization is completed by producing the droplets with diameters significantly smaller than initial spray diameter which is occurred at very high relative velocities and after a short distance from the discharge orifice.

1.5 Atomizers and pulverization

1.5.1 Introduction

Due to the importance of the atomization process in industrial areas, it is crucial to classify the different types of atomizers. This classification is according to the parameters such as geometry, usage environment and related forces or velocities and is not founded on atomization mechanisms (Lightfoot, 2007). In this part of the literature review, the different types of atomizers will be presented.

1.5.2 Different lubrication systems

According to the manufacturing process, there are internal and external lubrication systems. The main task of an MQL system is to supply the appropriate lubricants on the cutting edge (contact point of the tool).

- **Internal lubrication systems**

The best way of lubrication is the direct injection of lubricant on the cutting zone. In this method, the lubricant is continually available at the critical points during the entire cutting process. The using of MQCL with internal feeds enables us to achieve this idea. In the internal lubrication system, the lubricant arrives to the cutting zone through the spindle, tool revolver and the inner cooling channels of the tool (Unfallversicherung, 2010). This system is useful for very deep hole drilling at very high cutting speeds (table 1.1). In this way, we will have the maximum amount of lubricant during drilling process. This system needs special tools and appropriate machines but this equipment increase the process cost. There are two devices (one-channel and two-channel) which are used for internal lubrication (see Figure 1.4). These devices are different in term of required channels in the rotating chuck, spindles and the place of aerosol production. The internal lubrication systems do not need to adjust the feed nozzle. Therefore, there is not huge amount of loss due to dispersion (Unfallversicherung, 2010).

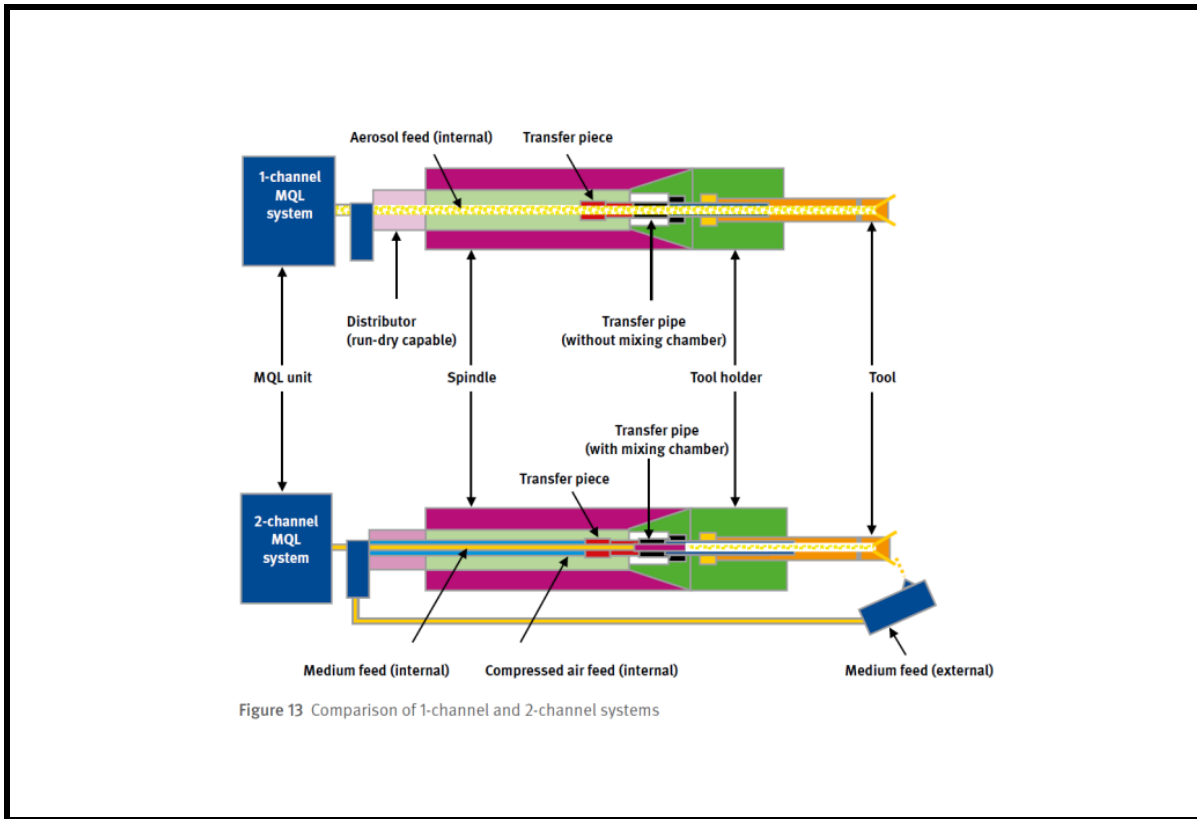


Figure 1.4 One-channel and Two-channel systems (Unfallversicherung, 2010)

❖ One and two channel devices

In the one-channel systems (see Figure 1.5) , there is a tank where the aerosol is generated with the aid of compressed air, and it arrives to tool through the rotary chuck, spindle and tool holder (Unfallversicherung, 2010). In the two-channel devices (see Figure 1.6); the aerosol production is performed in the mixture embedded in a pipe nozzle. Air and oil are fed separately using two channels through the tool spindle to the tool holder. The lubricant is transported via a high speed valve, where the metering process is done. Therefore the optimal quantity of the lubricant will be sent to the two channel rotary chuck. The transported lubricant and the supplied air are mixed in the mixing chamber of the pipe nozzle.

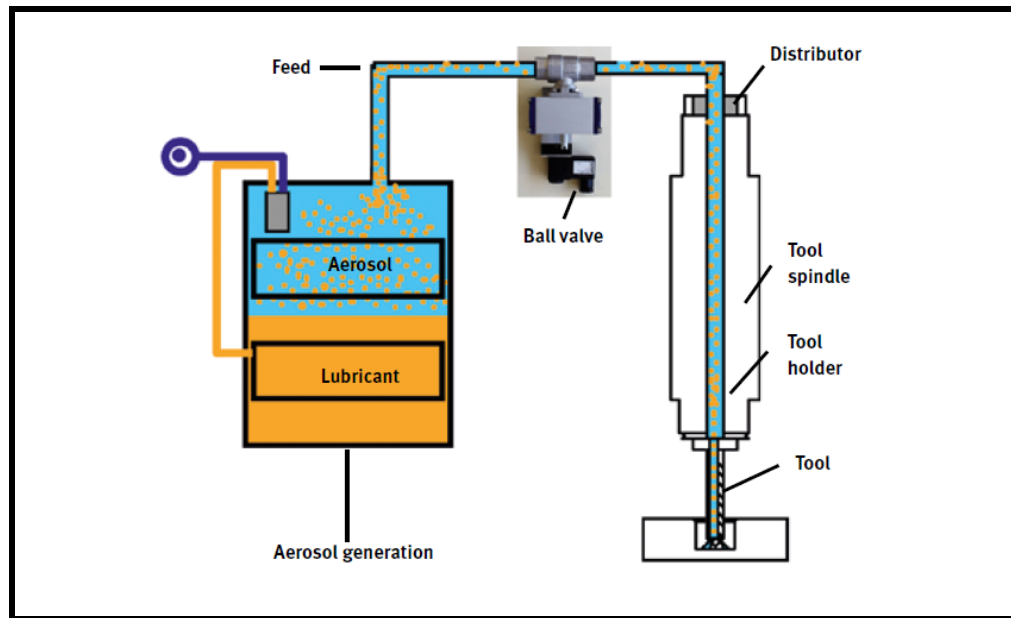


Figure 1.5 One-channel system for internal feed (Unfallversicherung, 2010)

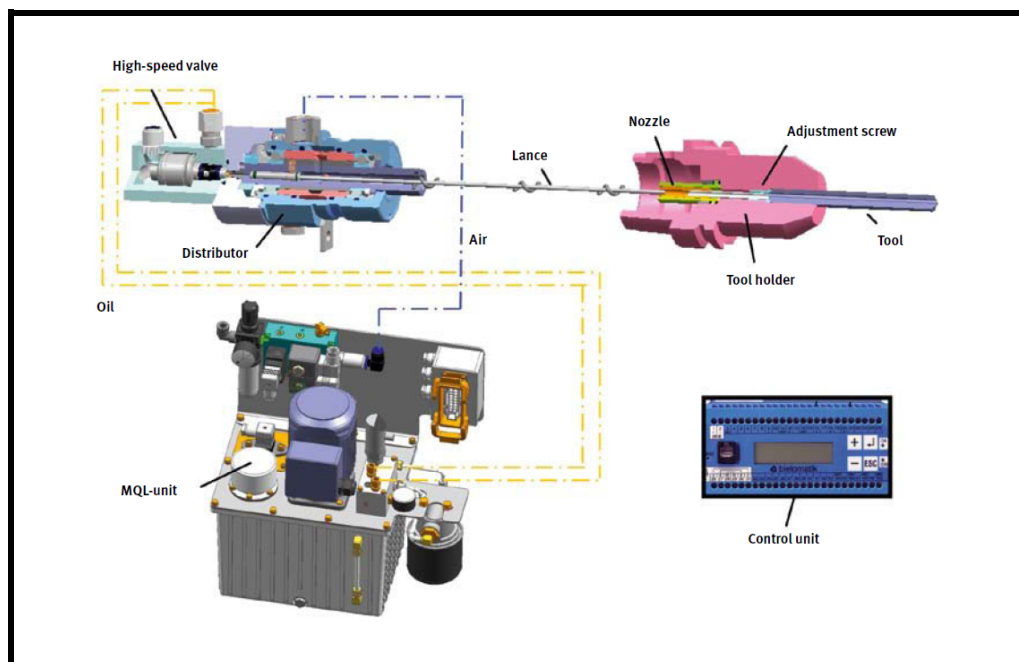


Figure 1.6 Two-channel system (Unfallversicherung, 2010)

- **External lubrication systems**

There are two types of external lubrication systems which transport the atomised lubricant and air to near the contact point. This system is appropriate for simple machining processes as well as turning, drilling, sawing and milling (table 1.1).

These systems work without using the special tools. The huge amount of loss due the dispersion and necessity of nozzle adjustment manually are the disadvantageous of this type of lubrication system.

In these systems, using the special tools is not necessary and the process cost is less than internal systems. But unlike internal systems, in external lubrication, there is a lot of loss due to the dispersion and the operator must adjust the nozzles manually.

- ❖ **Devices with metering pump² and with pressure tank**

In the metering pump devices (see Figure 1.7); a pneumatic micro-pump is responsible for the lubricant transportation. The controlling and regulation of the lubricant dosage is done by means of the stroke and frequency of the pump plunger.

In the pressure tank devices (see Figure 1.8); the lubricant will be exited with the pressure of the pressurized tank. By using the throttle valve and the supply pressure settings, metering will be done. Adjustments of tank pressure, atomisation of air and oil quantity separately, guarantee the good performance of this system (Unfallversicherung, 2010). Table 1.2 shows the comparison of devices with metering pump & pressure tank.

² A metering pump transfers an accurate volume of liquid during a specified time to produce a precise flow rate. (www.wikipedia.org/wiki/Metering_pump) *consulted on 10/June/2012*

Table 1.2 The comparison between metering pump and pressure tank
(Unfallversicherung, 2010)

	Metering pump	Pressure tank
Advantages	Exact dosage volume settings	Uniform lubrication stream
	Exact modular design	Lack of moving parts
	Possibility to install any number of pump elements	Lack of wear
Disadvantages	Pulsating lubricant stream	Precise adjustment of oil dosage volume is limited on some degrees
	Wear in moving parts	number of outputs is limited



Figure 1.7 Device with metering pump (Unfallversicherung, 2010)



Figure 1.8 Device with pressure tank (Unfallversicherung, 2010)

1.5.3 Nozzle performance properties

The performance of a nozzle will be presented by different nozzle characteristics which are described briefly as follows:

1. The injected liquid flow related on the nozzle feed pressure;
2. The injection angle of the spray produced by nozzle;
3. The ratio between the energy of the spray and the energy used by the nozzle;
4. The uniformity of the injected flow;
5. The droplet size distribution.

1.5.4 Different types of atomizers

In different industrial applications, the atomization processes of large number of nozzles are based on the capillary³ and aerodynamic⁴ break up. Besides these atomizers, there are others such as electro-spraying, plasma spraying and etc., which use the diverse types of energy to apply in atomization processes (Batarseh, 2009). The different types of atomizers used in most industrial applications will be described in following passages.

- **Pressure atomizers**

As explained previously, one of the important factors related to the atomization is to achieve the high relative velocity between the liquid and the surrounding air or gas. To approach this relative velocity, the pressure atomizers are used to convert the pressure into the required kinetic energy (Lefebvre, 1999). Various types of such atomizer, such as plain-orifice atomizers, simplex atomizers and the dual-orifice atomizers are described as follows.

- ❖ **Plain orifice atomizers**

The easiest technique to atomize a liquid is to inject it through a small circular hole. This system is occurred in the plain orifice atomizers. The liquid disintegration into small droplets is performed by injection at high velocity. The necessary velocity will be obtained by increasing the liquid pressure to the ambient gas pressure (almost 150 kPa). The increase in liquid injection pressure leads to increase in liquid jet turbulence and aerodynamic forces applied by the surrounding medium (Lefebvre, 1999). An illustration of this type of atomizer is shown in Figure 1.9.

3 Capillary action is a consequence of the liquid surface tension when liquid moves through thin tubes and capillary break up is a result of liquid ejection from a nozzle at high velocity and under the high injection pressure. (www.wikipedia.com) (consulted on 12/Aug.2012)

4 Aerodynamic breakup is due to the shear stresses at the liquid-gas interface. (www.wikipedia.com) (consulted on 12/Aug.2012)

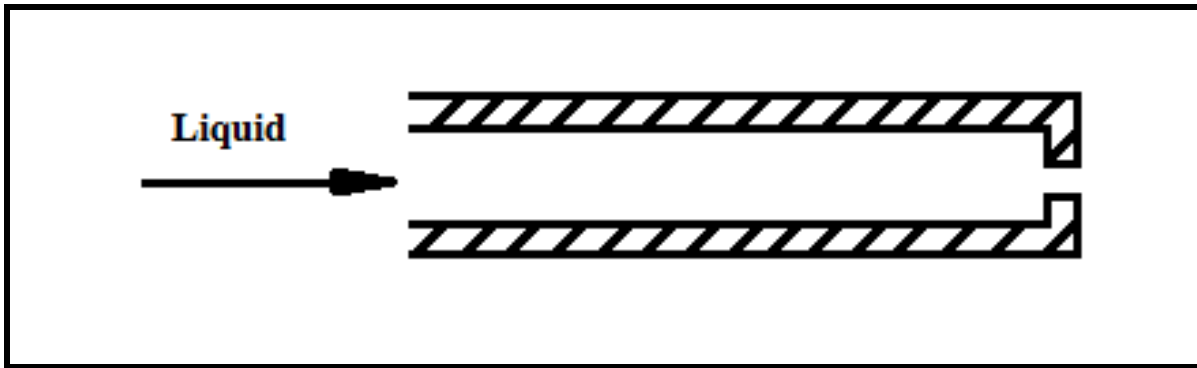


Figure 1.9 Plain orifice atomizer (Lefebvre, 1999)

Providing the narrow sprays with cone angles is one of the disadvantages of plain orifice atomizers.

❖ Simplex atomizers

The simplex atomizers function is based on liquid swirling motion accompanying the centrifugal forces. These types of the atomizers are used to achieve the wider cone angles compared with the plain orifice atomizers. As it is shown in Figure 1.10, liquid being injected into a swirl chamber passes through the tangential ports which are used to create a higher angular velocity and the air-cored vortex. At final orifice, the liquid which is under axial and radial forces will be injected as a hollow conical sheet (Lefebvre, 1999).

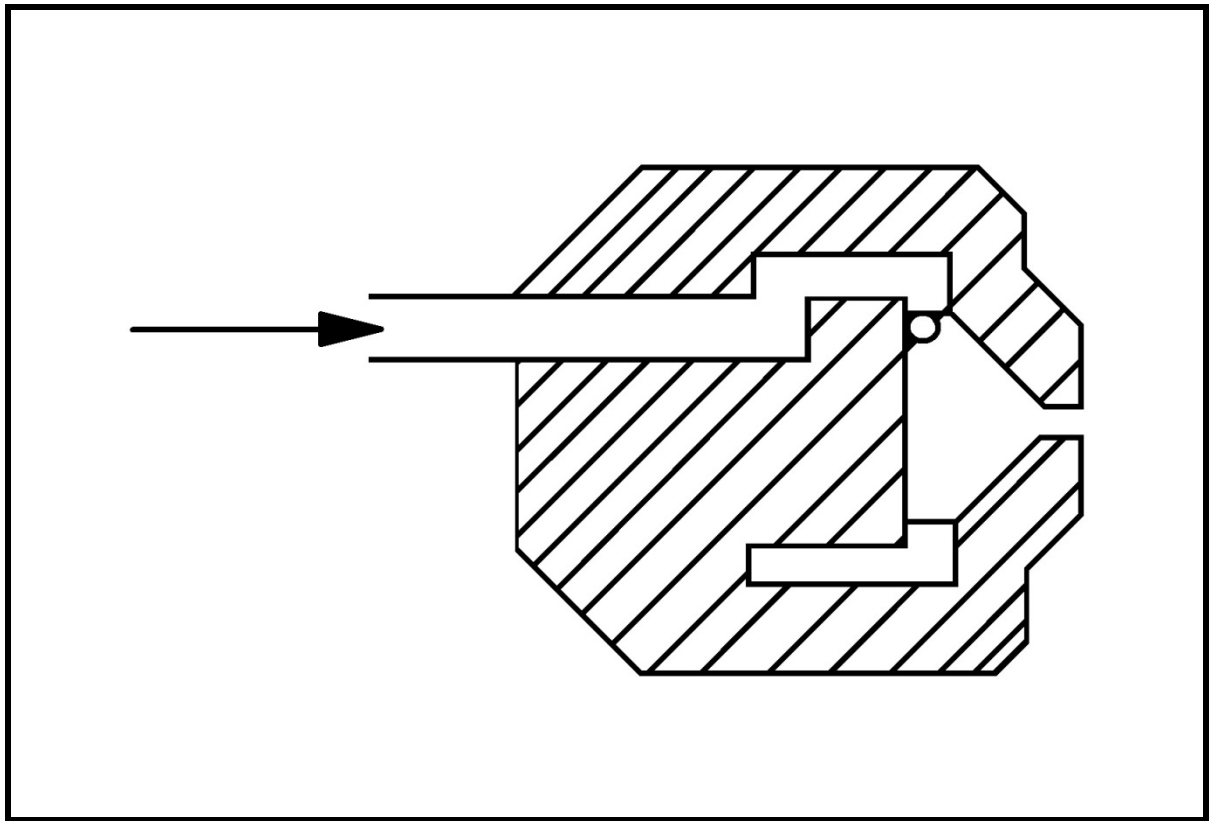


Figure 1.10 Simplex atomizer1(Lefebvre, 1999)

❖ Dual orifice atomizers

The dual orifice atomizers as shown in Figure 1.11 have two parts as primary or pilot nozzle and secondary or main nozzle. This type of atomizer could be compared with two simplex nozzles which are fitted concentrically. Depending on liquid quantity supplied in this nozzle, two different functions will be performed in this type of atomizer (Lefebvre, 1999).

- Liquid with low quantity: In this situation, the liquid flows through the small port of the primary nozzle where the liquid pressure will be increased. Due to the high pressure, the quality of liquid atomization will be improved;
- Liquid with high quantity: The increase in liquid amount and therefore the increase of the liquid pressure allow the port to open and enter the secondary nozzle. The atomization quality will be more and improves by increasing the amount of liquid and its pressure.

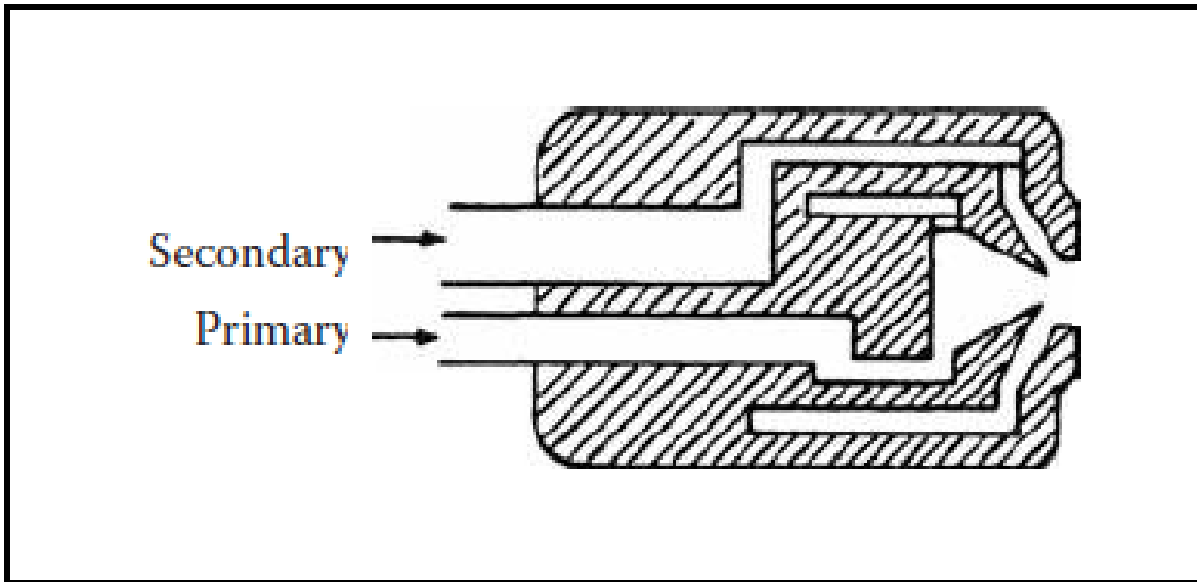


Figure 1.11 Dual orifice atomizer (Lefebvre, 1999)

❖ Spill return atomizers

The main difference between this atomizer and simplex one is the existence of a passage in the rear wall of the swirl chamber which allows the extra liquid to return back into the supplier tank (Lefebvre, 1999), (see Figure 1.12).

The advantages of this atomizer are as follow (Lefebvre, 1999):

- Providing a liquid injection at high pressure even at the lowest liquid flow rate;
- Excellent atomization quality;
- Absence of moving parts and independency from plugging by contaminations in the fuel.

The disadvantages of this atomizer are as follow (Lefebvre, 1999):

- High fuel-pump power necessity;
- Large variation in spray cone angle with the change in the fuel flow rate;
- Complexity of the flow rate metering;
- Need for a larger-capacity pump to create the high recirculation flow.

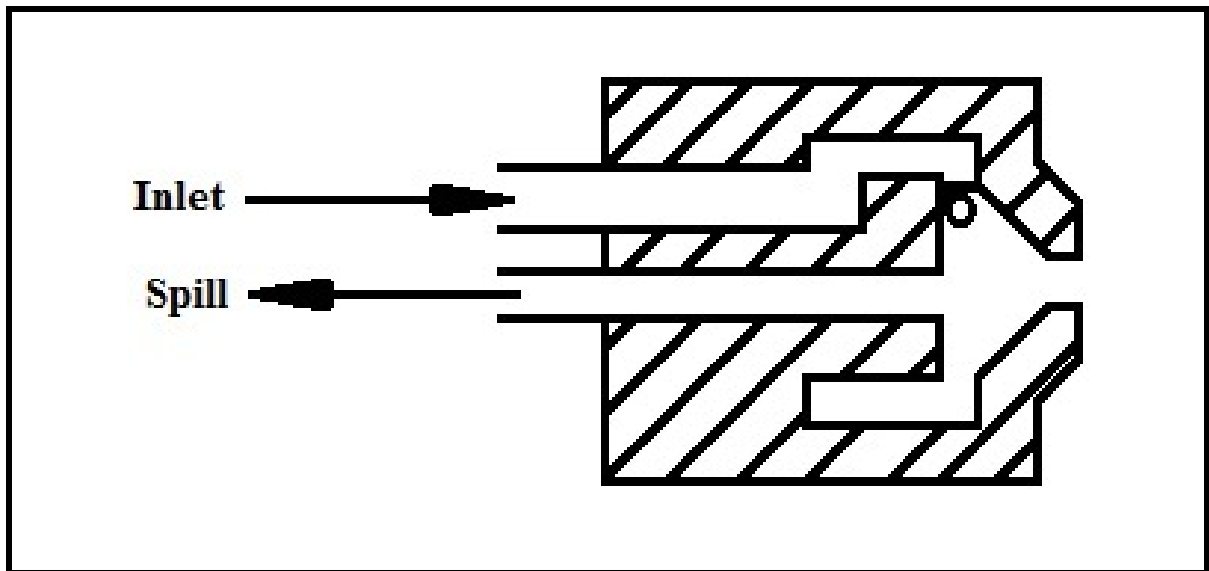


Figure 1.12 Spill return atomizers (Lefebvre, 1999)

- **Rotary atomizers**

The best example of the rotary atomizer is slinger system which is used in combination with a radial-annular combustion chamber. In this type of the atomizer, the low pressure liquid feeds into a hollow main shaft and gets injected radially through the shaft holes. The Slinger system fabricated by Turbomeca, the French company, is shown in Figure 1.13. The main advantages and disadvantages of this system are described as follow (Lefebvre, 1999):

Advantages:

- Simple system with low cost;
- Low pressure fuel pump necessity;
- Satisfactory atomization quality;
- Less impact of the viscosity and ability to use different types of liquid consequently.

Disadvantages:

- Slow response to the change in liquid flow due to the long flow path;
- Wall cooling especially when it is applied into engines with high pressure ratio.

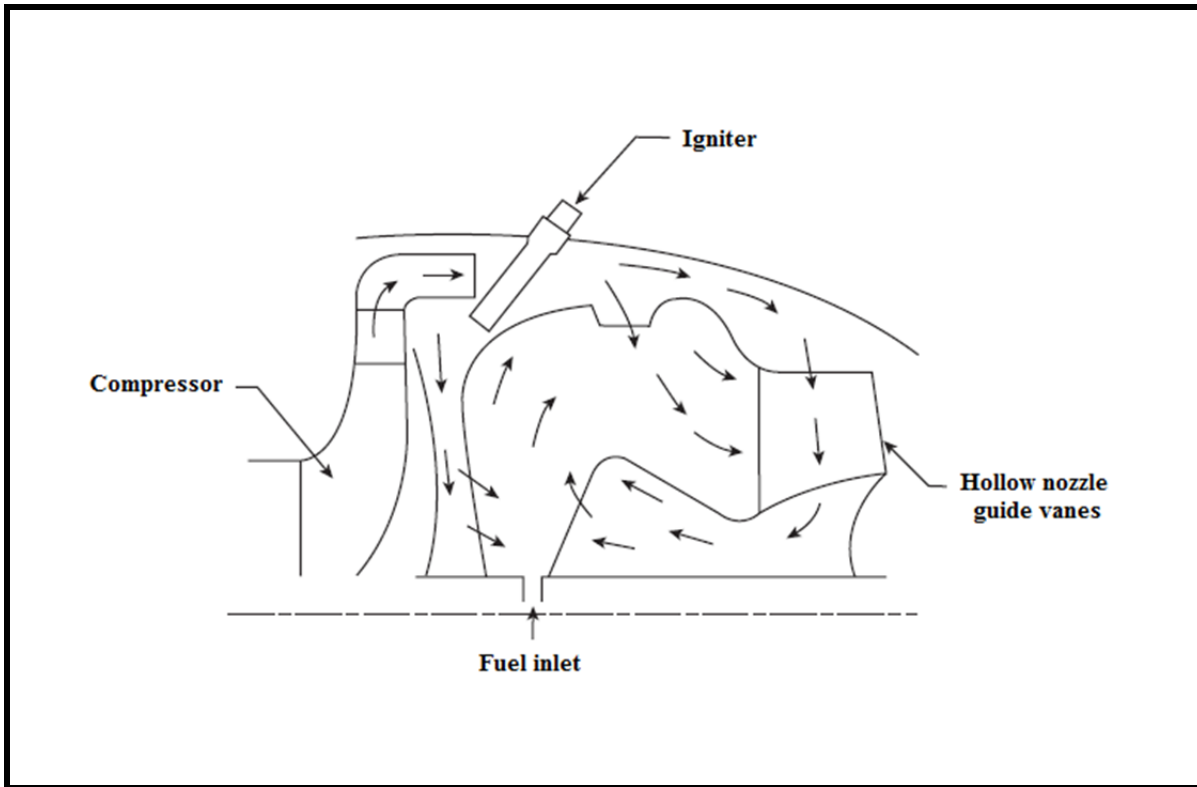


Figure 1.13 Turbomeca slinger system (Lefebvre, 1999)

- **Air assist atomizers**

There are two different types of the air assist atomizers such as internal-mixing and external-mixing configuration which are shown in Figures 1.14 – 15. These two types are very useful for atomizing the high viscosity liquids (Lefebvre, 1999).

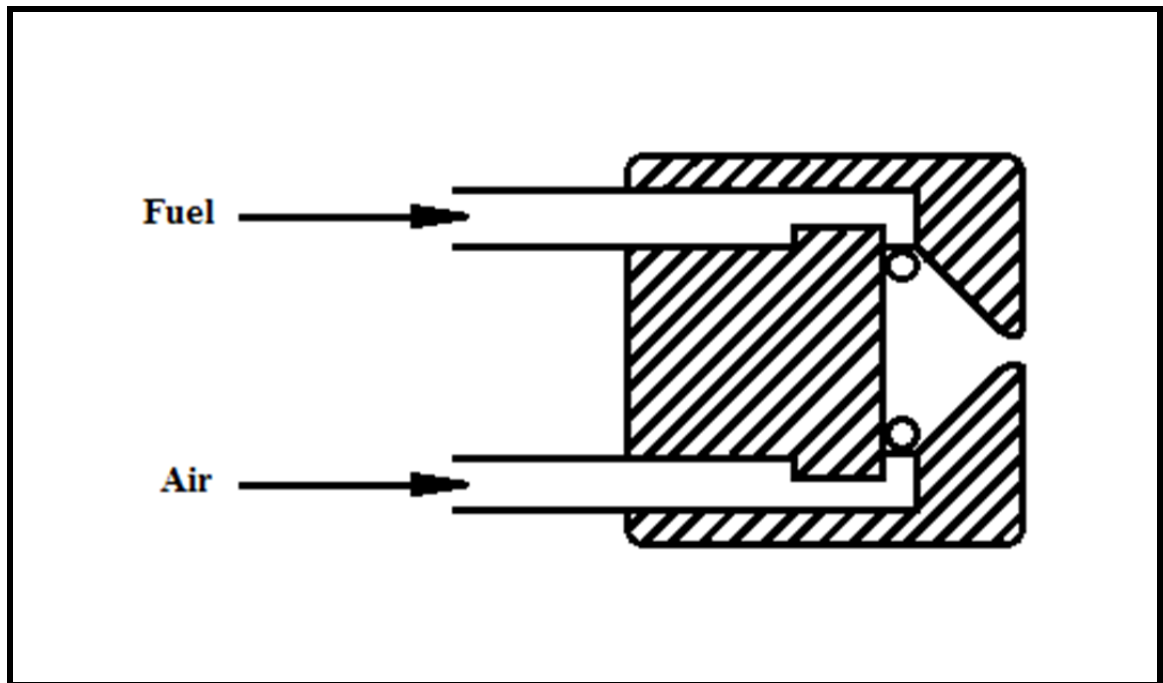


Figure 1.14 Internal-mixing air assist atomizers (Lefebvre, 1999)

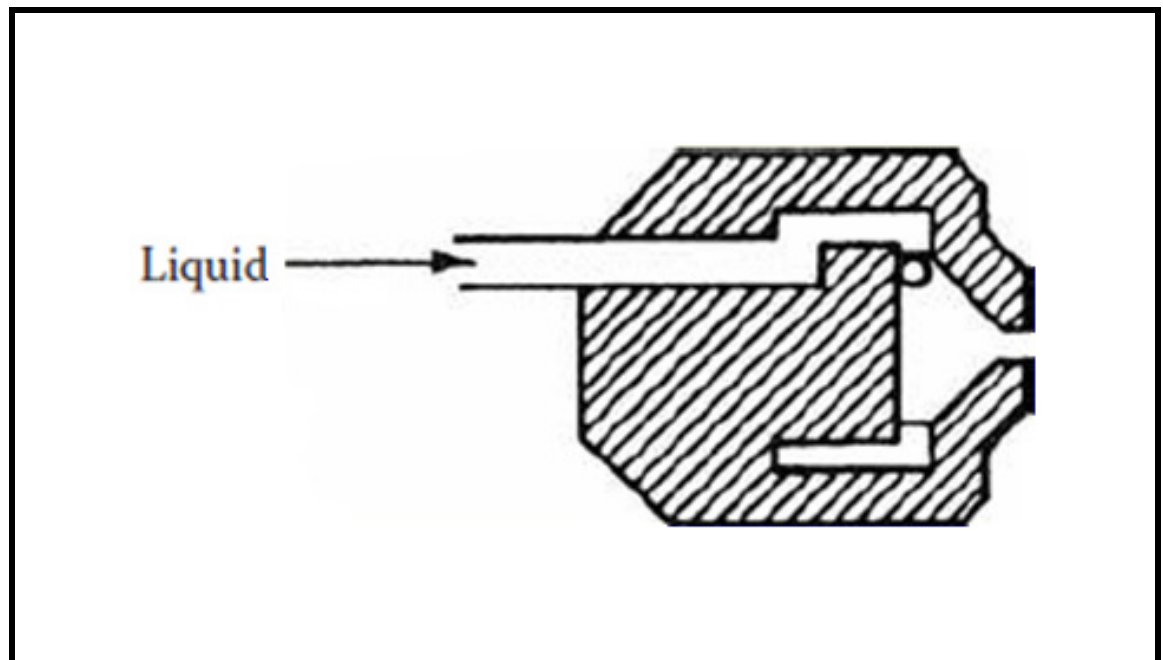


Figure 1.15 External-mixing air assist atomizers (Lefebvre, 1999)

The difference between the internal and the external mixing air assist atomizers is in the location of the air and the liquid mixture. In internal-mixing nozzle, the liquid and the air will be mixed before exiting through orifice.

In external-mixing atomizer the air and the liquid will be mixed at the discharge orifice. The main advantage of the external-mixing is the absence of the back pressure. This type of atomizer needs a higher air flow rate to approach the same atomization degree as that of the internal-mixing nozzle which is one of its inconveniences (Lefebvre, 1999).

- **Airblast atomizers**

The main function of the airblast atomizers is based on using the kinetic energy to transform the initial liquid-phase into the ligaments and droplets. This principal is the same as the one that is used in the air assist atomizers while the most important differences between these two nozzles are the air quantity employed and their atomizing velocity (Batarseh, 2009; Lefebvre, 1999).

The airblast nozzles produce the smaller sprays and they need the low pressure fuel pumps. This nozzle is very useful especially for high pressure combustion systems (Lefebvre, 1999) whereas the poor atomization associated with the low air velocity is the weak point of the airblast atomizers (Batarseh, 2009). Three types of the airblast atomizers which are described as follow are the plain-jet, the prefilming and the piloted airblast atomizers shown in Figure 1.16.

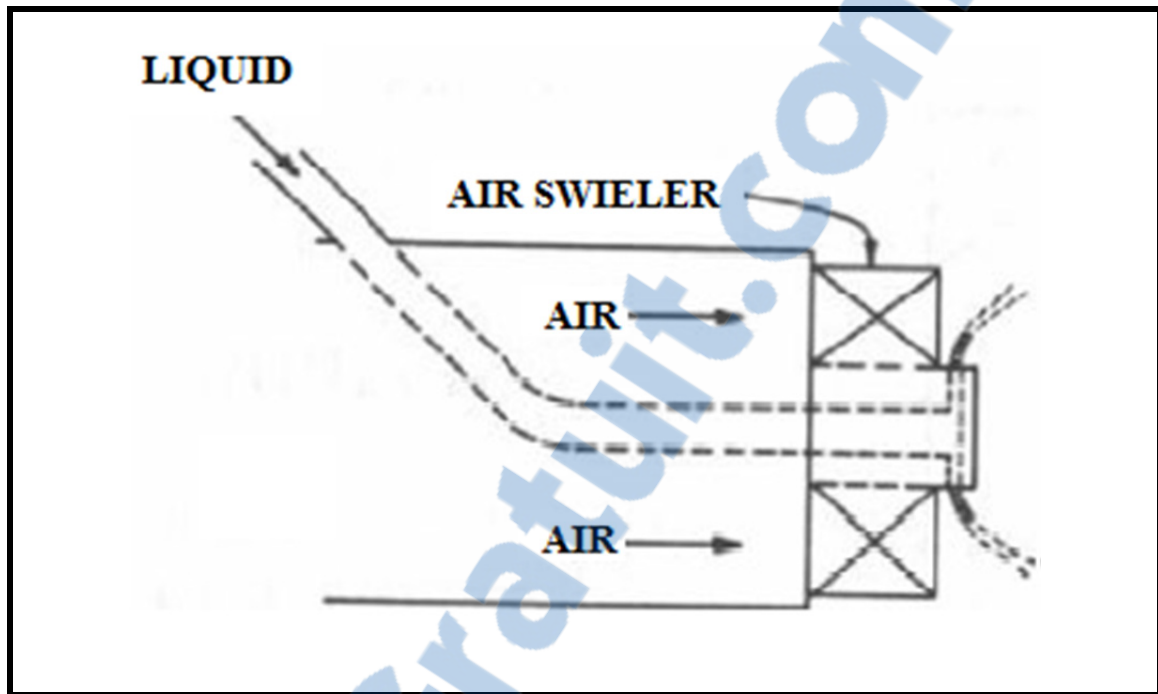


Figure 1.16(a) Plain-jet atomizer

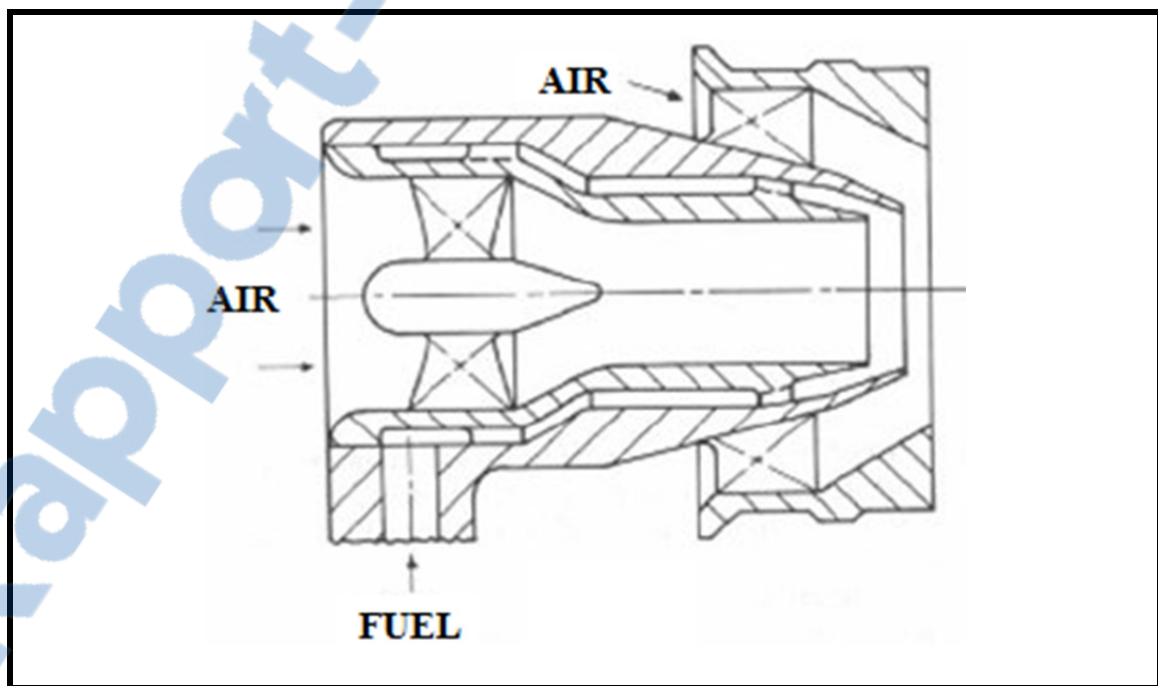


Figure 1.16(b) Prefilming

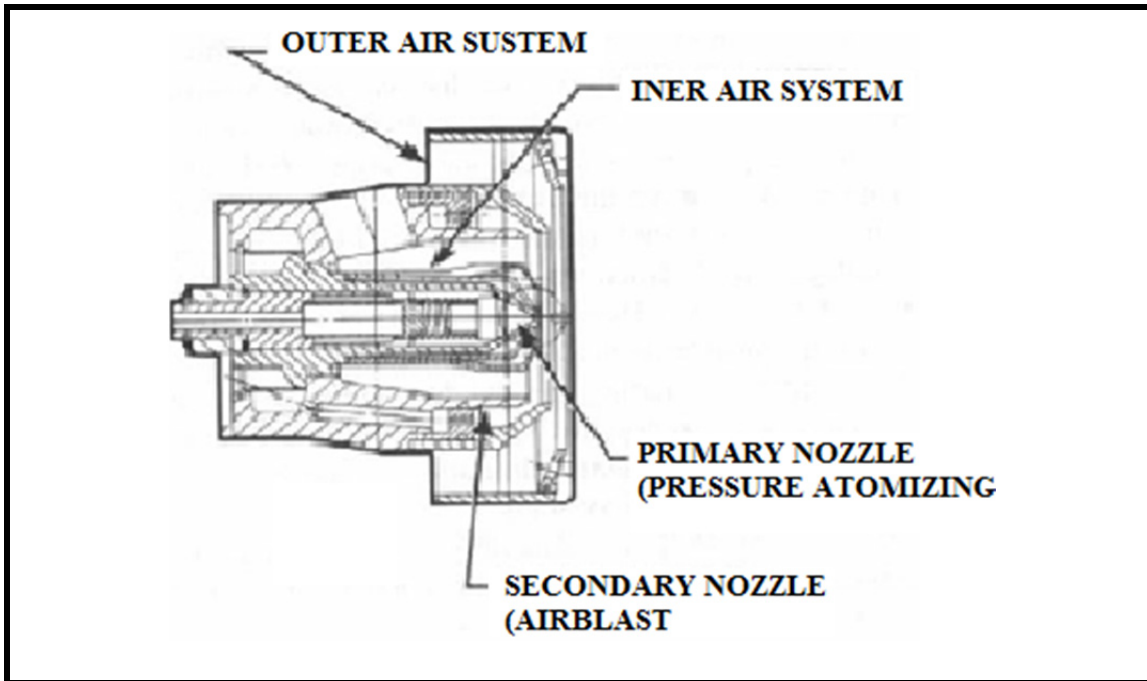


Figure 1.16(c) Piloted atomizer

Figure 1.16 Different types of the airblast atomizers (Lefebvre, 1999)

❖ Plain-jet airblast atomizers

The plain-jet airblast nozzle is the simplest form of airblast atomizers. Its function is based on the injection of a round jet of liquid along the axis of a generally co-flowing round jet of air (Lefebvre, 1999).

This type of the atomizer (see Figure 1.17) is very useful to study the influences of the air and the liquid characteristics on the mean drop size such as Nukiyama and Tanasawa (1939) investigations which will be described in part 1.6 of this chapter.

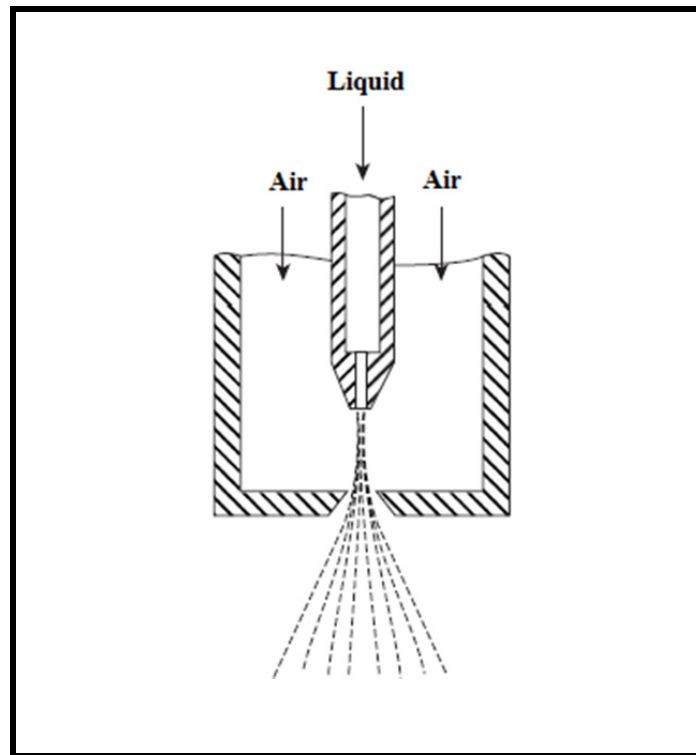


Figure 1.17 Plain-jet airblast atomizer (Lefebvre, 1999)

❖ Prefilming airblast atomizers

The airblast atomizers are usually used to increase the supplied air in order to increase the atomized liquid phase (Batarseh, 2009). Nowadays, in different industrial applications, the pre-filming airblast atomizers are the most useful nozzles in which the liquid is firstly spread out into a thin continuous sheet and then will be subjected to the atomizing action of the high-velocity air (Lefebvre, 1999). This type of atomizer is shown in Figure 1.18.



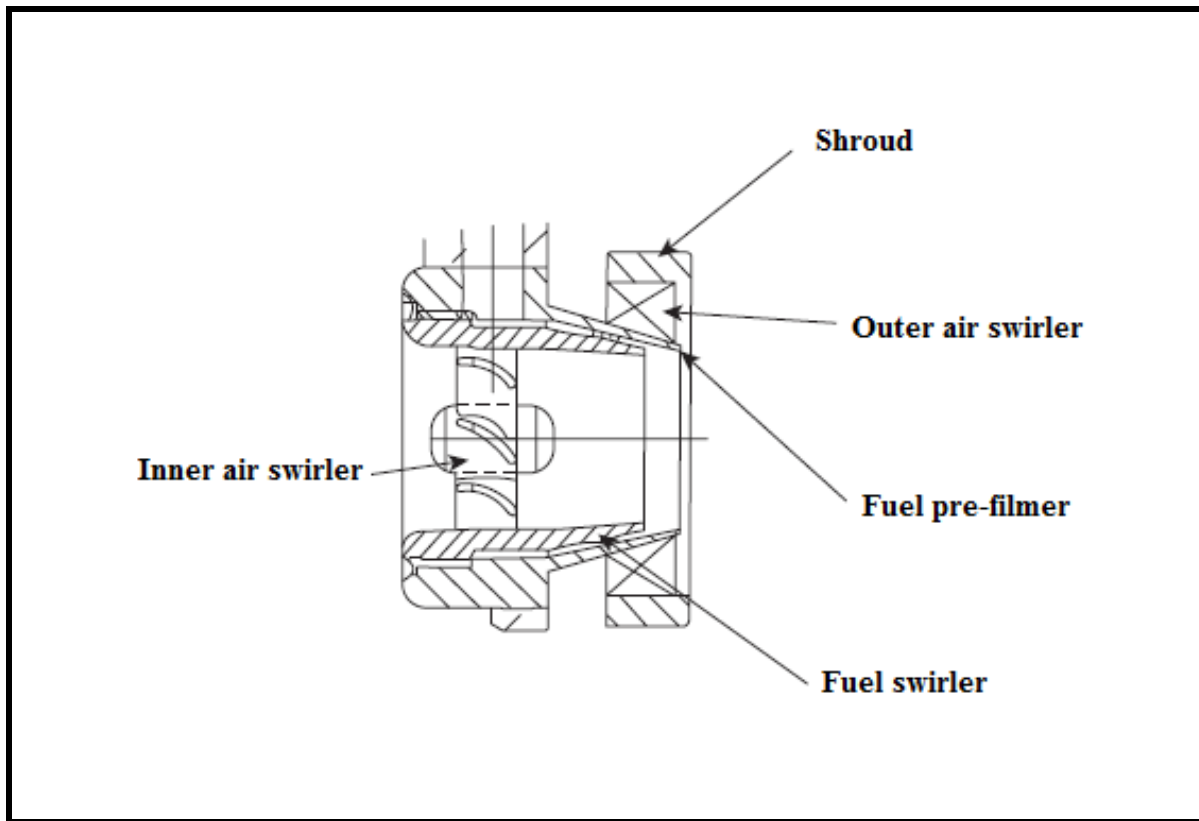


Figure 1.18 Pre-filming airblast atomizer (Lefebvre, 1999)

Due to use of pre-filmer nozzle structure, the liquid phase is pushed by a pressure swirl atomizer. As a result the gas phase will be interacted with the liquid film inside and outside the atomizer (Batareseh, 2009). The pre-filmer function is shown in Figure 1.19.

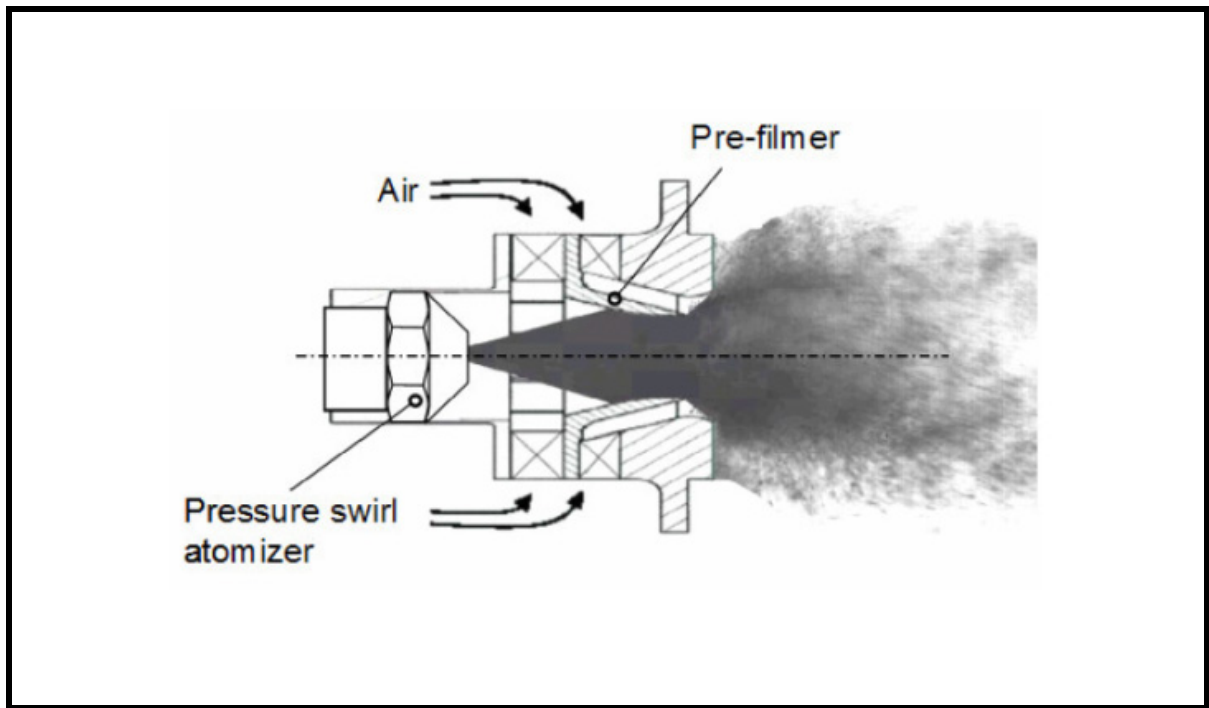


Figure 1.19 Prefilmer function in airblast atomizer (Batarseh, 2009)

❖ Piloted airblast atomizers

The main objective of piloted airblast atomizer (see Figure 1.20) is to increase the atomization performance when it is carried out using the low air velocity. This type of airblast nozzles is made by a prefilming airblast atomizer with a simplex pressure swirl nozzle which is installed on its centerline. Because of this structure, the piloted airblast atomizer is known as a hybrid injector (Lefebvre, 1999).

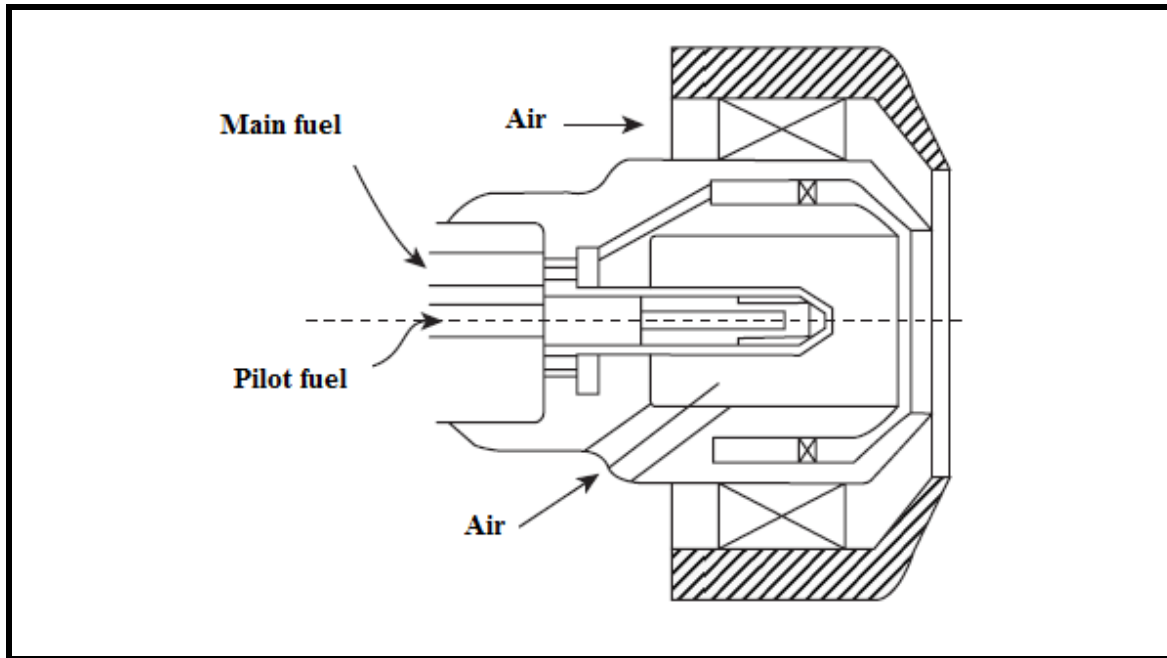


Figure 1.20 Piloted airblast atomizer (Lefebvre, 1999)

1.5.5 Common features of different twin-fluid atomizers

The various nozzles previously described are known as twin-fluid atomizers. The principal function of all twin-fluid atomizers is using the air as a first force in order to increase the atomization.

In these atomizers the injection of the low velocity air makes the bubbles which create a two-phase bubbly flow at the discharge orifice. The rapid expansion of the air bubbles emerged from the nozzle will break the liquid sheet up into small droplets (Lefebvre, 1999).

1.6 Prediction of mean drop size and drop size distribution

1.6.1 Introduction

Particle size measurement is become very important in research and development as well as in industrial applications (Lee Black, McQuay and Bonin, 1996). The increasing in pollutant emissions and the low price of residual fuel oils encourage researchers, scientists and engineers to investigate the droplet size distribution in the fuel nozzle sprays (Semião, Andrade and Carvalho, 1996). In engineering systems, the droplet size distribution is a

fundamental parameter to analyse the transport of the mass, momentum, and heat (Liu *et al.*, 2006). According to the atomization description, this process is complicated and because of its random nature, most of the practical atomizers do not produce sprays of homogeneous droplet size at any given operating conditions. Therefore, it is crucial to understand the investigation methods of the droplet size (Liu *et al.*, 2006).

1.6.2 Definition

All laser-based methods of the particle sizing are able to measure the spherical particles. Consequently, all the measured particles have the equivalent diameters if they are considered spherical (Lee Black, McQuay and Bonin, 1996).

All the particle size distribution functions are generally in relation to different aspects of flow such as volume or concentration. The basic mathematical function of the particle size distribution is a function of $f(d_i)$ which is the value of the particle size distribution function at the discrete values of the particle size, represented by d_i in equation 1.3 (Lee Black, McQuay and Bonin, 1996).

$$(d_{jk})_{j-k} = \frac{\sum_n d_i^j f(d_i)}{\sum_n d_i^k f(d_i)} \quad (1.3)$$

There are different definitions of mean particle diameters such as arithmetic mean, the surface mean, the volume mean and the Sauter mean, *etc.* Each one is known with a symbol like d_{10} , d_{20} , d_{30} , d_{32} , d_{43} , *etc.* which are used generally in equation 1.3. These symbols are used in the phenomena under the investigations, for example, d_{32} is used in the combustion related fields and d_{43} is used in the field of the chemical kinetics (Lee Black, McQuay and Bonin, 1996). The different definitions of the mean drop size are explained in table 1.3.

Table 1.3 Definitions and descriptions of mean particle diameter
(Lee Black, McQuay and Bonin, 1996)

Symbol	j,k	Name	Description
d_{10}	1,0	Arithmetic mean diameter	Normal average particle diameter of the size distribution
d_{20}	2,0	Surface mean	Diameter of a sphere with the average surface area of the particles in the size distribution
d_{30}	3,0	Volume mean diameter	Diameter of a sphere with the average volume of the particles in the size distribution
d_{21}	2,1	Surface diameter	Diameter of a sphere having the surface area of the average particle size in the distribution
d_{31}	3,1	Volume diameter	Diameter of a sphere having the volume of the average particle size in the distribution
d_{32}	3,2	Sauter mean diameter	Diameter of a sphere with the equivalent surface to volume ratio as all the particles in the size distribution
d_{43}	4,3	Weight mean	Diameter of a sphere having the average weight of all the particles in the size distribution

Between all these definitions, the Sauter Mean Diameter (SMD) is used more than the others due to its relevance to the rate of the evaporation and combustion (Lefebvre, 1980). Several parameters such as atomizing fluid properties, nozzle design and operating conditions affect the Sauter Mean Diameter (Semião, Andrade and Carvalho, 1996). The general function of SMD is:

$$SMD = \frac{\sum_i^{N_i} n_i d_i^3}{\sum_i^{N_i} n_i d_i^2} \quad (1.4)$$

where d_i and n_i are the droplet diameter (for airblast atomization process) and the number of the droplets per unit volume in size class N_i respectively (Liu *et al.*, 2006).

1.6.3 The empirical correlations related on the mean drop diameter

The SMD prediction for different types of atomizers such as airblast and Pressure-jet atomizers is based on semi-empirical correlations obtained from experimental data and the physical and dimensional analysis of the atomizing process. All of these equations are proposed related on different factors such as nozzle design features and physical flow properties of the air and the liquid employed (Lefebvre, 1980; Semião, Andrade and Carvalho, 1996). In this section, several predictions of SMD related to airblast atomizers are presented.

- **Plain-jet airblast atomizers Investigations**

- ❖ **Nukiyama and Tanasawa**

The coaxial two-fluid airblast atomizers are applicable in different industrial applications such as gas turbines and liquid propellant rocket engines (Liu *et al.*, 2006). Seventy years ago, the first investigation on plain-jet airblast atomizers was performed by Nukiyama and Tanasawa, who obtained a drop size equation as a function of the injection parameters. The airblast atomizer that is used in this study is shown in Figure 1.21. The measurements of gasoline, water, oils and solutions of alcohol and glycerin atomization were conducted by the sample collections of the spray on the glass slides coated by oil.

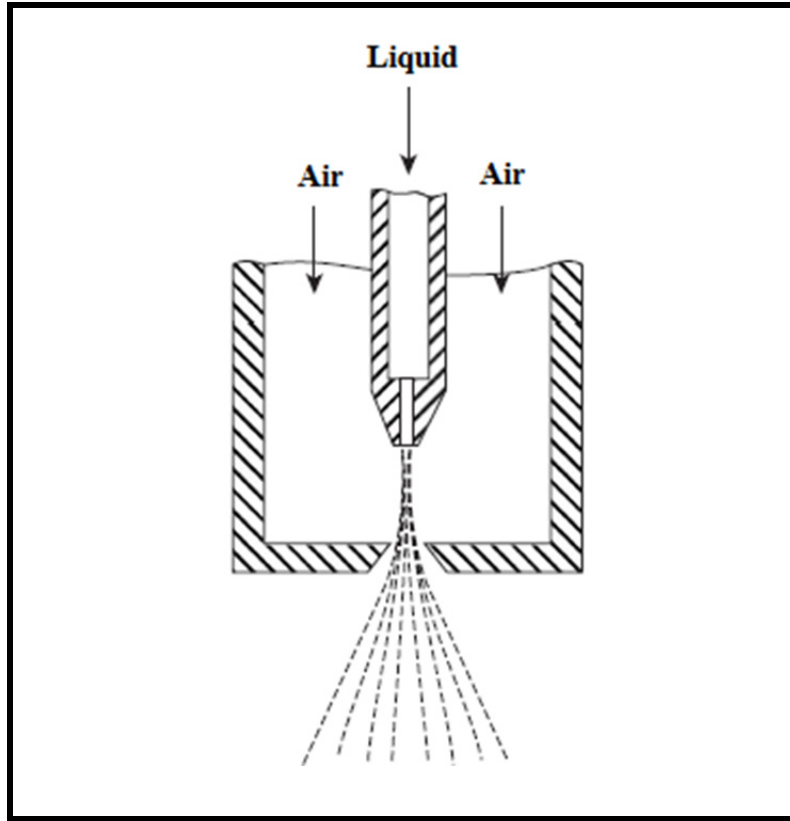


Figure 1.21 Nukiyama and Tanasawa plain-jet airblast atomizer
(Lefebvre, 1980; Liu *et al.*, 2006)

The analysis carried out by Nukiyama and Tanasawa led to the equation 1.5 for drop size in which the air density is kept constant (at the normal atmospheric value) during all experiments. This assumption is one of the major limitations of this equation because of the requirement of many combustion systems to operate over wide ranges of air pressure and temperature. Furthermore, the tests derived by Nukiyama and Tanasawa with different sizes and shapes of nozzles and orifices showed that these factors have almost no effect on mean drop size (Lefebvre, 1980; Liu *et al.*, 2006).

$$\text{SMD} = \frac{0.585}{U_R} \left(\frac{\sigma_L}{\rho_L} \right)^{0.5} + 53 \left(\frac{\mu_L^2}{\sigma_L \rho_L} \right)^{0.225} \left(\frac{Q_L}{Q_A} \right)^{1.5} \quad (1.5)$$

❖ Gretzinger and Marshall

Gretzinger and Marshall (Gretzinger and Marshall, 2004) were interested in the study of drop size distribution using two types of airblast atomizers such as converging and impingement nozzles. In converging nozzles which were used by Nukiyama and Tanasawa, the liquid will be contacted with the atomizing airstream at the throat of the air nozzle while in impingement nozzles, a central circular air tube is surrounded by an annular liquid channel (Lefebvre, 1980). The equations obtained by Gretzinger and Marshall are shown as follows (Equations 1.6 and 1.7 for converge and impingement nozzles respectively).

$$\text{MMD} = 2.6 \times 10^{-3} \left(\frac{\dot{m}_L}{\dot{m}_A} \right) \left(\frac{\mu_A}{\rho_A U_{AL}} \right)^{0.4} \quad (1.6)$$

$$\text{MMD} = 1.22 \times 10^{-4} \left(\frac{\dot{m}_L}{\dot{m}_A} \right)^{0.6} \left(\frac{\mu_A}{\rho_A U_{AL}} \right)^{0.15} \quad (1.7)$$

where MMD is Mass Mean Diameter (m) which is the drop diameter related to the 50% point on the cumulative mass distribution curve (Lefebvre, 1980).

Despite the lack of the direct study of the air viscosity which affects the mean drop size, an important characteristic of these equations is that they include the air viscosity parameter. It is concluded that increasing the nozzle size decreases the mean drop size which leads to produce the finer sprays (Lefebvre, 1980).

❖ Kim and Marshall

The two different forms of airblast atomizers are used during the research of the drop size distribution performed by Kim and Marshall (Kim and Marshall Jr, 1971). These forms are convergent single airblast nozzle and double concentric airblast atomizer. The first one works based on converging and expanding the atomizing air through a curl around a liquid nozzle. The other one is made of a secondary air nozzle which is placed axially in the liquid nozzle. The atomizer used in Kim and Marshall research is shown in Figure 1.22 (Lefebvre, 1980).

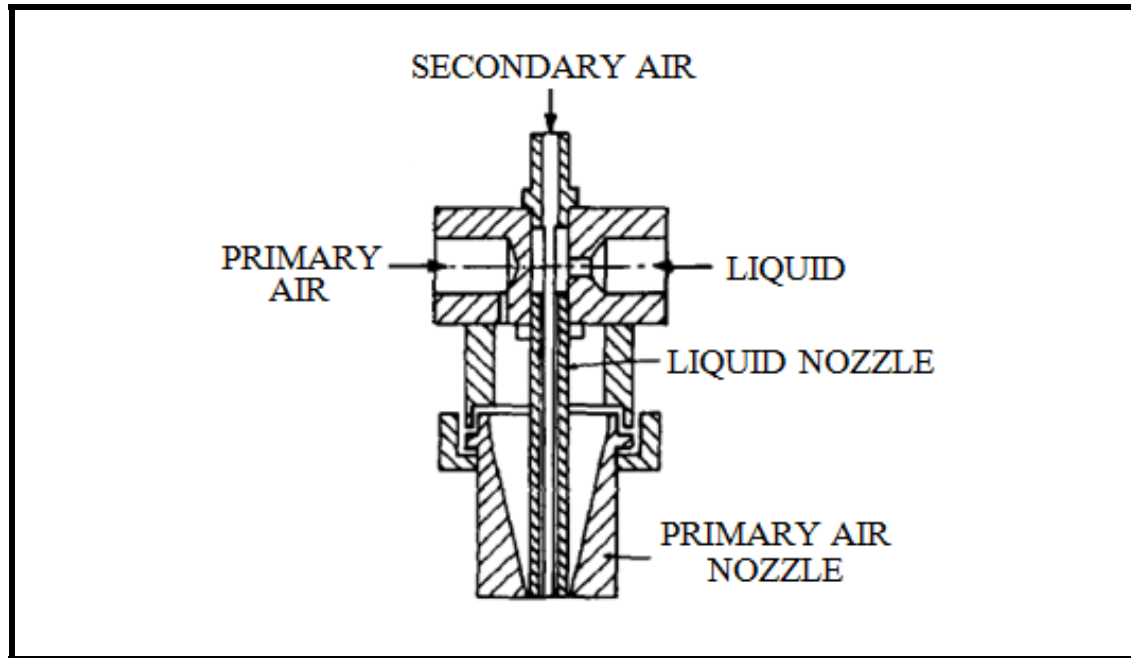


Figure 1.22 Kim & Marshall atomizer (Lefebvre, 1980)

The relevant measurements of drop size carried out by Kim and Marshall are according to the information shown in table 1.4 (Lefebvre, 1980).

Table 1.4 The parameters used in Kim and Marshall drop size measurements (Lefebvre, 1980)

Liquid viscosity	0.001- 0.050 kg/msec
Relative air velocity	75-393 m/sec
Air to liquid mass flow ratio	0.06-40
Liquid density	800- 960 kg/m ³
Air density	0.93-2.4 kg/m ³

The equations 1.8 and 1.9 are obtained from Kim and Marshal experiments for convergent single airblast nozzle and double concentric airblast atomizer respectively.

$$\text{MMD} = 5.36 \times 10^{-3} \frac{\sigma_L^{0.41} \mu_L^{0.32}}{(\rho_A U_R^2)^{0.57} A^{0.36} \rho_L^{0.16}} + 3.44 \times 10^{-3} \left(\frac{\mu_L}{\rho_L \sigma_L} \right)^{0.17} \left(\frac{\dot{m}_A}{\dot{m}_L} \right)^m \frac{1}{U_R^{0.54}} \quad (1.8)$$

$$\text{MMD} = 2.62 \frac{\sigma_L^{0.41} \mu_L^{0.32}}{(\rho_A U_R^2)^{0.72} \rho_L^{0.16}} + 1.06 \times 10^{-3} \left(\frac{\mu_L}{\rho_L \sigma_L} \right)^{0.17} \left(\frac{\dot{m}_A}{\dot{m}_L} \right)^m \frac{1}{U_R^{0.54}} \quad (1.9)$$

According to these equations, it is concluded that the significant operating variables in airblast atomization are the air/liquid mass ratio and the dynamic force. The increases in each one or both of them reduces the mean drop size (Lefebvre, 1980).

❖ Lorenzetto and Lefebvre

Lorenzetto and Lefebvre (1977) were a research group who investigated accurately the efficiency of plain-jet atomizers. The system which was used in their studies is shown in Figure 1.23. In this system, different parameters such as air/liquid ratio, air velocity, atomizer dimensions and the physical characteristics of liquid could be changed independently in a broad range (Lefebvre, 1980).

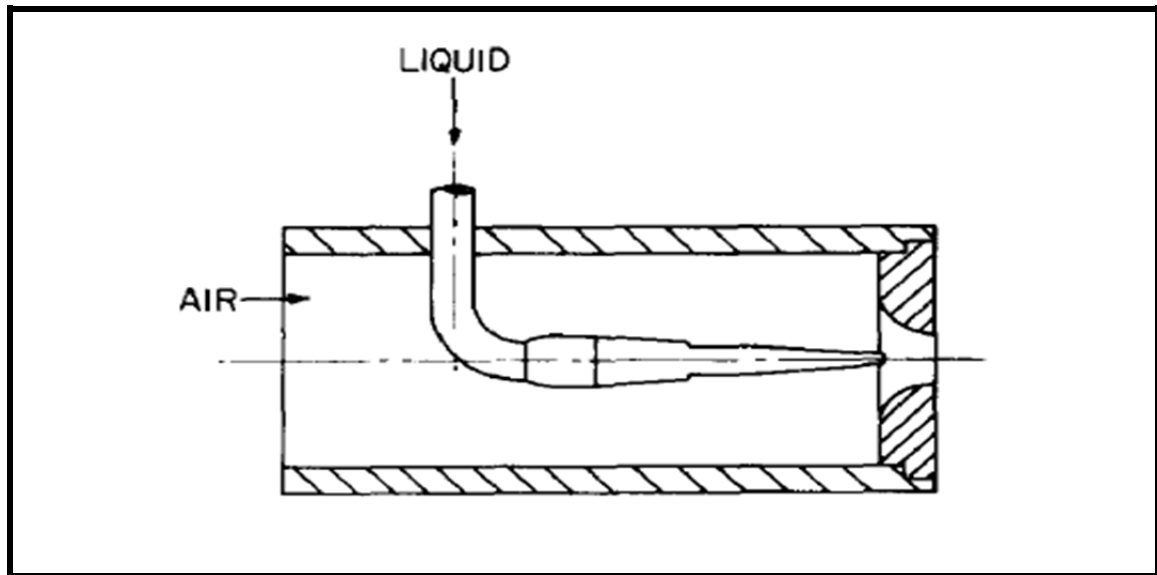


Figure 1.23 Lorenzetto and Lefebvre atomizer (Lefebvre, 1980)

This atomizer was also included the equipment which could produce a round jet of liquid surrounded by a co-axial and co-flowing stream of high velocity air. The drop size equation



obtained by Lorenzetto and Lefebvre (Equation 1.10), is determined using four liquid injectors with orifice diameters of 0.397, 0.794, 1.191 and 1.588 mm (Lefebvre, 1980).

$$\text{SMD} = 0.95 \left(\frac{(\sigma_L \dot{m}_L)^{0.33}}{U_R \rho_L^{0.37} \rho_A^{0.36}} \right) \left(1 + \frac{\dot{m}_L}{\dot{m}_A} \right)^{1.70} + 0.13 \mu_L \left(\frac{D_0}{\sigma_L \rho_L} \right)^{0.5} \left(1 + \frac{\dot{m}_L}{\dot{m}_A} \right)^{1.70} \quad (1.10)$$

The interests of this equation are the independent effect of the liquid flow rate and the notable influence of air/liquid ratio on SMD

❖ Jasuja

The other research of the mean drop size carried out by Jasuja (Jasuja, 1979) using a plain-jet airblast atomizer with kerosene and the other different fuels (see Figure 1.24).

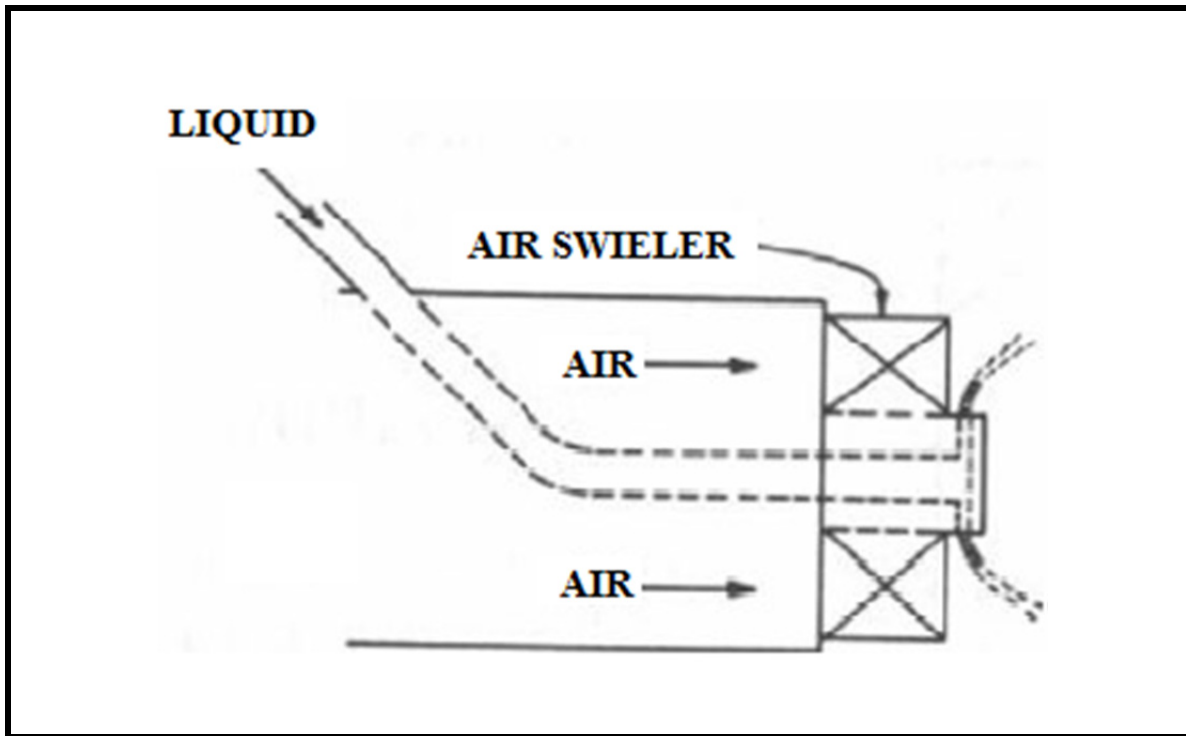


Figure 1.24 Plain-jet atomizer used by Jasuja (Lefebvre, 1980)

The SMD equation (Equation 1.11) obtained from this experimental work has the same characteristics of the Lorenzetto and Lefebvre equation with the exception of lower dependence of SMD on air/liquid mass ratio.

$$SMD = \frac{0.19}{U_A} \left(\frac{\sigma_L}{\rho_L \rho_A} \right)^{0.35} \left(1 + \frac{\dot{m}_L}{\dot{m}_A} \right)^{0.25} + 0.127 \left(\frac{\mu_L^2 D_0}{\sigma_L \rho_L} \right)^{0.5} \left(1 + \frac{\dot{m}_L}{\dot{m}_A} \right) \quad (1.11)$$

❖ Weiss and Worsham

According to Weiss and Worsham investigations (Weiss and Worsham, 1958) the most important parameter to control the mean drop size is the relative velocity between the air and the liquid. The research carried out by Weiss and Worsham contains both cross stream and co-stream injection of the liquid jets into the air at high velocity and it is based on the parameters shown in table 1.5 (Lefebvre, 1980).

Table 1.5 The parameters used in Weiss and Worsham drop size measurements (Lefebvre, 1980)

Air velocity	60 - 300 m/msec
Orifice diameters	1.2 - 4.8 mm
Liquid viscosities	0.0032 - 0.0113 kg/msec
Air densities	0.74 - 4.2 kg/m ³

The mean drop size equation (Equation 1.12) obtained from their experimental studies is based on dependence of the drop size distribution to the variety of excitable wavelengths on the surface of a liquid sheet (Lefebvre, 1980).

$$SMD \propto \left(\frac{U_L^{0.08} D_0^{0.16} \mu_L^{0.34}}{\rho_A^{0.30} U_R^{1.33}} \right) \quad (1.12)$$

- Prefilming airblast atomizers Investigations

- ❖ Rizkalla and Lefebvre

As previously explained, another kind of airblast atomizers which several researchers such as Rizkalla and Lefebvre (Lefebvre, 1980; Mandato *et al.*, 2012) used, is prefilming airblast atomizers (Figure 1.25). Rizkalla and Lefebvre used the light scattering method to examine the influence of the viscosity, density and the surface tension parameters on the mean drop size.

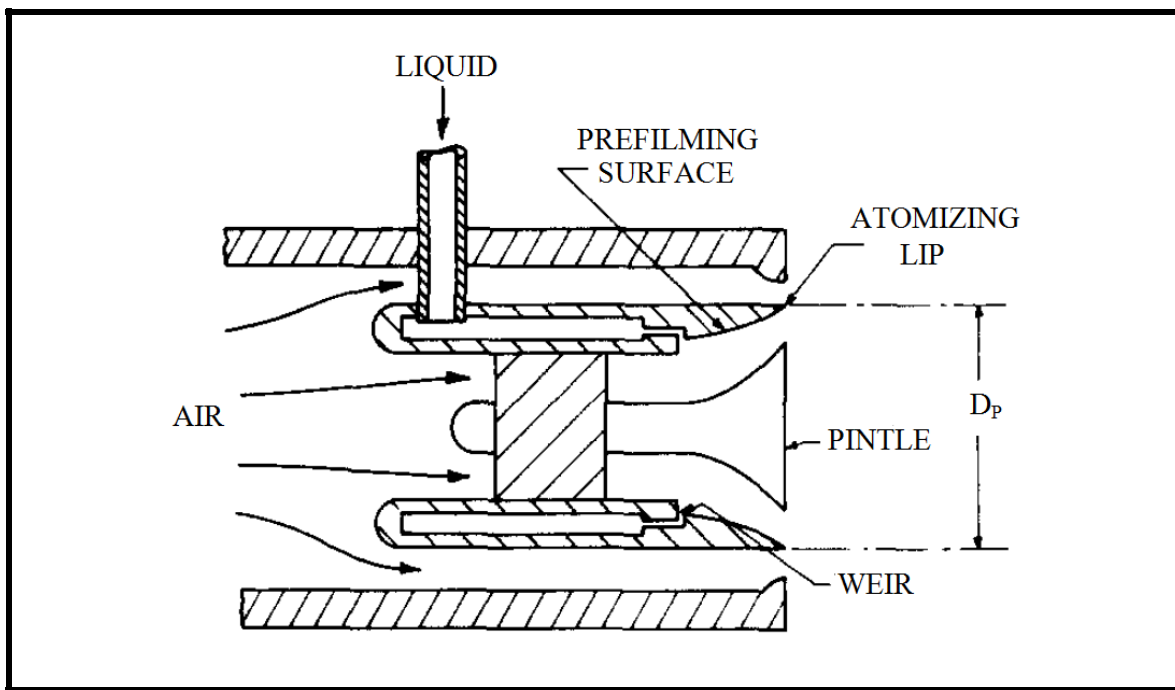


Figure 1.25 Rizkalla and Lefebvre atomizer (Lefebvre, 1980)

According to experimental results obtained by Rizkalla and Lefebvre, it was concluded that the main factors which affect the mean drop size are surface tension, air velocity and air density for the low viscosity liquids. Rizkalla and Lefebvre found that the liquid viscosity effect is independent from that of the air velocity. The equation obtained from the Rizkalla and Lefebvre researches (Equation 1.13), shows clearly this independence using two separate terms as air velocity and air density for the first one and the liquid viscosity as the second term (Lefebvre, 1980).

$$SMD = 3.33 \times 10^{-3} \frac{(\sigma_L \rho_L D_P)^{0.5}}{\rho_A U_A} \left(1 + \frac{\dot{m}_L}{\dot{m}_A}\right) + 13.0 \times 10^{-3} \left(\frac{\mu_L^2}{\sigma_L \rho_L}\right)^{0.425} D_P^{0.575} \left(1 + \frac{\dot{m}_L}{\dot{m}_A}\right)^2 \quad (1.13)$$

The comparison between prefilming and the plain-jet airblast nozzles carried out by Lefebvre and Rizkalla (see Figure 1.26), showed that the performance of the prefilming atomizers is better than that of the plain-jet atomizers particularly under the conditions such as low air/liquid ratio and/or low air velocity (Lefebvre, 1980).

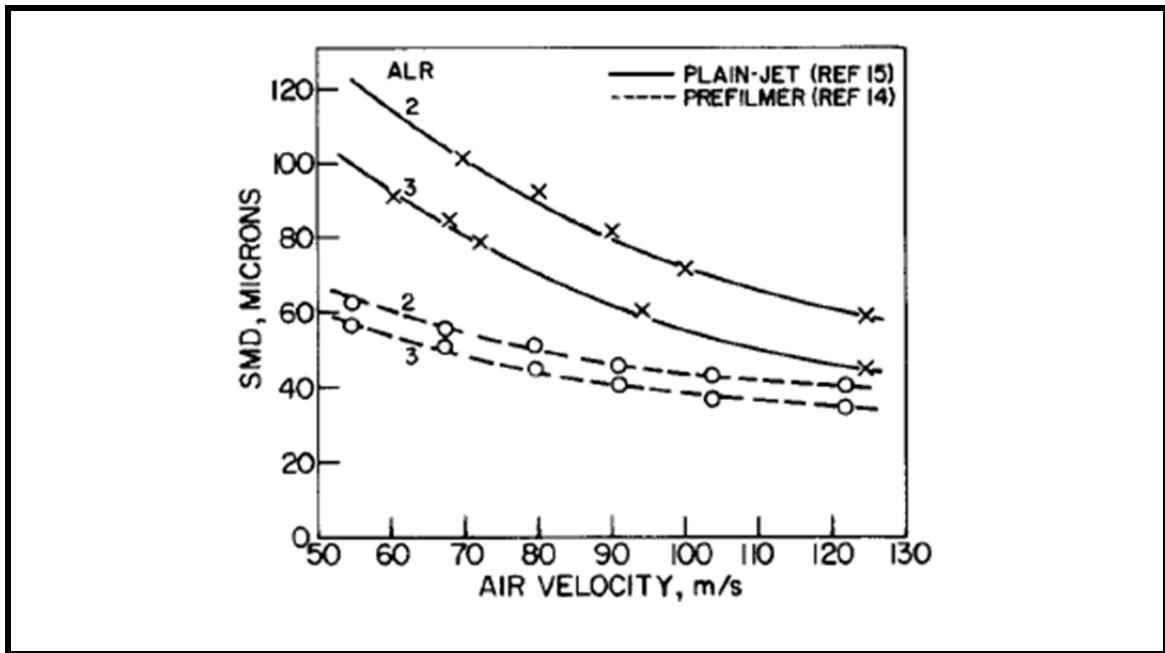


Figure 1.26 Atomizing efficiency of the plain-jet and the prefilming atomizers (Lefebvre, 1980)

1.6.4 The effects of variables on mean drop size

According to researches conducted on drop size distributions, the most important variables which affect mean drop size are viscosity, surface tension and density of liquid as well as the air velocity. Several effects of these properties and their results are explained in table 1.6 (Lefebvre, 1980). The influences of these parameters on plain-jet airblast atomizers are shown in Figures 1.27 and 1.29.

Table 1.6 The effects of the different variables on mean drop size (Lefebvre, 1980)

	Variable	Effects	Result
Liquid Properties	Viscosity	<ul style="list-style-type: none"> - Restraint of wave's constitution on the liquid surface; - Resistance against the deformation of the ligaments formed by removed liquid from the atomizing lip into drops. 	Increase in viscosity produces the larger drop size.
	Surface tension	<ul style="list-style-type: none"> - Resistance against the disturbance or deformation of the liquid surface; - Avoid to create the surface waves and delaying of ligament formation. 	Prevention of atomization
	Liquid density	Liquid density increasing: <ul style="list-style-type: none"> - Reduces the sheet thickness produced at the atomizing lip of the prefilming systems; - Increases the relative velocity of the plain-jet nozzles. 	Improvement of atomization
		In the prefilming atomizers: <ul style="list-style-type: none"> - The increase in distance of the coherent liquid sheets creates the ligaments in the lower relative velocity between the air and the liquid; - The liquid density increasing creates the more compact sprays. 	Increase the mean drop size
Air Properties	Air Velocity	In fuels with lower viscosity, the mean drop size is approximately inversely proportional to the air velocity.	

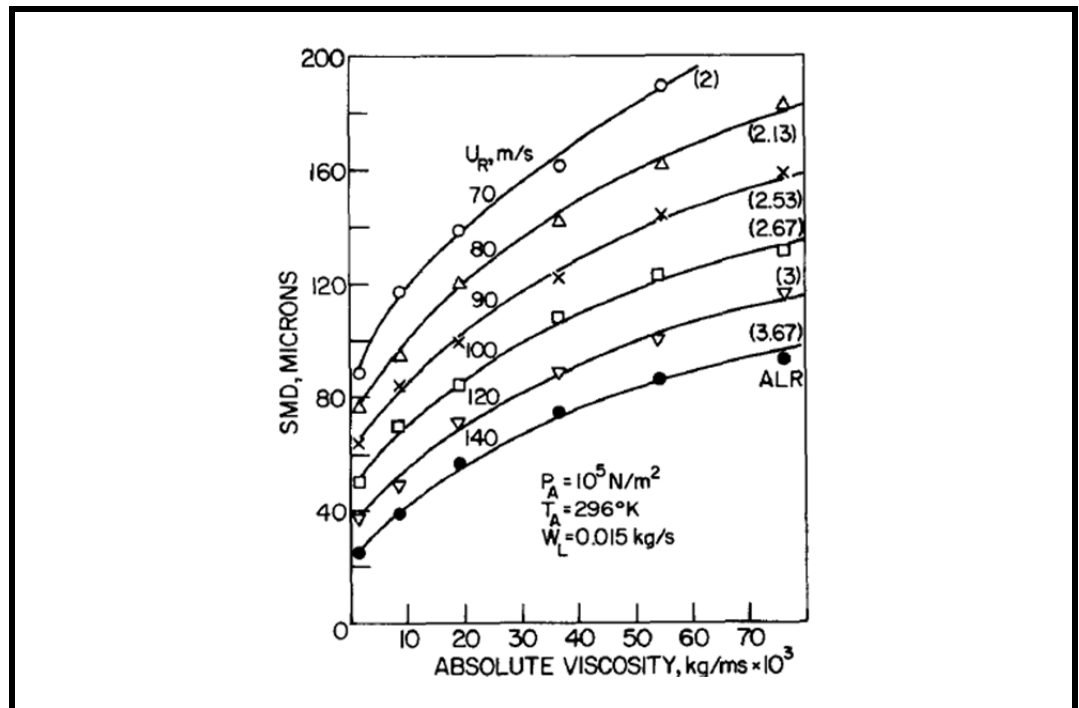


Figure 1.27 SMD variation related to liquid viscosity when using a plain-jet airblast atomizer (Lefebvre, 1980)

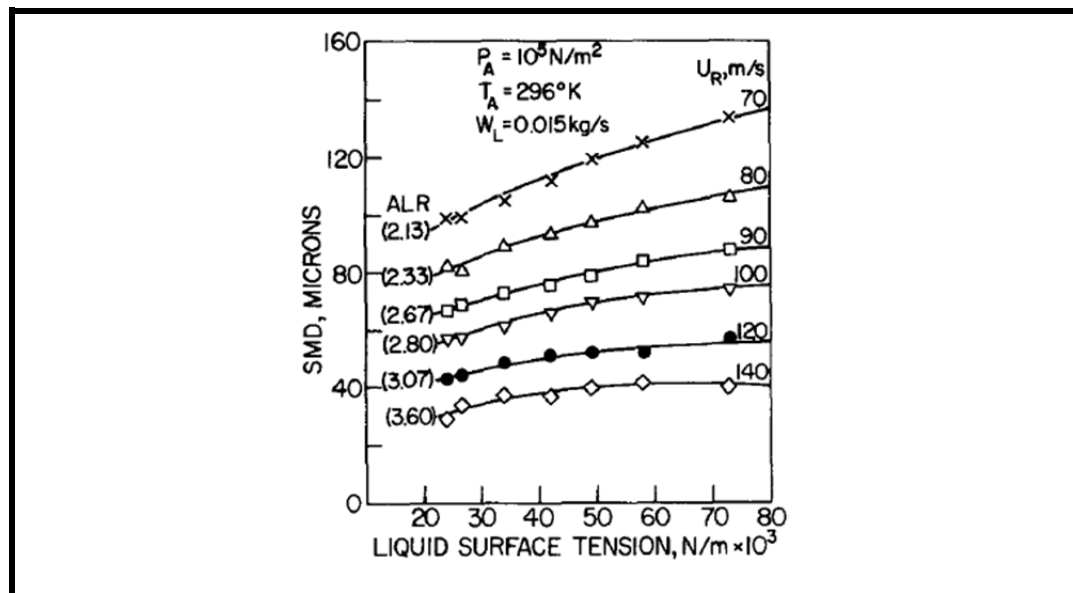


Figure 1.28 SMD variation related to surface tension when using for a plain-jet airblast atomizer (Lefebvre, 1980)

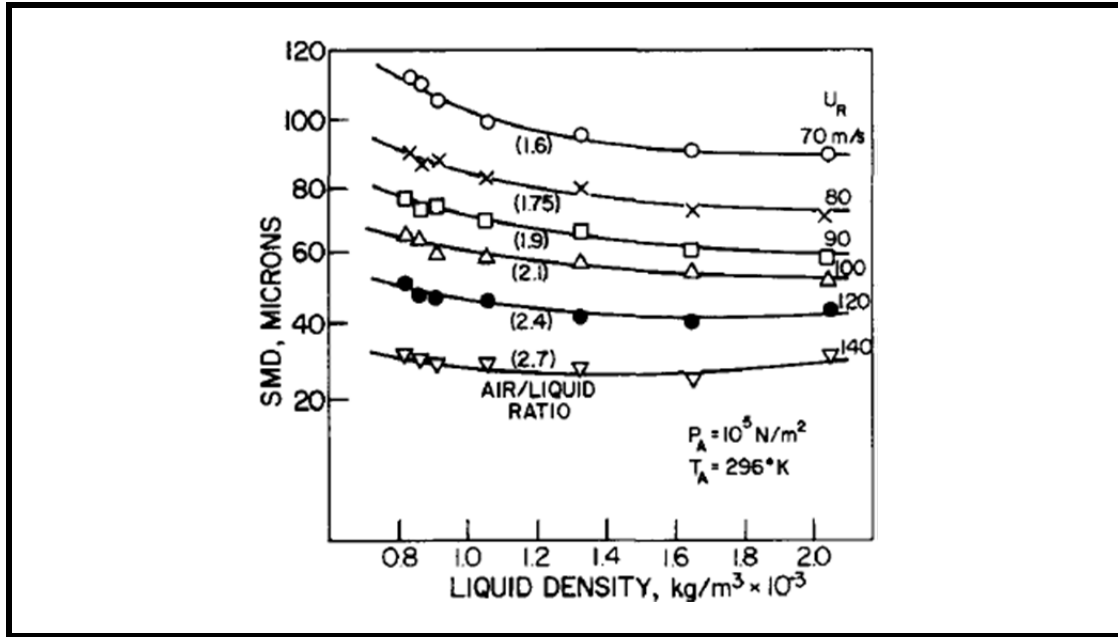


Figure 1.29 SMD variation related to liquid density when using a plain-jet airblast atomizer (Lefebvre, 1980)

1.7 Cutting parameter effects on machining quality characteristics

1.7.1 Cutting parameter effects on Surface Roughness

In manufacturing process, the improvement of surface quality is one of the major issues of interest for the customers. High quality products and reducing the machining cost become a goal in new industries. To achieve this target and in order to find the conditions in which the surface roughness value is decreased, different studies were carried out and the researchers could determine the various influences of cutting parameters such as cutting speed, feed rate and depth of cut on surface finish. The prediction of surface roughness is useful to achieve the better machining quality and therefore the final cost reduction. Surface roughness is generally determined by equation 1.14 as follow:

$$R_a = s^2 / 32r \quad (1.14)$$

where "s" is feed rate and "r" shows the nose radius. This model is not accurate due to lack of attention on the influences of the parameters such as tool geometry, machine tool rigidity,

cutting fluid application, cutting parameters and vibration in this model (Upadhyay, Jain and Mehta, 2012). Considering the researches carried out by Özel *et al.* (Özel, Hsu and Zeren, 2005) on AISI H13, the different parameters such as cutting edge geometry, workpiece hardness, cutting speed and feed rate affect the surface finish. They showed that lower edge radius and small workpiece hardness could increase the surface roughness. Davim and Figueira (Davim and Figueira, 2007) studied the surface roughness using the cold-work tool steel. Their experimental research confirmed that cutting time and feed rate are the most significant parameters on surface finish. The experimental analysis on hardened AISI 4140 carried out by Aslan *et al.* (Aslan, Camuşcu and Birgören, 2007) and the optimization performed on the experimental data showed that increase in cutting speed and feed rate, decreases and increases the surface roughness respectively.

1.7.2 Cutting parameter effects on cutting tool temperature

Heat generation problem during machining process is considerable. One of the reasons to increase the temperature during metal removal is because of reducing the time needed for machining (Bacci da Silva and Wallbank, 1999). Machining speed increasing and therefore increasing the chip formation causes to raise the plastic deformation and friction between the tool-chip interface which is a reason to heat generation (Sutter and Ranc, 2007). The different zones of heat generation during chip formation in orthogonal cutting process are shown in Figure 1.30.

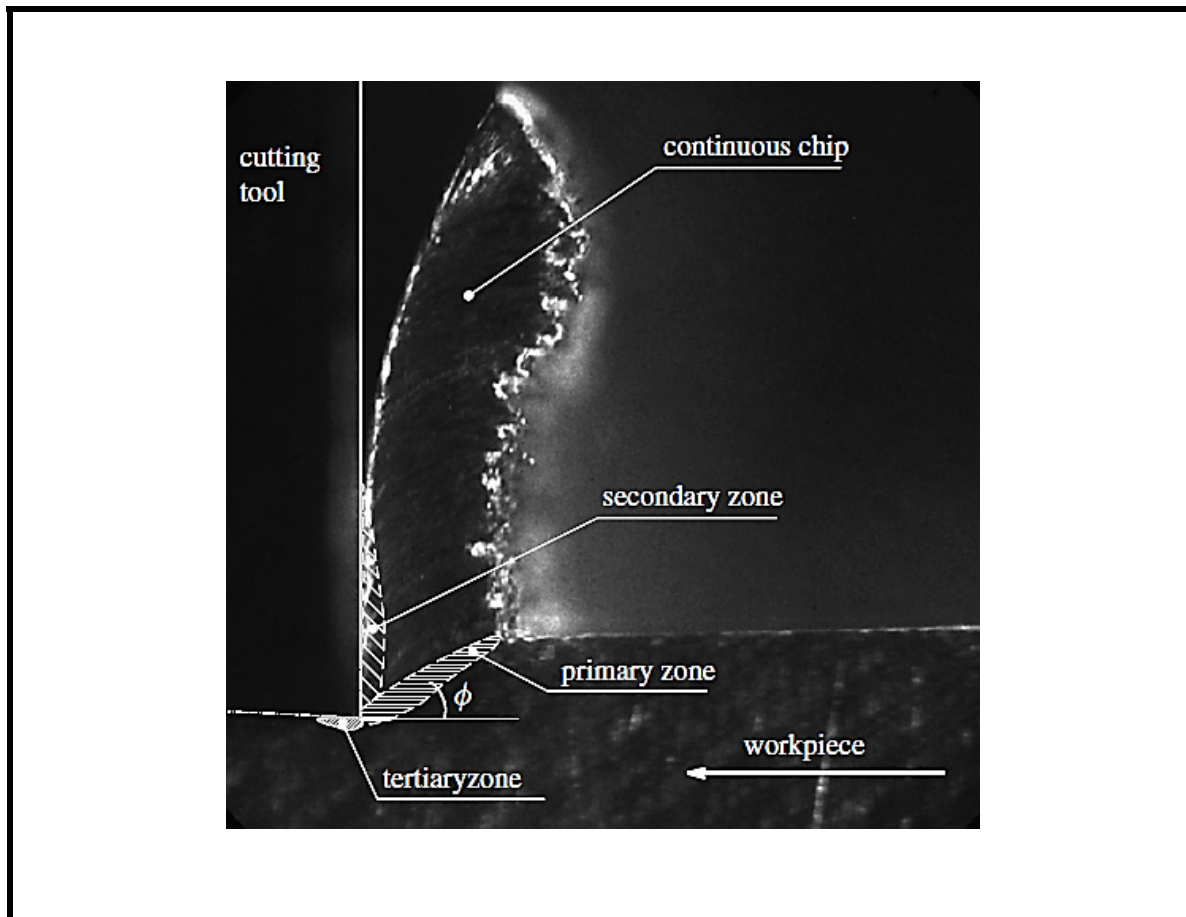


Figure 1.30 Heat generation zones (Sutter and Ranc, 2007)

According to Figure 1.30, the high shear deformation in primary zone starts to produce the heat generation. This temperature is increased because of the friction produced by tool chip contact. The deformation of the chip in secondary zone increases the temperature. Finally there is a tertiary zone situated under the tool tip where the plastic deformation and erosion between the tool flank face and the machined surface is created (Sutter and Ranc, 2007).

The different parts of machining process such as cutting fluid, workpiece, cutting tool and chips help to dissipate the generated heat. Between these items, the function of cutting fluid to reduce the heat generation is different. The role of coolant is removing the heat from the cutting zone whereas the lubricant facilitates the machining process and decreases the heat generation consequently (Bacci da Silva and Wallbank, 1999).

1.7.3 Cutting parameter effects on aerosol emission

- **Pre-cooling and pre-heating of workpiece materials**

Nowadays, several replacements exist to wet machining. These include cryogenic machining (for example liquid nitrogen) and dry machining. Cryogenic machining can be performed by pre-cooling the workpiece (Ding and Hong, 1998), by cooling the chip (Hong, Ding and Ekkens, 1999), or by cooling the tool-chip and tool-workpiece interfaces (Hong, 2006.).

It is found that pre-cooling a workpiece material leads to changes, at least 70%, in the chip formation, in the reduction of cutting forces and hence in a reduction in fine dust generation. Also, preheating the workpiece increases chip ductility and dust production levels.

The breakability of the chips will be increased by pre-cooling the workpiece, cooling the chip or cooling the interface of the chip –tool (Ding and Hong, 1998; Hong, Ding and Ekkens, 1999). Therefore the tool life can be increased while dust generation is minimized (Hong and Broome, 2000).

According to Balout *et al.* investigations (Balout, 2003), the ductile materials produce very fine dust particles (2.5 microns or less) with plastic deformation because they generate the microscopic friction. This amount of dust is more than dust generated by brittle materials which cannot undergo the plastic deformation.

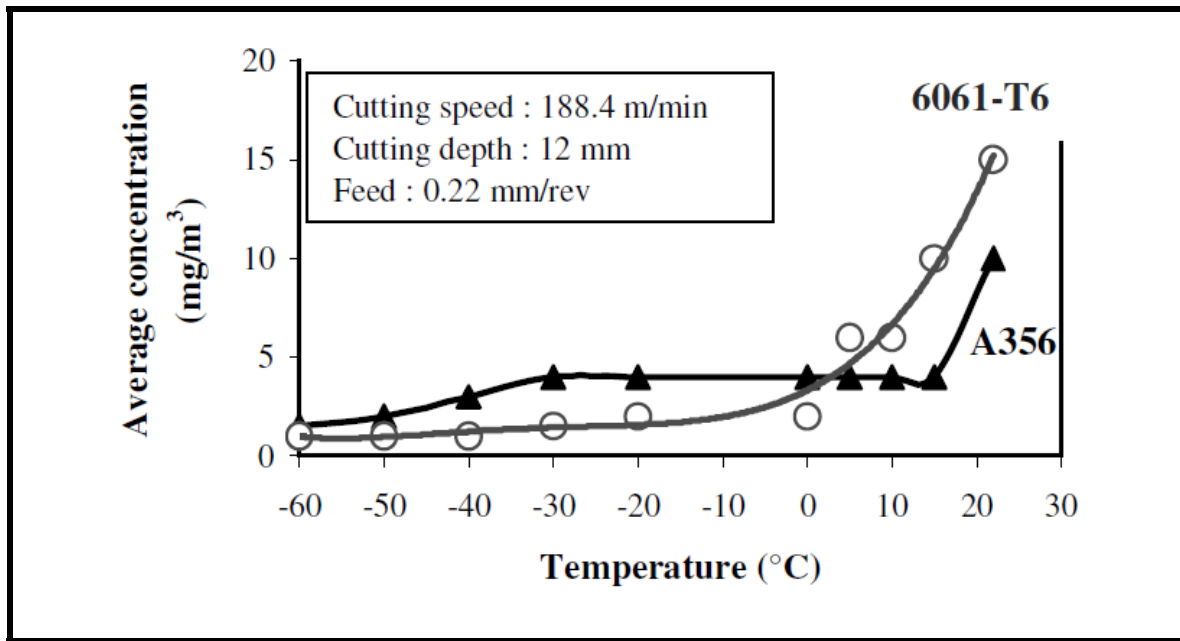


Figure 1.31 Average dust concentration when using A356 and AA6061 – T6 as a function of Workpiece Temperature (Balout, Songmene and Masounav, 2007)

According to Figure 1.31, the workpiece temperature has a significant effect on dust generation. The lower the temperature, the lower the amount of dust produced. Increasing the initial temperature of the material increases the plastic deformation in the chip. The five modes of dust generation during cutting process as shown in Figure 1.32 are as follows:

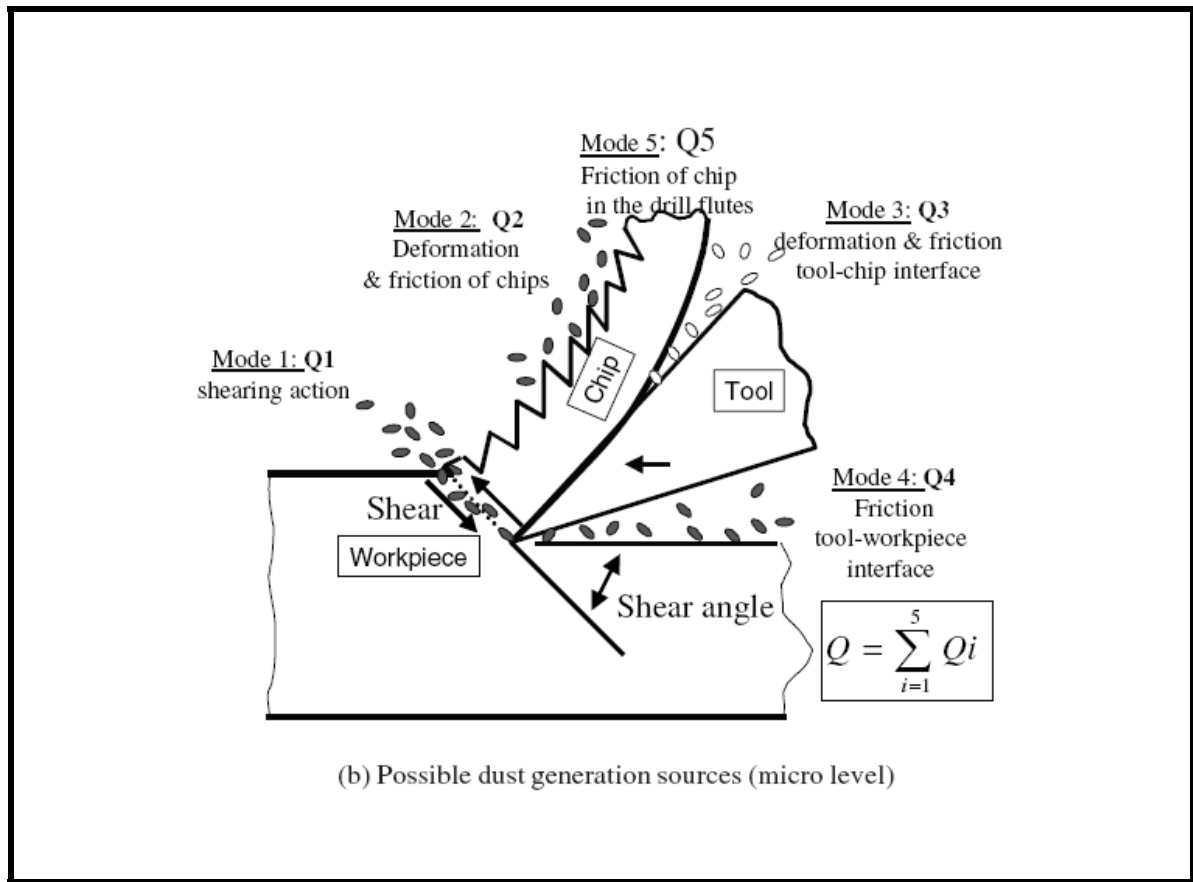


Figure 1.32 Possible dust generation sources (micro level)
(Balout, Songmene and Masounav, 2007)

- **Mode1:** Dust generation because of shearing action taking place in shear plane;
- **Mode2:** Dust generation because of the chip deformation which is happened during and immediately after chip formation;
- **Mode3:** Dust generation because of the chip sliding on the tool rake face (second deformation and friction);
- **Mode4:** Dust generation because of the tool rubbing on the fresh-cut surface;
- **Mode5:** Dust generation because of the friction occurring between the drill and the chip in the drill flute.

The question is that why the dust generation is reduced in the machining process of a pre-cooled workpiece. Due to cooling the workpiece, the material becomes less ductile and so the contact length at the tool-chip interface as well as the friction is decreased. Thus it

leads to the lower dust concentration. The ductility of the pre-cooled workpiece is reduced; the material becomes more brittle and produces semi-detached chips. This change in the mechanism of the chip formation reduces plastic deformation and dust production (Balout, Songmene and Masounav, 2007).

- **Tool lead angle effect in Dry cutting**

The research of Khettabi *et al.* 2007 (Khettabi, Songmene and Masounave, 2007) about lead angle and its effect on dust generation showed that the tool geometry has a significant influence on the dust emissions in machining, and this effect depends on material type.

The carried out experiments showed that a tool with a lead angle of 90° generates less dust than the other one with an angle of 70° or 110° . Machining a 6061-T6 aluminum alloy with a smaller lead angle generates more dust (Khettabi, Songmene and Masounave, 2007).

- **Speeds, materials and tool rake angles effects on orthogonal cutting**

Khettabi *et al.* (Khettabi, Songmene and Masounave, 2007) found that in turning, the tool lead angle affects the chip formation and the metallic particle generation. Ohbuchi and Obikawa (Ohbuchi and Obikawa, 2003) found that there is a critical speed and a critical unreformed chip thickness to better chip formation and efficient material removal. They also proved that these values are affected by rake angle. They found that for -15° or higher rake angle, the chip formed and it flows unconditionally whereas for the rake angle between -15° and -45° , decreasing the rake angle increases the critical speed. Because of the relationship between chip formation and shear angle, it is concluded that decreasing the chip thickness increases the friction and heat generation and also increases the dust emission. So based on the studies done by Fang (Fang, 2005), the negative rake angle increases the coefficient of friction and also the friction force. This result is contrary when using positive rake angle. In particular cases the negative rake angle can generate a small increasing in dust emission. So, using a null or low rake angle to reduce the dust emission is more advantageous. In orthogonal cutting, two dimensional modeling which simplifies the cutting process is possible. The tool geometry have a lot of effects on the metal cutting process as well as

shearing action, cutting force, temperature, deformation, surface roughness and chip formation.

In the oblique cutting, the tool lead angle has a significant effect on the chip shape but not on the chip segmentation mode. In the orthogonal cutting, the tool geometry includes the clearance angle, nose radius and the rake angle which affects the dust emission.

The study of Songmene *et al.* (Songmene, Balout and Masounave, 2008a; Songmene, Balout and Masounave, 2008b) shows that in low cutting speeds, machining is not recommended because of reduction in productivity but decreasing the dust emission and increasing the productivity are the most important reasons to recommend the high speed cutting.

The parameters such as chip ratio, chip segmentation and chip shape are very important to study the dust formation during machining (Khettabi, Songmene and Masounave, 2010). In table 1.7 the dust generation is compared using different cutting conditions and chip morphologies.

Table 1.7 Dust generation when using different cutting conditions and chip morphologies (Khettabi, Songmene and Masounave, 2010)

Cutting condition	Chip morphology	Dust emission
Negative tool rake angle	More brittle and segmented chips	Less dust
Positive tool rake angle	Less brittle and segmented chips	More dust

- **Modeling of particle emission**

Khettabi *et al.* (Khettabi, Songmene and Masounave, 2007; 2010) and Zaghbani *et al.* (Zaghbani, Songmene and Khettabi, 2009) showed the important effects of different cutting parameters, tool geometries and workpiece materials on metallic particle generation and proposed a semi-predictive model for fine metallic particle generation during the high speed milling respectively. The model for metallic particle emission during orthogonal cutting (Khettabi *et al.*, 2010) is created by studying the phenomenological aspects and energy combined with friction and plastic deformation materials. The different parameters used in

this study are force, shear stress, temperature, material properties and the chip flow localization parameter which is developed by Xie *et al.* (Xie, Bayoumi and Zbib, 1996). In this model, the new relationship is obtained as shown in equation 1.15 (Khettabi *et al.*, 2010):

$$D_u = A \times \frac{\beta_{\max} - \beta}{\beta_c} \times R_a \times \eta_s \cdot \left(\frac{V_0}{V}\right)^\delta \exp\left(\frac{E_A}{\tan \phi (1 - C_h \sin \theta) C_s \frac{F_{sh}}{b F_r}}\right) \quad (1.15)$$

where, D_u the Dust Unit, β the flow localisation parameter defined by Xie et al (Xie, Bayoumi and Zbib, 1996), E_A the energy activation, F_{sh} the shear force, C_s the cutting speed, F_r the feed rate, ϕ the shear angle, θ the tool rake angle and finally δ is the material parameter defined as follow:

$$\delta \equiv \begin{cases} \delta \geq 1 \rightarrow \text{Ductil materials} \\ 0.5 < \delta < 1 \rightarrow \text{Semi - ductil materials} \\ 0 < \delta \leq 0.5 \rightarrow \text{Brittle materials} \end{cases} \quad (1.16)$$

The δ parameter characterizes the effect of the material. This model is confirmed with the cutting turning tests and can predict the particle emission by investigating the different parameters such as cutting data, material properties and tool geometry. The analytical development and the experimental data are both used for developing this model.

According to Figures 1.33 and 1.34 (Khettabi *et al.*, 2010), it is concluded that increasing the cutting speed and tool rake angle, increases the particle emission but contrary, increasing the feed rate, decreases the particle emission. These experimental results confirm the model obtained by khettabi at al. (Khettabi *et al.*, 2010).

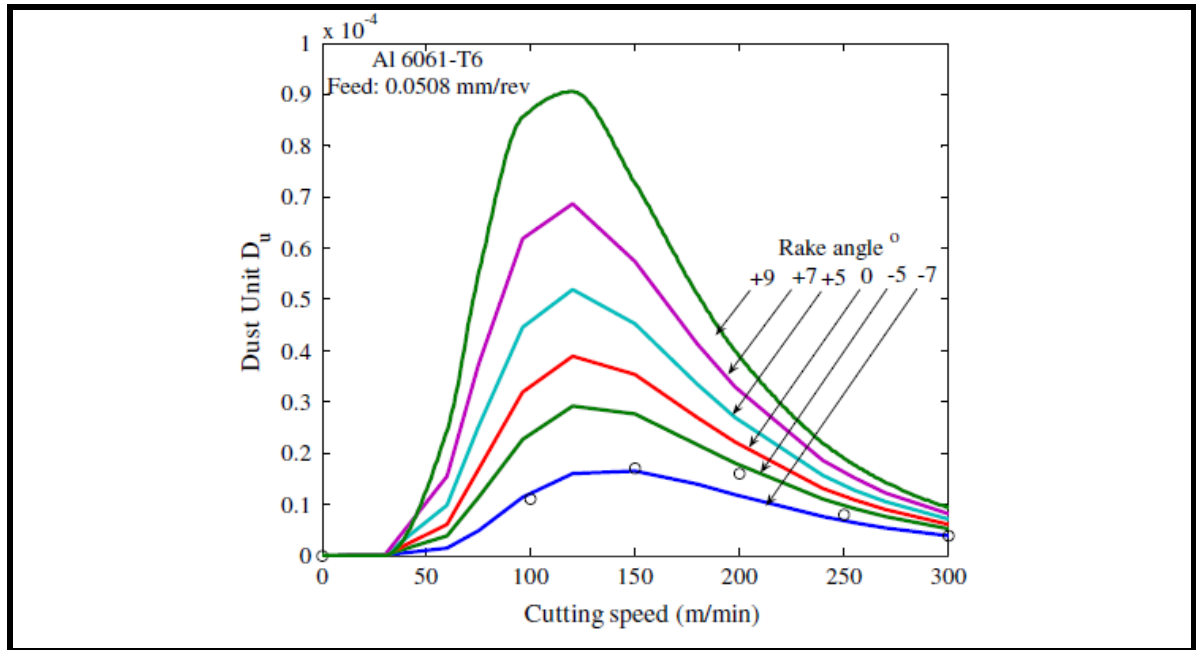


Figure 1.33 Dust emission varying on rake angle & cutting speed (dry machining of AA 6061-T6) (Khettabi *et al.*, 2010)

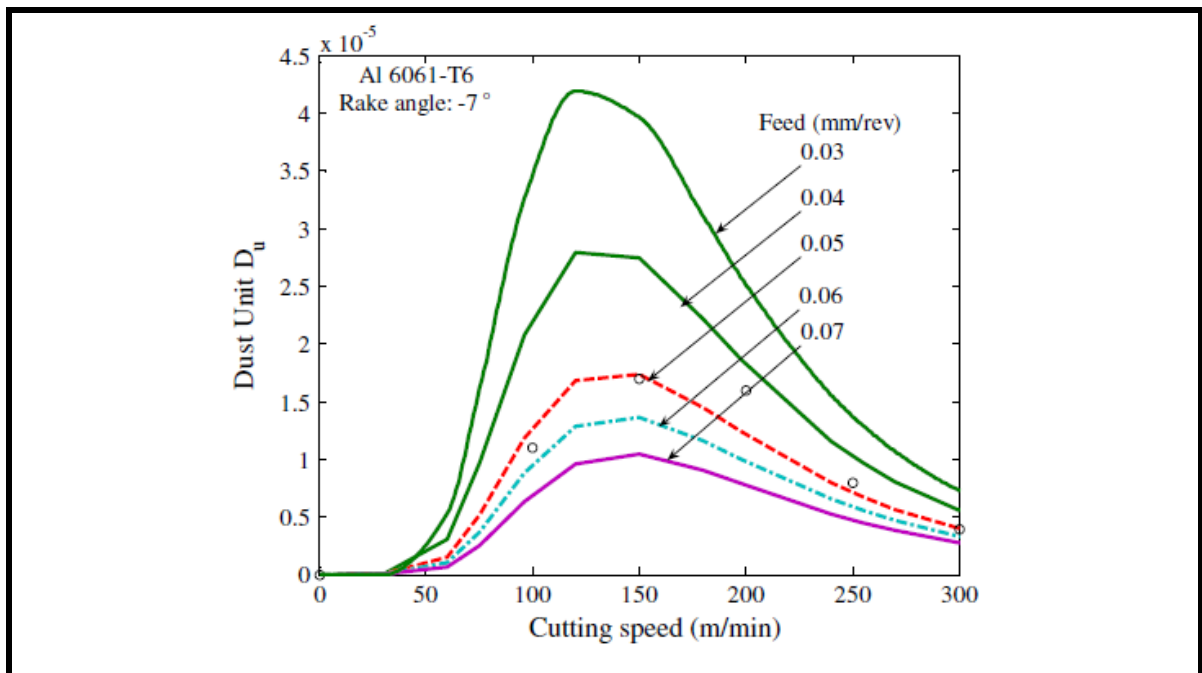


Figure 1.34 Dust emission varying on feed and cutting speed during (dry machining of AA6061) (Khettabi *et al.*, 2010)

1.8 Conclusion of literature review and refining of problematic

According to the literature review about MQCL and comparing it with dry and wet applications, it is concluded that MQCL method can improve the cutting performance more than the other machining modes because supplying the lubricant directly to the cutting zone reduces the cutting temperature which improves the chip-tool interaction. Because of tool wear reduction, MQCL improves tool lifetime. It leads also to better surface finish as compared with dry and wet machining.

The previous studies have shown that dry and semi-dry machining processes are environmental friendly and less dangerous. However, in some conditions, the large amounts of the fine and ultra-fine particles are produced. This problem in addition of particle emission hazardous, the investigation of particle sizes has become crucial. To accomplish this measurement, laser based techniques are very useful. The unique nature of the laser allows the accurate in-situ measurements in different environments where using the other kinds of particle sizing systems are impossible because of the various difficulties such as high temperature and risk of pollution which is dangerous for environment.

Considering the importance of the investigation of droplet size distribution and particle size measurement in different research and industrial applications, the principles and the applications of different atomization processes have been reviewed. According to the investigations and the empirical equations obtained from the Sauter mean diameter " d_{32} ", the most important parameters to control the mean droplet size are as follow:

- Liquid and gas mass flow rates and air to liquid mass flow rate ratio (ALR);
- The characteristics of the liquid such as viscosity, density and surface tension;
- The atomizer type such as plain-jet, prefilming and etc.

According to the investigations on the droplet size distribution described in this chapter, it is concluded that increasing the liquid viscosity, liquid density, surface tension and also decreasing the atomized air velocity increase the Sauter mean droplet diameter considerably. On the other hand, increasing the atomization pressure and ALR decreases the Sauter mean

diameter. Despite of existence of different sauter mean diameter empirical equations, these results show that under specified conditions, providing the qualified propositions for different equations is possible.

According to the literature review and despite of all the reported works on different machining modes, there is not considerably investigations about the effects of nozzle geometries and pump operations on machining quality indexes, especially in turning of aluminum alloy 6061-T6. The effects of cutting parameters on surface roughness, tool temperature and aerosol emission were always studied separately, therefore one of the major goals of this study is to find the cutting condition in which all the machining quality indicators achieve their optimal values.

CHAPTER 2

INSTRUMENTS AND EXPERIMENTAL PROCEDURES

2.1 Introduction

In the present research, using the proper measurement instruments and methods is crucial. This study is divided into two parts. The first one is about particle-sizing and the injection angle measurement and the second part is about the analysis of different cutting parameters effects on surface roughness, cutting tool temperature and aerosol emission. In order to measure the parameters such as Sauter mean diameter and also the quality indexes, different instruments have been used for the experiments which will be described in this chapter.

2.2 Instruments

2.2.1 Injectors

The experiments were carried out using six different plain-jet airblast atomizers fabricated by System Tecnolub sa, which are different in terms of the injection length and the orifice diameter as shown in table 2.1. Two of these injectors have the orifices with conical shape while the others are straight. The general configuration of these injectors is illustrated in Figure 2.1.

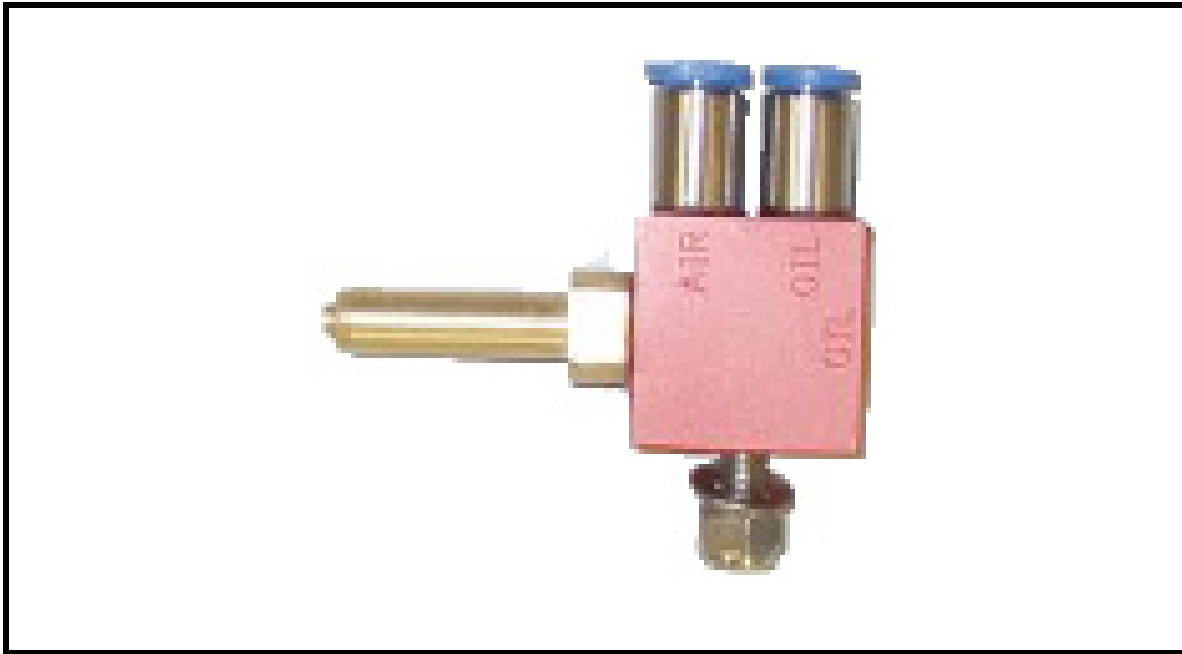


Figure 2.1(a)

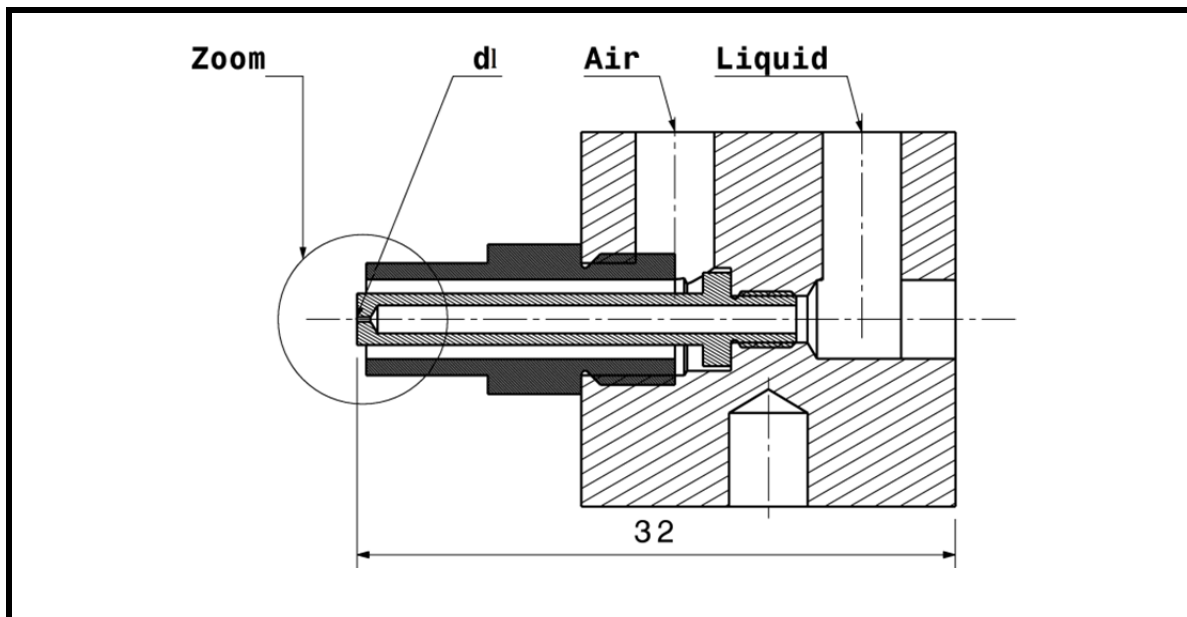


Figure 2.1(b)

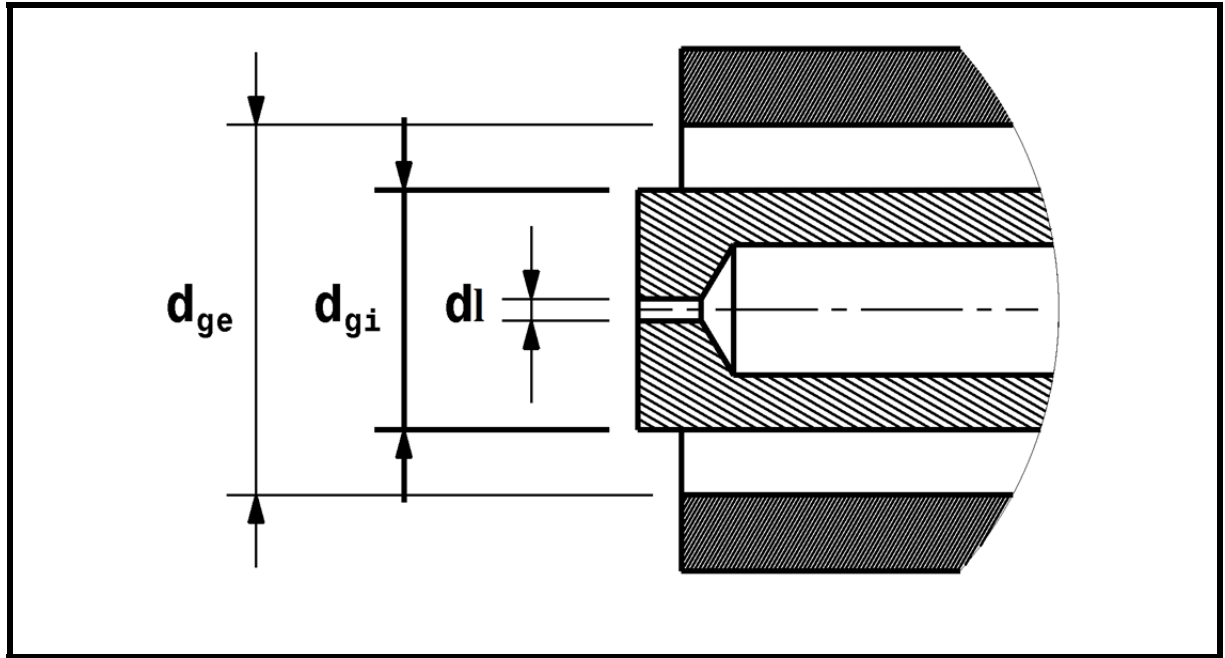


Figure 2.1(c)

Figure 2.1 Coaxial plain-jet airblast atomizer (Steimes *et al.*, 2012)

Table 2.1 Dimensions of atomizers

N	d_{ge} (mm)	d_{gi} (mm)	d_l (mm)	L_g (mm)	Liquid orifice shape
	External gas orifice diameter	Internal gas orifice diameter	Liquid orifice diameter	Length of injector	
1	4.25	2.75	0.25	10	Straight
2	4.25	2.75	0.25	20	Straight
3	4.25	2.75	0.25	33.5	Straight
4	4.25	2.75	1.00	33.5	Straight
5	4.25	2.75	0.25	20	Conical
6	4.25	2.75	0.35	20	Conical

In this research study, all the experiments are performed using Emultec VG lubricant which is a water-soluble (5% Solubility). This lubricant is based on esterified vegetable oils and is formulated without chlorine, formaldehyde-releasing bactericides, phenol derivatives, heavy

metals and silicones. The Emultec VG is recommended for the machining of aluminum alloy (except aeronautical aluminum) and the stainless steels. The characteristics of this emulsion (Manual, 2009) are as follow (table 2.2):

Table 2.2 EMULTEC VG specifications

Viscosity (at 40 °C) × 10³ (kg/m.s)	Density (at 15 °C) kg/m³	Surface tension ×10⁻³ (kg/s²)
1.0	1006.5	73

The other lubricant based on esterified vegetable oils used during the experiments is Mecagreen 550. Its characteristics are explained in table 2.3.

Table 2.3 Mecagreen-550 specifications (CONDAT Lubrifiants)

Lubricant Specification	MECAGREEN 550
Aspect	Limpid
Color	White
Odor	Low
Viscosity	21 mm ² /s
Solubility	Water 10 - 15 %
Biodegradability	Not Information
Application	Machining very hard chipping Aluminum, aluminum alloy, Stainless steel
Maximum storage	1 year

2.2.2 Laser diffraction system

As described in the previous chapter, one of the best systems to measure the droplet diameters and particle size distribution is laser diffraction system. In this work, in order to perform particle size analysis, the laser diffraction system, Helos-Vario/KR, produced by

Sympatec GmbH (a German company) was used. The operation of the HELOS (Helium-Neon Laser Optical System) is based on Mie Theory⁵ and the principle of the laser diffraction in the parallel laser beam for the hole measuring range is from 0.1 μm to 8750 μm . The system used in this study, Helos-Vario/KR, (see Figure 2.2) has two lenses, R3 and R6, which allow measuring the droplet size from 0.9 to 175 μm and from 9 to 1750 μm respectively. The evaluation of the particle size analysis data obtained from this system and also the instrument control has been driven by WINDOX 5 software.

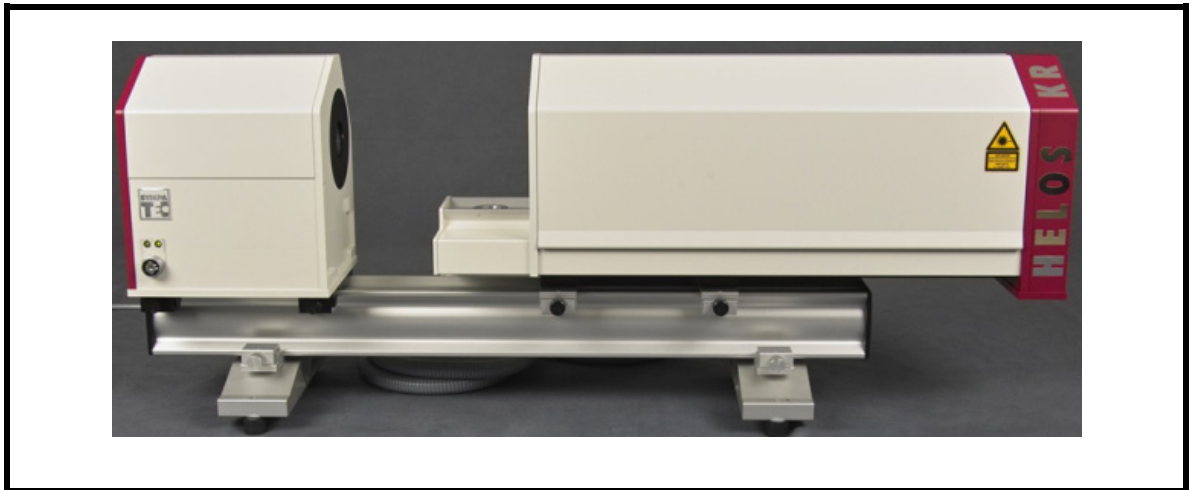


Figure 2.2 Helos-Vario/KR (www.sympatec.com), consulted on 02/Sep/2012

2.2.3 Pumps (GLS, SLS1.2-2 and DDA pumps) and flow sensor

In order to provide the necessary liquid flow rates, two different pumps were used. The injection methods such as pulsed and non-pulsed are the considerable difference between these two pumps. The GLS and SLS1.2-2 pumps as pulsed pump are used to providing the small liquid flow rates using a micro lubrication system (see Figures 2.3 – 2.4). These pumps are developed by a Belgium company, Systeme TecnoLub sa. In these machines, a volumetric micro pump injects a little quantity of the lubricant through a capillary tube to an outlet nozzle. At the same time, a low pressure pulverization air is injected to the cutting zone using

⁵ Lorenz-Mie theory is applicable to the spherical particles with diameter larger than the wavelength of the incident light. This theory is based on the refraction index and the diameter of the particle as well as the light wavelength (Lee Black, McQuay and Bonin, 1996).

a second capillary tube. The lubricant source is installed at the top of this machine and the flow rate could be adjusted by setting the micro pumps which allows settings from 1 to 180 strokes per minute. The adjustments of the micro lubrication systems are shown in table 2.4.

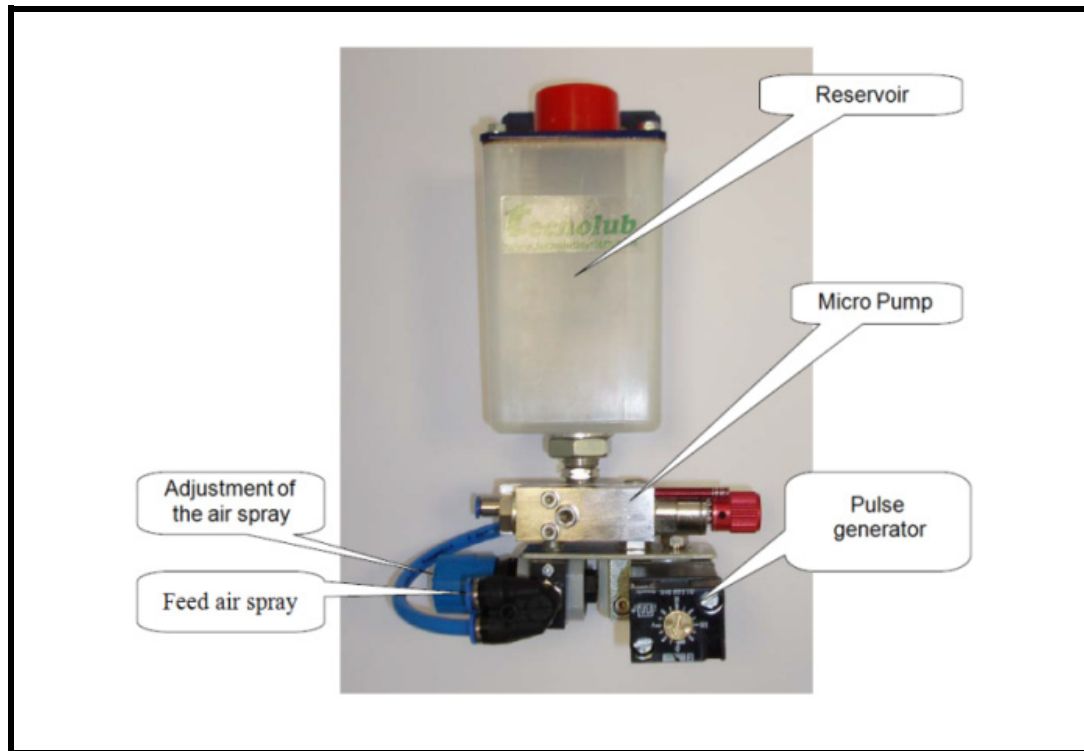


Figure 2.3 Microlubrication system (GLS pump) (Manual, Jan 2009)



Figure 2.4 Microlubrication system (SLS1.2-2 pump) (Manual, 2009)

Table 2.4 Adjustment of Microlubrication systems

	GLS pump	SLS1.2-2 pump
Maximum flow rate of Micro pump	5.4 ml/min	3.087 ml/min
Pulse generator	60 , 120 stroke/min	20, 50 and 90 stroke/min
Air spray pressure	1.4 bar	1.4 bar
Micro pump air control pressure	6 bar	6 bar

Digital dosing Advanced (DDA) pump (see Figure 2.5) as non-pulsed pump was used to produce the smooth and continuous liquid flow. The DDA pumps fabricated by a Danish company, GRUNDFOS Alldos, is a high-end pump model for extended flow and pressure ranges with sensor-based flow control and measurement functions to challenge the industrial applications.



Figure 2.5 Digital Dosing Advanced Pump (DDA) (GRUNDFOS, November 2010)

The significant difference between this pump and those of System Tecnolub sa; is that DDA pump doesn't need to program a number of strokes per pulse. Instead, the DDA pump is set to a volume per pulse and the required number of strokes will be calculated internally. The DDA pump is appropriate for the non-abrasive, inflammable and non- combustible liquids. The DDA pump used in this research is known as DDA7.5-16 FCM-PV/T/C-32U2U2FG as the reference (Table 2.5)

Table 2.5 DDA reference specifications (GRUNDFOS, November 2010)

DDA 7.5-16 FCM-PV/T/C-32U2U2FG	
DDA	Type range
7.5	Maximum flow (l/h)
16	Maximum pressure (bar)
FCM	Control variant (FC with flow measurement (DDA))
PV	Dosing head variant (PVDF (polyvinylidene fluoride))
T	Gasket material (PTFE)
C	Valve ball material (Ceramic)
3	Supply voltage (1 x 100-240 V, 50/60 Hz)
2	Valve type Spring-loaded : 1.45 psi (0.1 bar) suction opening pressure 1.45 psi (0.1 bar) discharge opening pressure
U2U2	Connection, suction/discharge (Hose 4/6 mm, 6/9 mm, 6/12 mm, 9/12 mm)
F	Mains plug (EU (Schuko))
G	Design (Grundfos Alldos)

To facilitate providing the suitable gas flow rate, a unidirectional flow sensor with maximum flow measuring range of 50 l/min fabricated by Festo Company was used. The reference of this flow meter (see Figure 2.6) is known as SFAB-50U-HQ6-2SA-M12 which is described in table 2.6.

Table 2.6 Flow sensor reference specifications (Manual, Aug 2012)

SFAB-50U-HQ6-2SA-M12	
SFAB	Flow sensor
50	Flow measuring range (l/min)
U	Flow input (Unidirectional)
H	Type of mounting (Via H-rail)
Q6	Pneumatic connection (Push-in connector 6 mm)
2SA	Electrical output (2x PNP or NPN, 1 analogue output 4 ... 20 mA)
M12	Electrical connection (Straight plug, M12x1, 5-pin)



Figure 2.6 Flow sensor (Manual, Aug 2012)

2.2.4 TSI 8532 DustTrak – II aerosol monitor

In many researches, the dust generated measurement during the cutting operation is one of the interesting studies. Different instruments for particle measuring are available in which the various techniques such as electrostatic, optical, filter, etc.; are used. The TSI 8532 DustTrak – II aerosol monitor (see Figure 2.7) as a laser based instrument was used in the second part of these experiments in order to measure the maximum mass concentration of dust.



Figure 2.7 TSI 8532- DustTrak II aerosol monitor (Manual, Jan 2012)

This device equipped with different impactors allows the operator to measure the particle size in a range of 0.1 to 10 μm and the aerosol concentration range between 0.001 and 150 mg/m^3 . The maximum of the dust concentration during each test was obtained using the TSI



8532 DustTrak. The interval time for these tests was adjusted for 4 minutes and the calibration was performed at the beginning of the experiments using the zero filters.

2.2.5 Profilometer

In order to measure the surface, Taylor-Hobson Surtronic3+ as shown in Figure 2.8 was used.



Figure 2.8 Profilometer, Surtronic3+ (SalesBrochure) *consulted on 15/Aug./2012*

This Profilometer was used for the long rod of aluminum alloy 6061-T6 during the experiments with the GLS pump but the Mitutoyo machine as shown in Figure 2.9 was used to measure the surface roughness of short rod of 6061-T6 Aluminum alloy during the experiments with the SLS1.2-2 pump.

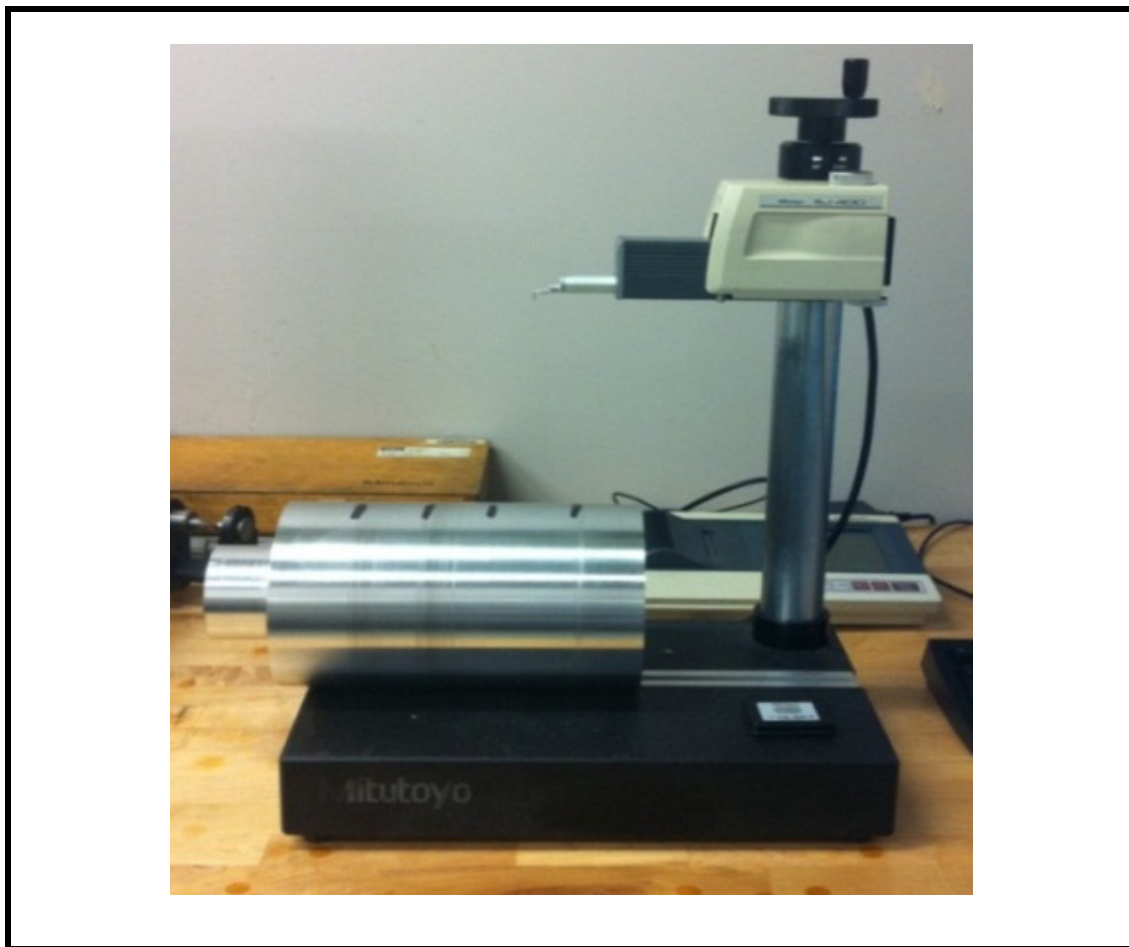


Figure 2.9 Profilometer, Mitutoyo

2.3 Installation and experimental procedures

As it is explained at the beginning of this chapter, the experiments were carried out in two different sections that their procedures will be described as follow.

2.3.1 Particle sizing and injection angle measurement

The aim of the first part is the particle sizing analysis, measuring the Sauter mean diameter as well as the injection angle and finally comparing the results obtained from different atomizers (table 2.1). All of these experiments are performed at room temperature using six gas flow rates and four liquid flow rates as are mentioned in table 2.7.

Table 2.7 Gas and Liquid flow rates

Gas flow rate (l/min)						Liquid flow rate (ml/min)	
						Microlub Pump	DDA Pump
20	25	30	35	40	45	2.1	2.1
							4.2
						4.2	10
							17.5

The measurements were repeated 3 times at every operating condition (30 measurements during 30 sec) and the arithmetic mean was used to eliminate the influence of the randomness in the atomization process. For particle sizing, the injectors were mounted perpendicularly at the distance of 5 cm from the laser beam where two lenses of the laser diffraction system were positioned at the distance of 50 cm.

In order to measure the injection angle, the nozzle was placed perpendicularly at the distance of 10 cm from a ruler fixed on the table. The first contact points of two sheets that are moving towards each other parallel to the ruler and the injected liquid were observed on the ruler. These two points and the tip of the injector form a triangle which helps us to find the injection angle. The illustration of this experiment is schematically shown in Figure 2.10.

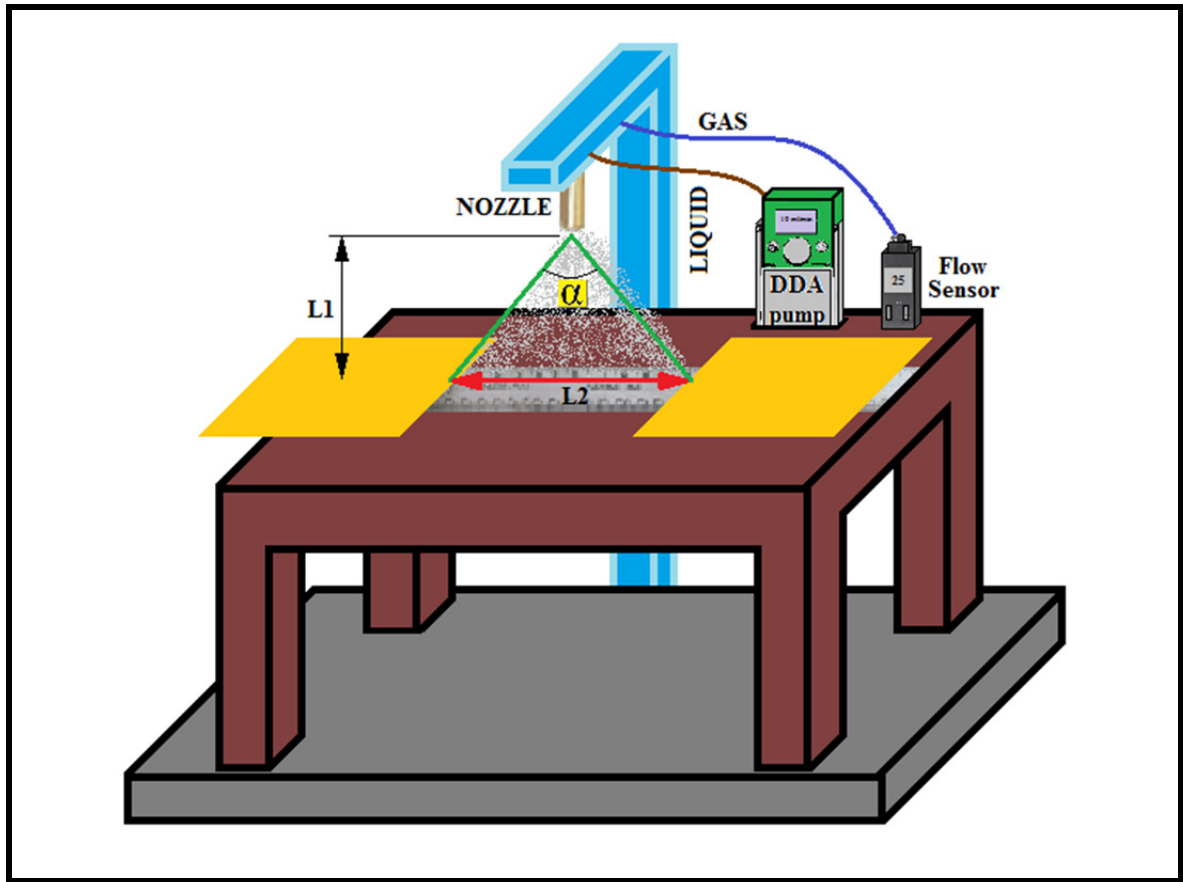


Figure 2.10 Injection angle experiment procedure

2.3.2 Machining quality characteristics measurements

In this study, the machining experiments were carried out on the rods of the aluminium alloy 6061-T6 during the turning operations. Different cutting speeds and feed rates were used under MQC, wet and dry machining methods. Each test is performed on the 100 mm of the rod length. The two different airblast atomizers with straight shape of liquid orifice (Lg20dl0.25 and Lg33.5dl1.00) were used in MQC experiments. These injectors are placed perpendicularly at the distance of 10 cm from the tip of the inserts as shown in Figure 2.11.

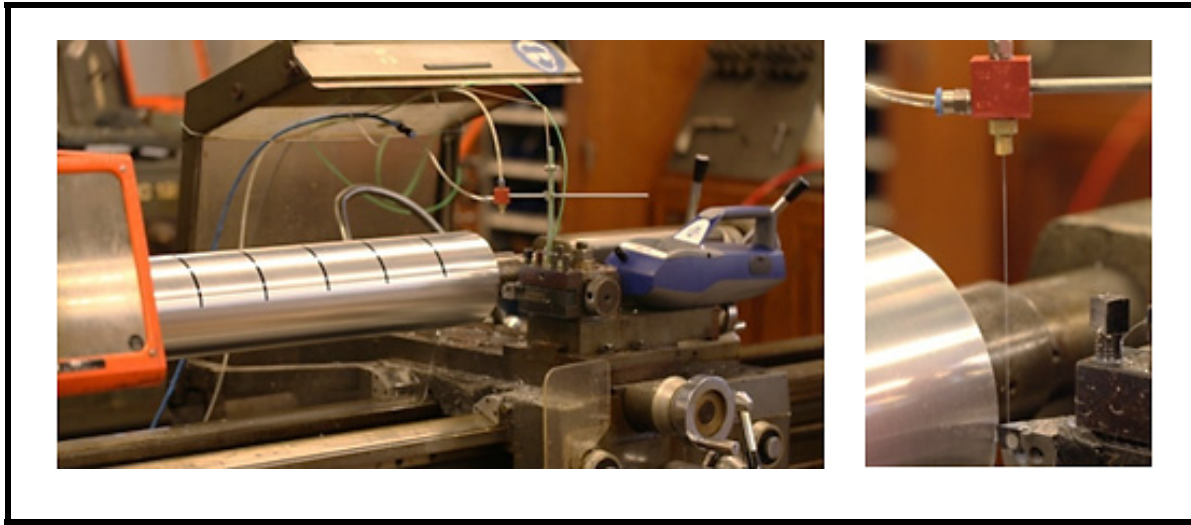


Figure 2.11 The position of injectors

All of the cutting parameters related on the three machining modes (MQC, dry and wet) are given in table 2.8 for the tests carried out by DDA pump and in table 2.9 for the test performed by SLS1.2-2 pump.

Table 2.8 Cutting parameters (Experiments using DDA pump)

Cutting parameters \ Lubrication mode	MQC	DRY	WET
Cutting Speed (m/min)	163 to 633	163 to 633	163 to 633
Feed Rate: (mm/Rev)	0.1 - 0.15 - 0.2	0.1 - 0.15 - 0.2	0.1 - 0.15 - 0.2
Radial depth of cut (mm)	1	1	1
Liquid flow rate (ml/min)	4.2 - 10 - 17.5	-	2600
Gas flow rate (l/min)	15 - 25 - 35 - 45	-	-

Table 2.9 Cutting parameters (Experiments using SLS1.2-2 pump)

Lubrication mode Cutting parameters	MQC	DRY	WET
Cutting Speed (m/min)	79 - 116 - 163 - 206 - 442 - 660		
Feed Rate (mm/Rev)	0.10 - 0.15 - 0.20		
Radial depth of cut (mm)	1	1	1
Liquid flow rate (ml/min)	0.686 - 1.715 - 3.087	-	2600

The cutting temperature measurement was carried out using a thermocouple installed perpendicular to the tool tip at a distance of 6 mm (see Figure 2.12). The temperatures were measured at the second during each test and the maximum of them was chosen for the analysis.

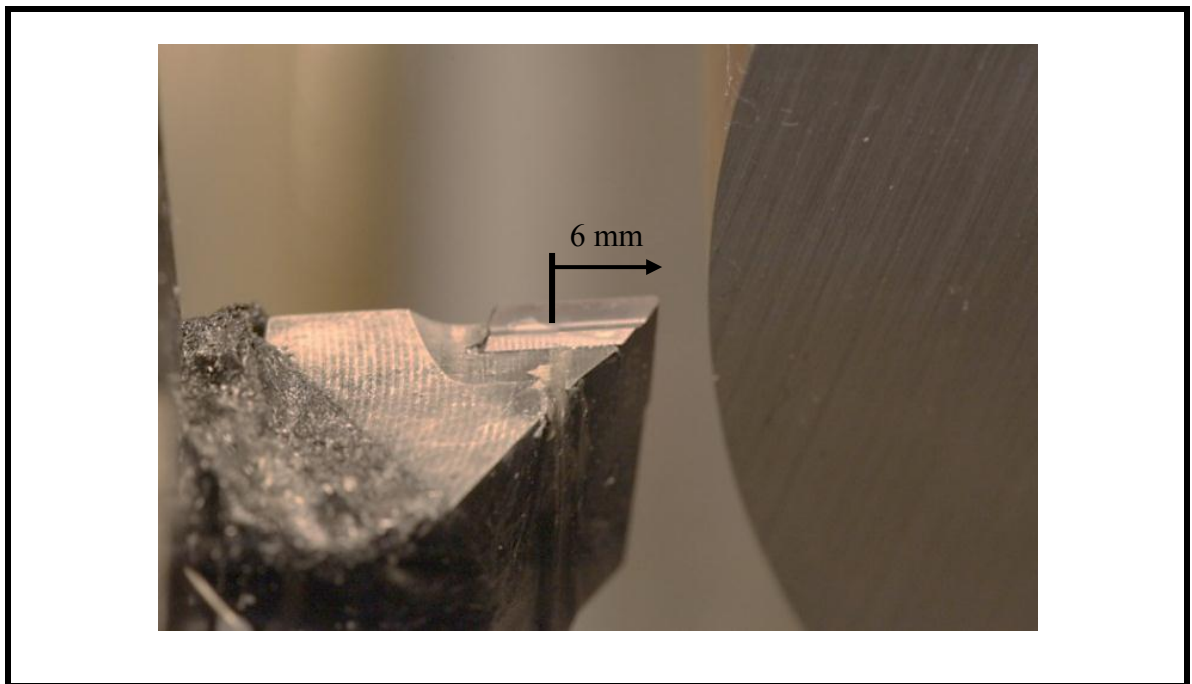


Figure 2.12 The position of thermocouple

2.4 Conclusion

In the present study the turning of aluminum alloy 6061-T6 was carried out on a conventional machine and using the different water soluble coolants such as Emultec and Mecagreen-550 which are the esterified vegetable oils. In these experiments the airblast plain-jet injectors with different geometries and two pumps, continuous and discontinuous, were used. In order to measure the aerosol emission and dust concentration, the TSI 8532 DustTrak – II monitor was used. This apparatus was useful to detect the particles in a range of 0.1 to 10 μm of size and aerosol concentration ranging between 0.001 and 150 mg/m^3 . The results obtained using all of these instruments, are analysed and discussed in the next chapters.

CHAPTER 3

EFFECTS OF ATOMIZER GEOMETRIES ON PARTICLE SIZING AND INJECTION ANGLE

3.1 Introduction

The aim of this chapter is to investigate the effects of plain-jet airblast atomizer geometries and the injection methods (pulsed and non-pulsed) on particle sizing and injection angle. In order to validate this part of experimental study, the particle sizing results will be compared with the empirical equation obtained by Lorenzetto and Lefebvre (section 1.6.3 of chapter 1). This part of experiments is carried out using the six plain-jet airblast atomizers. Based on the geometry, these nozzles are divided into three categories consisting of various liquid jet diameters, various lengths and various liquid orifice shapes. All these three groups are indicated in table 3.1.

Table 3.1 Dimensions of the atomizers

	Lg (mm)	dl (mm)	d_{ge} (mm)	d_{gi} (mm)	Liquid orifice shape
1st gr.	33.5	0.25	4.25	2.75	Straight
	33.5	1.00	4.25	2.75	Straight
2th gr.	10	0.25	4.25	2.75	Straight
	20	0.25	4.25	2.75	Straight
	33.5	0.25	4.25	2.75	Straight
3th gr.	20	0.25	4.25	2.75	Straight
	20	0.25	4.25	2.75	Conical

In this table, Lg is the length of the injector, d_{ge}, d_{gi} and dl are the external and internal gas orifice diameter and liquid orifice diameter respectively. All of these nozzles have the same area of the gas nozzle cross section. The investigations were performed using 4 liquid flow

rates that for each one, the 6 various gas flow rates are applied. The two different pumps such as GLS and DDA allow us to compare the results during this research.

All of the analyses are carried out using multilevel factorial design method with 2 factor interactions which are obtained due to the Statgraphics software (statistical analysis software). The significant parameters identification is done using the method of analysis of variance (ANOVA).

3.2 Effects of liquid orifice diameter

3.2.1 Sauter mean diameter (SMD)

The effect of the liquid orifice diameter on the Sauter mean diameter (SMD) of coaxial two-fluid airblast atomizers has been investigated when using the first group of the nozzles specified in table 3.1.

To compare the results of GLS and DDA pumps in each experiment, the air and Emultec VG are used as gas and liquid with specified flow rates as shown in Table 3.2.

Table 3.2 Gas and liquid flow rates

Gas volumetric flow rate (l/min)	20	25	30	35	40	45
Liquid volumetric flow rate (ml/min)	2.1			4.2		

The effects of each parameter such as gas and liquid flow rates as well as orifice diameters and their interaction effects on particle sizing and injection angle are studied based on the ANOVA as shown in Tables 3.3-3.4 for GLS and DDA pumps respectively.

Table 3.3 The ANOVA table of SMD when using nozzles with different diameters and GLS pump

N	Source	Sum of Squares	Df	Mean Square	F-Ratio	P %
1	\dot{q}_g	17992.10	1	17992.1	102.39	0
2	\dot{q}_l	130.48	1	130.48	0.74	40.08
3	dl	3340.82	1	3340.82	19.01	0.04
4	$\dot{q}_g \times \dot{q}_l$	162.397	1	162.40	0.92	34.99
5	$\dot{q}_g \times d_l$	707.741	1	707.74	4.03	6.09
6	$\dot{q}_l \times d_l$	109.654	1	109.65	0.62	44.04
7	Total error	2987.26	17	175.72		
8	Total (corr.)	25430.4	23			

Table 3.4 The ANOVA table of SMD when using nozzles with different diameters and DDA pump

N	Source	Sum of Squares	Df	Mean Square	F-Ratio	P %
1	\dot{q}_g	13847.60	1	13847.6	121.18	0
2	\dot{q}_l	54.5715	1	54.57	0.48	49.89
3	dl	5.7722	1	5.77	0.05	82.49
4	$\dot{q}_g \times \dot{q}_l$	28.7296	1	28.73	0.25	62.25
5	$\dot{q}_g \times d_l$	395.771	1	395.77	3.46	8.01
6	$\dot{q}_l \times d_l$	21.2252	1	21.23	0.19	67.19
7	Total error	1942.62	17	114.27		
8	Total (corr.)	16296.2	23			

According to the P-value definition, all the parameters in which the P-value is less than 5% have the significant effect on the obtained correlations and the R-squared statistic indicates the percentage of the variability in the investigated parameter where the fitted model is explained.

According to the tables 3.3-3.4 and the previous descriptions, the R-squared for GLS and DDA pumps are 88.25 % and 83.87 %, respectively. Considering the P-values in each table, it is concluded that in the pulsed injection, the gas flow rate and the liquid orifice diameter have the most significant effects. Whereas, the gas flow rate is the only considerable parameter when using the non-pulsed pump. These results are visible in the Pareto charts corresponding to each pump as follows (see Figures 3.1 – 3.2).

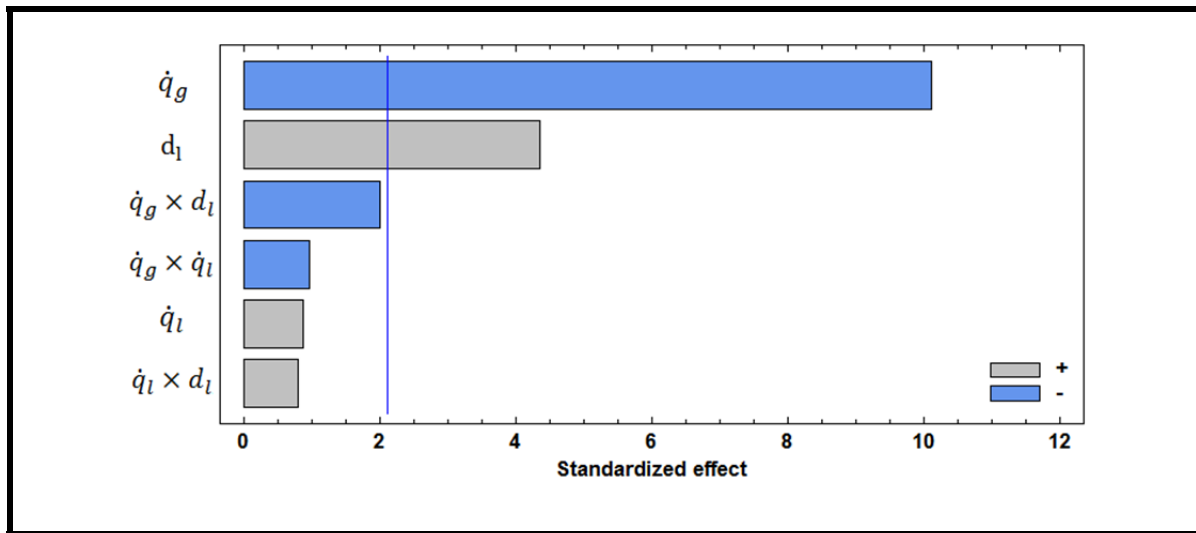


Figure 3.1 Pareto chart of SMD when using nozzles with different diameter and GLS pump

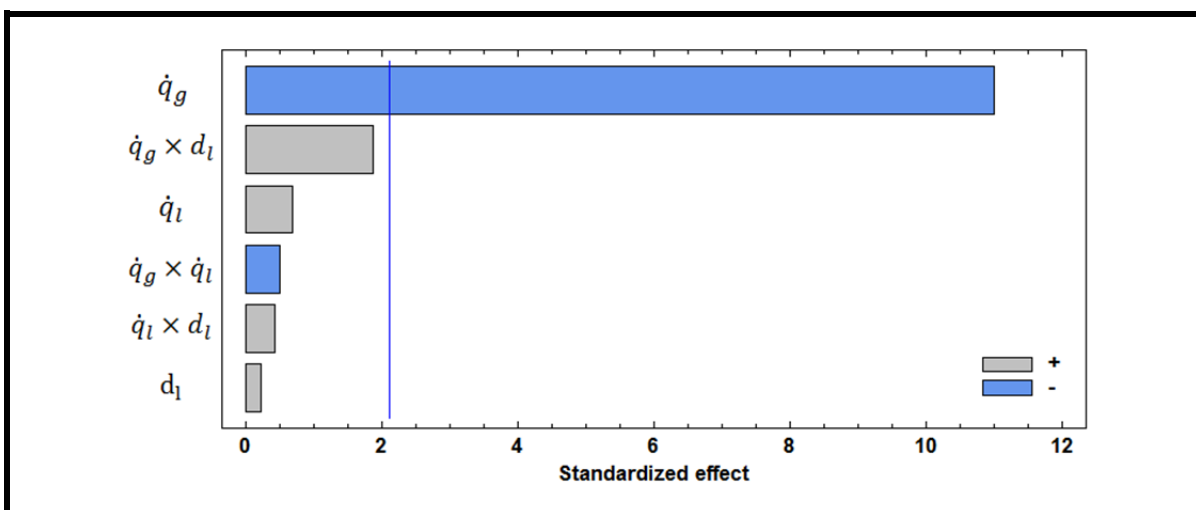


Figure 3.2 Pareto chart of SMD when using nozzles with different diameter and DDA pump

Based on the experimental data and the statistical analysis, the following empirical equations (see Eqs. 3.1-3.2) are formulated to predict the SMD obtained from GLS and DDA pumps where \dot{q}_g , dl , and SMD are in liter per minute, millimeter and micrometer respectively. The SMD values corresponding to these equations are plotted in Figure 3.3.

$$SMD = 153.18 - 3.21\dot{q}_g + 31.46dl \quad (3.1)$$

$$SMD = 141.68 - 2.81\dot{q}_g \quad (3.2)$$

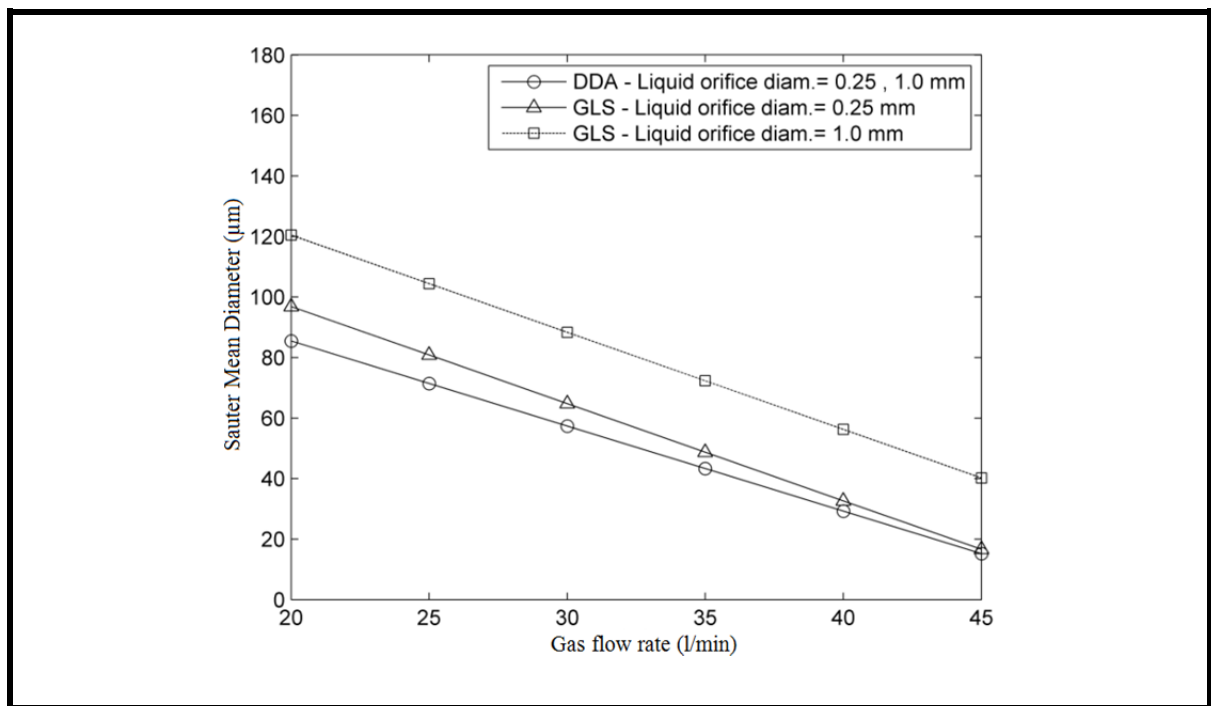


Figure 3.3 SMD related to gas flow rate for GLS and DDA pumps when using nozzles with different liquid orifice diameters

According Figure 3.3, in both of pumps the SMD is linearly reduced where the gas flow rate increases. In the pulsed pump, the atomizer with lower liquid orifice diameter produces the lower droplet size which means good atomization. The droplet size is independent from the liquid orifice diameter when using continuous pump.

According to experimental observation; a better atomization was consistently achieved when using DDA pump. Figure 3.3 shows that in higher gas flow rates, the SMD values are similar in pulsed and non-pulsed pumps when using atomizers with lower liquid orifice diameter.

3.2.2 Injection angle

According to the ANOVA results presented in Tables 3.5 – 3.6, it is clear that in pulsed and non-pulsed pumps, the parameters such as gas flow rate, liquid flow rate and liquid orifice diameter have the significant effects on the injection angle. Furthermore, the injection angle is affected by interaction effects between liquid flow rate and liquid orifice diameter when using pulsed pump while the continuous pump is influenced by the interaction effect between gas and liquid flow rates. It is substantial that in both of these pumps, liquid flow rate is the most effective parameter on the injection angle.

The R-squared for GLS and DDA pumps are 99.64% and 97.83 % respectively and the percentage contribution of each parameter affecting injection angle are shown in table 3.7.

Table 3.5 The ANOVA table of injection angle when using nozzles with different diameters and GLS pump

N	Source	Sum of Squares	Df	Mean Square	F-Ratio	P %
1	\dot{q}_g	87.5618	1	87.56	110.05	0
2	\dot{q}_l	3343.18	1	3343.18	4201.77	0
3	dl	146.817	1	146.82	184.52	0
4	$\dot{q}_g \times \dot{q}_l$	16.856	1	16.86	21.19	0.03
5	$\dot{q}_g \times d_l$	19.0948	1	19.09	24	0.01
6	$\dot{q}_l \times d_l$	87.0966	1	87.10	109.46	0
7	Total error	13.5262	17	0.80		
8	Total (corr.)	3714.13	23			

Table 3.6 The ANOVA table of injection angle when using nozzles with different diameters and DDA pump

N	Source	Sum of Squares	Df	Mean Square	F-Ratio	P %
1	\dot{q}_g	125.357	1	125.36	315.78	0
2	\dot{q}_l	146.372	1	146.37	368.72	0
3	dl	29.018	1	29.02	73.1	0
4	$\dot{q}_g \times \dot{q}_l$	3.73296	1	3.73	9.4	0.07
5	$\dot{q}_g \times d_l$	0.02860	1	0.029	0.07	79.16
6	$\dot{q}_l \times d_l$	0.00010	1	0.0001	0.0003	98.73
7	Total error	6.74856	17	0.40		
8	Total (corr.)	311.258	23			

Table 3.7 Percentage contribution of parameters affecting injection angle

Percentage Contribution						
	\dot{q}_g (l/min)	\dot{q}_l (ml/min)	dl (mm)	$\dot{q}_g \times \dot{q}_l$ (l/min)× (ml/min)	$\dot{q}_g \times dl$ (l/min)×(mm)	$\dot{q}_l \times dl$ (ml/min)× (mm)
GLS pump	2.35	90.01	3.95	0.45	0.51	2.34
DDA pump	40.27	47.02	9.32	1.20	-	-

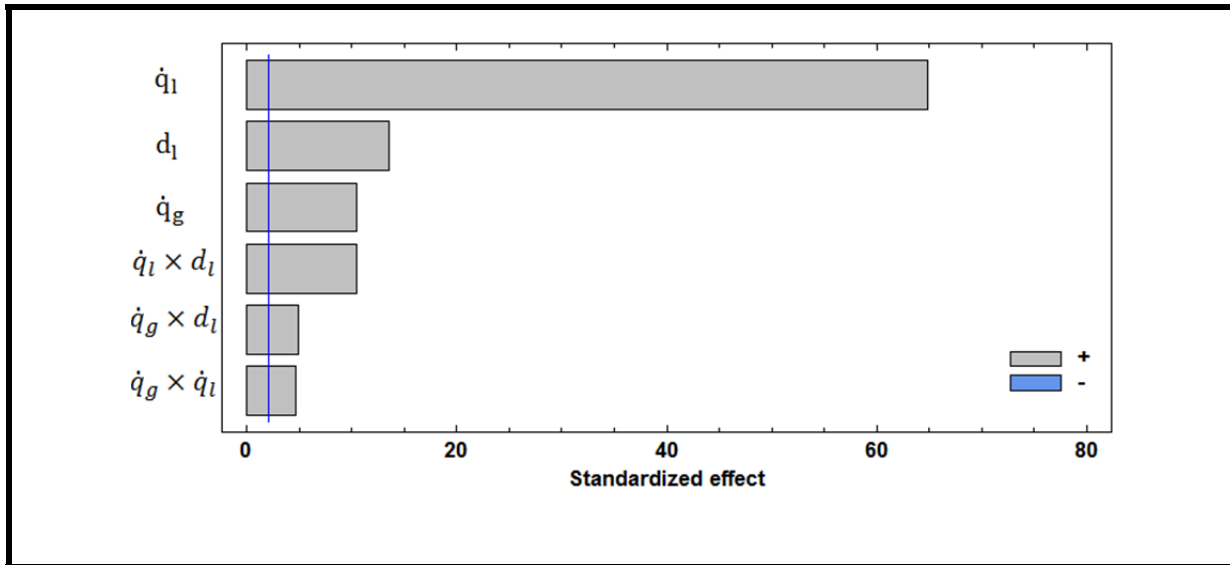


Figure 3.4 Pareto chart of injection angle when using nozzles with different diameters and GLS pump

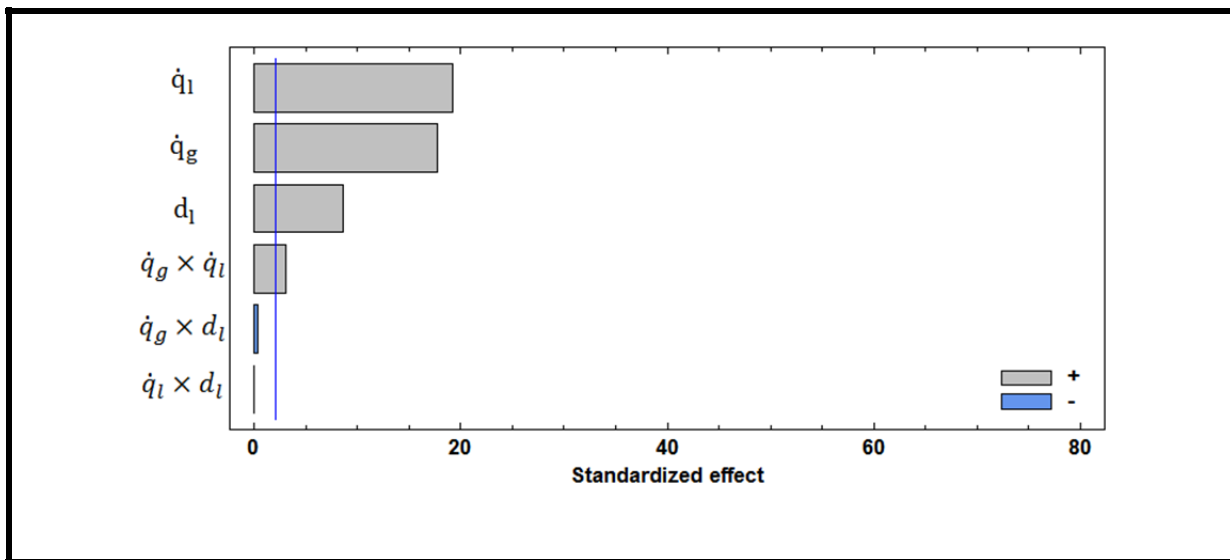


Figure 3.5 Pareto chart of injection angle when using nozzles with different diameters and DDA pump

The experimental equations obtained from the statistical analysis (Equations 3.3 and 3.4 for GLS and DDA pumps respectively) are plotted (see Figures 3.6 – 3.7) in order to investigate the behaviour of the nozzles with different liquid orifice diameters and the influences of the pumps features.

$$\alpha = -0.72 - 0.24\dot{q}_g + 5.18\dot{q}_l - 17.70d_l + 0.09\dot{q}_g\dot{q}_l + 0.28\dot{q}_gd_l + 4.84\dot{q}_ld_l \quad (3.3)$$

$$\alpha = 2.71 + 0.12\dot{q}_g + 0.92\dot{q}_l + 2.93d_l + 0.04\dot{q}_g\dot{q}_l \quad (3.4)$$

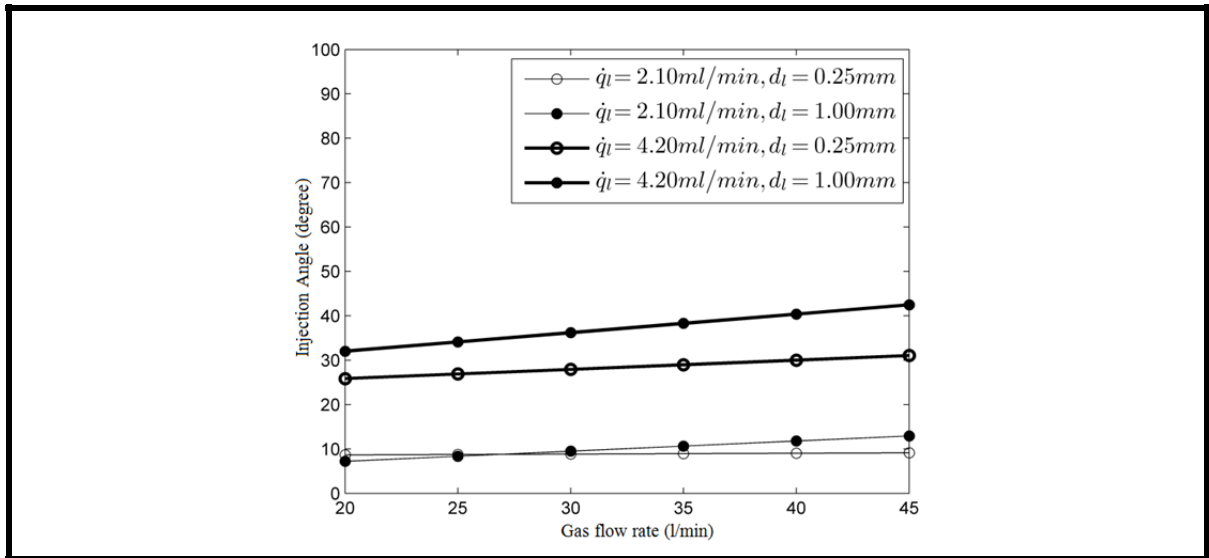


Figure 3.6 Injection angle related to gas flow rate for GLS pump when using nozzles with different liquid orifice diameters

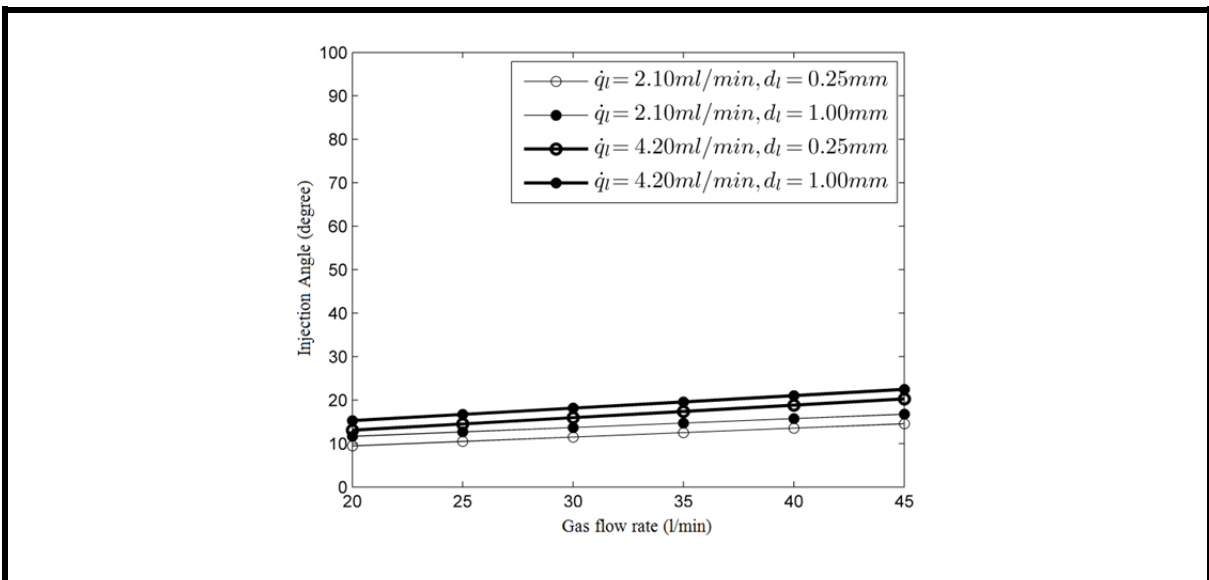


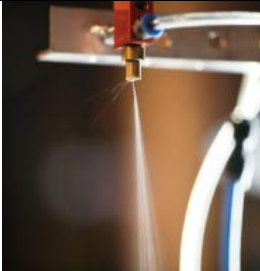


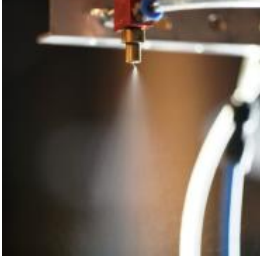
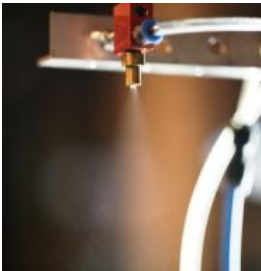




Figure 3.7 Injection angle related to gas flow rate for DDA pump when using nozzles with different liquid orifice diameters

According to the Figures 3.6 - 3.7, it is clear that the injection angle is increased due to increase in the liquid and gas flow rates as well as in the liquid orifice diameter. However, this increase is carried out regularly in DDA pump while in GLS pump is performed smoothly in the lowest liquid flow rate and the liquid orifice diameter. As shown in Figure 3.6, increasing the liquid orifice diameter when using higher liquid flow rate leads to considerable increase in the injection angle. To better understand the influences of the studied parameters on injection angle, several real examples are shown in table 3.8.

Table 3.8 Examples of the measured injection angle

	$\dot{q}_l = 4.2 \text{ ml/min}$	$\dot{q}_l = 10.0 \text{ ml/min}$	$\dot{q}_l = 17.5 \text{ ml/min}$
$\dot{q}_g = 20 \text{ l/min}$	 $\alpha = 10.66^\circ$	 $\alpha = 18.92^\circ$	 $\alpha = 20.22^\circ$
$\dot{q}_g = 30 \text{ l/min}$	 $\alpha = 16.50^\circ$	 $\alpha = 21.88^\circ$	 $\alpha = 24.27^\circ$
$\dot{q}_g = 40 \text{ l/min}$	 $\alpha = 20.04^\circ$	 $\alpha = 23.17^\circ$	 $\alpha = 29.33^\circ$

3.3 Effects of atomizer length

In this section, where the second group of nozzles as shown in table 3.1 are used, the effects of the atomizer length on SMD and injection angle are investigated. The similar analysis method as previous section has been used. Therefore, the results and their conclusions are only being explained.

3.3.1 Sauter mean diameter (SMD)

According to the ANOVA tables 3.9 - 3.10 of GLS and DDA pumps with the R-squared of 75.72% and 74.29% respectively, it is observed that the P-value of gas flow rate in both of these pumps is less than 5%. Therefore, the only parameter which has the significant effect on SMD is gas flow rate.

The empirical equations obtained from the experiments and statistical analysis (Equations 3.5 - 3.6 for GLS and DDA pumps respectively) are plotted in Figure 3.8 which simplifies the investigation of the nozzle length effects on SMD.

$$\text{SMD} = 148.42 - 2.86 \dot{q}_g \quad (3.5)$$

$$\text{SMD} = 144.46 - 2.88 \dot{q}_g \quad (3.6)$$

Table 3.9 The ANOVA table of SMD when using nozzles with different lengths and GLS pump

N	Source	Sum of Squares	Df	Mean Square	F-Ratio	P %
1	\dot{q}_g	21121.8	1	21121.8	85.13	0
2	\dot{q}_l	195.234	1	195.23	0.79	38.23
3	L	179.097	1	179.10	0.72	40.25
4	$\dot{q}_g \times \dot{q}_l$	61.5634	1	61.56	0.25	62.22
5	$\dot{q}_g \times L$	262.444	1	262.44	1.06	31.22
6	$\dot{q}_l \times L$	228.182	1	228.18	0.92	34.55
7	Total error	7195.42	29	248.12		
8	Total (corr.)	29635.1	35			

Table 3.10 The ANOVA table of SMD when using nozzles with different lengths and DDA pump

N	Source	Sum of Squares	Df	Mean Square	F-Ratio	P %
1	\dot{q}_g	21789.1	1	21789.1	75.82	0
2	\dot{q}_l	650.049	1	650.05	2.26	14.34
3	L	652.292	1	652.29	2.27	14.27
4	$\dot{q}_g \times \dot{q}_l$	523.092	1	523.09	1.82	18.77
5	$\dot{q}_g \times L$	18.7561	1	18.76	0.07	80.02
6	$\dot{q}_l \times L$	377.611	1	377.61	1.31	2.61
7	Total error	8334.06	29	287.38		
8	Total (corr.)	32411.3	35			

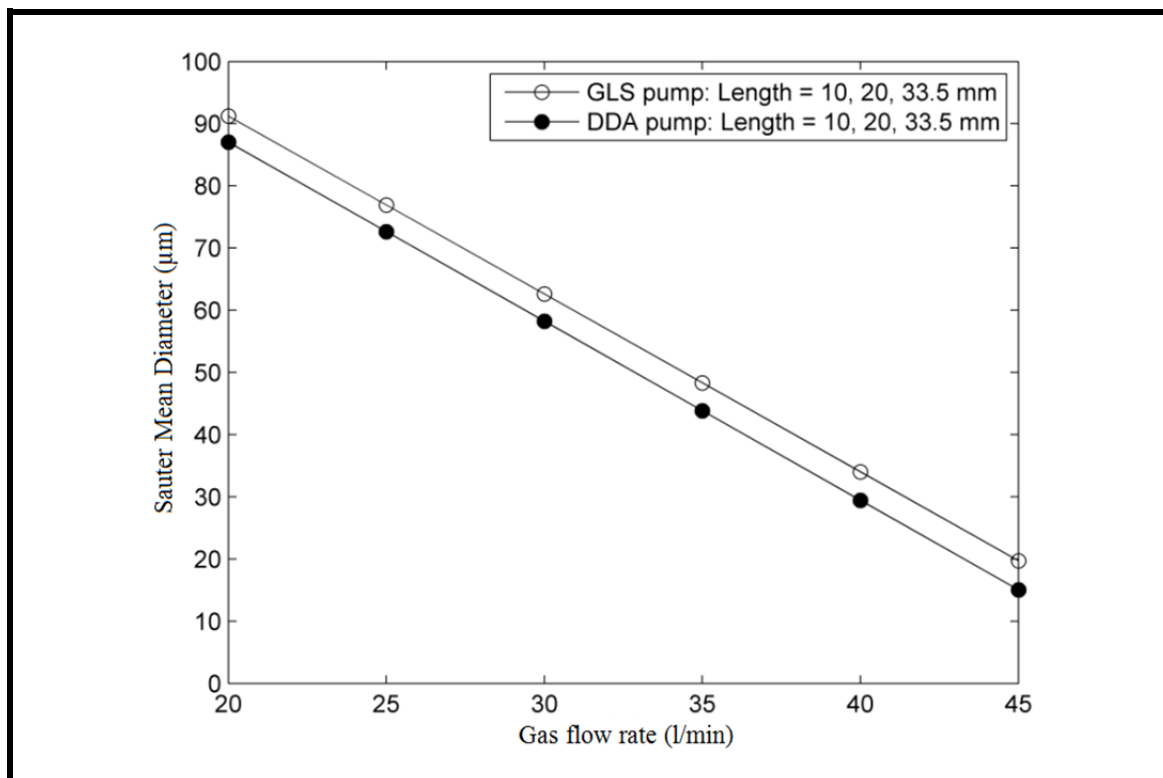


Figure 3.8 SMD related to gas flow rate when using nozzles with different lengths

Based on Figure 3.8, it is concluded that the quality of atomization is independent of the pump type and it regularly increases when using injectors with different lengths. However, the SMD values in DDA pump are always less than that in GLS pump. This means that the better atomization occurs in continuous pumps.

3.3.2 Injection angle

According to the ANOVA tables 3.11-3.12 with 91.03% and 89.30% of R-squared for GLS and DDA pumps respectively, it is clear that due to the P-values, the gas and liquid flow rates are the most effective parameters on the injection angle using both of the pumps while the substantial effect of atomizer length occurs when using DDA pump.

The empirical equations 3.7 – 3.8 obtained using the GLS and DDA pumps, are shown graphically in Figures 3.9 - 3.10. These Figures show that the injection angle increases due to increase in the air and liquid flow rate. In pulsed pump the increase is occurred independently from the injector length while in DDA pump the increase in the atomizer length decreases the injection angle.

$$\alpha = -15.09 + 0.23 \dot{q}_g + 8.40 \dot{q}_l \quad (3.7)$$

$$\alpha = -5.11 + 0.38 \dot{q}_g + 2.99 \dot{q}_l - 0.07 L \quad (3.8)$$

Table 3.11 The ANOVA table of injection angle when using nozzles with different lengths and GLS pump

N	Source	Sum of Squares	Df	Mean Square	F-Ratio	P %
1	\dot{q}_g	134.344	1	134.34	13.19	0.11
2	\dot{q}_l	2771.49	1	2771.49	271.98	0
3	L	0.04590	1	0.05	0.005	94.69
4	$\dot{q}_g \times \dot{q}_l$	25.4758	1	25.48	2.5	12.46
5	$\dot{q}_g \times L$	23.2511	1	23.25	2.28	14.17
6	$\dot{q}_l \times L$	7.14443	1	7.14	0.7	40.92
7	Total error	295.437	29	10.19		
8	Total (corr.)	3291.82	35			

Table 3.12 The ANOVA table of injection angle when using nozzles with different lengths and DDA pump

N	Source	Sum of Squares	Df	Mean Square	F-Ratio	P %
1	\dot{q}_g	379.137	1	379.14	117.26	0
2	\dot{q}_l	344.645	1	344.65	106.6	0
3	L	14.9172	1	14.92	4.61	4.02
4	$\dot{q}_g \times \dot{q}_l$	0.73250	1	0.73	0.23	63.77
5	$\dot{q}_g \times L$	11.569	1	11.57	3.58	6.86
6	$\dot{q}_l \times L$	12.5602	1	12.56	3.88	5.83
7	Total error	93.7628	29	3.23		
8	Total (corr.)	876.093	35			

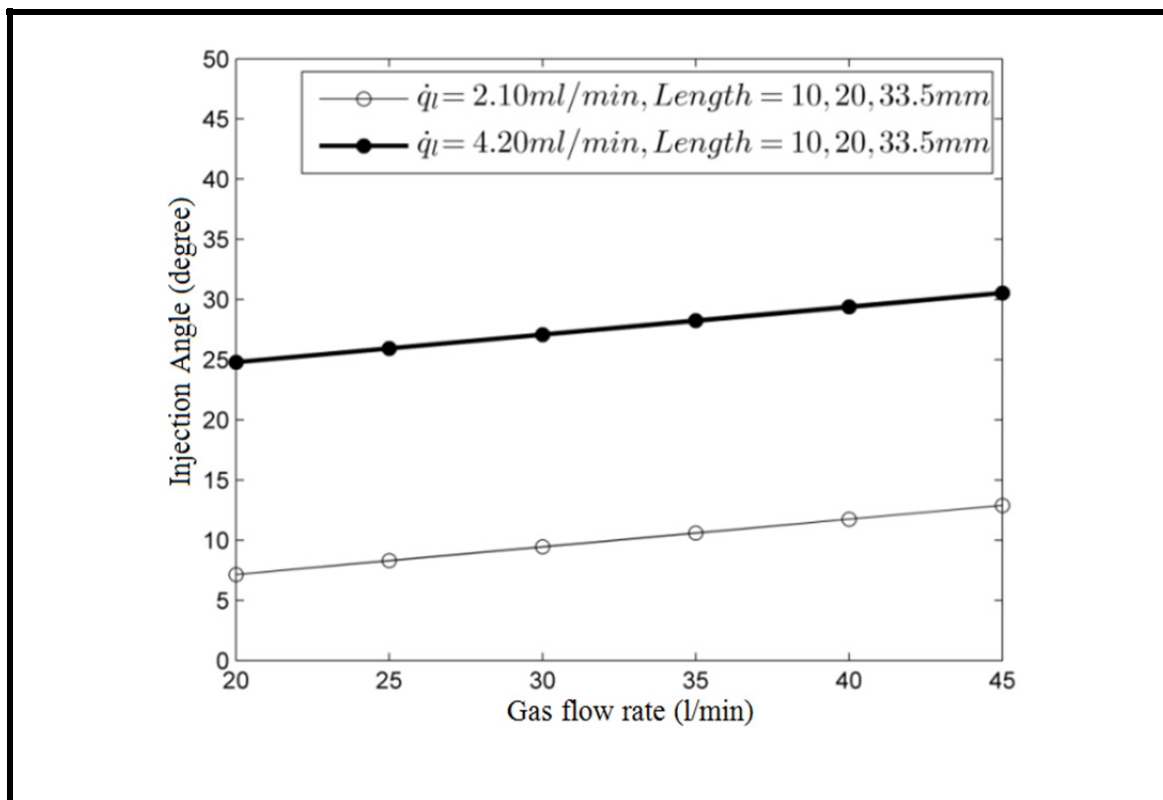


Figure 3.9 Injection angle related to gas flow rate when using nozzles with different lengths and GLS pump

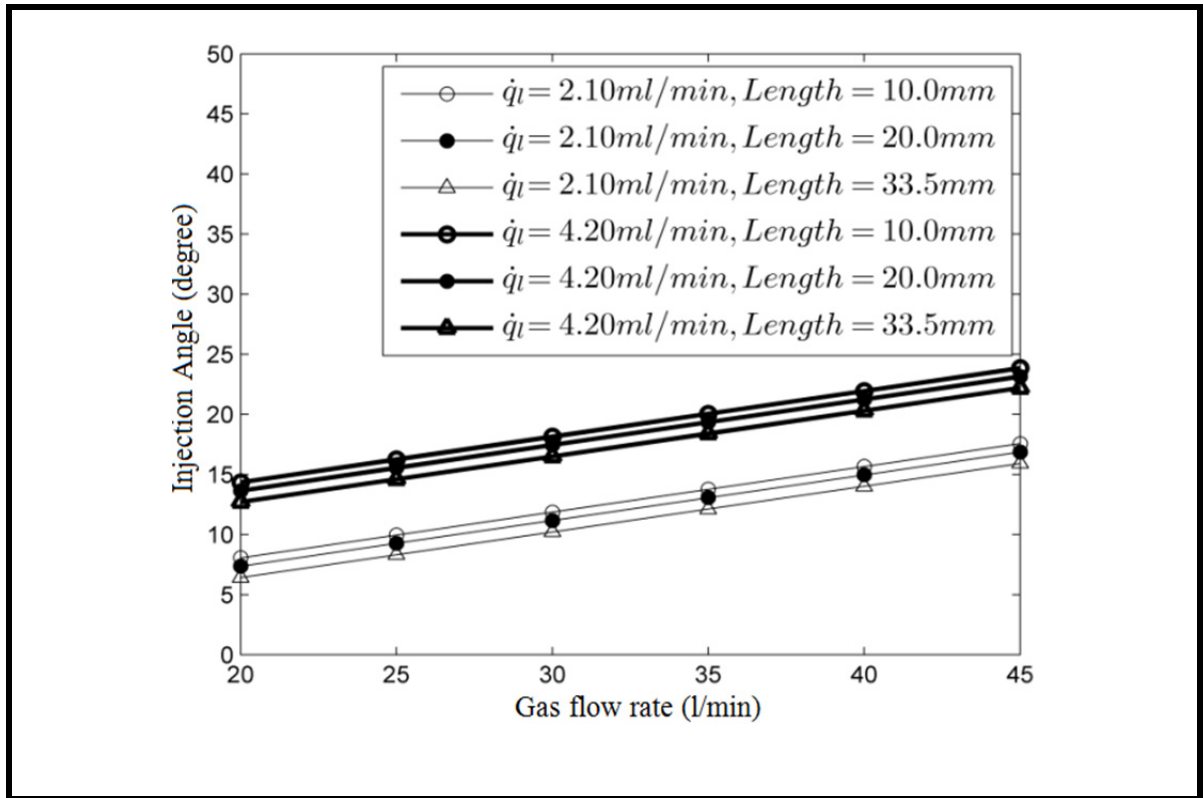
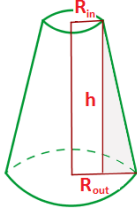



Figure 3.10 Injection angle related to gas flow rate when using nozzles with different lengths and DDA pump

3.4 Effects of liquid orifice shape

In this section, the effects of the liquid orifice shape of atomizers on the particle sizing and the injection angle is investigated. Two nozzles with the same length and liquid orifice diameter are used where their liquid orifices are straight and conical. The shape of the orifices and the difference between the fraction of internal and external liquid orifice diameters (R) are presented in table 3.13.

Table 3.13 Liquid orifice shapes

Liquid orifice shape	Conical	Straight
		
$R = R_{in} / R_{out}$	0.21	1

3.4.1 Sauter mean diameter (SMD)

The ANOVA tables 3.14 - 3.15 with 84.75% and 83.54% of R-squared for GLS and DDA pumps respectively, show that the most effective parameters on SMD are the gas flow rate and liquid orifice shape for both of the pumps. However, the effect of the interaction effects between these two parameters on SMD is observed only by using non-pulsed pump.

The empirical equations 3.9 – 3.10 for GLS and DDA pumps respectively are being plotted in Figure 3.11. This Figure helps us to investigate the behaviour of each nozzle and injection method.

$$SMD = 336.79 - 7.13 \dot{q}_g - 205.58 R + 4.50 \dot{q}_g R \quad (3.9)$$

$$SMD = 180.49 - 2.90 \dot{q}_g - 44.71 R \quad (3.10)$$

Table 3.14 The ANOVA table of SMD when
using nozzles with different orifice shapes and GLS pump

N	Source	Sum of Squares	Df	Mean Square	F-Ratio	P %
1	\dot{q}_g	33989.9	1	33989.9	60.58	0
2	\dot{q}_l	1.6485	1	1.65	0.003	95.74
3	R	13200.9	1	13200.9	23.53	0.01
4	$\dot{q}_g \times \dot{q}_l$	267.405	1	267.41	0.48	49.93
5	$\dot{q}_g \times R$	5525.58	1	5525.58	9.85	0.6
6	$\dot{q}_l \times R$	17.7332	1	17.73	0.03	86.1
7	Total error	9538.53	17	561.09		
8	Total (corr.)	62541.7	23			

Table 3.15 The ANOVA table of SMD when
using nozzles with different orifice shapes and DDA pump

N	Source	Sum of Squares	Df	Mean Square	F-Ratio	P %
1	\dot{q}_g	14704	1	14704	53.18	0
2	\dot{q}_l	389.057	1	389.06	1.41	25.18
3	R	7484.66	1	7484.66	27.07	0.01
4	$\dot{q}_g \times \dot{q}_l$	343.414	1	343.41	1.24	28.06
5	$\dot{q}_g \times R$	933.634	1	933.63	3.38	8.37
6	$\dot{q}_l \times R$	0.98820	1	0.99	0.003	95.3
7	Total error	4700.15	17	276.48		
8	Total (corr.)	28555.9	23			

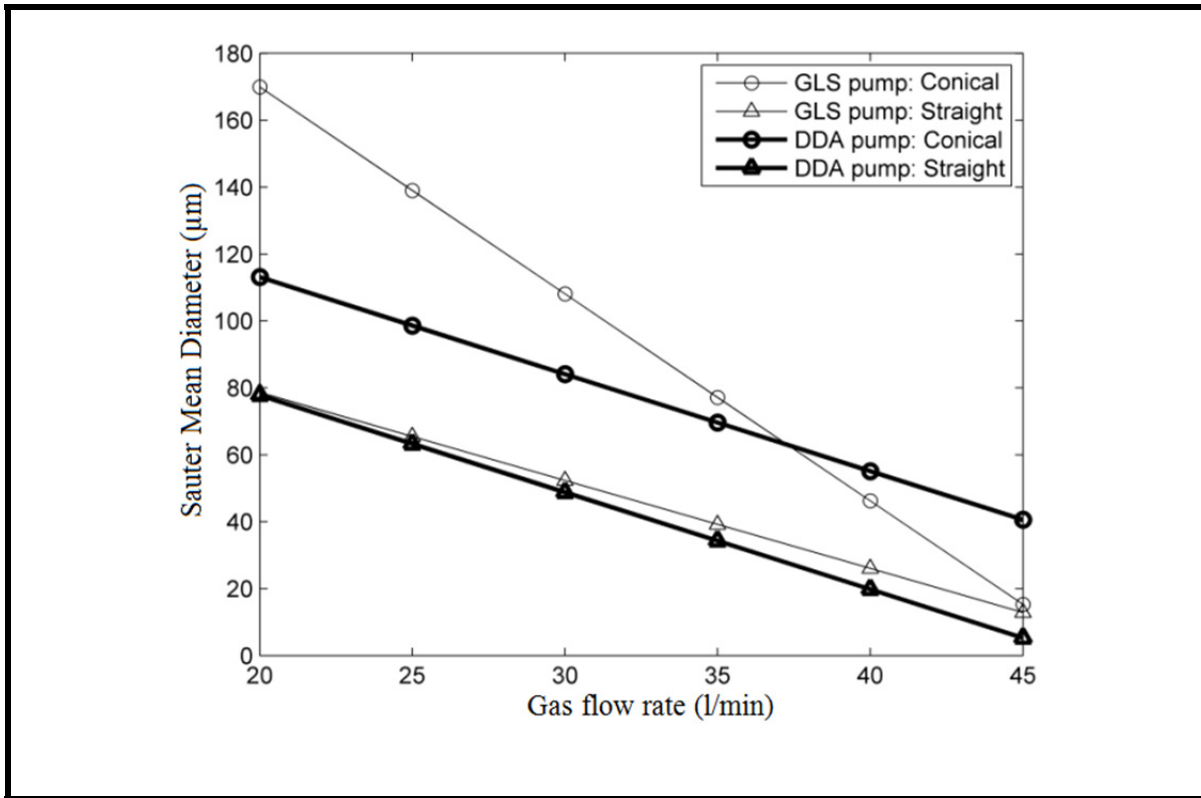


Figure 3.11 SMD related to gas flow rate when using nozzles with different orifice shapes

According to Figure 3.11, the increase in gas flow rate decreases particle diameters when using nozzles with different liquid orifice shapes. It is observed that the nozzles with straight liquid orifice shape improve the atomization quality more than that of the other liquid orifice shape.

Figure 3.11 shows that the SMD variations are parallel in both of the nozzles when using DDA pump while a convergence between the results is observed in the higher gas flow rates when using pulsed pump.

3.4.2 Injection angle

The analysis of variance of the results obtained from the injection angle investigations shows that all of the parameters such as gas flow rate, liquid flow rate and liquid orifice shape have the significant effects on the injection angle. This result is obviously shown in ANOVA

tables 3.16 - 3.17 with 99.76% and 96.95% of R-squared for GLS and DDA pumps respectively.

According to the experimental equations 3.11-3.12 using GLS and DDA pumps and the related graphs as shown in Figures 3.12-3.13 it is concluded that the increase in gas flow rate increases the injection angle in both of the pumps. This result is independent from liquid flow rate and liquid orifice shape.

$$\alpha = 0.26 + 0.002 \dot{q}_g + 0.23 \dot{q}_l + 3.66 R + 0.068 \dot{q}_g \dot{q}_l + 2.33 \times \dot{q}_l R \quad (3.11)$$

$$\alpha = -16.05 + 0.51 \dot{q}_g + 5.38 \dot{q}_l + 4.74 R - 2.53 \dot{q}_l R \quad (3.12)$$

Table 3.16 The ANOVA table of injection angle when using nozzles with different orifice shapes and GLS pump

N	Source	Sum of Squares	Df	Mean Square	F-Ratio	P %
1	\dot{q}_g	80.6896	1	80.69	591.38	0
2	\dot{q}_l	389.057	1	389.06	2851.43	0
3	R	452.489	1	452.49	3316.32	0
4	$\dot{q}_g \times \dot{q}_l$	8.79692	1	8.797	64.47	0
5	$\dot{q}_g \times R$	0.23374	1	0.23	1.71	2.08
6	$\dot{q}_l \times R$	22.3687	1	22.37	163.94	0
7	Total error	2.31953	17	0.14		
8	Total (corr.)	955.954	23			

Table 3.17 The ANOVA table of injection angle when using nozzles with different orifice shapes and DDA pump

N	Source	Sum of Squares	Df	Mean Square	F-Ratio	P %
1	\dot{q}_g	458.957	1	458.96	268.13	0
2	\dot{q}_l	393.174	1	393.17	229.7	0
3	R	38.9131	1	38.91	22.73	0.02
4	$\dot{q}_g \times \dot{q}_l$	2.22501	1	2.23	1.3	27
5	$\dot{q}_g \times R$	4.99023	1	4.99	2.92	10.59
6	$\dot{q}_l \times R$	26.3761	1	26.38	15.41	0.11
7	Total error	29.0986	17	1.71		
8	Total (corr.)	953.734	23			

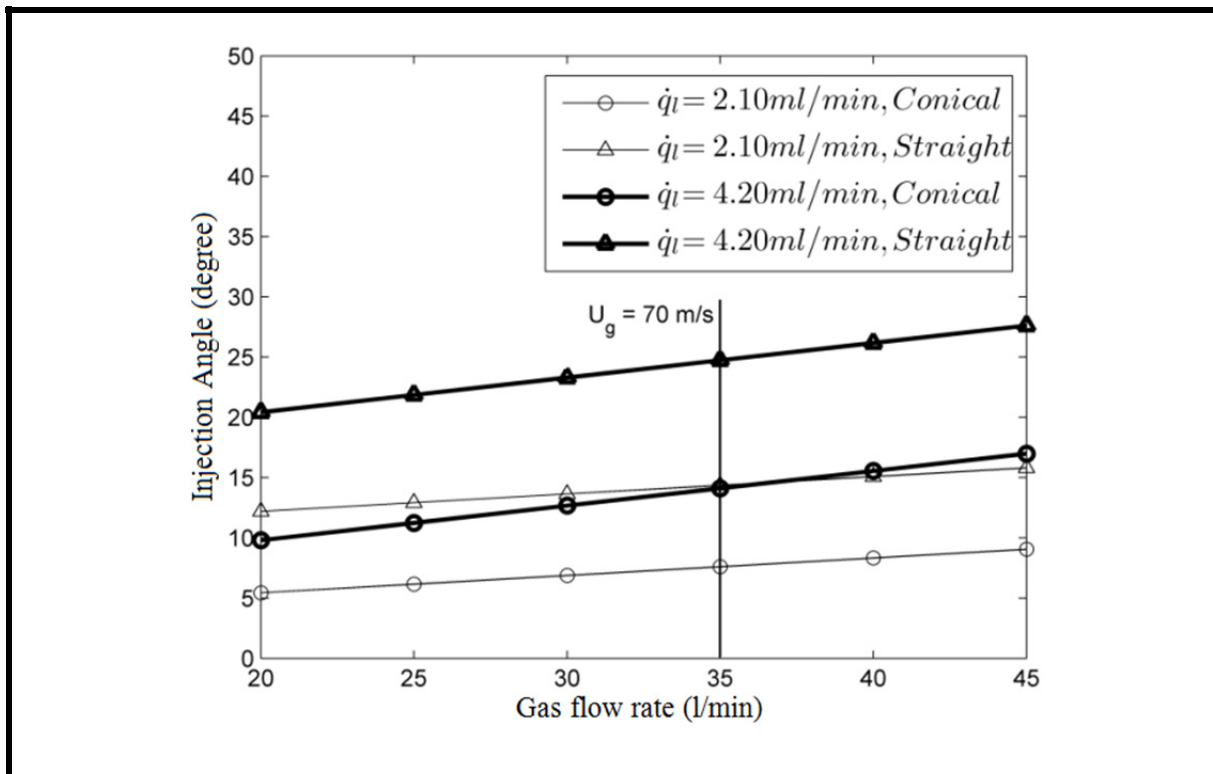


Figure 3.12 Injection angle related to gas flow rate when using nozzles with different orifice shapes and GLS pump

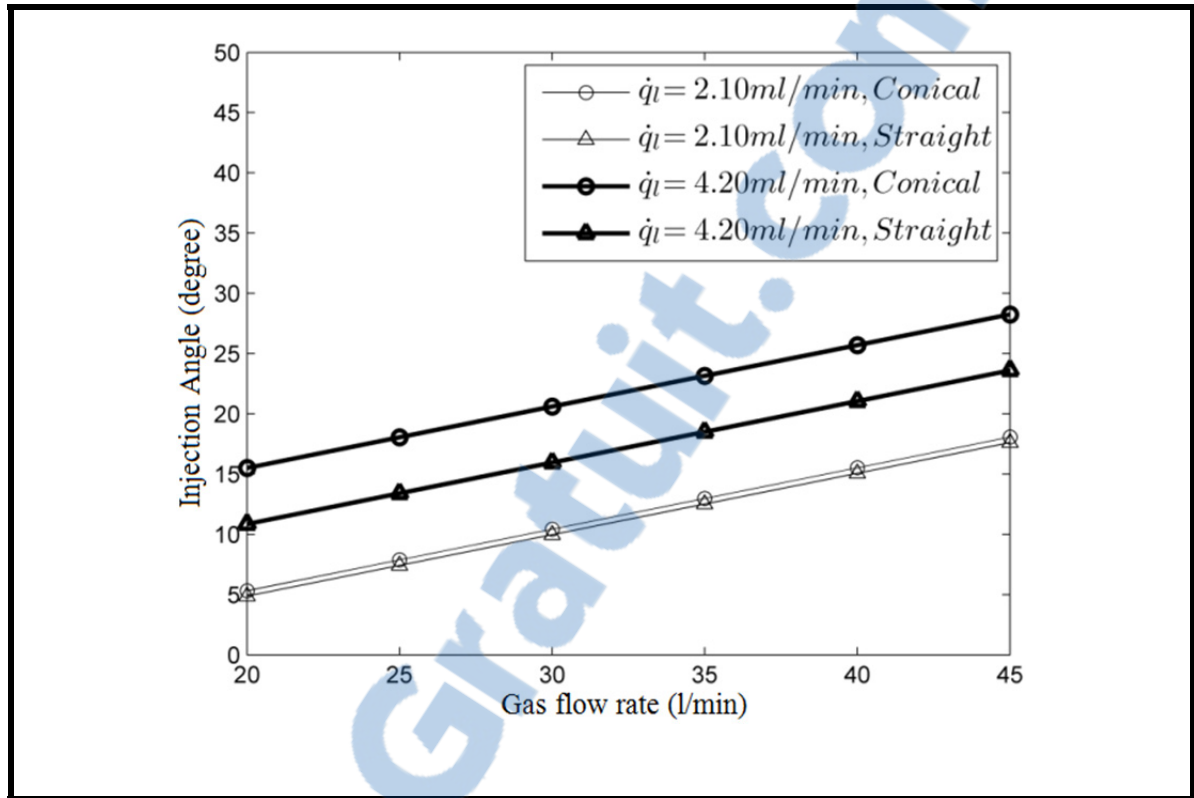


Figure 3.13 Injection angle related to gas flow rate when using nozzles with different orifice shapes and DDA pump

There are few differences between the injection angle distribution in DDA and GLS pumps with regards to different liquid flow rates and liquid orifice shapes which are explained as follow:

In DDA pump:

- In higher liquid flow rates, the injection angle is always higher than that in lower liquid flow rates;
- In each liquid flow rate, the injection angle is higher in the nozzles with conical liquid orifice and the lubrication could be carried out in the larger surface of cutting zone.

In GLS pump:

- Contrary to the DDA pump, in each liquid flow rate, the injection angle is higher in the nozzles with straight liquid orifice;

- In different gas velocities, the following relationships exist:

$$\begin{cases} U_g < 70 \text{ m/s} \Rightarrow \alpha_{\dot{q}_l=2.1 \frac{\text{ml}}{\text{min}}}^{\text{straight}} > \alpha_{\dot{q}_l=4.2 \frac{\text{ml}}{\text{min}}}^{\text{conical}} \\ U_g = 70 \text{ m/s} \Rightarrow \alpha_{\dot{q}_l=2.1 \frac{\text{ml}}{\text{min}}}^{\text{straight}} = \alpha_{\dot{q}_l=4.2 \frac{\text{ml}}{\text{min}}}^{\text{conical}} \\ U_g > 70 \text{ m/s} \Rightarrow \alpha_{\dot{q}_l=2.1 \frac{\text{ml}}{\text{min}}}^{\text{straight}} < \alpha_{\dot{q}_l=4.2 \frac{\text{ml}}{\text{min}}}^{\text{conical}} \end{cases}$$

3.5 Atomizer geometry effects on SMD and injection angles when using continuous pump and high liquid flow rates

In this section, the three groups of nozzles and different gas and liquid flow rates indicated in tables 3.1 – 3.18 respectively are employed to investigate the effects of the nozzle geometries on SMD and injection angle. In this study, the injection is carried out using the continuous pump (DDA pump) and higher liquid flow rates.

Table 3.18 Gas and liquid flow rates

Gas volumetric flow rate (l/min)	20	25	30	35	40	45
Liquid volumetric flow rate (ml/min)	2.1	4.2	10	17.5		

The ANOVA will be used in this section to interpret the results obtained through experimental works.

3.5.1 Liquid orifice diameter effects

According to the tables 3.19 - 3.20, it is observed that the most effective parameters in SMD are gas flow rate, liquid flow rate, interactions effects between gas and liquid flow rate and interaction effect between gas flow rate and liquid orifice diameter. However, the parameters such as gas flow rate, liquid flow rate, liquid orifice diameter and interaction effects between liquid flow rate and liquid orifice diameter have the considerable effects on injection angle.

Table 3.19 The ANOVA table of SMD when using nozzles with different liquid orifice diameter and DDA pump

N	Source	Sum of Squares	Df	Mean Square	F-Ratio	P %
1	\dot{q}_g	47722.1	1	47722.1	159.91	0
2	\dot{q}_l	4435.94	1	4435.94	14.86	0.04
3	dl	219.989	1	219.99	0.74	39.56
4	$\dot{q}_g \times \dot{q}_l$	3356.65	1	3356.65	11.25	0.17
5	$\dot{q}_g \times d_l$	2331.23	1	2331.23	7.81	0.79
6	$\dot{q}_l \times d_l$	299.733	1	299.73	1.00	32.21
7	Total error	12235.8	41	298.43		
8	Total (corr.)	67252.8	47			

Table 3.20 The ANOVA table of injection angle when using nozzles with different liquid orifice diameter and DDA pump

N	Source	Sum of Squares	Df	Mean Square	F-Ratio	P %
1	\dot{q}_g	377.866	1	377.87	27.84	0
2	\dot{q}_l	4649.32	1	4649.32	342.54	0
3	dl	482.169	1	482.17	35.52	0
4	$\dot{q}_g \times \dot{q}_l$	9.10481	1	9.10	0.67	41.75
5	$\dot{q}_g \times d_l$	0.31256	1	0.31	0.02	88.01
6	$\dot{q}_l \times d_l$	186.739	1	186.74	13.76	0.06
7	Total error	556.502	41	13.57		
8	Total (corr.)	6149.71	47			

Referring to the main effect plots of SMD and injection angle (see Figures 3.14 – 3.15), it is concluded that increasing gas and liquid flow rates increases and decreases the SMD respectively. According to Figure 3.15, higher injection angle can be obtained when using higher levels of experimental parameters.

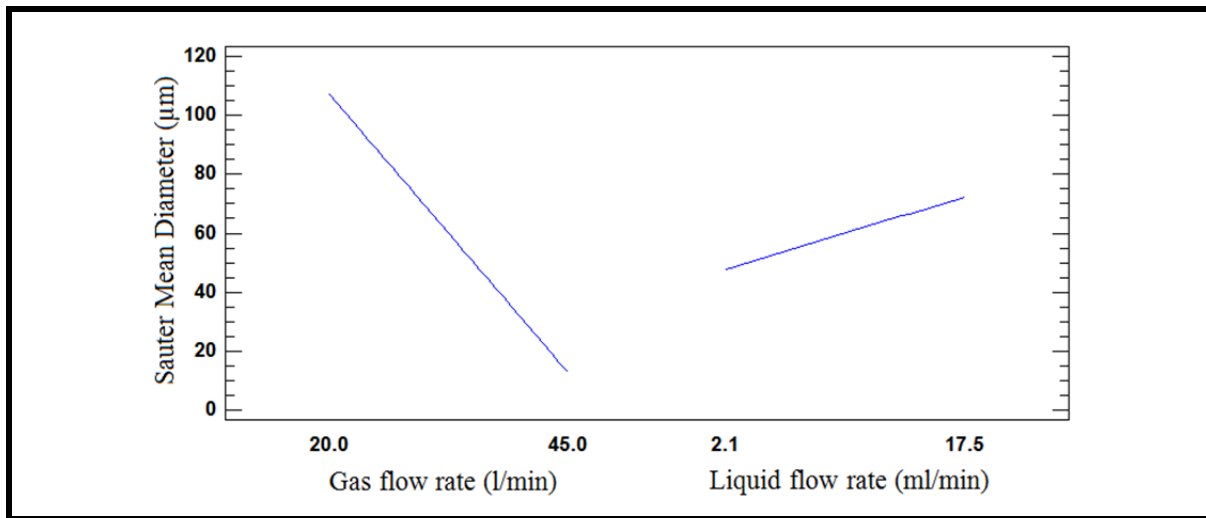


Figure 3.14 Main effect plot of SMD when using nozzles with different liquid orifice diameters and DDA pump

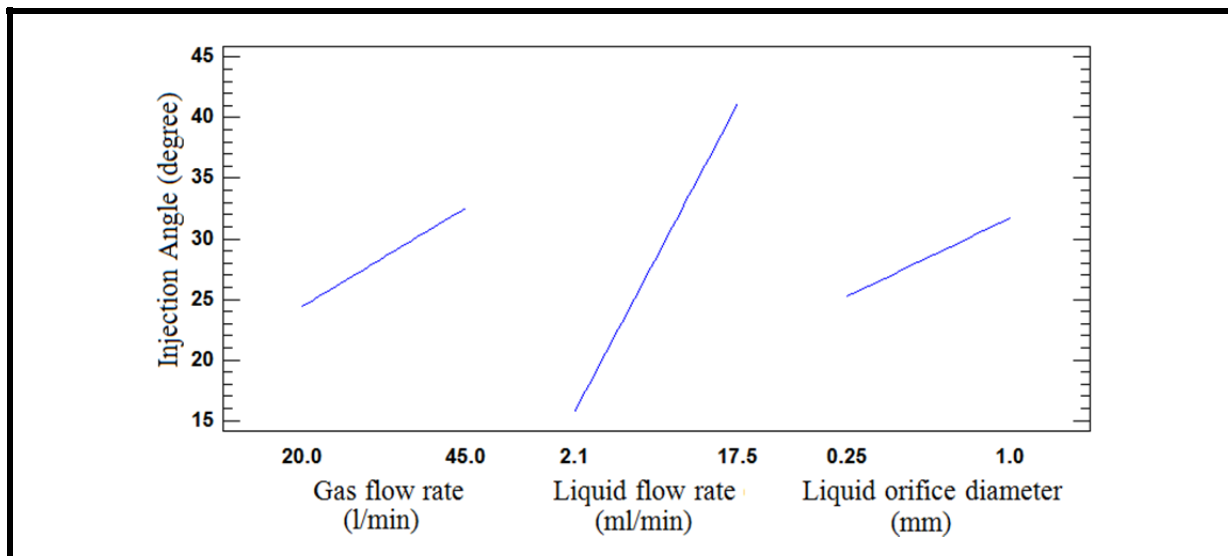


Figure 3.15 Main effect plot of injection angle when using nozzles with different liquid orifice diameters and DDA pump

3.5.2 Atomizer length effects

According to table 3.21, all of the parameters indicated in this table have the significant effects on SMD. The ANOVA table 3.22 shows that except the interaction effects between

the gas and liquid flow rate and between the gas flow rate and injector length, the other parameters indicated have the considerable effects on injection angle.

Table 3.21 The ANOVA table of SMD when using nozzles with different lengths and DDA pump

N	Source	Sum of Squares	Df	Mean Square	F-Ratio	P %
1	\dot{q}_g	188337	1	188337	138.66	0
2	\dot{q}_l	62412	1	62412	45.95	0
3	L	48001.3	1	48001.3	35.34	0
4	$\dot{q}_g \times \dot{q}_l$	41178.1	1	41178.1	30.32	0
5	$\dot{q}_g \times L$	12404.9	1	12404.9	9.13	0.36
6	$\dot{q}_l \times L$	23406.7	1	23406.7	17.23	0.01
7	Total error	88290.1	65	1358.31		
8	Total (corr.)	434070	71			

Table 3.22 The ANOVA table of injection angle when using nozzles with different lengths and DDA pump

N	Source	Sum of Squares	Df	Mean Square	F-Ratio	P %
1	\dot{q}_g	822.162	1	822.16	70.31	0
2	\dot{q}_l	2014.58	1	2014.58	172.28	0
3	L	352.293	1	352.29	30.13	0
4	$\dot{q}_g \times \dot{q}_l$	2.48501	1	2.49	0.21	64.63
5	$\dot{q}_g \times L$	34.9066	1	34.91	2.99	8.88
6	$\dot{q}_l \times L$	342.056	1	342.06	29.25	0
7	Total error	760.078	65	11.69		
8	Total (corr.)	4156.15	71			

According to Figures 3.16 and 3.17, increasing the gas flow rate and length of injector decreases the particle diameters while increasing the liquid flow rate has the inverse effect on SMD. According to Figure 3.17, it is observed that increasing the all of indicated parameters increases the injection angle.

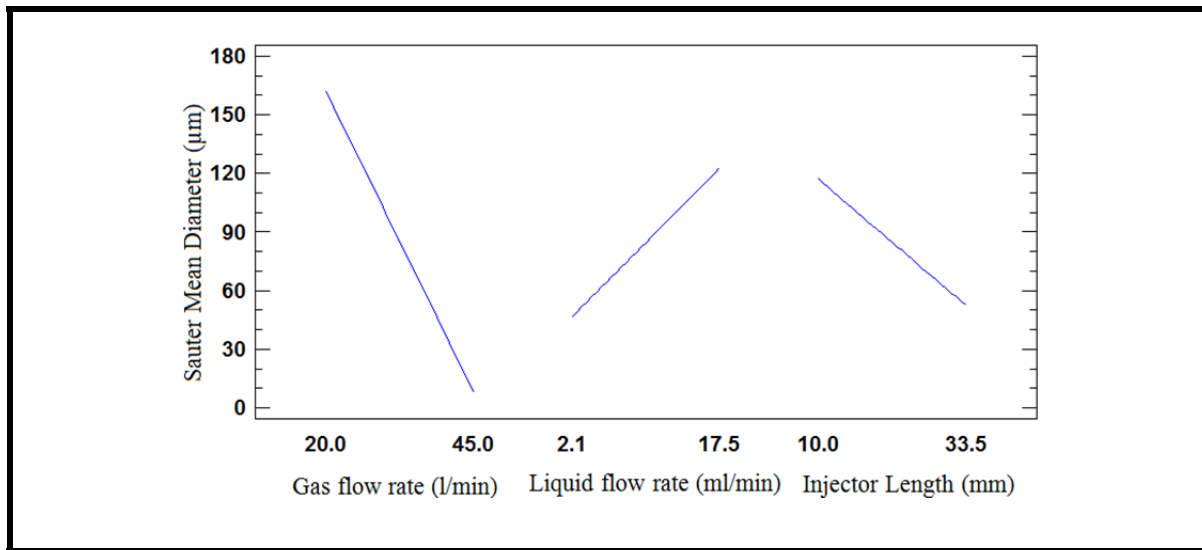


Figure 3.16 Main effect plot of SMD when using nozzles with different lengths and DDA pump

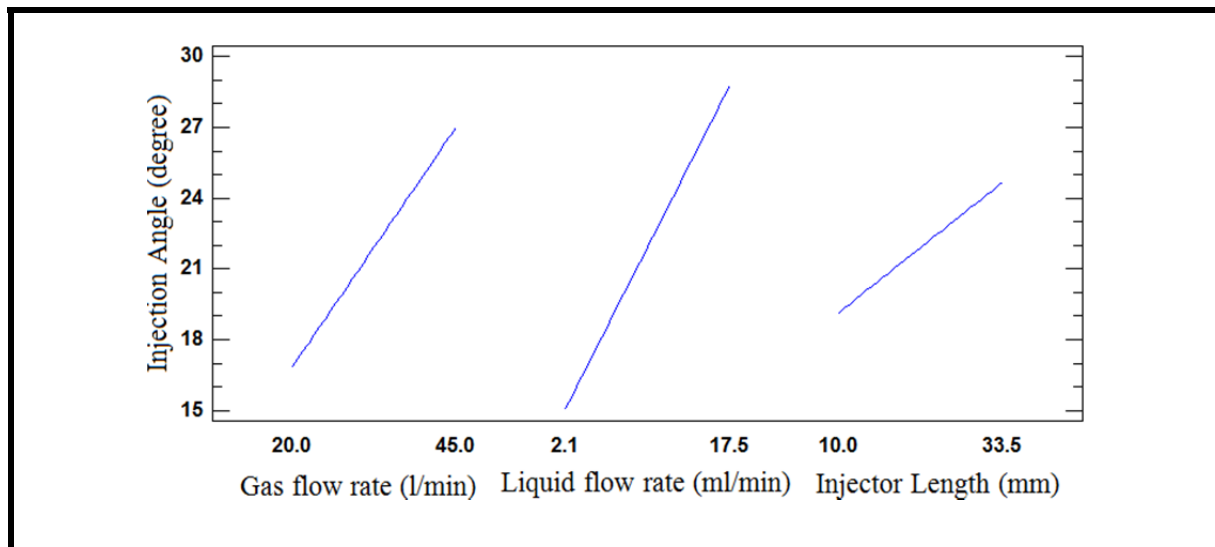


Figure 3.17 Main effect plot of injection angle when using nozzles with different lengths and DDA pump

3.5.3 Liquid orifice shape effects

According to tables 3.23 and 3.24, all of the parameters such as gas flow rate, liquid flow rate and liquid orifice shape have the significant effects on the SMD and injection angle. The interaction effects between liquid and gas flow rate with liquid orifice shape with 0.66% and

2.6% of P-values are also the significant parameters on SMD and injection angle respectively. According to Figures 3.18 and 3.19, increasing the gas and liquid flow rates decreases and increases the SMD respectively while increasing the both of these parameters increases the injection angle. These Figures show that the injectors with straight liquid orifice shape produce the particles with lower diameters and lower injection angles.

Table 3.23 The ANOVA table of SMD when using nozzles with different liquid orifice shapes and DDA

N	Source	Sum of Squares	Df	Mean Square	F-Ratio	P %
1	\dot{q}_g	85811.6	1	85811.6	93.11	0
2	\dot{q}_l	57002.3	1	57002.3	61.85	0
3	R	33469.3	1	33469.3	36.32	0
4	$\dot{q}_g \times \dot{q}_l$	20344.4	1	20344.4	22.08	0
5	$\dot{q}_g \times R$	766.584	1	766.58	0.83	36.71
6	$\dot{q}_l \times R$	7547.12	1	7547.12	8.19	0.66
7	Total error	37784.9	41	921.58		
8	Total (corr.)	223514	47			

Table 3.24 The ANOVA table of injection angle when using nozzles with different liquid orifice shapes and DDA

N	Source	Sum of Squares	Df	Mean Square	F-Ratio	P %
1	\dot{q}_g	830.25	1	830.25	94.25	0
2	\dot{q}_l	1333.39	1	1333.39	151.36	0
3	R	69.0906	1	69.09	7.84	0.77
4	$\dot{q}_g \times \dot{q}_l$	0.00598	1	0.006	0.0007	97.93
5	$\dot{q}_g \times R$	47.038	1	47.04	5.34	2.6
6	$\dot{q}_l \times R$	1.17917	1	1.18	0.13	71.63
7	Total error	361.18	41	8.81		
8	Total (corr.)	2684.99	47			

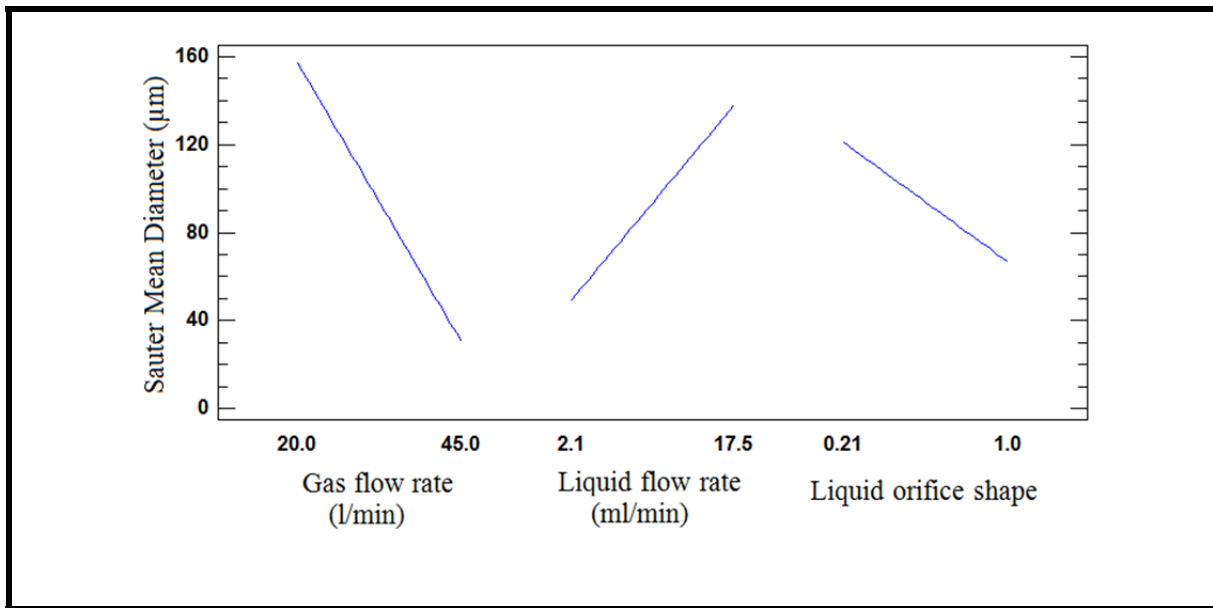


Figure 3.18 Main effect plot of SMD when using nozzles with different liquid orifice shapes and DDA

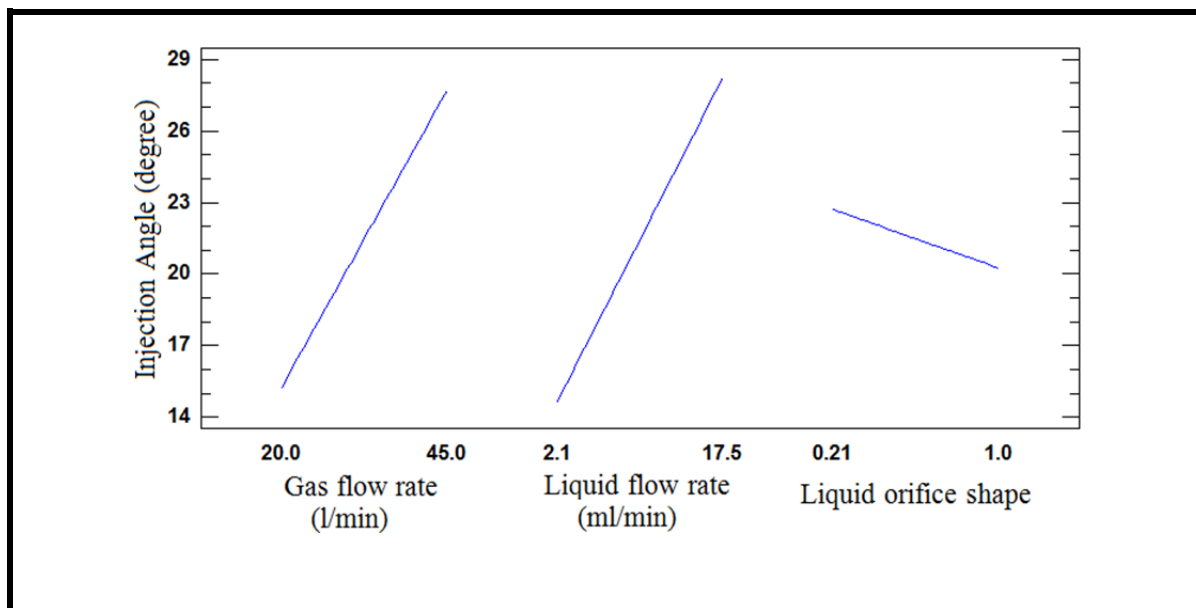


Figure 3.19 Main effect plot of injection angle when using nozzles with different liquid orifice shapes and DDA

3.6 Validation of the Sauter mean diameter (SMD) experimental results

According to section 1.6.3 of literature review, the investigations of Lorenzetto and Lefebvre (1977) on the efficiency of plain-jet airblast atomizers were carried out using the atomizers with different geometries and different liquid and air properties such as air/liquid ratio, air velocities as well as viscosity, surface tension and density of liquid.

Lorenzetto and Lefebvre found an equation (Equation 3.13) for SMD using the nozzles which could produce a round jet of the liquid surrounded by a co-axial and co-flowing stream of high velocity air (Lefebvre, 1980).

$$\text{SMD} = 0.95 \left(\frac{(\sigma_L \dot{m}_L)^{0.33}}{U_R \rho_L^{0.37} \rho_g^{0.30}} \right) \left(1 + \frac{\dot{m}_L}{\dot{m}_g} \right)^{1.70} + 0.13 \mu_L \left(\frac{dl}{\sigma_L \rho_L} \right)^{0.5} \left(1 + \frac{\dot{m}_L}{\dot{m}_g} \right)^{1.70} \quad (3.13)$$

Where \dot{m}_L and \dot{m}_g are the mass flow rates for the liquid and the gas respectively.

Due to using the same injectors in this research as those are used by Lorenzetto and Lefebvre and in order to validate the SMD results obtained experimentally using laser diffraction, a comparison between the measured SMD using nozzles with different liquid jet orifice diameter and the Lorenzetto and Lefebvre correlation (Equation 3.13) is performed as shown in Figures 3.20 and 3.21.

According to these Figures, it is concluded that in both of the injectors, increasing the gas flow rate increases the atomization efficiency which is the result of decreasing the SMD. On the contrary, increasing the liquid flow rate increases the SMD which lead to the weak atomization. In both of the injectors, a good conformity between the experimental and theoretical results especially in higher liquid and gas flow rates is shown. The differences between the initial conditions used by Lorenzetto and Lefebvre (Lefebvre, 1980) and those used in present research(see Table 3.25) lead to diverge between the results when using lower gas flow rates.

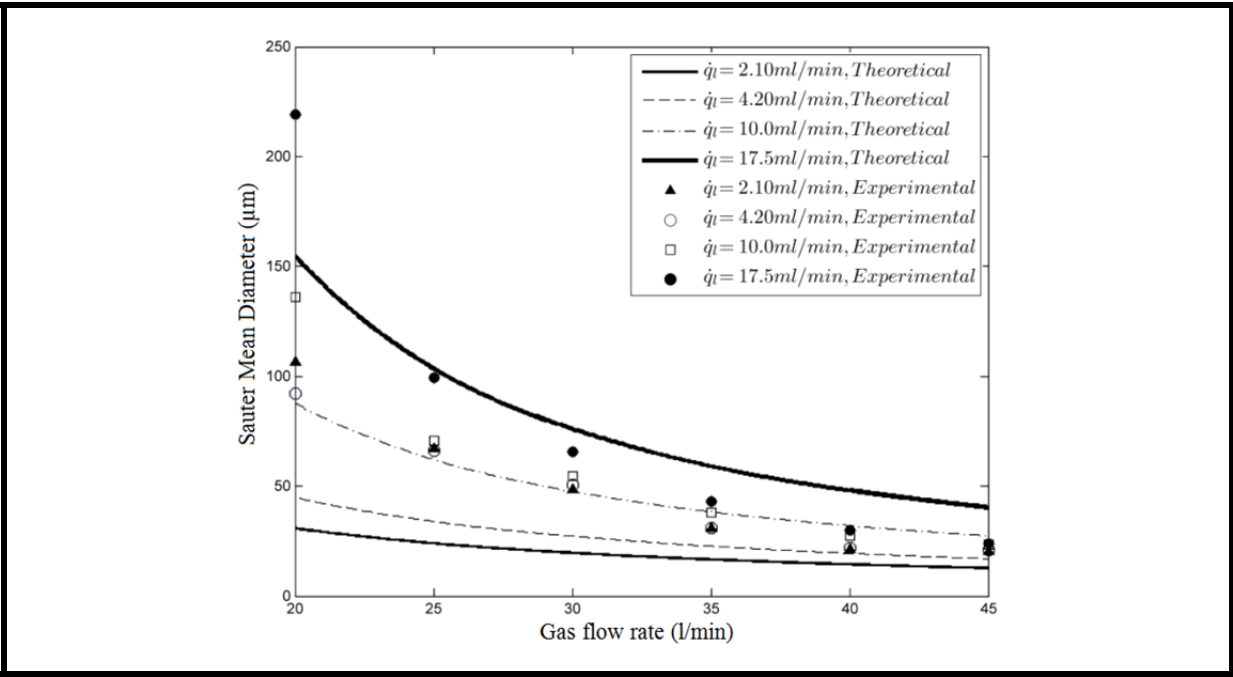


Figure 3.20 Particle sizing validation for the injector Lg20.0dl0.25

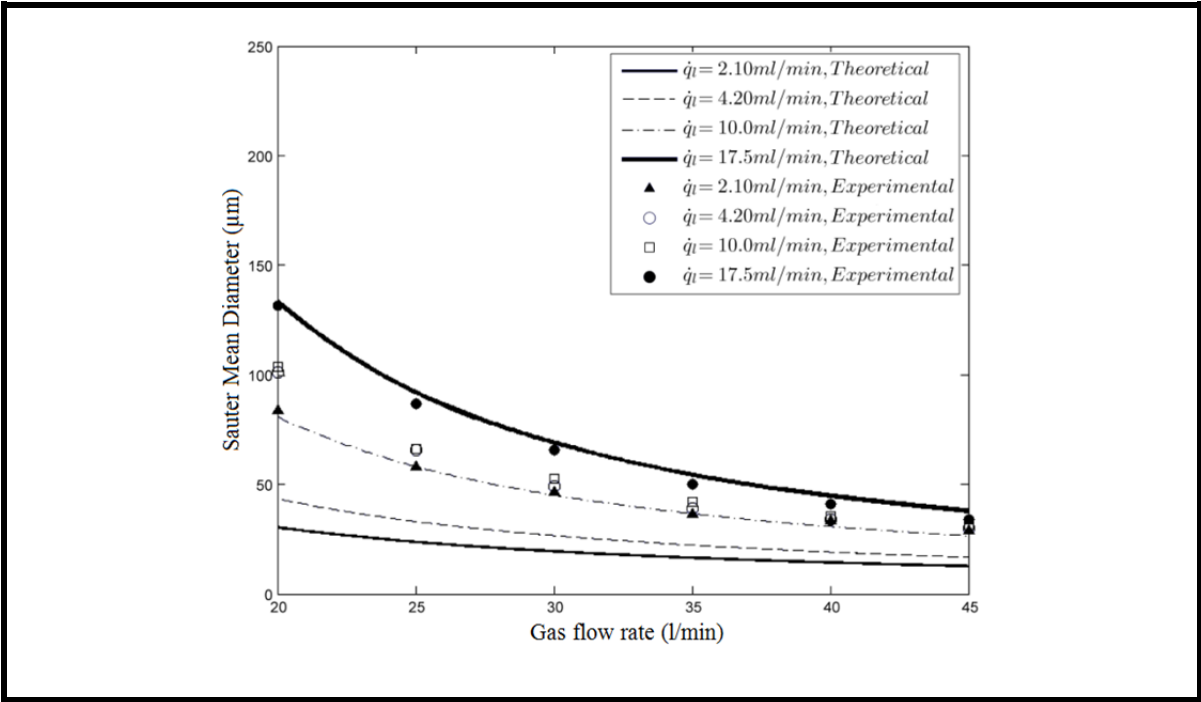


Figure 3.21 Particle sizing validation for the injector Lg33.5dl1.00

According to this conditions, the range of the gas velocity in theoretical result is 60-180 m/s while in the present experiments, the gas velocity is less than 60 m/s for the gas flow rates under 30 l/min. Comparing both of the liquid orifice diameter results, the experiments are more conform with theory in higher liquid jet diameter where the liquid diameters is closer to those which were used in Lorenzetto and Lefebvre investigations.

Table 3.25 Initial conditions of the experimental and theoretical studies

Investigator	Type of atomization	Liquid employed	Liquid properties				Gas properties			Air/liquid mass ratio
			$\sigma_l \times 10^{-3}$ (kg/s ²)	ρ_l (kg/m ³)	$\mu_l \times 10^3$ (kg/m.s)	dl (mm)	P_g (10 ⁻⁵ Pa)	T_g (°K)	U_g (m/s)	
Lorenzetto & Lefebvre	Plain-jet	water, kerosine special solutions	26	794	10	0.397	1.0	295	60	1
			-	-	-	-			-	-
			76	2180	76	1.588			180	16
Current research	Plain-jet	Emultec VG (5% solubility)	73	1006.5	1.0	0.25 & 1.0	1.0	293.15	40.4 - 91.0	1.38 - 25.71

With respect to theoretical results for low liquid flow rates (2.1 and 4.2 ml/min), it is clear that the divergence between these results will be reduced in very high gas flow rates. This difference is because of the air/liquid mass ratio range used in both of these researches. According to table 3.25, the air/liquid mass ratio of Lorenzetto and Lefebvre investigation was in the range of 1 - 16 but this parameter for the present experiments is in the range of 1.38 - 25.71. The values of air/liquid mass ratio presented in table 3.26 show more conformity between the experiments and theory in higher liquid flow rates.

Table 3.26 Experimental air/liquid mass ratio

Gas mass flow rate ($\times 10^{-4}$) (kg/sec)	4.01	5.01	6	7.02	8.02	9
Liquid mass flow rate ($\times 10^{-6}$) (kg/sec)	Gas/Liquid mass ratio					
35	11.45	14.31	17.14	20.05	22.91	25.71
70	5.72	7.15	8.57	10.02	11.45	12.85
170	2.35	2.94	3.53	4.12	4.72	5.29
290	1.38	1.73	2.06	2.42	2.77	3.10

3.7 Conclusion

According to the analysis performed in the present chapter it is concluded that:

1. The better atomization is attained using the continuous pumps;
2. The quality of atomization in the nozzles with straight liquid orifice shape is better than the atomizers with conical liquid orifice shape;
3. For both of the pumps (pulsed and continuous) studied, the injection angle is increased when increasing the gas or liquid flow rates as well as liquid orifice diameter of nozzle;
4. In the nozzles with conical liquid orifice shape, the injection angle is higher when using the continuous pump. This means this type of nozzles can lubricate a greater cutting zone;
5. The injection angle is independent of the injector length in pulsed pumps.

CHAPTER 4

MACHINING PERFORMANCE WHEN TURNING AA6061-T6 WITH PULSED AND CONTINUOUS COOLING/LUBRICATION

4.1 Introduction

The present chapter contains the investigation of the process parameter effects on the quality indexes of machining such as surface roughness, cutting tool temperature and dust and aerosol emission during the turning of aluminum alloy 6061-T6. The principal goal of this study is to find the cutting conditions which optimize the quality of machining and reduce the tool temperature as well as the aerosol generation in turning of aluminum alloy 6061-T6 when using MQC.

4.2 Surface roughness investigation using the pulsed and continuous pumps when turning aluminum alloy 6061-T6

4.2.1 Introduction

The surface roughness is one of the important factors to evaluate the machining accuracy. To obtain the better surface quality, the cutting parameters such as feed rate, cutting speed and depth of cut must be controlled.

The research is divided into two sections. The first one was carried out using the pulsed pump such as SLS1.2-2 (see Figure 2.4) and the continuous pump (DDA pump) was used in the next section. All of the experiments were performed under various machining modes included dry, wet and MQC.

The principal aims of this study are as follow:

- Investigating the effects of cutting parameters on surface roughness;
- Comparing cutting parameter effects on surface roughness when using pulsed and non-pulsed pumps;
- Choosing the nozzle which are geometrically effective to optimize the quality of surface finish

4.2.2 Effect of cutting parameters on surface roughness when using pulsed pump

According to experimental results, the surface roughness variations related to different cutting speeds are shown in Figures 4.1 to 4.3 when using feed rate as mentioned in table 2.9.

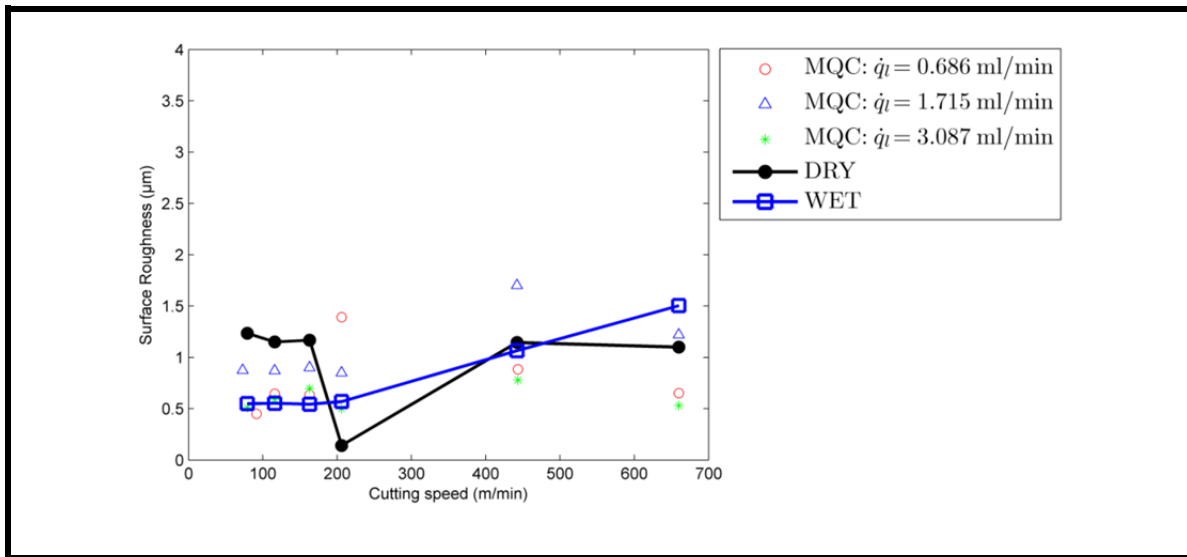


Figure 4.1 Surface roughness (μm) variations related to cutting speed (m/min) where feed rate = 0.10 mm/rev

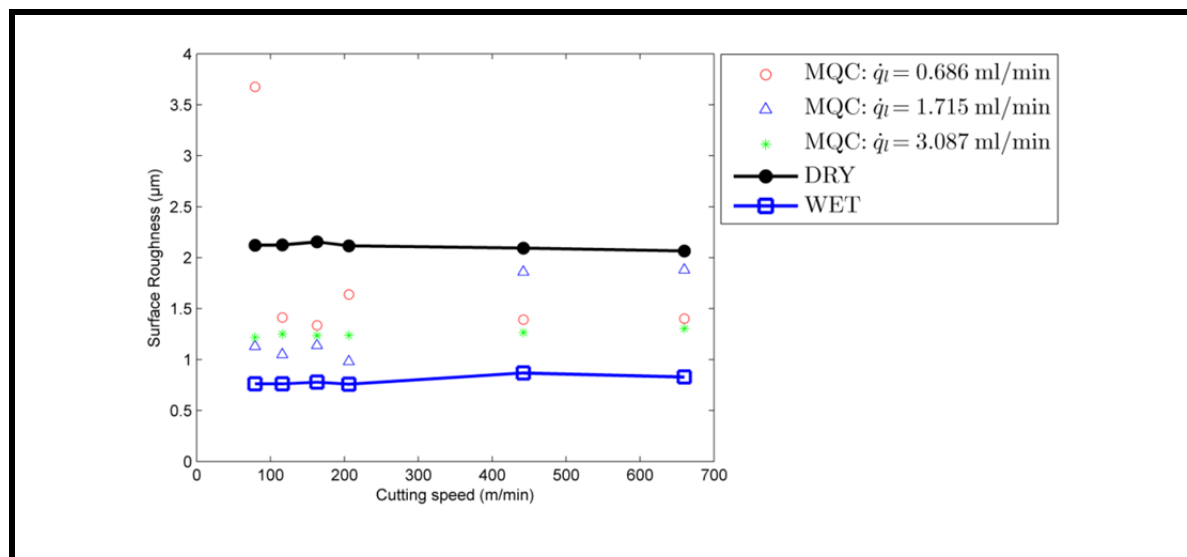


Figure 4.2 Surface roughness (μm) variations related to cutting speed (m/min) where feed rate = 0.15 mm/rev

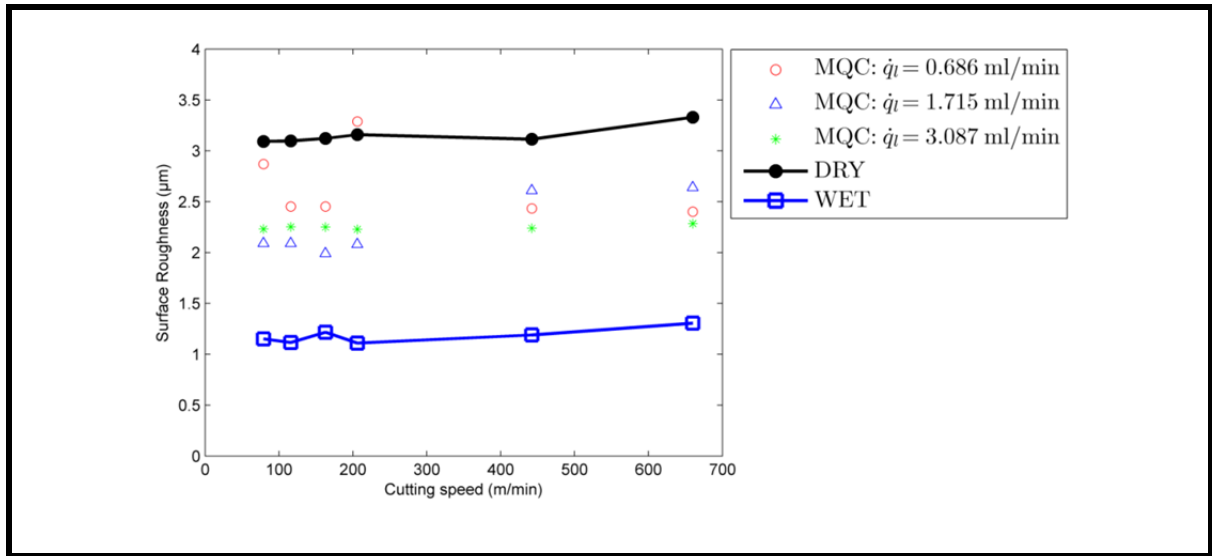


Figure 4.3 Surface roughness (μm) variations related to cutting speed (m/min) where feed rate = 0.20 mm/rev

According to Figures 4.1 to 4.3, it is observed that increasing the feed rate decreases the surface roughness during wet machining mode more than that dry or MQC. In wet lubrication method and using lower and higher cutting speeds, the surface roughness is increased and decreased when feed rate is raised; Whereas, in all of the range of cutting speed, the surface roughness is increased during dry machining.

According to ANOVA table 4.1 with 71.06% of R-squared, it is observed that using the pulsed pump, the parameters such as feed rate and cutting speed have the significant effects on surface roughness when turning aluminum alloy 6061-T6 (see Figures 4.1 to 4.3) .

Table 4.1 The ANOVA table of surface roughness when using pulsed pump

N	Source	Sum of Squares	Df	Mean Square	F-Ratio	P %
1	\dot{q}_l	0.14	1	0.14	1.05	31
2	F_r	1.60	1	1.60	12.29	0
3	C_s	13.02	1	13.02	99.84	0
4	$\dot{q}_l \times F_r$	0.19	1	0.19	1.46	23
5	$\dot{q}_l \times C_s$	0.07	1	0.07	0.53	47
6	$F_r \times C_s$	0.03	1	0.03	0.2	65
7	Total error	6.13	47	0.13		
8	Total (corr.)	21.18	53			

According to the main effect plot and Pareto chart (see Figures 4.4 – 4.5), it is clear that increasing the both of feed rate and cutting speed increases the surface roughness while the effect of liquid flow rate on surface roughness is not considerable. Figure 4.4 shows that in MQC lubrication mode, the best surface finish will be obtained in lower feed rate and lower cutting speed.

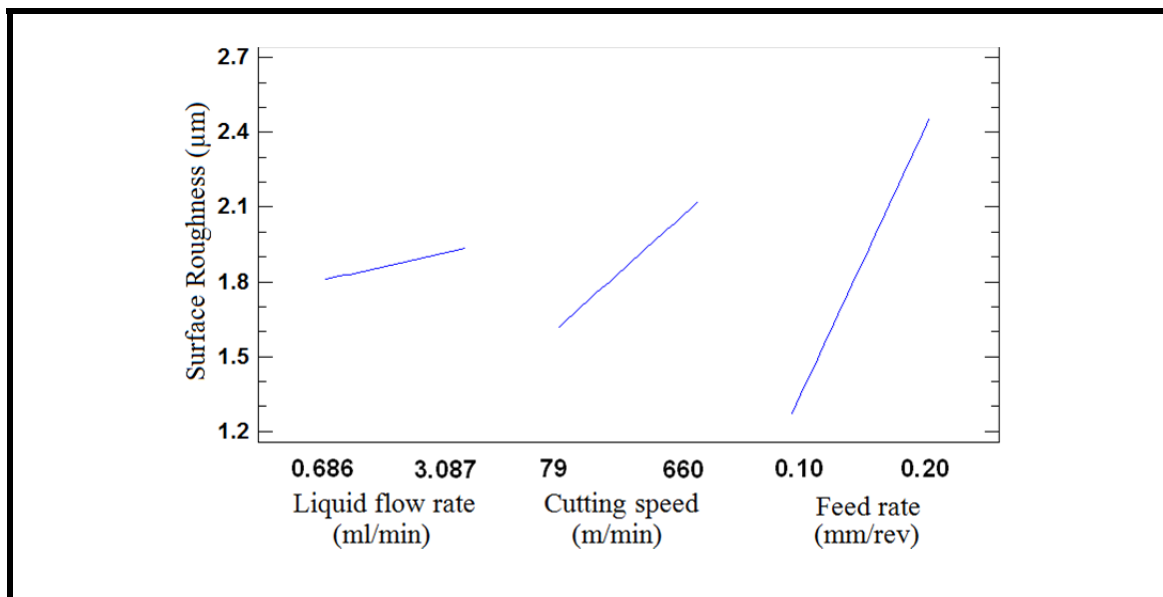


Figure 4.4 Main effect plot of surface roughness analysis when using pulsed pump

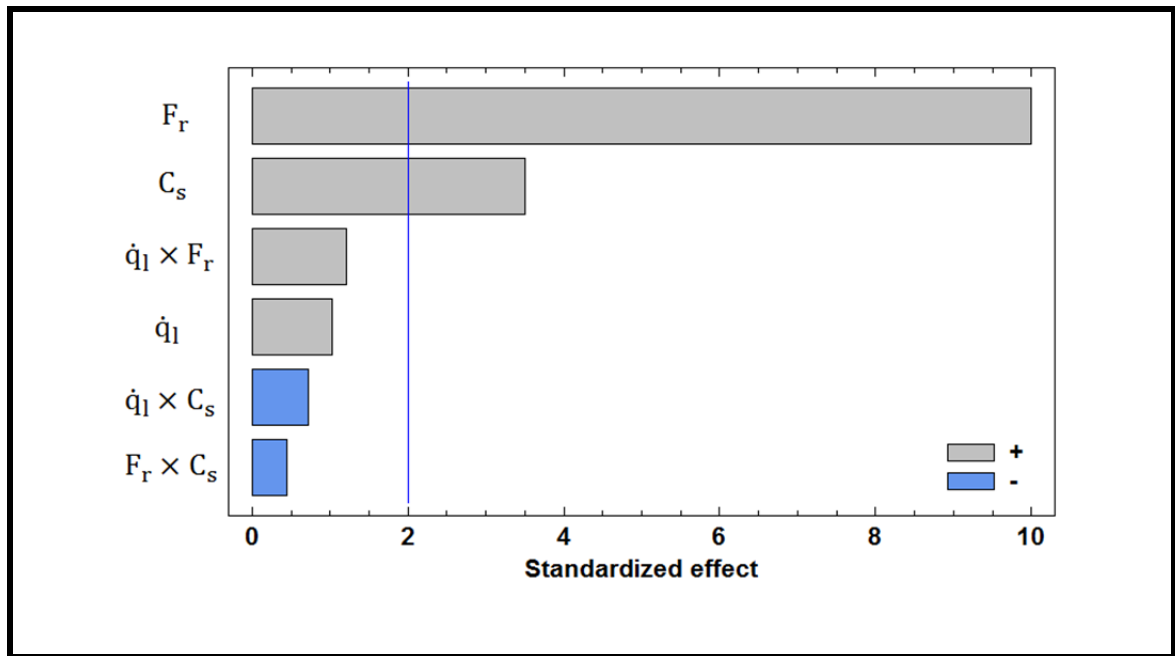


Figure 4.5 Pareto chart of surface roughness analysis when using pulsed pump

4.2.3 Effect of cutting parameters on surface roughness when using continuous pump

In these experiments, the investigations are carried out based on the different cutting parameters such as feed rate, cutting speed and also the gas and liquid flow rates as shown in table 2.8. The two nozzles with different length and liquid orifice diameters are used and the depth of cut fixed in 2 mm diameter. According to experimental observations, the surface roughness variations related to different cutting speeds are shown in Figures 4.6 and 4.7 when using three different feed rates and two types of nozzles.

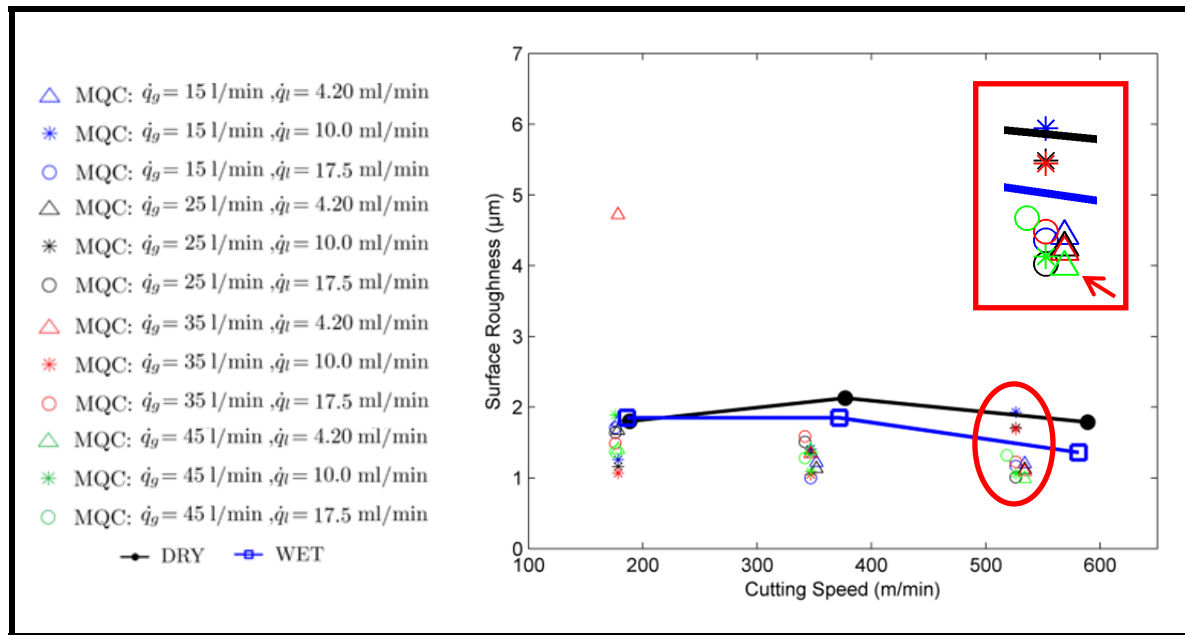


Figure 4.6 (a) Feed rate = 0.10 mm/rev

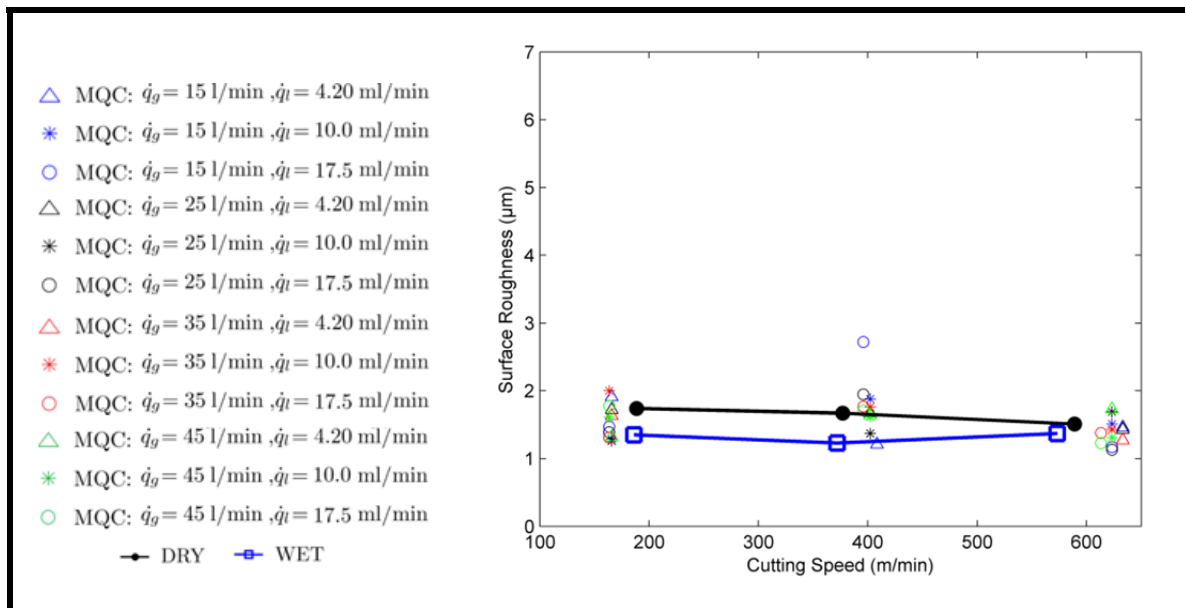


Figure 4.6 (b) Feed rate = 0.15 mm/rev

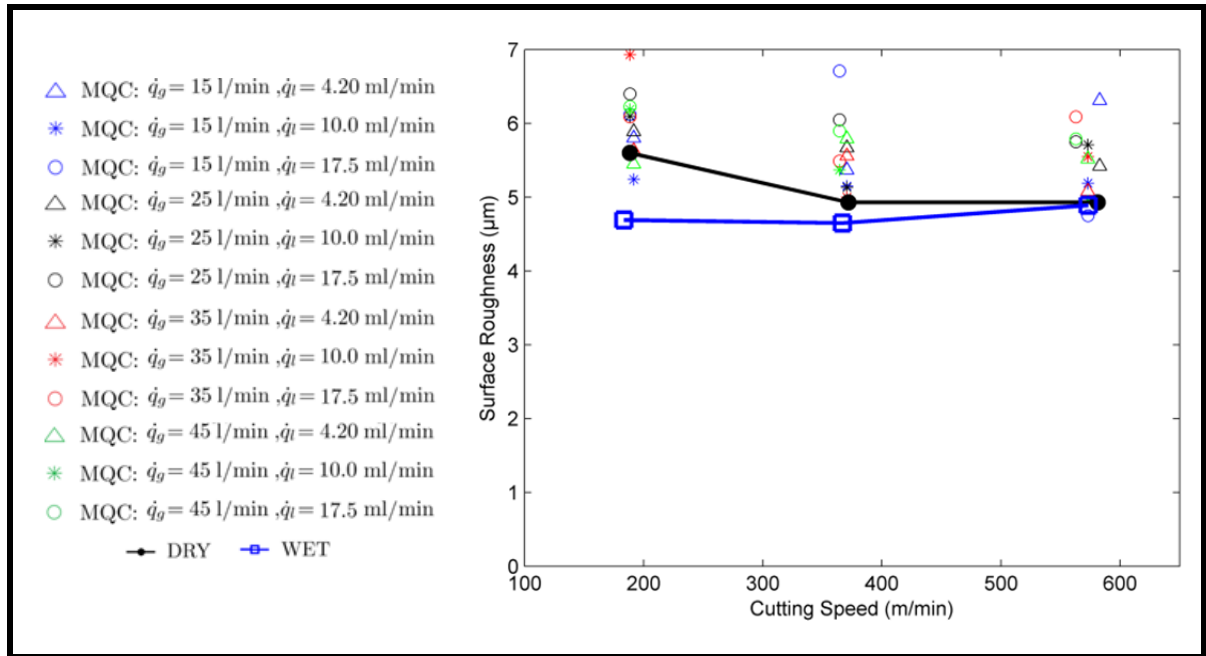


Figure 4.6 (c) Feed rate = 0.20 mm/rev

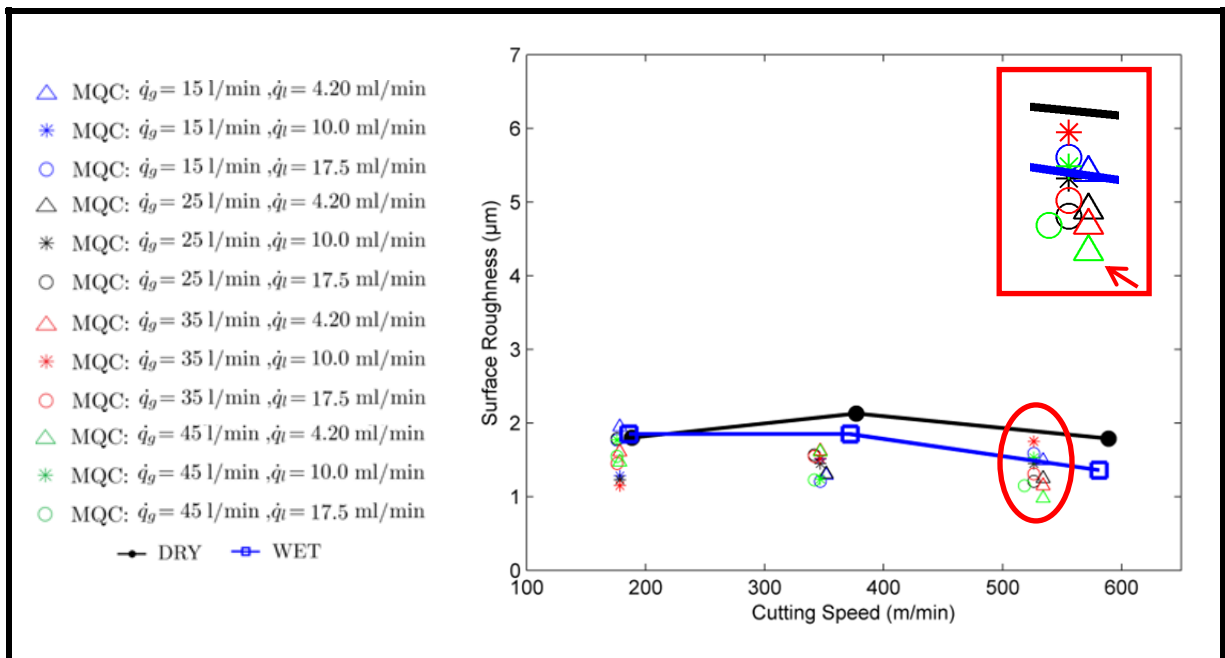
Figure 4.6 Lg20.0dl0.25 – Surface roughness (μm) variations related to cutting speed (m/min)

Figure 4.7 (a) Feed rate = 0.10 mm/rev

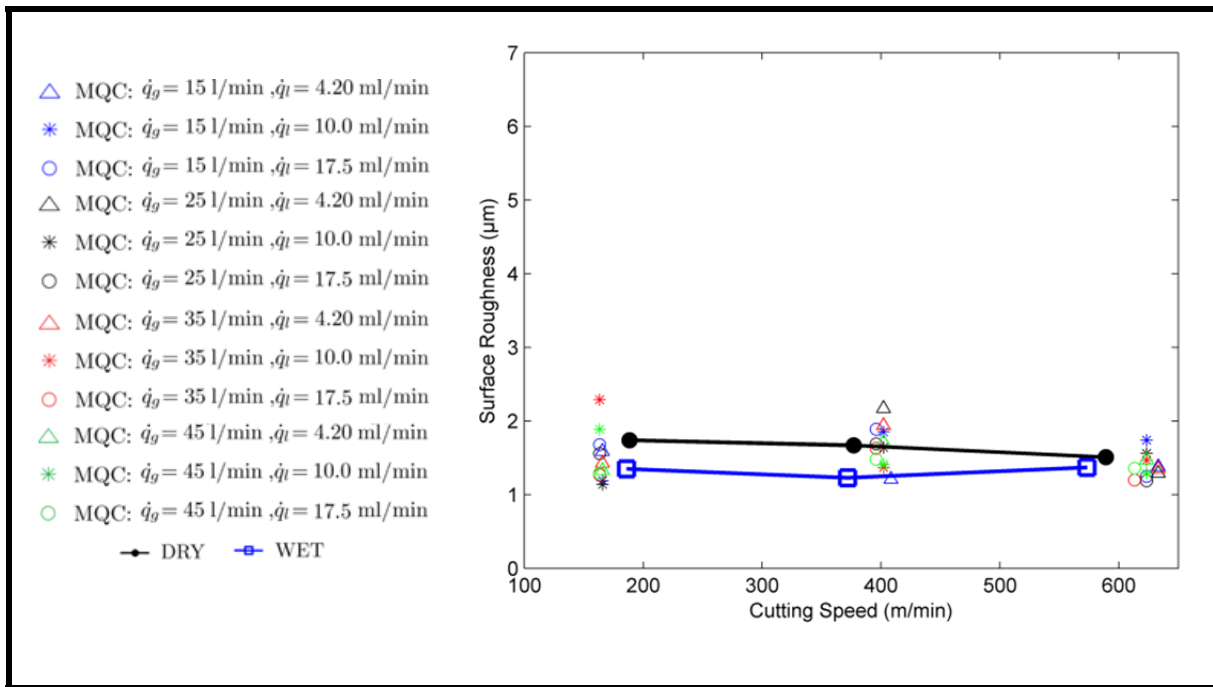


Figure 4.7 (b) Feed rate = 0.15 mm/rev

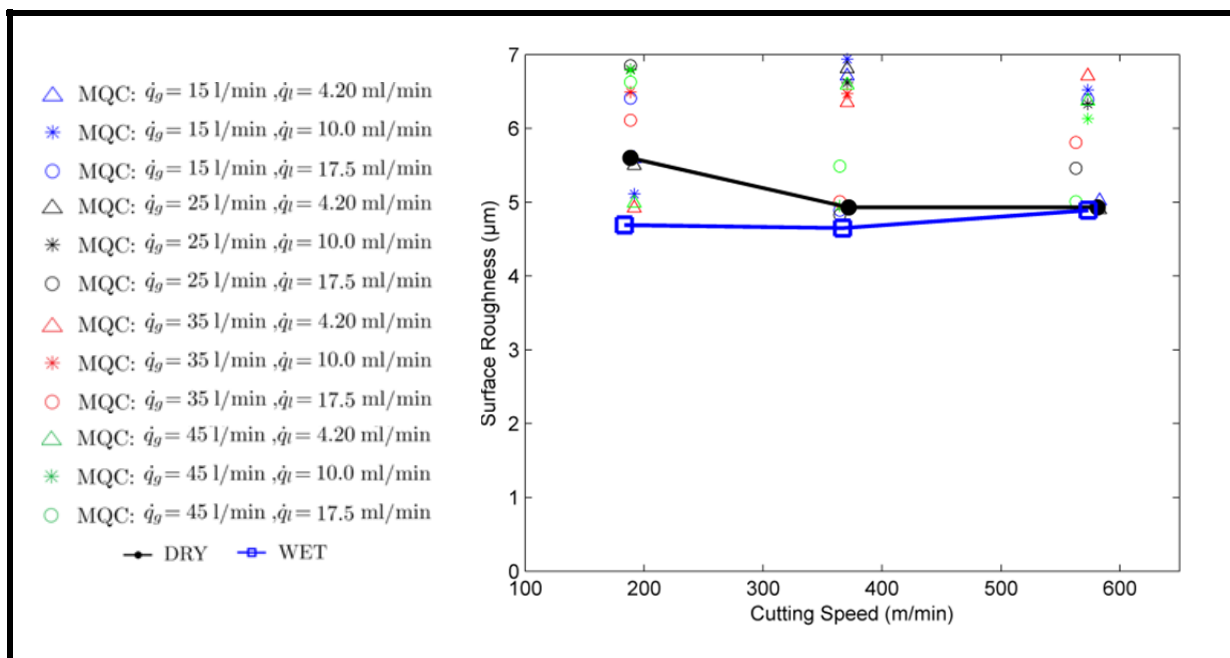


Figure 4.7 (c) Feed rate = 0.20 mm/rev

Figure 4.7 Lg33.5dl1.00 - Surface roughness (μm) variations related to cutting speed (m/min)

According to Figures 4.6 and 4.7, it is observed that increasing the feed rate improves the surface finish in wet machining further than that in dry and MQC modes. To explain these Figures especially in MQC machining mode and in order to find the better conditions in which the surface finish improves, it is helpful to analyse the parameters which have the most significant effects on surface roughness

According to tables 4.2 - 4.3, feed rate has the most significant effect on surface roughness using both nozzles.

Table 4.2 The ANOVA table of surface roughness when using Lg20.0dl0.25

N	Source	Sum of Squares	Df	Mean Square	F-Ratio	P %
1	\dot{q}_g	0.01	1	0.01	0.01	93
2	\dot{q}_l	0.55	1	0.55	0.46	50
3	C_s	0.81	1	0.81	0.68	41
4	F_r	12.82	1	12.82	10.72	0
5	$\dot{q}_g \times \dot{q}_l$	0.00	1	0.00	0	99
6	$\dot{q}_g \times C_s$	0.01	1	0.01	0.01	91
7	$\dot{q}_g \times F_r$	0.00	1	0.00	0	96
8	$\dot{q}_l \times C_s$	0.10	1	0.10	0.08	78
9	$\dot{q}_l \times F_r$	0.78	1	0.78	0.65	42
10	$C_s \times F_r$	0.31	1	0.31	0.26	61
11	Residual	116.01	97	1.20		
12	Total (corr.)	447.24	107			

Table 4.3 The ANOVA table of surface roughness when using Lg33.5dl1.00

N	Source	Sum of Squares	Df	Mean Square	F-Ratio	P %
1	\dot{q}_g	0.00	1	0.00	0	99
2	\dot{q}_l	0.17	1	0.17	0.13	72
3	Cs	0.58	1	0.58	0.42	52
4	Fr	17.97	1	17.97	13.08	0
5	$\dot{q}_g \times \dot{q}_l$	0.04	1	0.04	0.03	86
6	$\dot{q}_g \times C_s$	0.01	1	0.01	0	95
7	$\dot{q}_g \times F_r$	0.00	1	0.00	0	100
8	$\dot{q}_l \times C_s$	0.05	1	0.05	0.03	86
9	$\dot{q}_l \times F_r$	0.10	1	0.10	0.07	79
10	$C_s \times F_r$	0.52	1	0.52	0.38	54
11	Residual	133.27	97	1.37		
12	Total (corr.)	501.14	107			

Referring to Figures 4.8 and 4.9 for Lg20.0dl0.25 and Lg33.5dl1.00 nozzles ($\dot{q}_g = 45$ l/min & $\dot{q}_l = 17.5$ ml/min), it is clear that an increase in the feed rate when using these injectors increases the surface roughness while increasing cutting speed decreases surface roughness. It means that the optimum surface finish is obtained in lower feed rate and higher cutting speed. According to these conditions and regarding the Figures 4.6(a) and 4.7(a), it is observed that the surface finish is better in MQC than wet and dry machining modes.

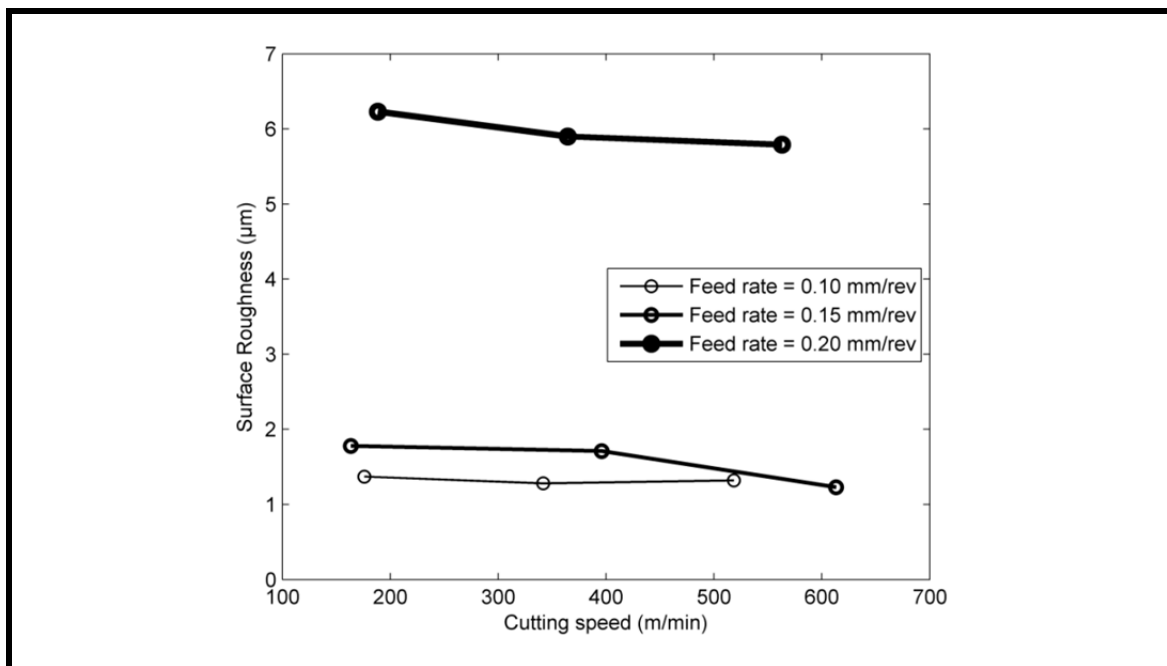


Figure 4.8 Feed rate effects on surface roughness when using Lg20.0dl0.25

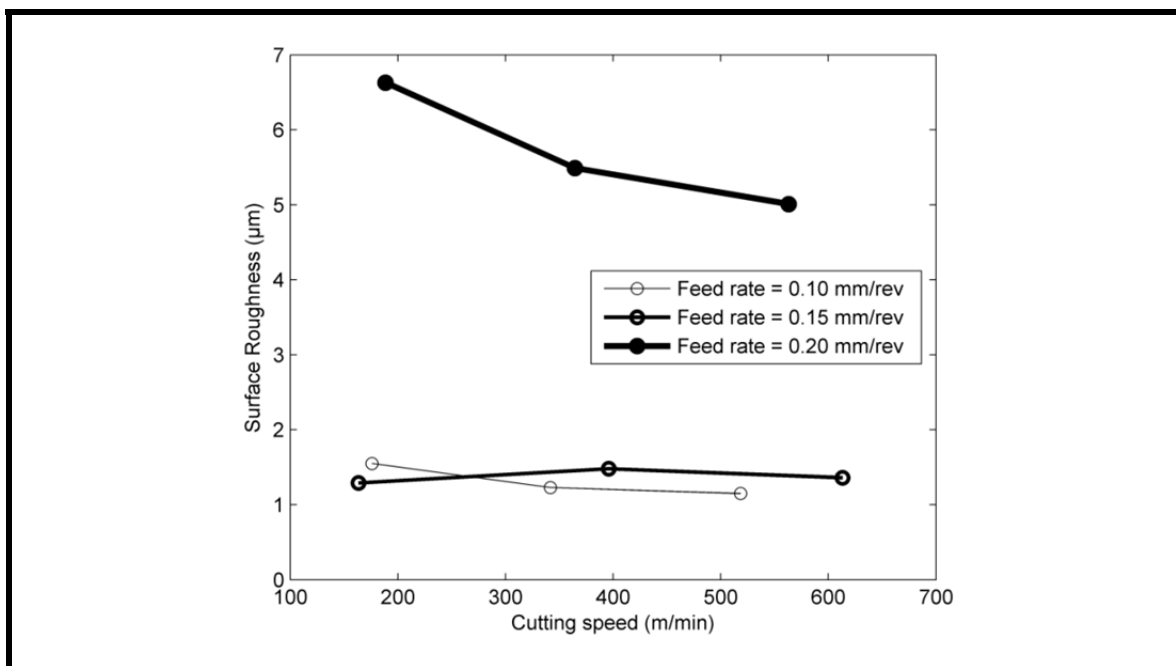


Figure 4.9 Feed rate effects on surface roughness when using Lg33.5dl1.00



Although the gas and liquid flow rates have no significant effect on surface roughness, this quality indicator is affected by these parameters because of their influences on atomization quality as explained earlier in sections 3.5.1 and 3.5.2 of chapter 3.

It is previously observed that in continuous pump, increasing the gas flow rate and decreasing the liquid flow rate decreases SMD when using injectors with different lengths and different liquid orifice diameters. This result improves the atomization quality (see Figures 3.14 and 3.16)

According to Figures 4.6(a) and 4.7(a), the minimum of surface roughness using Lg20.0dl0.25 and Lg33.5dl1.00 are achieved respectively in maximum and minimum of gas and liquid flow rates (45 l/min and 4.2 ml/min). In order to select one of these injectors which leads to better surface finish and considering the results obtained from Figures 3.14 and 3.15 (the diameter has no effect on SMD while the increase in the injector length decreases the particle diameters), it is concluded that the injector Lg33.5dl1.00 is the preferable atomizer which produces the best surface finish.

This conclusion could be approved according to the minimum values of **surface** roughness obtained during the MQC experiments which are 0.99 and 0.98 μm for Lg20.0dl0.25 and Lg33.5dl1.00 nozzles respectively. It is also interesting to know that according to Figures 3.15 and 3.17 of chapter 3, increasing the both of length and liquid orifice diameter increases the injection angle which means that lubrication could be carried out in the larger surface of cutting zone when using Lg33.5dl1.00 atomizer.

4.3 Cutting tool temperature and dust concentration investigation using the continuous pumps when turning of aa6061-t6

4.3.1 Introduction

In the cutting zone, the heat generation will be occurred in three different zones such as primary shear zone, tool-chip interface and tool-workpiece interface. The increase in temperature in primary shear zone is influenced by characteristics of the workpiece and chip material. The heat generation in the other two areas affects the tool wear at tool face and

flank respectively (Liu *et al.*, 2006). Due to these effects, the temperature is one of the main limitations in the selection of cutting parameters such as feed rate and cutting speed. The criteria such as surface roughness, productivity, cycle time etc., are not the only effective parameters on the machining performance. Another indicator which is very important to protect the environment and the operator health is the dust generation during the different machining methods. The dusts can be created under two forms of solid and liquid. The solid form will be generated during dry and wet machining whereas the generation of the liquid form of the dust will be occurred where the cutting fluids are used (Strutt, 1879) In this section, the effects of different cutting parameters and conditions on cutting tool temperature and dust emission is studied.

4.3.2 Effect of cutting parameters on tool temperature

In this section, the effects of the process parameters on cutting tool temperature is investigated using a thermocouple installed perpendicular to the tool tip at a distance of 6 mm (see Figure 2.12). All of the experiments of MQC mode are carried out using the same cutting parameters as shown in table 2.8 and the wet machining was performed using the liquid flow rate of 2.6 l/min. The tool temperature variations related to cutting speed when using different feed rates are shown in Figures 4.10 and 4.11. Based on these Figures, it is observed that the heat generation increases by decreasing the quantity of lubricant. This result is totally independent of the cutting speed and feed rate.

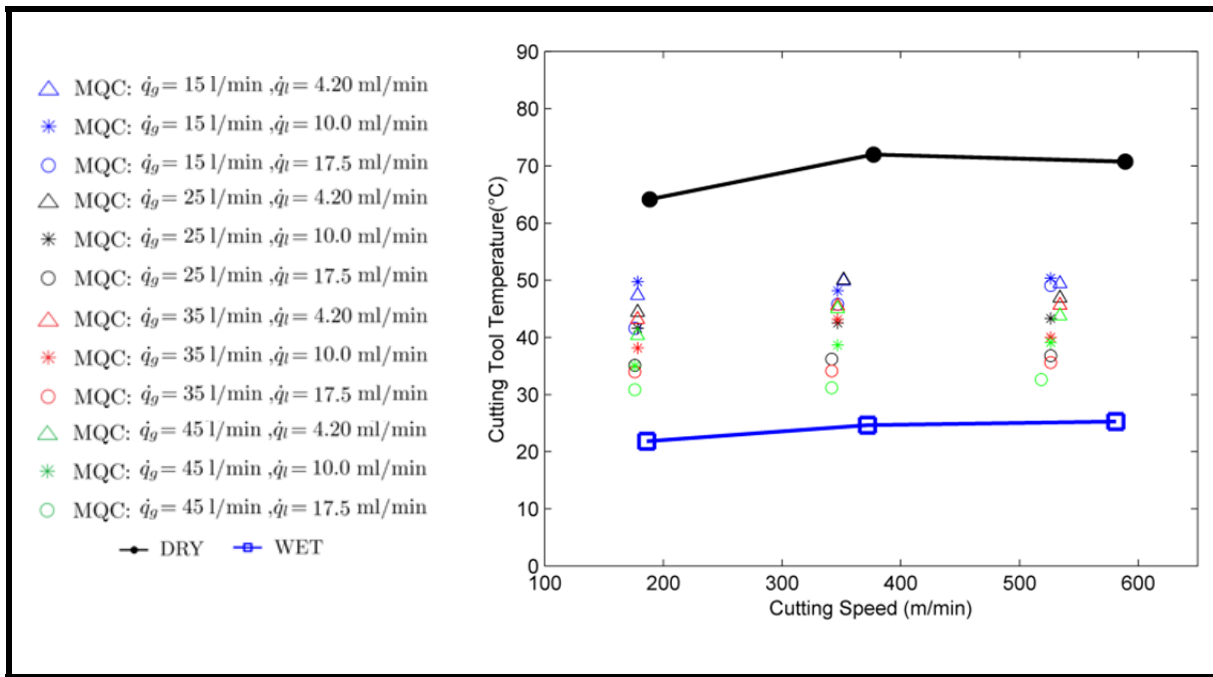


Figure 4.10 (a) Feed rate = 0.10 mm/rev

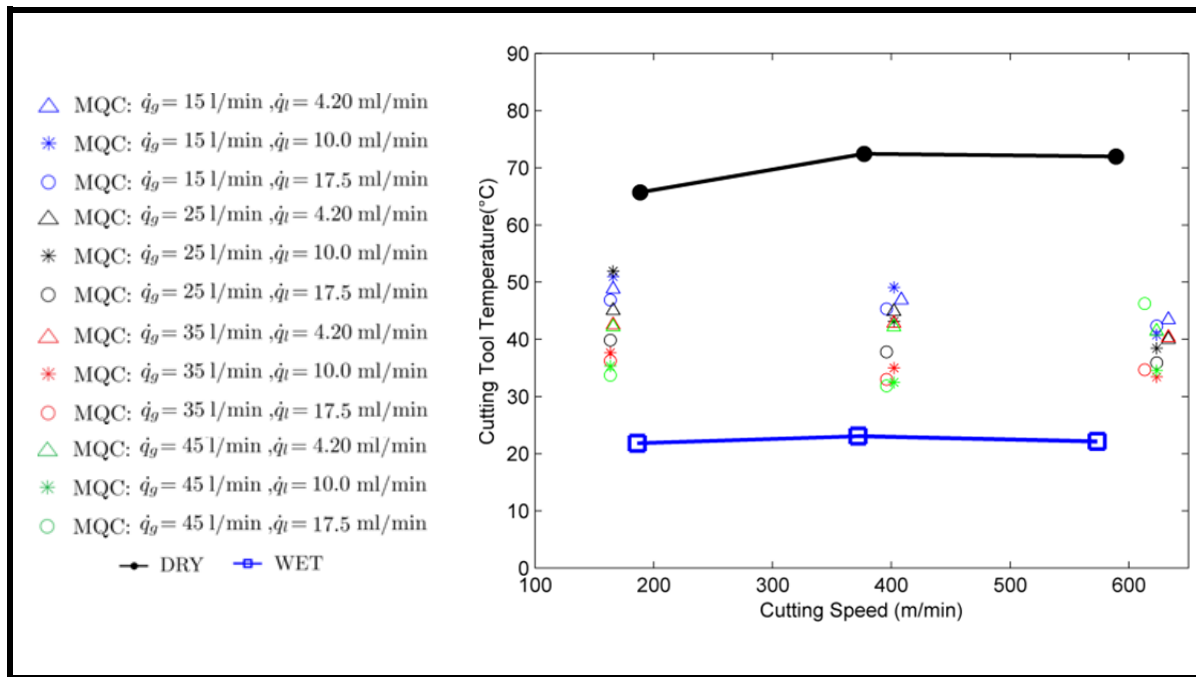


Figure 4.10 (b) Feed rate = 0.15 mm/rev

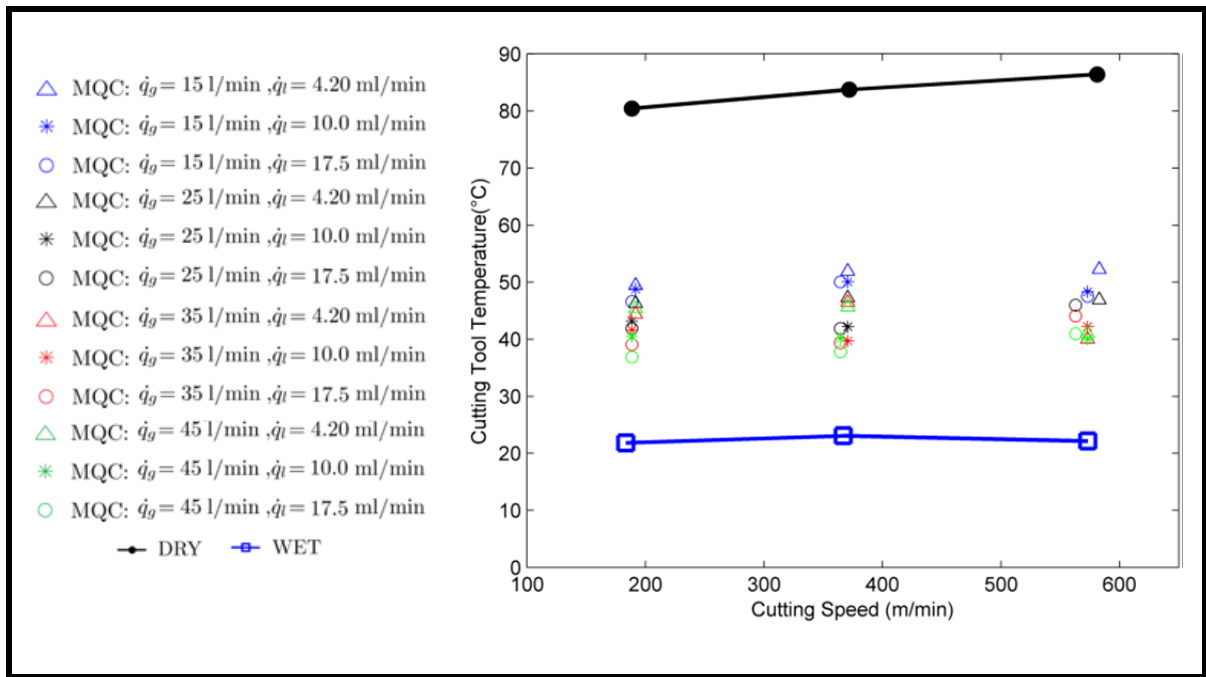


Figure 4.10 (c) Feed rate = 0.20 mm/rev

Figure 4.10 Lg20.0dl0.25 – tool temperature (°C) variations related to cutting speed (m/min)

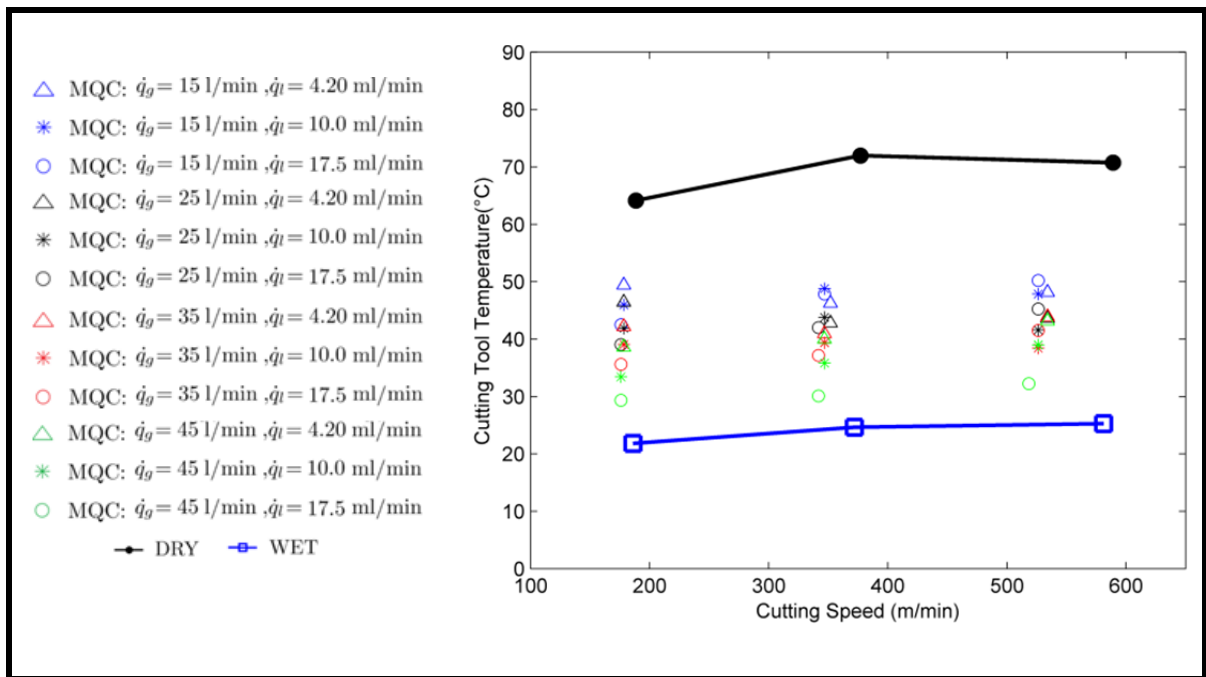


Figure 4.11 (a) Feed rate = 0.10 mm/rev

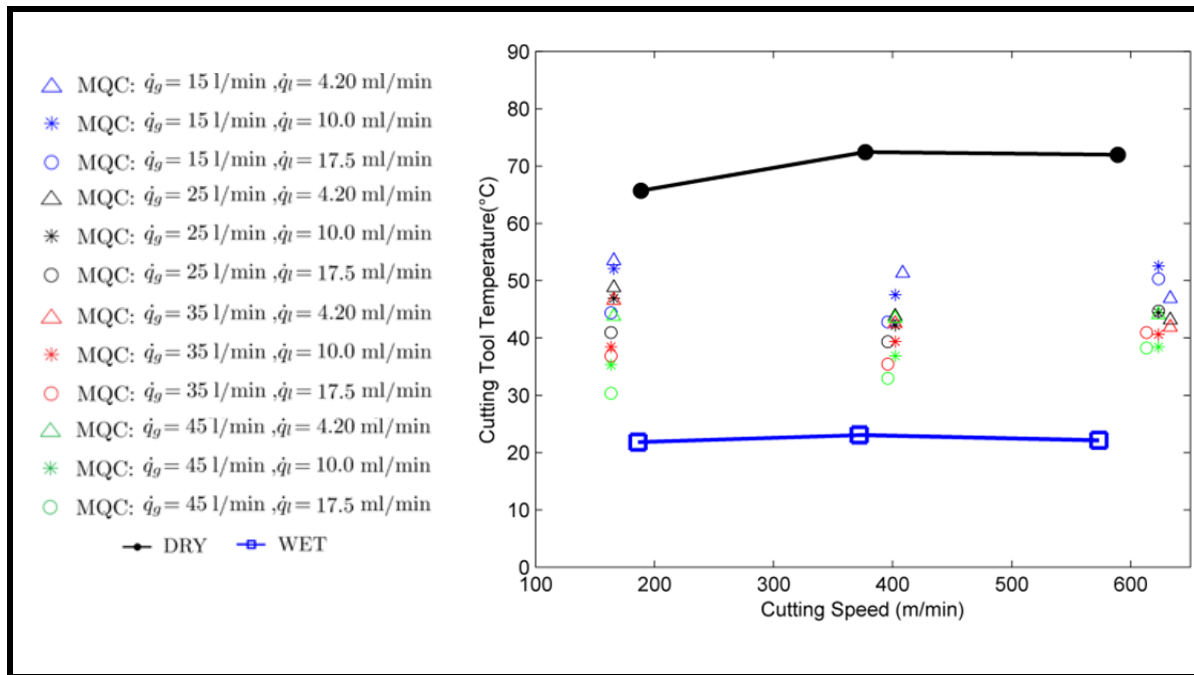


Figure 4.11 (b) Feed rate= 0.15 mm/rev

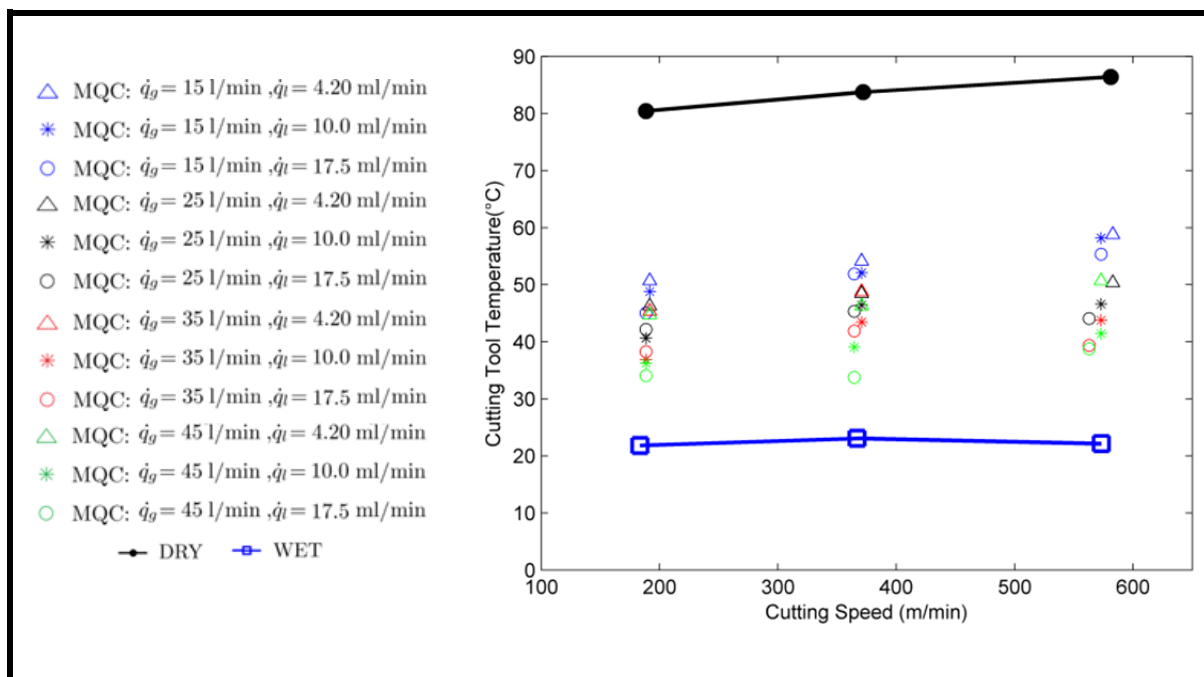


Figure 4.11 (c) Feed rate = 0.20 mm/rev

Figure 4.11 Lg20dl0.25 - tool temperature (°C) variations related to cutting speed (m/min)

To explain the effects of cutting parameters on tool temperature particularly when using MQC, the statistical analysis is performed. According to tables 4.4 and 4.5, it is inferred that in Lg20.0dl0.25 nozzle, the parameters with considerable effects on tool temperature are the gas and liquid flow rate as well as the interaction effects between liquid flow rate and cutting speed while in Lg33.5dl1.00 the cutting speed as well as the interaction effects between gas and liquid flow rate (\dot{q}_g & \dot{q}_l), cutting speed and liquid flow rate (C_s & \dot{q}_l) and finally between cutting speed and feed rate have the most significant influences on the tool temperature.

Table 4.4 The ANOVA table of cutting tool temperature when using Lg20.0dl0.25

N	Source	Sum of Squares	Df	Mean Square	F-Ratio	P %
1	\dot{q}_g	64.40	1	64.40	6.39	1
2	\dot{q}_l	42.99	1	42.99	4.27	4
3	C_s	10.50	1	10.50	1.04	31
4	F_r	3.08	1	3.08	0.31	58
5	$\dot{q}_g \times \dot{q}_l$	11.32	1	11.32	1.12	29
6	$\dot{q}_g \times C_s$	28.89	1	28.89	2.87	9
7	$\dot{q}_g \times F_r$	0.04	1	0.04	0	95
8	$\dot{q}_l \times C_s$	40.76	1	40.76	4.04	5
9	$\dot{q}_l \times F_r$	5.69	1	5.69	0.57	45
10	$C_s \times F_r$	8.14	1	8.14	0.81	37
11	Residual	977.53	97	10.08		
12	Total (corr.)	2563.01	107			

Table 4.5 The ANOVA table of cutting tool temperature when using Lg33.5dl1.00

N	Source	Sum of Squares	Df	Mean Square	F-Ratio	P %
1	\dot{q}_g	21.16	1	21.16	3.5	6
2	\dot{q}_l	0.17	1	0.17	0.03	87
3	C_s	34.82	1	34.82	5.76	2
4	F_r	10.04	1	10.04	1.66	20
5	$\dot{q}_g \times \dot{q}_l$	68.12	1	68.12	11.27	0
6	$\dot{q}_g \times C_s$	1.34	1	1.34	0.22	64
7	$\dot{q}_g \times F_r$	2.90	1	2.90	0.48	49
8	$\dot{q}_l \times C_s$	38.86	1	38.86	6.43	1
9	$\dot{q}_l \times F_r$	13.99	1	13.99	2.32	13
10	$C_s \times F_r$	41.89	1	41.89	6.93	1
11	Residual	586.11	97	6.04		
12	Total (corr.)	3478.64	107			

Considering the similar initial conditions to perform the experiments using both of the injectors and referring to the experimental studies carried out by the other researchers about the effects of parameters such as cutting speed and feed rate on cutting tool temperature, the following questions are considerable:

- Why these parameters don't have the significant effects on tool temperature when using Lg20.0dl0.25?
- Why the feed rate has no significant effects on tool temperature when using Lg33.5dl1.00?

Two different hypotheses can be proposed to explain these questions. At first point of view, this inconvenience can be occurred due to the experimental errors such as the poor positioning of thermocouple. The second hypothesis comes from the behaviour of the nozzle geometry and its effects on the atomization performance and the injection angle.

According to the performed analysis of SMD and the injection angle in chapter 3 and referring to the Figures 3.14 to 3.17, it is observed that the atomization quality and the

injection angle are decreased when using injectors with smaller length and liquid orifice diameter. This result helps us to conclude that in Lg20.0dl0.25 the lubrication was more concentrated on the cutting zone and the vaporization due to the increase in cutting speed and/or feed rate was less than that in Lg33.5dl1.00. Consequently, these two parameters have no significant effects on cutting tool temperature when using smaller injector.

To investigate the effects of cutting parameters on tool temperature with respect to the Figures 4.12 to 4.15, it is clearly shown that increasing the gas and liquid flow rate decreases the tool temperature and increasing the cutting speed when using Lg33.5dl1.00 increases the cutting tool temperature proportionally while this parameter has non-considerable effect when using Lg20.0dl0.25. The reason of cutting speed effect on tool temperature, can be explained by the plastic deformation occurred in the shear zone because of increasing the cutting speed. The rapid plastic deformation creates the high friction between the tool and the workpiece. Despite of considerable heat evacuation through the chips, the rest of the heat is transferred to the tool. This problem can be the cause of the tool wear as well as the material deformation especially in very high temperature.

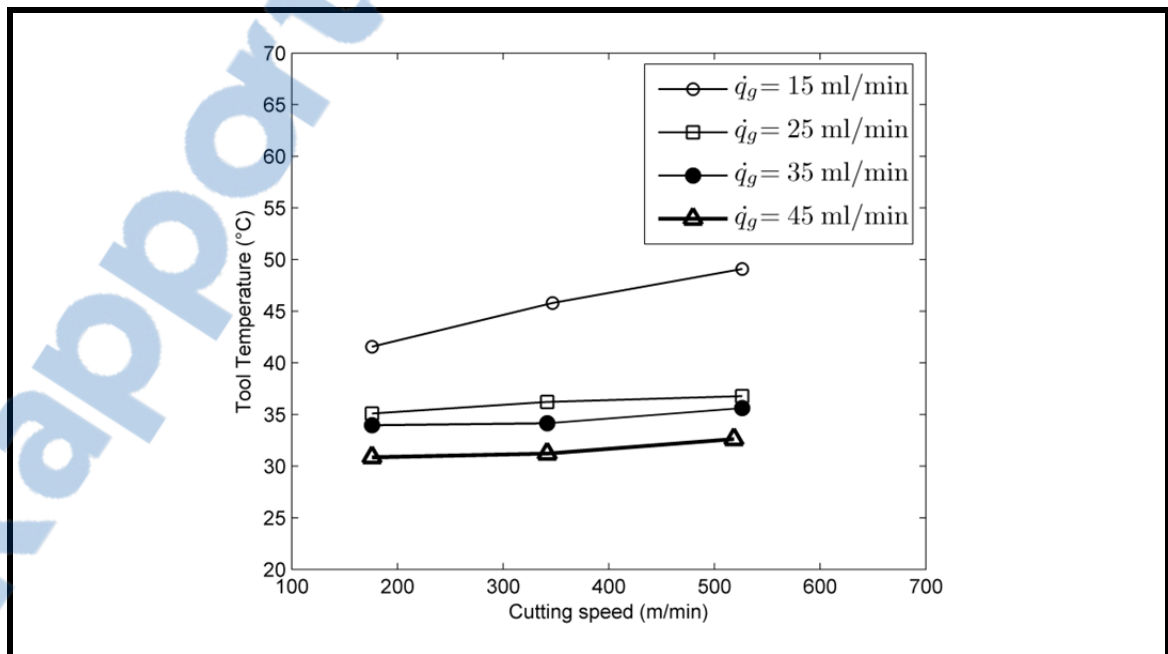


Figure 4.12 Gas flow rate effects on tool temperature when using Lg20.0dl0.25

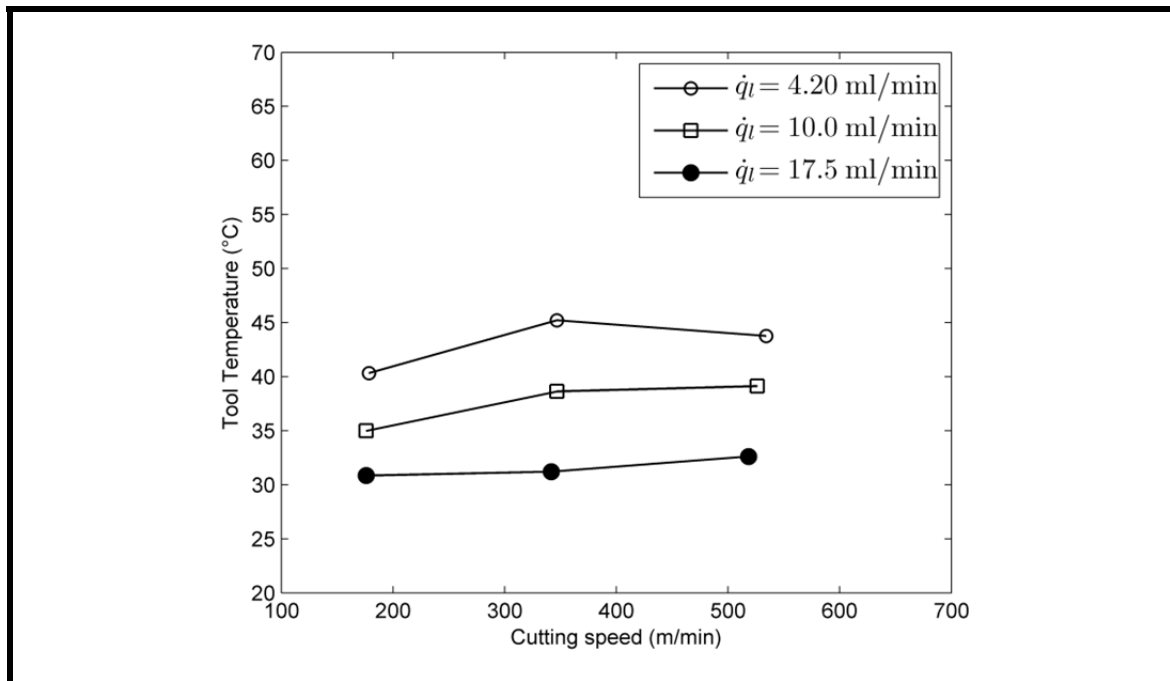


Figure 4.13 Liquid flow rate effects on tool temperature when using Lg20.0dl0.25

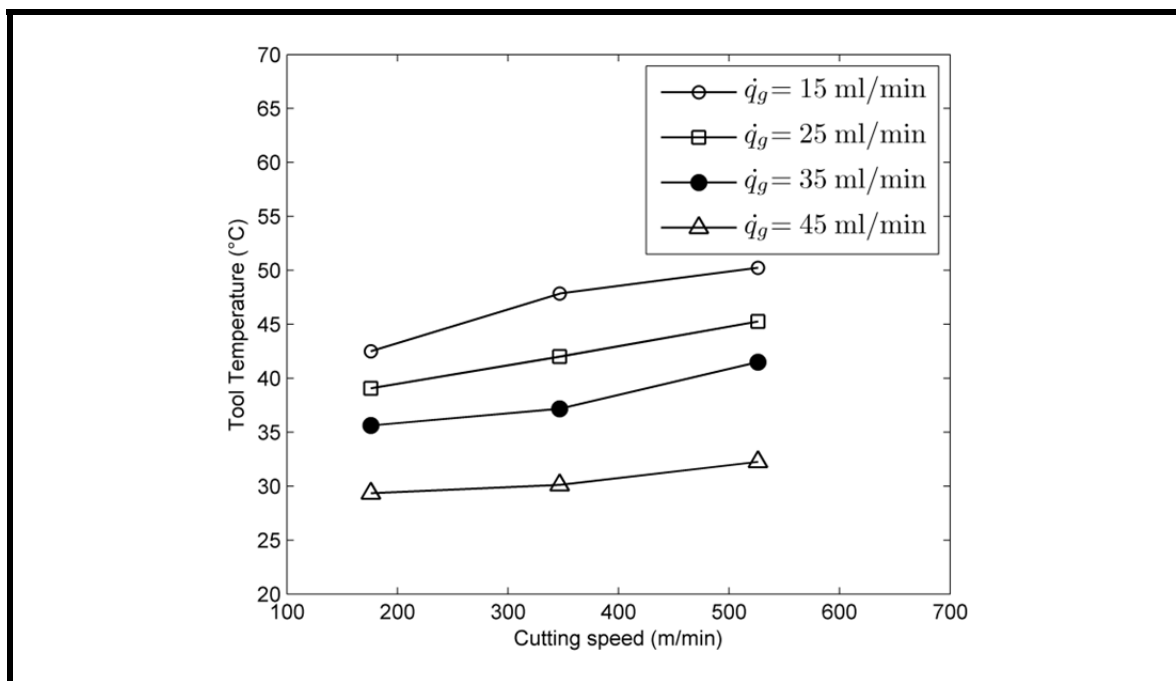


Figure 4.14 Gas flow rate effects on tool temperature when using Lg33.5dl1.0

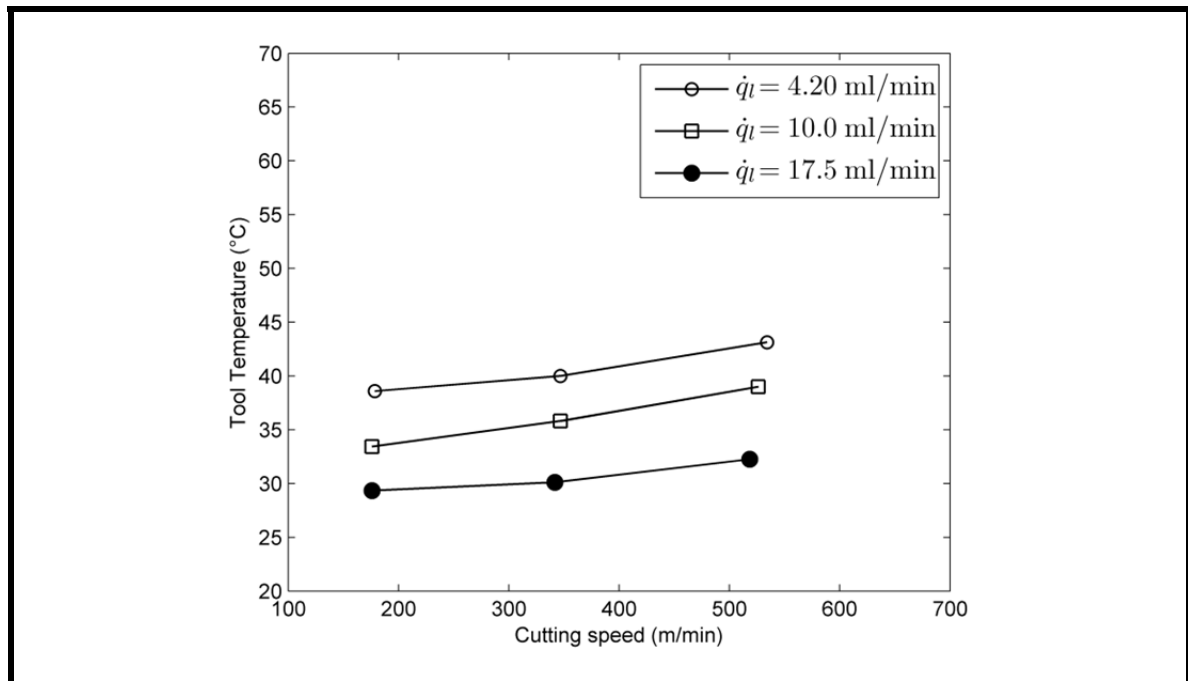


Figure 4.15 Liquid flow rate effects on tool temperature when using Lg33.5dl1.0

4.3.3 Effect of cutting parameters on dust concentration (Dc)

In order to find the cutting parameter effects on dust generation during dry, wet and MQC machining modes, the average of particle concentration was measured through the experiments.

All of these experiments were carried out using two nozzles (Lg33.5dl1.0 and Lg20.0dl0.25) and the similar cutting conditions as previously used. Measuring the dust concentration (solid and liquid particles) was performed using a laser photometer (TSI8532 DustTrak) which is capable to measure the concentration of the particle size range of 0.1 to 10 μm was used.

According to Figures 4.16 and 4.17 and considering the reduction of particle diameters when using the nozzle with higher length (Lg33.5dl1.00 in this study), it is visible at first glance that decreasing the particle size (in any gas flow rate) decreases the dust concentration when turning of aluminum alloy 6061-T6 by MQC machining mode. The other initial conclusion obtained from these Figures is that the dust concentration in dry machining is generally less

than that in two other methods which is logical due to the elimination of the liquid particles produced from cutting fluids through dry machining.

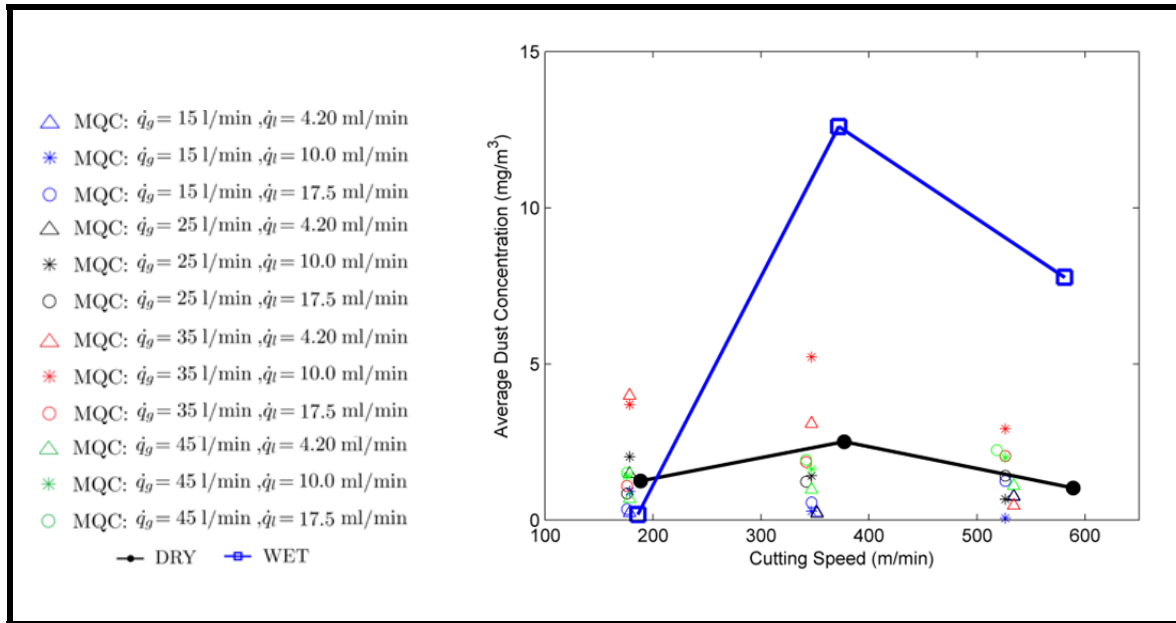


Figure 4.16 (a) Feed rate = 0.10 mm/rev

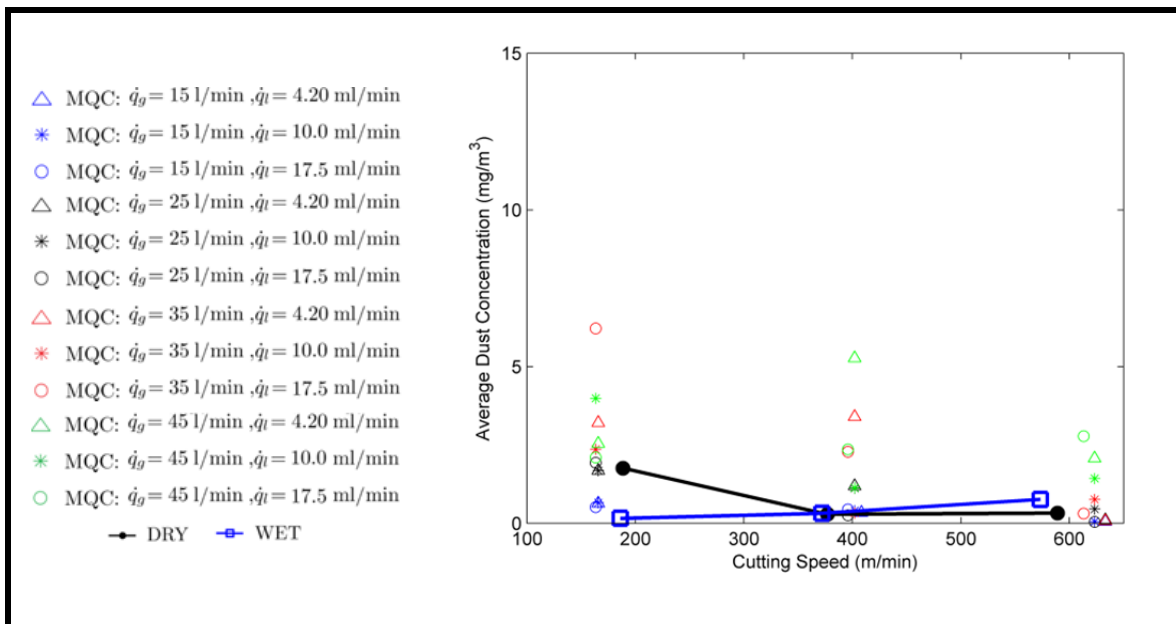


Figure 4.16 (b) Feed rate = 0.15 mm/rev

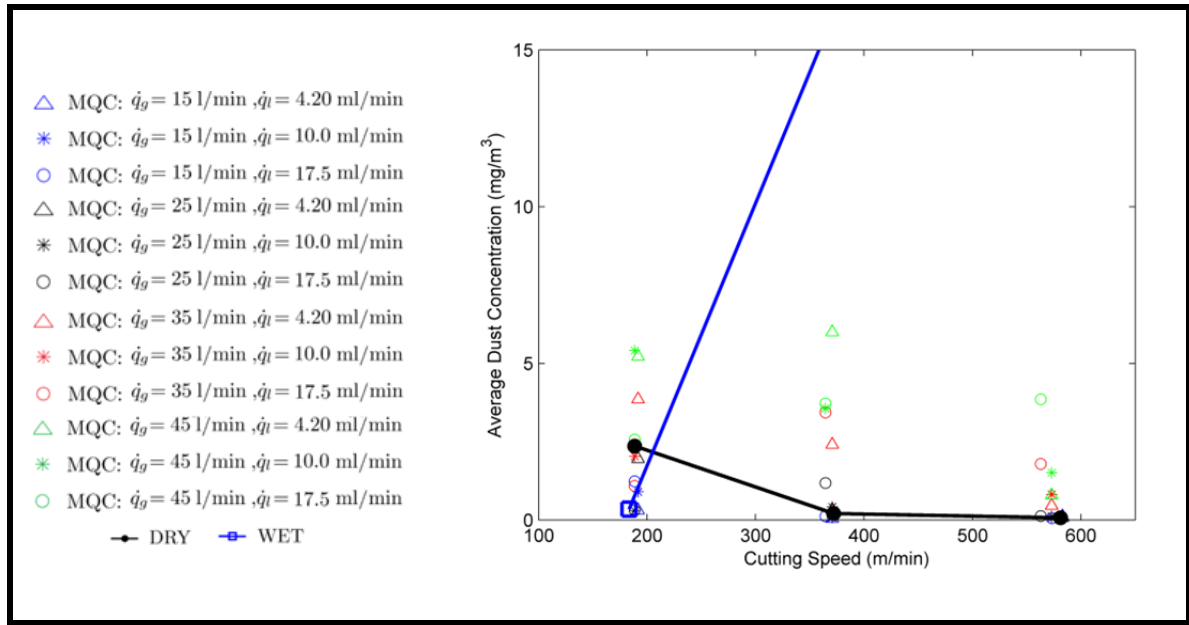


Figure 4.16 (c) Feed rate = 0.20 mm/rev

Figure 4.16 Lg20.0dl0.25 – dust concentration (mg/m³) variations related to cutting speed (m/min)

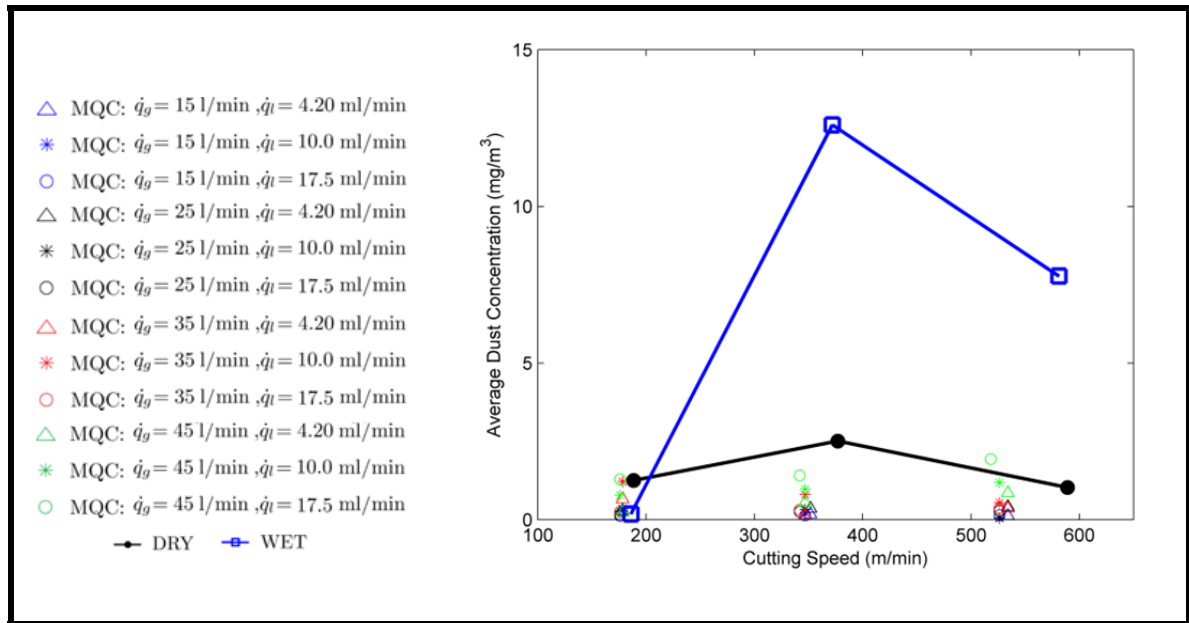


Figure 4.17 (a) Feed rate = 0.10 mm/rev

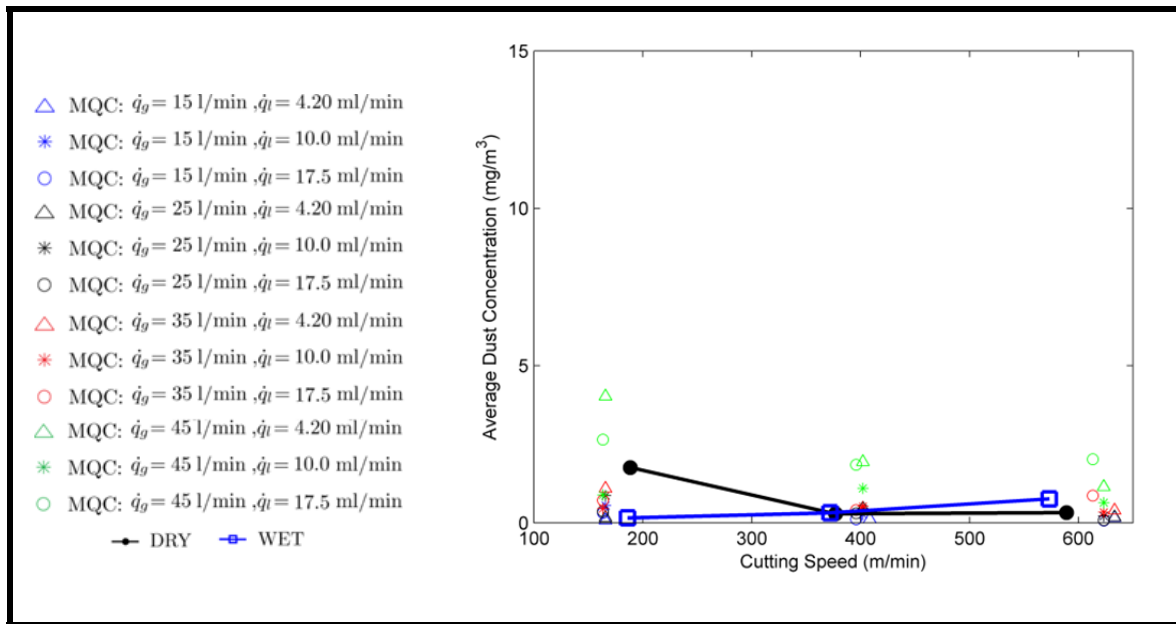


Figure 4.17 (b) Feed rate = 0.15 mm/rev

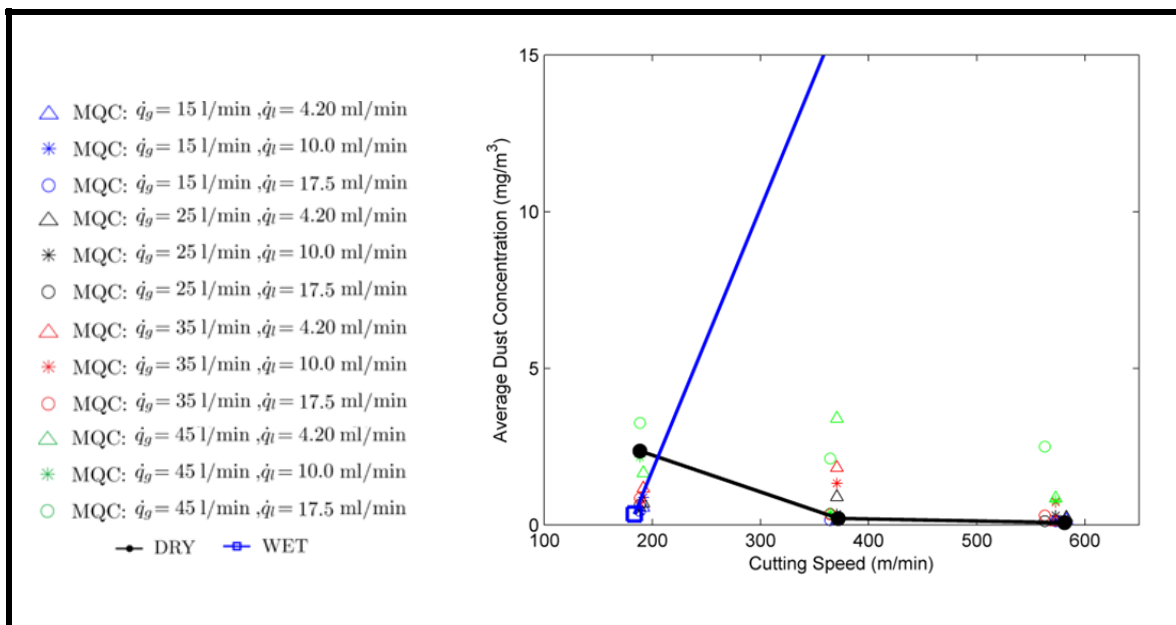


Figure 4.17 (c) Feed rate = 0.20 mm/rev

Figure 4.17 Lg33.5dl1.00 – dust concentration (mg/m³) variations related to cutting speed (m/min)

The different effects of cutting parameters such as cutting speed, feed rate, gas and liquid flow rates on dust concentration are shown in Figures 4.18 to 4.23.

According to the Figures 4.18 and 4.19, increasing the gas flow rate and cutting speed in both of the injectors increases and decreases the dust concentration respectively. Increasing the liquid flow rate in Lg20.0dl0.25 increases the dust concentration whereas increasing the liquid flow rate using Lg33.5dl1.00 has the inverse effect on dust concentration (see Figures 4.20 - 4.21). With respect to Figures 4.22 and 4.23, it is concluded that increasing the feed rate, increases the dust concentration.

As described in chapter 3 about the inverse effect of the liquid flow rate when using these two nozzles, the increasing in the liquid flow rate increases both SMD and injection angle regardless the length of the nozzle and its liquid orifice diameter. According to the results obtained from chapter 3, the increasing in the nozzle length and liquid orifice diameter decreases the SMD and increases the injection angle respectively.

It is concluded that in smaller injector, Lg20.0dl0.25, the increasing of the liquid flow rate accompanying of the small nozzle length and liquid orifice diameter leads to increase the dust concentration. This result is inversely occurred in Lg33.5dl1.00 due to the decreasing in SMD.

Considering the literature review, one of the important parameters influenced on dust generation is the friction. This result is useful to explain the effect of the feed rate on dust concentration where the increasing in the feed rate increases the friction. As it is previously obtained, the increasing in the cutting speed decreases the surface roughness and minimizing the roughness can be beneficial to reduce the particle emissions (Khettabi *et al.*, 2010). Consequently, the decreasing in dust concentration due to the increase in cutting speed can be explained.

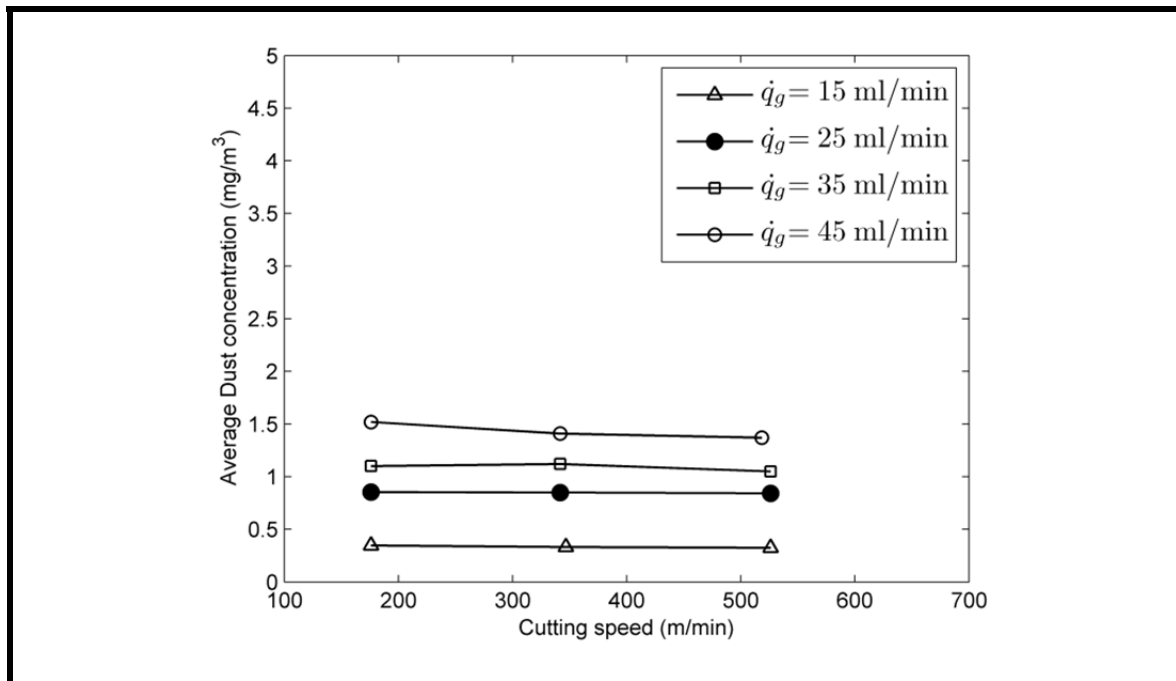


Figure 4.18 Gas flow rate effects on dust concentration when using Lg20.0dl0.25

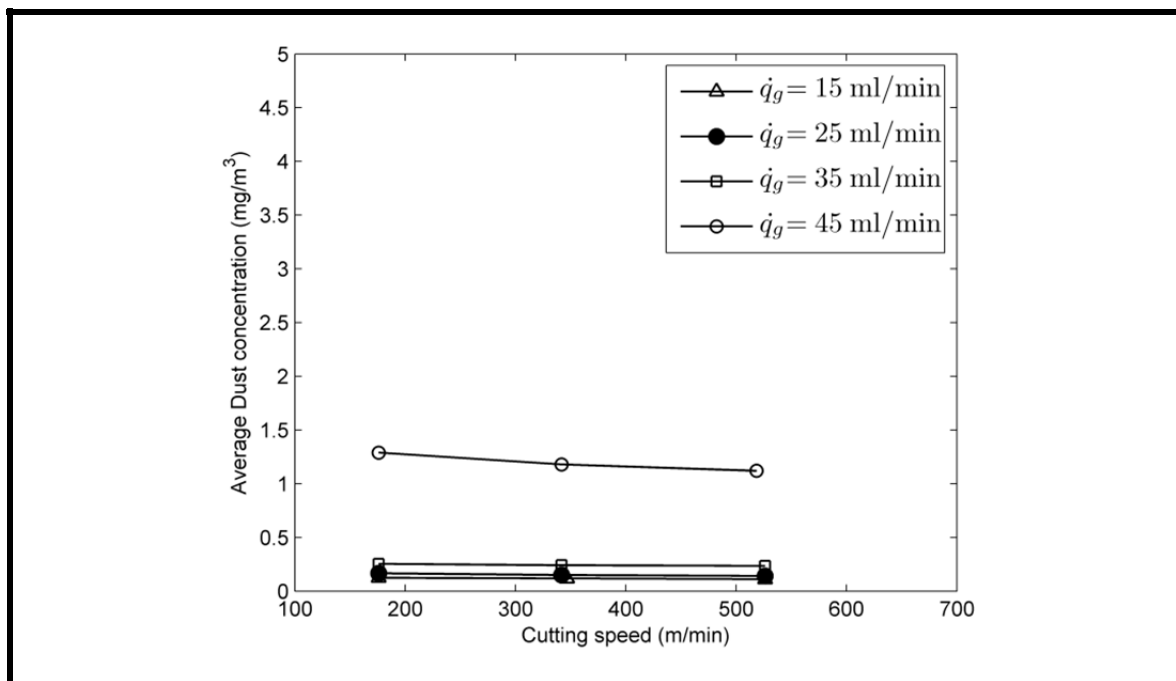


Figure 4.19 Gas flow rate effects on dust concentration when using Lg33.5dl1.00

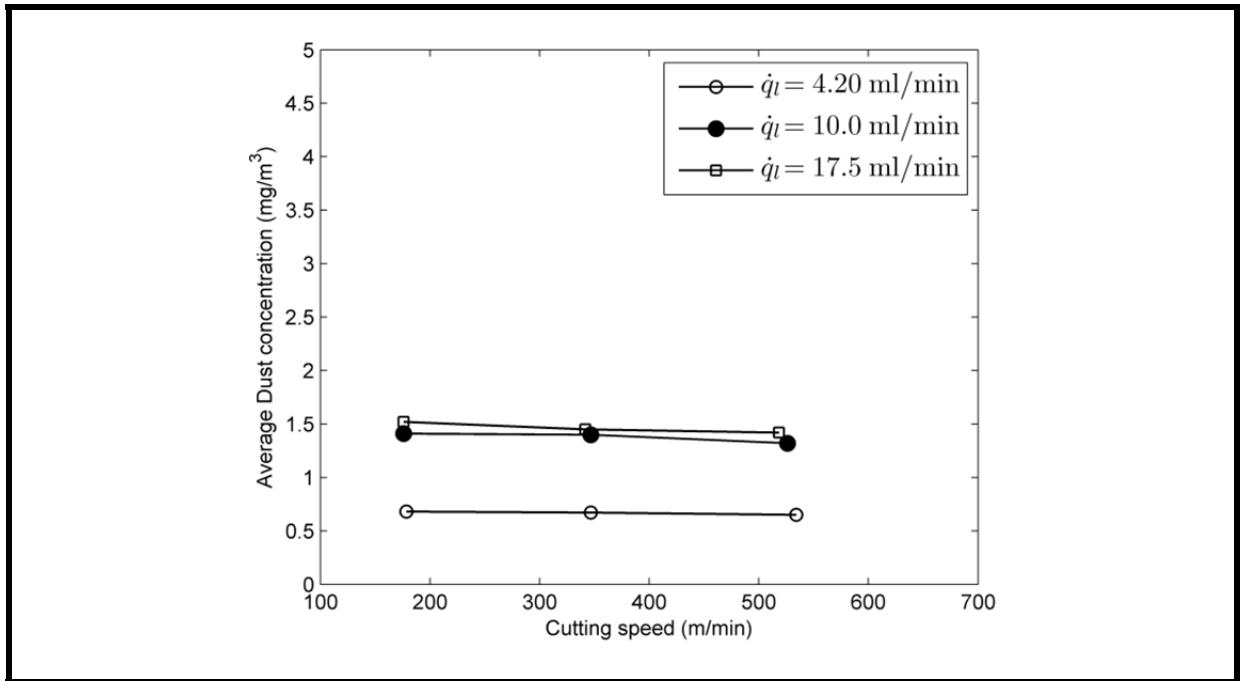


Figure 4.20 Liquid flow rate effects on dust concentration when using Lg20.0dl0.25

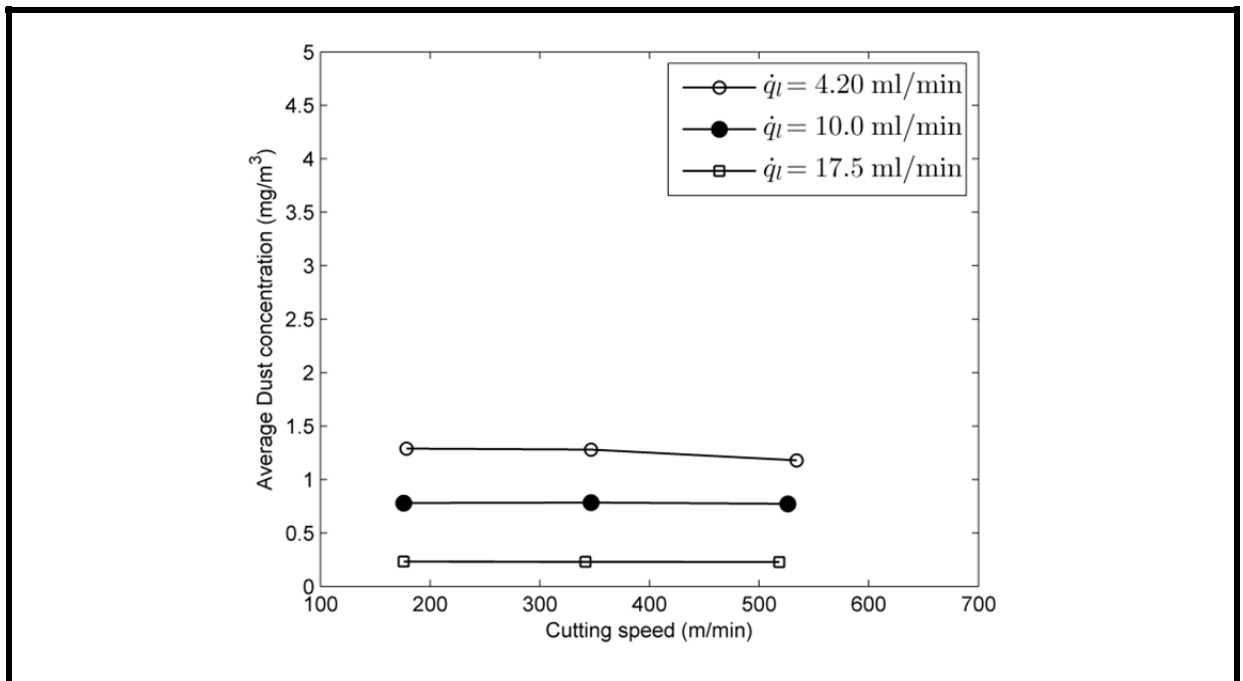


Figure 4.21 Liquid flow rate effects on dust concentration when using Lg33.5dl1.00

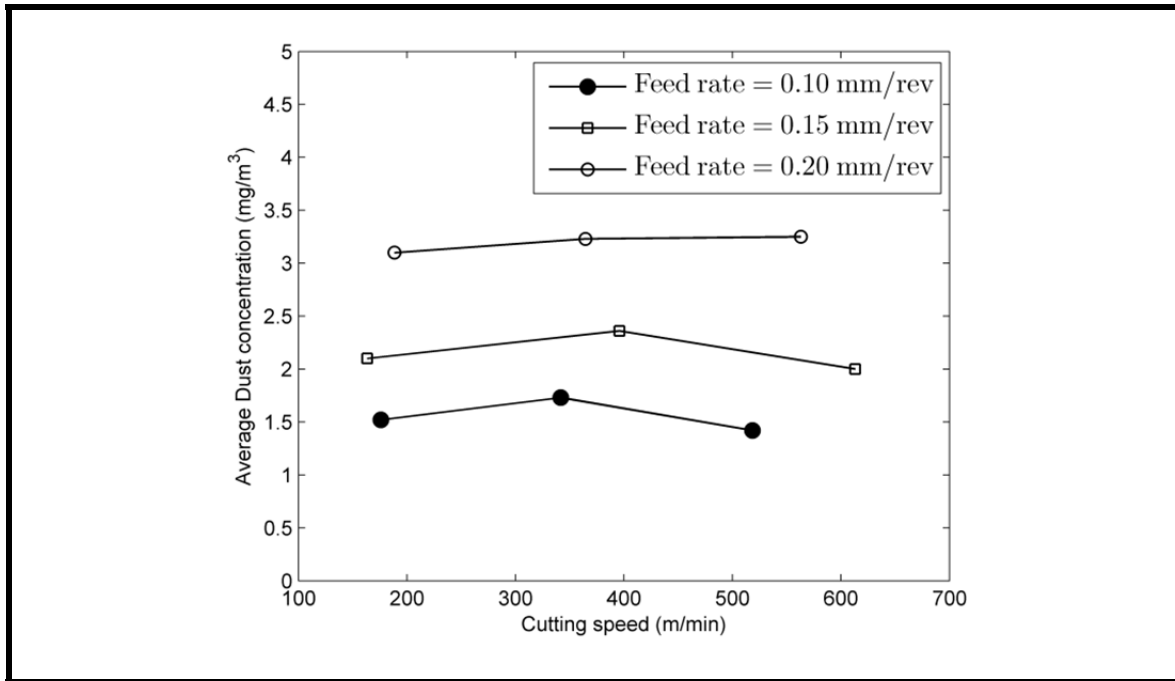


Figure 4.22 Feed rate effects on dust concentration when using Lg20.0dl0.25

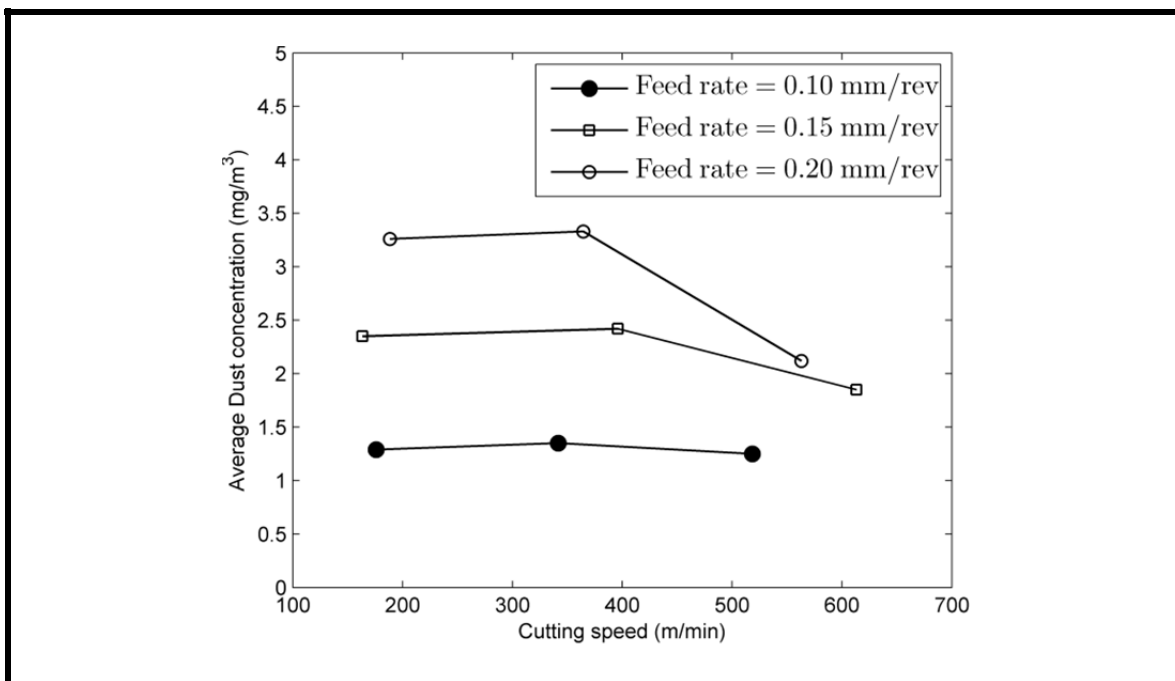


Figure 4.23 Feed rate effects on dust concentration when using Lg33.5dl1.00

4.4 Multiple response optimization of machining

4.4.1 Introduction

In the previous sections, the influence of different cutting parameters on surface roughness, tool temperature and aerosol emission were investigated and the better conditions are found for each of these quality factors. The optimum condition found for each response was not necessarily compatible in other responses. In this situation, it is essential to find an area where all the experimental responses realize the specifications imposed to attain the recommended goals. In the present study the objective is to minimize all three of these factors which give the best surface finish, longer tool lifetime and cleaner environment and also the better productivity.

4.4.2 Desirability Function

One of the most popular methods employed for real-time optimization of numerous independent or unrelated responses is Desirability Function method which is very simple and easy to apply (He and Zhu, 2009). This approach was suggested firstly by Harrington (Harrington, 1965), but the Derringer and Suich (Derringer, 1980) proposed a more overall desirability function which is usable to the researchers. In this method, the desirability function D_i (Equation 4.1) converts each response into a dimensionless value (d_i ; $i=1,2,3,\dots,n$) between 0 and 1 which is identified as desirability:

$$D_i = \sqrt[m]{d_1 \times d_2 \times d_3 \times \dots \times d_n} \quad (4.1)$$

where m is the number of responses.

In order to find the Desirability of each response it is important to know about the goal of optimization which is minimizing, maximizing (called one-sided transformation) or obtaining the precise target value (called two-sided transformation). If the $\hat{y}_i(x)$ is the fitted value of response variable $y_i(x)$ where x_i is the input process parameters, the one sided transformations are as follow (Wan and Birch, 2011; Wan and Birch, 2011):

- When the goal is to minimize the i^{th} response (Equation.4.2):

$$d_i = \begin{cases} 1 & \hat{y}_i(x) < L \\ \left[\frac{\hat{y}_i(x) - H}{L - H} \right]^w & L \leq \hat{y}_i(x) \leq H \\ 0 & \hat{y}_i(x) > H \end{cases} \quad (4.2)$$

- When the goal is to maximize the i^{th} response (Equation. 4.3):

$$d_i = \begin{cases} 0 & \hat{y}_i(x) < L \\ \left[\frac{\hat{y}_i(x) - L}{H - L} \right]^w & L \leq \hat{y}_i(x) \leq H \\ 1 & \hat{y}_i(x) > H \end{cases} \quad (4.3)$$

- Finally, two-sided transformation is performed due to the below equations (Equation.4.4):

$$d_i = \begin{cases} 0 & \hat{y}_i(x) < L \\ \left[\frac{\hat{y}_i(x) - L}{T - L} \right]^{w1} & L \leq \hat{y}_i(x) \leq T \\ \left[\frac{\hat{y}_i(x) - H}{H - T} \right]^{w2} & T \leq \hat{y}_i(x) \leq H \\ 0 & \hat{y}_i(x) > H \end{cases} \quad (4.4)$$

where L, U and T are the minimum, maximum and target values respectively. In these equations, w is the weight value which is determined by the analyst. This value depends on the importance level of the responses and can be 1 if the importance level of all the responses is the same. According to the experiments carried out using two atomizers, Lg20.0dl0.25 and Lg33.5dl1.00, as shown in the table 4.6, the cutting parameters used to obtain the optimum of each response (Surface Roughness, Tool Temperature and Aerosol Emission) are different. In this case, it is indispensable to achieve the optimum setting level in which all of these responses take their minimum values.

Table 4.6 Quality responses statistical results

	Responses	R ²	R2 adjusted	P-value	F-ratio	Input parameters to achieve the optimum value			
						q _g (l/min)	q _l (ml/min)	Cs (m/min)	Fr (mm/Rev)
Lg20.0dl0.25	Surface Roughness (μm)	74.36	71.72	0	28.14	45	4.20	534.07	0.10
	Cutting Tool Temperature (°C)	69.87	66.77	0	22.50	45	17.5	175.93	0.10
	Average Dust Concentration (mg/m ³)	53.86	49.11	0	11.32	15	10.0	526.22	0.10
Lg20.0dl0.25	Surface Roughness (μm)	73.44	70.71	0	26.83	45	4.20	534.07	0.10
	Cutting Tool Temperature (°C)	85.25	83.73	0	56.08	45	17.5	175.93	30.85
	Average Dust Concentration (mg/m ³)	55.51	50.93	0	12.10	25	17.5	623.30	0.15

Therefore, the equations 4.1 and 4.2 are useful to attain this goal. The values of desirability function for each nozzle are presented in tables A1 and A2 in appendix1 and appendix2. In these tables, the value of D_i (max) for Lg20.0dl0.25 and Lg33.5dl1.00 are 0.961 and 0.973 respectively which show the optimum setting levels of process parameters for each of these nozzles.

These levels are similar for both of the atomizers (see Tables 4.7 and 4.8). The results show that the optimum input values of multiple response optimizations regarding the better productivity rate is high feed rate, higher gas flow rate, higher liquid flow rate and higher cutting speed.

Table 4.7 Optimum setting level when using Lg20.0dl0.25 nozzle

N	Experimental input variables				Experimental responses				Desirability
	Gas flow rate (l/min)	Liquid flow rate (ml/min)	Cutting speed Cs (m/min)	Feed rate Fr (mm/Rev)	Surface Roughness Ra (μm)	Cutting Tool Temperature T (°C)	Average Dust concentration Dc (mg/m ³)	Material removal rate Q (mm ³ /min)	
	Minimum				0.99	30.85	0.046	211.12	Di(max)
	Maximum				6.93	52.23	6.22	1399.40	
	Average				2.905	42.211	1.513	677.45	
72	45	17.5	613.24	0.15	1.36	46.28	2.78	1002.83	0.961

Table 4.8 Optimum setting level when using Lg33.5dl1.00 nozzle

N	Experimental input variables				Experimental responses				Desirability
	Gas flow rate (l/min)	Liquid flow rate (ml/min)	Cutting speed Cs (m/min)	Feed rate Fr (mm/Rev)	Surface Roughness R_a (μm)	Cutting Tool Temperature T ($^{\circ}\text{C}$)	Average Dust concentration D_c (mg/m^3)	Material removal rate Q (mm^3/min)	
Minimum					0.98	29.35	0.049	211.12	Di(max)
Maximum					6.94	58.82	4.02	1400.40	
Average					2.976	43.277	0.701	679.48	
72	45	17.5	613.2 4	0.15	1.23	38.28	2.02	1103.83	0.973

The optimum setting level values of this study (see Table 4.9) confirm that the better surface finish, the minimum of cutting tool temperature and aerosol emission and the better productivity are obtained using the Lg33.5dl1.00 nozzle which validate the results obtained previously.

Table 4.9 Optimum response values for two different nozzles

	Surface Roughness (μm)	Cutting Tool Temperature ($^{\circ}\text{C}$)	Average Dust concentration (mg/m^3)	Material removal rate (mm^3/min)
Lg20.0dl0.25	1.36	46.28	2.78	1002.83
Lg33.5dl1.00	1.23	38.28	2.02	1103.83

According to table 4.10 (for Lg33.5dl1.00), it is observed that all the cutting parameters and their interactions have the significant effect on desirability function R-squared of 99.14 %.

Table 4.10 The ANOVA table of desirability function when using Lg33.5dl1.00 nozzle

N	Source	Sum of Squares	Df	Mean Square	F-Ratio	P %
1	\dot{q}_g	0.10	1	0.10	450.51	0.00
2	\dot{q}_l	0.09	1	0.09	404.89	0.00
3	C_s	0.00	1	0.00	13.77	0.03
4	F_r	2.24	1	2.24	10200.4	0.00
5	$\dot{q}_g \times \dot{q}_l$	0.00	1	0.00	17.11	0.01
6	$\dot{q}_g \times C_s$	0.01	1	0.01	31.13	0.00
7	$\dot{q}_g \times F_r$	0.01	1	0.01	28.92	0.00
8	$\dot{q}_l \times C_s$	0.01	1	0.01	26.84	0.00
9	$\dot{q}_l \times F_r$	0.01	1	0.01	27.32	0.00
10	$C_s \times F_r$	0.00	1	0.00	5.83	1.77
11	Residual	0.02	97	0.00		
12	Total (corr.)	2.48	107			

CONCLUSION

Following the conducted experimental study and the performed analysis in this research, the main conclusions are presented in two sections:

- a) The effects of nozzle geometries and different pumps (pulsed and non-pulsed) on Sauter mean diameter and injection angle;
- b) The effects of cutting conditions on quality parameters such as surface finish, cutting tool temperature and dust concentration and the optimum conditions estimation.

In the first part, three types of nozzles with different lengths, liquid orifice diameters and liquid orifice shapes were investigated. The main conclusions are as follows:

1. Effects on atomization:

- Liquid orifice diameter effect: The droplet size in continuous pump is independent from the liquid orifice diameter of nozzle while in the pulsed pump; the smaller liquid orifice diameter leads to the better atomization;
- Injector length effect: The length of injector has no significant effect on atomization. In other word, depending on gas flow rate, the particle size vary regardless the injector length;
- Liquid orifice shape: The atomization quality in the nozzle with straight liquid orifice is better than that of the conical liquid orifice shape;

According to different pumps, the better atomization is always occurred when using continuous pump.

2. Effects on Mixed air-liquid injection angle:

- Liquid orifice diameter effect: For continuous and pulsed pumps, an increase in flow rates (liquid or gas) or in the liquid orifice diameter of nozzle leads to a larger injection angle;
- Injector length effect: The injection angle is independent of the injector length in discontinuous pump while in continuous pump; the injectors with smaller lengths can lubricate a larger surface of cutting zone when using lower liquid flow rates;

- Liquid orifice shape: The injection angle is better (larger) in the nozzle with conical liquid orifice shape when using continuous pump;

The conclusions obtained from turning of aluminum alloy 6061-T6 are divided into four categories as follows:

❖ **Surface Roughness :**

- Comparing the different lubrication modes, it is concluded that increasing the feed rate improves the surface finish during wet machining further than that in dry and MQC modes;
- When using pulsed pump, the optimum surface finish is achieved in lower feed rate, lower cutting speed and lower gas flow rate. . In this condition, the better surface finish is obtained using the MQC mode;
- In order to achieve the best surface finish, the lower feed rate and the higher cutting speed are the optimum cutting conditions when using continuous pumps. In this case, the surface finish is always better in MQC than that in wet and dry machining modes;
- Despite the fact that gas and liquid flow rates have no significant effect on surface roughness, this quality indicator is affected by these parameters through their influences on atomization quality. As a result, comparing two nozzles, the injector with bigger dimensions is the preferable atomizer which produces the best surface finish;

❖ **Cutting Tool Temperature:**

- Heat generation increases by decreasing the quantity of the lubricant. This result is totally independent of the cutting speed and feed rate;
- The increase in the gas and liquid flow rate decreases the tool temperature in both of the nozzles when using MQC machining mode. In this mode and using Lg33.5dl1.00 nozzle, the increase in cutting speed increases the cutting tool temperature proportionally. This parameter has non-considerable effect when using the lg20.0dl0.25;
- Comparing different nozzles, the cutting speed and feed rate have no significant effect on the tool temperature when using the nozzle with smaller length and liquid orifice diameter. The two following hypotheses could explain this behaviour:

- I. The experimental errors such as the poor positioning of thermocouple;
- II. The behaviour of the nozzle geometry and its effects on the atomization performance as well as the injection angle which leads to the more concentration of lubricant on the cutting zone and less vaporization due to the increase in speed and/or feed rate.

❖ **Dust Concentration:**

- During dry machining mode, the dust concentration generally less than that in wet and MQC modes. This result is due to the elimination of the liquid particles produced from cutting fluids during dry machining;
- Increasing the gas flow rate and cutting speed in both of the injectors (Lg33.5dl1.00 and Lg20.0dl0.25) increases and decreases the dust concentration respectively. However, the increase in liquid flow rate in smaller injector, increases the dust concentration whereas this effect is inverse using the injector with higher length and liquid orifice diameter;
- The increase in feed rate increases the dust concentration due to the increasing of the friction;

❖ **Optimization**

According to desirability function and optimization performed on the obtained results for all the responses, it is concluded that optimum level setting for multiple response optimization is the high feed rate, higher cutting speed and higher liquid and gas flow rates. In these conditions the productivity is also better than the other conditions. Comparing two different nozzles, it is confirmed that the nozzle with bigger length and liquid orifice diameter leads to optimum values of all the quality indexes.

RECOMMENDATIONS

The analysis of the results presented in this thesis identified a number of directions, and tasks.

The first recommendation addresses the repeating of the investigation of the process parameter effects on the quality indexes of machining such as surface roughness, cutting tool temperature and dust and aerosol emission during the turning of aluminum alloy 6061-T6 using the pulsed pumps and the same conditions as those used in ULB. This new investigation will help us to compare the influences of injection methods such as pulsed and continuous.

The other proposition is to repeat the cutting tool temperature analysis using a thermocouple installed exactly at the tip of cutting tool in order to avoid the inaccurate temperature during machining.

Regarding the investigation of sauter mean diameter done by Lorenzetto and Lefebvre which is based on the exponential model, as a future work, it is also recommended to refine the analysis using this model.

APPENDIX 1

Table A1 Multiple response optimization when using Lg20.0dl0.25 nozzle

N	Experimental input variables				Experimental responses				Desirability
	Gas flow rate \dot{q}_g (l/min)	Liquid flow rate \dot{q}_l (ml/min)	Cutting speed C_s (m/min)	Feed rate F_r (mm/rev)	Surface roughness R_a (μm)	Cutting Tool Temperature T ($^{\circ}\text{C}$)	Average Dust concentration D_c (mg/m^3)	Material removal rate Q (mm^3/min)	D_i
1	1	1	1	1	1.79	47.373	0.232	214.13	0.509
2	2	1	1	1	1.67	44.395	1.48	214.13	0.607
3	3	1	1	1	4.72	43.141	3.99	214.13	0.638
4	4	1	1	1	1.40	40.319	0.681	214.13	0.635
5	1	2	1	1	1.26	49.724	0.919	214.13	0.622
6	2	2	1	1	1.16	41.573	2.03	214.13	0.680
7	3	2	1	1	1.07	38.125	3.7	214.13	0.700
8	4	2	2	1	1.89	34.99	1.41	211.12	0.696
9	1	3	2	1	1.71	41.573	0.347	211.12	0.707
10	2	3	2	1	1.64	35.1	0.853	211.12	0.749
11	3	3	2	1	1.49	33.96	1.1	211.12	0.765
12	4	3	2	1	1.37	30.85	1.52	211.12	0.762
13	1	1	3	1	1.22	49.881	0.243	422.23	0.521
14	2	1	3	1	1.13	50.038	0.21	422.23	0.558
15	3	1	4	1	1.34	45.492	3.09	416.20	0.576
16	4	1	4	1	1.39	45.022	0.98	416.20	0.580
17	1	2	4	1	1.41	48.157	0.286	416.20	0.557
18	2	2	4	1	1.35	42.514	1.42	416.20	0.591
19	3	2	4	1	1.05	43.141	5.22	416.20	0.607
20	4	2	4	1	1.09	38.633	1.63	416.20	0.612

Table A1 Multiple response optimization when using Lg20.0dl0.25 nozzle (*continued*)

N	Experimental input variables				Experimental responses				Desirability
	Gas flow rate \dot{q}_g (l/min)	Liquid flow rate \dot{q}_l (ml/min)	Cutting speed C_s (m/min)	Feed rate F_r (mm/rev)	Surface roughness R_a (μm)	Cutting Tool Temperature T ($^{\circ}\text{C}$)	Average Dust concentration D_c (mg/m^3)	Material removal rate Q (mm^3/min)	D_i
21	1	3	4	1	1.00	45.806	0.562	416.20	0.595
22	2	3	5	1	1.51	36.22	1.23	410.17	0.628
23	3	3	5	1	1.59	34.15	1.86	410.17	0.644
24	4	3	5	1	1.28	31.21	1.93	410.17	0.650
25	1	1	6	1	1.20	49.411	0.771	640.89	0.400
26	2	1	6	1	1.12	46.903	0.745	640.89	0.412
27	3	1	6	1	1.09	45.649	0.465	640.89	0.420
28	4	1	6	1	0.99	43.768	1.1	640.89	0.434
29	1	2	7	1	1.93	50.351	0.058	631.46	0.414
30	2	2	7	1	1.71	43.298	0.67	631.46	0.431
31	3	2	7	1	1.69	40.006	2.92	631.46	0.441
32	4	2	7	1	1.06	39.125	2	631.46	0.447
33	1	3	7	1	1.17	49.097	1.25	631.46	0.418
34	2	3	7	1	1.01	36.78	1.42	631.46	0.439
35	3	3	7	1	1.23	35.62	2.05	631.46	0.463
36	4	3	8	1	1.32	32.62	2.24	622.04	0.471
37	1	1	9	2	1.91	48.784	0.638	298.58	0.591
38	2	1	9	2	1.72	45.022	1.68	298.58	0.720
39	3	1	9	2	1.63	42.514	3.21	298.58	0.774
40	4	1	9	2	1.32	42.2	2.54	298.58	0.799
41	1	2	9	2	1.29	50.978	0.655	298.58	0.756
42	2	2	9	2	1.26	51.919	1.68	298.58	0.656

Table A1 Multiple response optimization when using Lg20.0dl0.25 nozzle (*continued*)

N	Experimental input variables				Experimental responses				Desirability
	Gas flow rate \dot{q}_g (l/min)	Liquid flow rate \dot{q}_l (ml/min)	Cutting speed C_s (m/min)	Feed rate F_r (mm/rev)	Surface roughness R_a (μm)	Cutting Tool Temperature T ($^{\circ}\text{C}$)	Average Dust concentration D_c (mg/m^3)	Material removal rate Q (mm^3/min)	D_i
43	3	2	10	2	2.00	37.655	2.36	294.053	0.682
44	4	2	10	2	1.61	35.304	3.99	294.05	0.701
45	1	3	10	2	1.47	46.903	0.513	294.05	0.658
46	2	3	10	2	1.39	39.849	1.93	294.05	0.693
47	3	3	10	2	1.31	36.244	6.22	294.05	0.719
48	4	3	10	2	1.78	33.736	2.1	294.05	0.745
49	1	1	11	2	1.21	46.903	0.337	735.13	0.610
50	2	1	12	2	1.67	44.865	1.19	723.82	0.683
51	3	1	12	2	1.64	42.827	3.4	723.82	0.725
52	4	1	12	2	1.64	42.2	5.27	723.82	0.749
53	1	2	12	2	1.88	49.097	0.404	723.82	0.702
54	2	2	12	2	1.37	43.141	1.12	723.82	0.754
55	3	2	12	2	1.76	34.99	0.329	723.82	0.786
56	4	2	12	2	1.62	32.482	1.13	723.82	0.806
57	1	3	13	2	2.72	45.335	0.446	712.51	0.776
58	2	3	13	2	1.95	37.812	0.254	712.51	0.822
59	3	3	13	2	1.77	33	2.28	712.51	0.850
60	4	3	14	2	1.71	31.885	2.36	712.51	0.869
61	1	1	14	2	1.46	43.454	0.054	1140.02	0.569
62	2	1	14	2	1.43	40.006	0.103	1140.02	0.611
63	3	1	15	2	1.27	40.319	0.073	1140.02	0.639
64	4	1	15	2	1.73	41.417	2.07	1121.93	0.658

Table A1 Multiple response optimization when using Lg20.0dl0.25 nozzle (*continued*)

N	Experimental input variables				Experimental responses				Desirability
	Gas flow rate \dot{q}_g (l/min)	Liquid flow rate \dot{q}_l (ml/min)	Cutting speed C_s (m/min)	Feed rate F_r (mm/rev)	Surface roughness R_a (μm)	Cutting Tool Temperature T ($^{\circ}\text{C}$)	Average Dust concentration D_c (mg/m^3)	Material removal rate Q (mm^3/min)	D_i
65	1	2	15	2	1.51	40.79	0.055	1121.93	0.618
66	2	2	15	2	1.69	38.438	0.452	1121.93	0.823
67	3	2	15	2	1.43	33.423	0.761	1121.93	0.859
68	4	2	15	2	1.31	34.52	1.43	1121.93	0.878
69	1	3	15	2	1.17	42.357	0.049	1121.93	0.868
70	2	3	16	2	1.13	35.931	0.046	1121.93	0.917
71	3	3	16	2	1.38	34.677	0.309	986.25	0.945
72	4	3	17	2	1.36	46.276	2.78	1002.33	0.961
73	1	1	17	3	5.80	49.411	0.313	459.93	0.415
74	2	1	17	3	5.89	46.276	1.95	459.93	0.468
75	3	1	17	3	5.63	44.395	3.85	459.93	0.475
76	4	1	17	3	5.45	45.335	5.22	459.93	0.446
77	1	2	18	3	5.24	48.784	0.898	459.93	0.457
78	2	2	18	3	6.10	43.141	0.295	452.39	0.500
79	3	2	18	3	6.93	41.573	2.04	452.39	0.506
80	4	2	18	3	6.19	40.476	5.41	452.39	0.483
81	1	3	18	3	6.12	46.589	1.24	452.39	0.493
82	2	3	18	3	6.40	41.887	0.313	452.39	0.530
83	3	3	18	3	6.09	39.065	1.09	452.39	0.536
84	4	3	19	3	6.23	36.871	2.57	452.39	0.520
85	1	1	19	3	5.37	51.919	0.049	889.70	0.411
86	2	1	19	3	5.67	47.216	0.324	889.70	0.430

Table A1 Multiple response optimization when using Lg20.0dl0.25 nozzle (*continued*)

N	Experimental input variables				Experimental responses				Desirability
	Gas flow rate \dot{q}_g (l/min)	Liquid flow rate \dot{q}_l (ml/min)	Cutting speed C_s (m/min)	Feed rate F_r (mm/rev)	Surface roughness R_a (μm)	Cutting Tool Temperature T ($^{\circ}\text{C}$)	Average Dust concentration D_c (mg/m^3)	Material removal rate Q (mm^3/min)	D_i
87	3	1	19	3	5.56	46.433	2.41	889.70	0.434
88	4	1	19	3	5.79	45.649	6	889.70	0.422
89	1	2	19	3	5.15	50.038	0.077	889.70	0.417
90	2	2	19	3	5.13	42.2	0.419	889.70	0.440
91	3	2	20	3	5.00	39.692	0.312	889.70	0.446
92	4	2	20	3	5.37	40.163	3.56	874.62	0.440
93	1	3	20	3	6.71	50.038	0.126	874.62	0.425
94	2	3	20	3	6.05	41.887	1.18	874.62	0.452
95	3	3	20	3	5.49	39.379	3.43	874.62	0.461
96	4	3	20	3	5.90	37.812	3.72	874.62	0.457
97	1	1	21	3	6.31	52.232	0.126	1399.40	0.264
98	2	1	21	3	5.42	46.903	0.076	1399.40	0.268
99	3	1	22	3	5.08	40.006	0.462	1375.26	0.284
100	4	1	22	3	5.52	40.946	0.791	1375.26	0.280
101	1	2	22	3	5.19	48.314	0.062	1375.26	0.271
102	2	2	22	3	5.71	42.2	0.122	1375.26	0.280
103	3	2	22	3	5.55	42.2	0.819	1375.26	0.283
104	4	2	22	3	4.95	40.006	1.51	1375.26	0.282
105	1	3	22	3	4.75	47.53	0.06	1375.26	0.261
106	2	3	23	3	5.75	45.962	0.127	1351.14	0.289
107	3	3	23	3	6.09	44.081	1.79	1351.13	0.296
108	4	3	23	3	5.79	40.946	3.85	1351.13	0.298

Table A1 Multiple response optimization when using Lg20.0dl0.25 nozzle (*continued*)

N	Experimental input variables				Experimental responses				Desirability
	Gas flow rate q _g (l/min)	Liquid flow rate q _l (ml/min)	Cutting speed C _s (m/min)	Feed rate F _r (mm/rev)	Surface roughness R _a (μm)	Cutting Tool Temperature T (°C)	Average Dust concentration D _c (mg/m ³)	Material removal rate Q (mm ³ /min)	
MINIMUM					0.99	30.85	0.046	211.12	D _i (max)
MAXIMUM					6.93	52.23	6.22	1399.40	
AVERAGE					2.905	42.211	1.513	677.45	
72	45	17.5	613.24	0.15	1.36	46.28	2.78	1002.33	0.961

APPENDIX 2

Table A2 Multiple response optimization when using Lg33.5dl1.00 nozzle

N	Experimental input variables				Experimental responses				Desirability
	Gas flow rate \dot{q}_g (l/min)	Liquid flow rate \dot{q}_l (ml/min)	Cutting speed C_s (m/min)	Feed rate F_r (mm/rev)	Surface roughness R_a (μm)	Cutting Tool Temperature T ($^{\circ}\text{C}$)	Average Dust concentration D_c (mg/m^3)	Material removal rate Q (mm^3/min)	D_i
1	1	1	1	1	1.95	49.411	0.277	214.13	0.682
2	2	1	1	1	1.61	46.433	0.272	214.13	0.703
3	3	1	1	1	1.61	42.2	0.655	214.13	0.713
4	4	1	1	1	1.47	38.595	0.233	214.13	0.715
5	1	2	1	1	1.28	45.962	0.355	214.13	0.712
6	2	2	1	1	1.23	41.887	0.289	214.13	0.737
7	3	2	1	1	1.15	39.065	1.21	214.13	0.750
8	4	2	2	1	1.77	33.423	0.78	211.11	0.751
9	1	3	2	1	1.77	42.51	0.124	211.11	0.747
10	2	3	2	1	1.79	39.065	0.167	211.11	0.775
11	3	3	2	1	1.45	35.62	0.254	211.11	0.787
12	4	3	2	1	1.55	29.35	1.29	211.11	0.786
13	1	1	3	1	1.29	46.276	0.172	422.23	0.510
14	2	1	3	1	1.31	42.827	0.351	422.23	0.532
15	3	1	4	1	1.62	40.946	0.154	416.20	0.542
16	4	1	4	1	1.61	40.006	0.541	416.20	0.548
17	1	2	4	1	1.51	48.784	0.219	416.20	0.525
18	2	2	4	1	1.45	43.768	0.328	416.20	0.548
19	3	2	4	1	1.52	39.379	0.806	416.20	0.562
20	4	2	4	1	1.24	35.81	0.974	416.20	0.569

Table A2 Multiple response optimization when using Lg33.5dl1.00 nozzle (*continued*)

N	Experimental input variables				Experimental responses				Desirability
	Gas flow rate \dot{q}_g (l/min)	Liquid flow rate \dot{q}_l (ml/min)	Cutting speed C_s (m/min)	Feed rate F_r (mm/rev)	Surface roughness R_a (μm)	Cutting Tool Temperature T ($^{\circ}\text{C}$)	Average Dust concentration D_c (mg/m^3)	Material removal rate Q (mm^3/min)	D_i
21	1	3	4	1	1.21	47.843	0.135	416.20	0.544
22	2	3	5	1	1.57	42	0.25	410.17	0.574
23	3	3	5	1	1.55	37.18	0.309	410.17	0.590
24	4	3	5	1	1.23	30.12	1.41	410.17	0.596
25	1	1	6	1	1.49	48.157	0.123	640.89	0.289
26	2	1	6	1	1.25	43.611	0.413	640.89	0.300
27	3	1	6	1	1.15	43.925	0.364	640.89	0.307
28	4	1	6	1	0.98	43.141	0.852	640.89	0.325
29	1	2	7	1	1.53	47.843	0.049	631.46	0.301
30	2	2	7	1	1.45	41.573	0.061	631.46	0.317
31	3	2	7	1	1.75	38.438	0.542	631.46	0.327
32	4	2	7	1	1.53	39	1.18	631.46	0.334
33	1	3	7	1	1.59	50.23	0.142	631.46	0.299
34	2	3	7	1	1.21	45.26	0.283	631.46	0.323
35	3	3	7	1	1.31	41.5	0.36	631.46	0.350
36	4	3	8	1	1.15	32.25	1.93	622.03	0.355
37	1	1	9	2	1.59	53.486	0.081	298.58	0.742
38	2	1	9	2	1.43	48.784	0.164	298.58	0.763
39	3	1	9	2	1.43	46.589	1.09	298.58	0.782
40	4	1	9	2	1.33	43.768	4.02	298.58	0.793
41	1	2	9	2	1.19	52.075	0.548	298.58	0.751
42	2	2	9	2	1.14	46.903	0.863	298.58	0.780

Table A2 Multiple response optimization when using Lg33.5dl1.00 nozzle (continued)

N	Experimental input variables				Experimental responses				Desirability
	Gas flow rate \dot{q}_g (l/min)	Liquid flow rate \dot{q}_l (ml/min)	Cutting speed C_s (m/min)	Feed rate F_r (mm/rev)	Surface roughness R_a (μm)	Cutting Tool Temperature T ($^{\circ}\text{C}$)	Average Dust concentration D_c (mg/m^3)	Material removal rate Q (mm^3/min)	D_i
43	3	2	10	2	2.29	38.44	0.45	294.05	0.800
44	4	2	10	2	1.89	35.304	0.89	294.05	0.813
45	1	3	10	2	1.68	44.395	0.316	294.05	0.759
46	2	3	10	2	1.56	40.946	0.366	294.05	0.801
47	3	3	10	2	1.27	36.87	0.72	294.05	0.825
48	4	3	10	2	1.29	30.36	2.65	294.05	0.838
49	1	1	11	2	1.21	51.292	0.117	735.13	0.588
50	2	1	12	2	2.17	43.768	0.458	723.82	0.604
51	3	1	12	2	1.94	42.51	0.365	723.82	0.617
52	4	1	12	2	1.71	43.454	1.94	723.82	0.627
53	1	2	12	2	1.85	47.53	0.262	723.82	0.591
54	2	2	12	2	1.64	42.2	0.453	723.82	0.615
55	3	2	12	2	1.37	39.379	0.525	723.82	0.632
56	4	2	12	2	1.41	36.871	1.1	723.82	0.644
57	1	3	13	2	1.89	42.827	0.117	712.53	0.585
58	2	3	13	2	1.69	39.379	0.304	712.51	0.618
59	3	3	13	2	1.63	35.46	0.41	712.51	0.640
60	4	3	13	2	1.48	32.95	1.85	712.51	0.662
61	1	1	14	2	1.38	46.903	0.164	1140.02	0.861
62	2	1	14	2	1.29	43.141	0.182	1140.02	0.887
63	3	1	14	2	1.35	41.887	0.393	1140.02	0.905
64	4	1	15	2	1.47	44.081	1.15	1121.92	0.916

Table A2 Multiple response optimization when using Lg33.5dl1.00 nozzle (*continued*)

N	Experimental input variables				Experimental responses				Desirability
	Gas flow rate \dot{q}_g (l/min)	Liquid flow rate \dot{q}_l (ml/min)	Cutting speed C_s (m/min)	Feed rate F_r (mm/rev)	Surface roughness R_a (μm)	Cutting Tool Temperature T ($^{\circ}\text{C}$)	Average Dust concentration D_c (mg/m ³)	Material removal rate Q (mm ³ /min)	D_i
65	1	2	15	2	1.74	52.546	0.215	1121.93	0.882
66	2	2	15	2	1.56	44.395	0.22	1121.93	0.915
67	3	2	15	2	1.47	40.633	0.337	1121.93	0.936
68	4	2	15	2	1.29	38.438	0.643	1121.93	0.949
69	1	3	15	2	1.25	50.351	0.076	1121.93	0.908
70	2	3	15	2	1.19	44.708	0.086	1121.93	0.947
71	3	3	16	2	1.20	40.946	0.863	1103.83	0.971
72	4	3	16	2	1.23	38.28	2.02	1103.83	0.973
73	1	1	17	3	5.59	50.66	0.554	459.93	0.460
74	2	1	17	3	5.50	46.28	0.69	459.93	0.474
75	3	1	17	3	4.92	45.34	1.17	459.93	0.477
76	4	1	17	3	4.99	44.708	1.66	459.93	0.471
77	1	2	17	3	5.11	48.784	0.883	459.93	0.490
78	2	2	18	3	6.80	40.63	0.464	452.39	0.508
79	3	2	18	3	6.49	36.871	0.716	452.39	0.512
80	4	2	18	3	6.79	36.244	2.17	452.39	0.504
81	1	3	18	3	6.41	45.022	0.447	452.39	0.522
82	2	3	18	3	6.85	42.2	0.641	452.39	0.542
83	3	3	18	3	6.11	38.282	0.855	452.39	0.547
84	4	3	18	3	6.63	34.05	3.26	452.39	0.538
85	1	1	19	3	6.71	54.113	0.149	889.70	0.337
86	2	1	19	3	6.81	48.47	0.893	889.70	0.351

Table A2 Multiple response optimization when using Lg33.5dl1.00 nozzle (*continued*)

N	Experimental input variables				Experimental responses				Desirability
	Gas flow rate \dot{q}_g (l/min)	Liquid flow rate \dot{q}_l (ml/min)	Cutting speed C_s (m/min)	Feed rate F_r (mm/rev)	Surface roughness R_a (μm)	Cutting Tool Temperature T ($^{\circ}\text{C}$)	Average Dust concentration D_c (mg/m^3)	Material removal rate Q (mm^3/min)	D_i
87	3	1	19	3	6.35	48.784	1.83	889.70	0.358
88	4	1	19	3	6.59	46.276	3.4	889.70	0.359
89	1	2	19	3	6.94	52.075	0.236	889.70	0.355
90	2	2	19	3	6.62	46.433	0.346	889.70	0.373
91	3	2	19	3	6.47	43.454	1.33	889.670	0.382
92	4	2	20	3	4.95	39.065	0.379	874.62	0.388
93	1	3	20	3	4.89	51.919	0.156	874.62	0.381
94	2	3	20	3	4.83	45.335	0.355	874.62	0.403
95	3	3	20	3	5.01	41.887	0.341	874.62	0.414
96	4	3	20	3	5.49	33.75	2.12	874.62	0.414
97	1	1	21	3	5.02	58.816	0.156	1400.39	0.138
98	2	1	21	3	4.90	50.351	0.236	1398.39	0.146
99	3	1	22	3	6.71	50.665	0.098	1375.26	0.164
100	4	1	22	3	6.37	50.665	0.85	1375.26	0.167
101	1	2	22	3	6.52	58.189	0.16	1375.26	0.156
102	2	2	22	3	6.33	46.589	0.299	1375.26	0.168
103	3	2	22	3	6.13	43.768	0.729	1375.26	0.175
104	4	2	22	3	6.13	41.417	0.782	1375.26	0.178
105	1	3	22	3	6.39	55.367	0.125	1375.26	0.162
106	2	3	23	3	5.46	44.081	0.124	1351.14	0.192
107	3	3	23	3	5.81	39.379	0.302	1351.14	0.201
108	4	3	23	3	5.01	38.752	2.5	1351.14	0.205

Table A2 Multiple response optimization when using Lg33.5dl1.00 nozzle (*continued*)

Z	Experimental input variables				Experimental responses				Desirability
	Gas flow rate ḡ _g (l/min)	Liquid flow rate ḡ _l (ml/min)	Cutting speed C _s (m/min)	Feed rate F _r (mm/rev)	Surface roughness R _a (μm)	Cutting Tool Temperature T (°C)	Average Dust concentration D _c (mg/m ³)	Material removal rate Q (mm ³ /min)	
MINIMUM					0.98	29.35	0.049	211.12	D _i (max)
MAXIMUM					6.94	58.82	4.02	1400.40	
AVERAGE					2.976	43.277	0.701	679.48	
72	45	17.5	613.24	0.15	1.23	38.28	2.02	1103.83	0.973

BIBLIOGRAPHY

- Aslan, E., N. Camuşcu and B. Birgören. 2007. « Design optimization of cutting parameters when turning hardened AISI 4140 steel (63 HRC) with $\text{Al}_2\text{O}_3 + \text{TiCN}$ mixed ceramic tool ». *Materials & design*, vol. 28, n° 5, p. 1618-1622.
- Bacci da Silva, M., and J. Wallbank. 1999. « Cutting temperature: prediction and measurement methods—a review ». *Journal of materials processing technology*, vol. 88, n° 1, p. 195-202.
- Balout, B. 2003. Master thesis « Usinage a sec des alliages legers et des composites ». *Ecole de Technologie Superieure (Canada)*, p. 164.
- Balout, B., V. Songmene and J. Masounav. 2007. « An Experimental Study of Dust Generation During Dry Drilling of Pre-Cooled and Pre-Heated Workpiece Materials ». *Journal of Manufacturing Processes*, vol. 9, n° 1.
- Batarseh, F.Z.M. 2009. « Spray generated by an airblast atomizer: atomization, propagation and aerodynamic instability ».
- Cassin, C., and G. Boothroyd. 1965. « Lubricating action of cutting fluids ». *Journal of mechanical engineering science*, vol. 7, n° 1, p. 67-81.
- Castleman, RA. 1932. *The mechanism of atomization accompanying solid injection*. US Government Printing Office.
- Charudatt, R. Bhale. « Seminar On Dry Machining Process Dry Machining Process ».
- CONDAT Lubrifiants, www.condat.fr. « Technical sheet of MecaGreen 550 Lubricant ».
- Davim, J.P., and L. Figueira. 2007. « Machinability evaluation in hard turning of cold work tool steel (D2) with ceramic tools using statistical techniques ». *Materials & design*, vol. 28, n° 4, p. 1186-1191.
- Derringer, G. 1980. « Simultaneous optimization of several response variables ». *J. Quality Technol.*, vol. 12, p. 214-219.
- DGUV. 2010. « Information Minimum quantity lubrication for machining operations ». p. 84.
- Diakodimitris, C., P. Hendrick and YR Iskandar. « Study of Minimum Quantity Cooling (MQC) on the tool temperature in milling operations ».

- Ding, Y., and S.Y Hong. 1998. « Improvement of Chip Breaking in Machining Low Carbon Steel by Cryogenically Precooling the Workpiece ». *Journal of Manufacturing Science and Engineering*, vol. 120, n° 1, p. 76-83.
- Fang, N. 2005. « Tool-chip friction in machining with a large negative rake angle tool ». *Wear*, vol. 258, n° 5, p. 890-897.
- Gretzinger, J., and WR Marshall. 2004. « Characteristics of pneumatic atomization ». *AIChE Journal*, vol. 7, n° 2, p. 312-318.
- Grundfos, instructions. November 2010. « SMART Digital - DDA, Installation and operating instructions ».
- Harrington, EC. 1965. « The desirability function ». *Industrial quality control*, vol. 21, n° 10, p. 494-498.
- He, Z., and PF Zhu. 2009. « A hybrid genetic algorithm for multiresponse parameter optimization within desirability function framework ». In *Industrial Engineering and Engineering Management, 2009. IE&EM'09. 16th International Conference on*. p. 612-617. IEEE.
- Hede, P.D., P. Bach and A.D. Jensen. 2008. « Two-fluid spray atomisation and pneumatic nozzles for fluid bed coating/agglomeration purposes: A review ». *Chemical Engineering Science*, vol. 63, n° 14, p. 3821-3842.
- Hong, S.Y. 2006. . « Lubrication mechanisms of LN2 in ecological cryogenic machining ». *Machining science and technology*, vol. 10, n° 1, p. 133-155.
- Hong, S.Y. , and M. Broome. 2000. « Economical and ecological cryogenic machining of AISI 304 austenitic stainless steel ». *Clean Technologies and Environmental Policy*, vol. 2, n° 3, p. 157-166.
- Hong, S.Y., Y. Ding and R.G. Ekkens. 1999. « Improving low carbon steel chip breakability by cryogenic chip cooling ». *International Journal of Machine Tools and Manufacture*, vol. 39, n° 7, p. 1065-1085.
- Jasuja, AK. 1979. « Atomization of crude and residual fuel oils ». *Journal of Engineering for Power*, vol. 101, p. 250.
- Jun, M.B.G., S.S. Joshi, R.E. DeVor and S.G. Kapoor. 2008. « An experimental evaluation of an atomization-based cutting fluid application system for micromachining ». *Journal of manufacturing science and engineering*, vol. 130, n° 3.
- Kalpakjian, S. and Schmid, S.R. (Chapter 8). 2008. *Manufacturing Processes for Engineering Materials*, 5th ed.: Pearson Education.

- Khettabi, R., V. Songmene and J. Masounave. 2007. « Effect of tool lead angle and chip formation mode on dust emission in dry cutting ». *Journal of Materials Processing Technology*, vol. 194, n° 1-3, p. 100-109.
- Khettabi, R., V. Songmene and J. Masounave. 2010. « Effects of Speeds, Materials, and Tool Rake Angles on Metallic Particle Emission During Orthogonal Cutting ». *Journal of materials engineering and performance*, vol. 19, n° 6, p. 767-775.
- Khettabi, R., V. Songmene, I. Zaghbani and J. Masounave. 2010. « Modeling of Particle Emission During Dry Orthogonal Cutting ». *Journal of materials engineering and performance*, vol. 19, n° 6, p. 776-789.
- Kim, KY, and WR Marshall Jr. 1971. « Drop-size distributions from pneumatic atomizers ». *AIChE Journal*, vol. 17, n° 3, p. 575-584.
- Lee Black, D., M.Q. McQuay and M.P. Bonin. 1996. « Laser-based techniques for particle-size measurement: a review of sizing methods and their industrial applications ». *Progress in energy and combustion science*, vol. 22, n° 3, p. 267-306.
- Lefebvre, A.H. 1980. « Airblast atomization ». *Prog. Energy Combust. Sci.*, vol. 6, p. 233-261.
- Lefebvre, A.H. 1989. *Atomization and sprays*. CRC.
- Lefebvre, Arthur Henry. 1999. *Gas Turbine Combustion*, second Taylor and Francis 400 p.
- Lightfoot, M.D. 2007. *A Fundamental Classification of Atomization Processes*. DTIC Document.
- Liu, H.F., W.F. Li, X. Gong, X.K. Cao, J.L. Xu, X.L. Chen, Y.F. Wang, G.S. Yu, F.C. Wang and Z.H. Yu. 2006. « Effect of liquid jet diameter on performance of coaxial two-fluid airblast atomizers ». *Chemical Engineering and Processing: Process Intensification*, vol. 45, n° 4, p. 240-245.
- Mandato, S., E. Rondet, G. Delaplace, A. Barkouti, L. Galet, P. Accart, T. Ruiz and B. Cuq. 2012. « Liquids' atomization with two different nozzles: Modeling of the effects of some processing and formulation conditions by dimensional analysis ». *Powder Technology*.
- Manual, FESTO. Aug 2012. « Flow sensors SFAB ».
- Manual, Tecnolub 2009. « Micro lubrication on Air - Oil ».
- Manual, Tecnolub Jan 2009. « Microlubrication GLS0.4-1 ».

- Manual, TSI Model 8530/8531/8532. Jan 2012. « DUSTTRAK™ II Aerosol Monitor, Operation and Service Manual ».
- Ohbuchi, Y. , and T. Obikawa. 2003. « Finite element modeling of chip formation in the domain of negative rake angle cutting. Transactions of the ASME ». *Journal of Engineering Materials and Technology*, vol. 125, n° 3, p. 324-328.
- Özel, T., T.K. Hsu and E. Zeren. 2005. « Effects of cutting edge geometry, workpiece hardness, feed rate and cutting speed on surface roughness and forces in finish turning of hardened AISI H13 steel ». *The International Journal of Advanced Manufacturing Technology*, vol. 25, n° 3, p. 262-269.
- SalesBrochure, Taylo Hubson. « Rapid on the shopfloor Surface Texture Measurement, www.taylor-hobson.com », *consulted on 15/Aug./2012*.
- Semião, V., P. Andrade and M.G. Carvalho. 1996. « Spray characterization: numerical prediction of Sauter mean diameter and droplet size distribution ». *Fuel*, vol. 75, n° 15, p. 1707-1714.
- Shaw, MC, JD Pigott and LP Richardson. 1951. « Effect of cutting fluid upon chip–tool interface temperature ». *Trans. ASME*, vol. 71, p. 45-56.
- Songmene, V. , B. Balout and J. Masounave. 2008a. « Clean machining: Experimental investigation on dust formation Part I: Influence of machining parameters and chip formation ». *International Journal of Environmentally Conscious Design & Manufacturing*, vol. 14, n° 1, p. 1-16.
- Songmene, V., B. Balout and J. Masounave. 2008b. « Clean machining: Experimental investigation on dust formation-Part II: Influence of machining strategies and drill condition ». *International Journal of Environmentally Conscious Design & Manufacturing*, vol. 14, n° 1, p. 17-33.
- Steimes, J., C. Diakodimitris, M. Di-Matteo and P. Hendrick. 2012. « A laser diffraction study on droplet diameters in two lubrication systems ». *Int Symp on Applications of Laser Techniques to Fluid Mechanics* p. 12.
- Strutt, JW. 1879. « On the instability of jets ». Vol. 10, p. 4-13.
- Sutter, G., and N. Ranc. 2007. « Temperature fields in a chip during high-speed orthogonal cutting—An experimental investigation ». *International Journal of Machine Tools and Manufacture*, vol. 47, n° 10, p. 1507-1517.
- Unfallversicherung, Deutsche Gesetzliche. 2010. « Information: Minimum quantity lubrication for machining operations ». p. 84.

- Upadhyay, V., PK Jain and NK Mehta. 2012. « In-process prediction of surface roughness in turning of Ti-6Al-4V alloy using cutting parameters and vibration signals ». *Measurement*.
- Wan, Wen, and Jeffrey B Birch. 2011. « Using a modified genetic algorithm to find feasible regions of a desirability function ». *Quality and Reliability Engineering International*, vol. 27, n° 8, p. 1173-1182.
- Weber, C. 1931. « Disintegration of liquid jets ». *Zeitschrift für Angewandte Mathematik und Mechanik*, vol. 11, n° 2, p. 136-159.
- Weiss, M.A., and C.H. Worsham. 1958. *Atomization in High Velocity Air Streams*. Esso Research and Engineering Company.
- www.sympatec.com. « Sympatec, GmbH, System-Partikel-Technik. », *consulted on 02/Sep/2012*.
- Xie, JQ, AE Bayoumi and HM Zbib. 1996. « A study on shear banding in chip formation of orthogonal machining ». *International Journal of Machine Tools and Manufacture*, vol. 36, n° 7, p. 835-847.
- Zaghbani, I., V. Songmene and R. Khettabi. 2009. « Fine and ultrafine particle characterization and modeling in high-speed milling of 6061-T6 aluminum alloy ». *Journal of materials engineering and performance*, vol. 18, n° 1, p. 38-48.